Universidade de Aveiro Departamento de Química
2019

Ângela da Conceição Relvas Guerra

Estudo metabolómico dos efeitos de compostos da casca de eucalipto em células humanas de mama tumorais e não tumorais

Metabolomics study of the effects of eucalyptus bark compounds on human breast tumor and non-tumor epithelial cells

Universidade de Aveiro Departamento de Química
2019

Ângela da Conceição Relvas Guerra

Estudo metabolómico dos efeitos de compostos da casca de eucalipto em células humanas de mama tumorais e não tumorais

Metabolomics study of the effects of eucalyptus bark compounds on human breast tumor and non-tumor epithelial cells

Tese apresentada à Universidade de Aveiro para cumprimento dos requisitos necessários à obtenção do grau de Doutor em Bioquímica, realizada sob a orientação científica do Doutora Iola Melissa Fernandes Duarte, Investigadora Principal do CICECO – Instituto de Materiais de Aveiro, do Departamento de Química da Universidade de Aveiro e da Doutora Maria de Fátima Pereira Duarte, Investigadora Auxiliar do Centro de Biotecnologia Agrícola e Agro-Alimentar do Alentejo (CEBAL).

Apoio financeiro da FCT e do POPH/FSE (SFRH/BD/98635/2013) no âmbito do III Quadro Comunitário de Apoio, e projeto NEucBark– New valorization strategies for Eucalyptus spp. Bark Extracts (PTDC/AGR-FOR/3187/2012) financiado pelo Fundo Europeu de Desenvolvimento Regional (FEDER) através do Programa Operacional Fatores de Competitividade (COMPETE); da Universidade de Aveiro – projeto CICECO-Instituto de Materiais de Aveiro, FCT Ref. UID/CTM/50011/2019, financiado por fundos nacionais através da FCT/MCTES. Agradece-se ainda à Rede Nacional de RMN (RNRMN), apoiada por fundos FCT, à empresa Bruker BioSpin (Rheinstetten, Germany) e ao projeto “Biodata.pt – Infraestrutura Portuguesa de Dados Biológicos” (REF: LISBOA-01-0145-FEDER-022231) co-financiado pelo POR Lisboa, através do programa FEDER e por fundos nacionais através da FCT/MEC (PIDDAC).

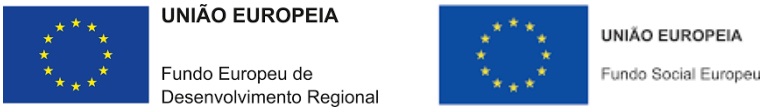

Aos meus Pais
Joaquina Relvas e Manuel Guerra

Ao Filipe

À Abelhinha

"Adeus Hans Castorp, filho ingénuo e traquinas da vida! A tua história chegou ao fim. Terminámos a narrativa. Não foi uma história nem longa nem curta, apenas hermética. Não foi por ti que a contámos (…), mas pela história em si. Não deixou, todavia, de ser a tua história (…)"

In A Montanha Mágica, Thomas Mann

o júri

presidente

Doutor Joaquim Arnaldo Carvalho Martins
Professor Catedrático do Departamento de Eletrónica, Telecomunicações e Informática da Universidade de Aveiro

Doutora Maria De Fátima Monginho Baltazar
Professora Associada da Escola de Ciências da Saúde da Universidade do Minho

Doutora Andreia Ferreira De Castro Gomes
Professora Auxiliar do Departamento de Biologia da Escola de Ciências da Universidade do Minho

Doutora Maria Paula Matos Marques
Professora Auxiliar com Agregação do Departamento de Ciências da Vida da Faculdade de Ciências e Tecnologia da Universidade de Coimbra

Doutora Ana Maria Pissarra Coelho Gil
Professora Associada com Agregação do Departamento de Química da Universidade de Aveiro

Doutora Iola Melissa Fernandes Duarte
Equiparada a Investigadora Principal do Departamento de Química da Universidade de Aveiro

agradecimentos

Em primeiro lugar, gostaria de agradecer à Doutora Iola Duarte, por ter aceitado ser minha orientadora, pelo apoio, disponibilidade e ajuda em todas as fases de execução deste trabalho. À minha co-orientadora, Doutora Fátima Duarte, a minha "mãe" na ciência. Obrigado por todos os ensinamentos, conselhos, apoio e incentivo, mas sobretudo obrigado pelo exemplo. Por nos mostrares todos os dias que podemos sempre fazer mais e ser melhores.

À Professora Doutora Maria do Rosário Domingues pelo incansável apoio e incentivo durante o período de aulas do programa doutoral e à Doutora Helena Oliveira, o meu agradecimento pela realização dos ensaios de citometria.

À Joana Carrola por toda a preciosa ajuda, ensinamentos com o RMN e amizade.

A todos os colegas do CEBAL em especial aos meninos do CS. Aos colegas e ex-colegas que passaram pelo grupo dos Compostos Bioactivos, obrigado pelas valiosas discussões, ajuda e palavras de incentivo.

À Daniela por todas as horas partilhadas no 15, sempre cheias de sorrisos. Só nós sabemos o que o carrinho sofreu no verão de 2016. Ao Miguel por todas as conversas desconexas e pela preocupação por tudo estar escuro. Às minhas meninas, Ana e Olinda, fundamentais em todas as fases. Obrigado pelo incansável apoio, generosa paciência e amizade gigantesca.

À Joana Rita por estar sempre tão perto, mesmo estando longe.

À minha Paula por ser sempre a minha inspiração. À Maria e ao Martim por me mostrarem nos momentos mais difíceis, o que realmente é importante.

Ao Filipe. Fomos sempre dois em todas as vitórias e derrotas deste doutoramento. Sabes uma coisa?

Aos meus pais, obrigado por tudo…

palavras-chave

Extrato lipofilico da casca externa de *Eucalyptus nitens*; ácidos betulínico e ursólico; cancro da mama triplo negativo; células não-tumorais epiteliais de mama; metabolismo celular; metabolómica; ressonância magnética nuclear.

resumo

A exploração agroindustrial do eucalipto para a produção de pasta de celulose gera uma grande quantidade de resíduos de biomassa, casca em especial. A casca de *Eucalyptus* spp é uma fonte generosa de diversos triterpenóides, principalmente ácidos triterpénicos. Os ácidos triterpénicos têm demostrado capacidade de modular inúmeras vias de sinalização envolvidas no processo de carcinogénese, que, por sua vez, poderão estar intrinsecamente relacionadas com a reprogramação metabólica celular. Dada a escassa informação sobre a atividade modulatória dos compostos da casca de eucalipto no metabolismo, o trabalho realizado nesta tese pretendeu determinar, de forma abrangente, os efeitos metabólicos de um extrato lipofílico da casca externa de *E. nitens* e de dois ácidos triterpénicos (betulínico e ursólico) em células de cancro da mama triplo negativo e células epiteliais não tumorais de mama. Para este efeito, utilizou-se a metabolómica por espectroscopia de RMN, que permitiu uma análise integrada de meio de cultura e extratos celulares (aquosos e orgânicos). O Capítulo 1 introduz alguns aspetos gerais sobre o cancro da mama, como a classificação em subtipos e a abordagem terapêutica, e informa acerca do uso de compostos naturais derivados de plantas no tratamento do cancro, focando-se nos ácidos triterpénicos. Seguidamente, as principais desregulações no metabolismo associadas ao cancro da mama são apresentadas, bem como o conhecimento atual sobre a modulação metabólica induzida por ácidos triterpénicos e outros isoprenóides. Finalmente, apresenta-se a abordagem metabolómica, em conjunto com um breve estado da arte sobre as suas aplicações no estudo de células tumorais de mama e a sua reposta metabólica a compostos naturais derivados de plantas. No Capítulo 2, a atividade metabólica basal e a composição dos dois tipos de células utilizados neste trabalho (células de cancro da mama triplo negativo MDA-MB-231, e células epiteliais mamárias não tumorais MCF-10A) são detalhadamente descritas. Os padrões de consumo e excreção celulares, juntamente com a análise do endometaboloma polar e da composição lipídica sugeriram diferenças em várias vias metabólicas, relacionadas com as maiores necessidades das células tumorais em termos de biossíntese, produção de energia e controlo do estado redox. O Capítulo 3 aborda os efeitos de um extrato lipofílico da casca externa de *E. nitens* no metabolismo das células MDA-MB-231 e MCF-10A. As células MDA-MB-231 incubadas com este extrato (15 µg/mL) mostraram grandes alterações no metaboloma celular. Diversas vias metabólicas aparentaram ser moduladas de forma a favorecer o incremento da respiração mitocondrial, facto evidenciado pelo aumento significativo da razão NAD^+/NADH em células tratadas. Observou-se também a diminuição da expressão proteica de colina quinase (ChoK-α) e do teor relativo em fosfocolina, habitualmente associada a um fenótipo agressivo de cancro da mama. Nas células epiteliais de mama MCF-10A, o extrato lipofílico da casca externa de *E. nitens* originou, em geral, um efeito mais moderado, caracterizado pela intensificação da glicólise, não tendo produzido quaisquer efeitos na composição lipídica das células.

resumo (cont.)

A resposta metabólica das células de cancro da mama triplo negativo e das células epiteliais não-tumorais de mama ao ácido betulínico e ao ácido ursólico (ácidos triterpénicos abundantes no extrato lipofílico da casca externa de *E. nitens*) é apresentada no Capítulo 4. Nas células MDA-MB-231, o ácido betulínico pareceu ter induzido um aumento na glicólise e na atividade do ciclo dos ácidos tricarboxílicos, em conjunto com a hidrólise de lípidos neutros e acumulação de fosfolípidos de membrana. Os efeitos do ácido ursólico foram menos acentuados após as 48h de incubação, mas após um período de recuperação em meio de cultura celular, foi observada a diminuição da glicólise e dos níveis de ATP. Nas células MCF-10A, ambos os ácidos triterpénicos aparentaram reprogramar intensamente o metabolismo da glucose no sentido da degradação de glicogénio, intensificação da glicólise, aumento da via biossintética das hexosaminas, degradação da membrana celular e formação de gotas lipídicas (possivelmente para eliminar espécies tóxicas). Em suma, esta tese contribui de forma significativa para fazer avançar o conhecimento sobre a atividade metabólico-modulatória do extrato lipofílico da casca externa de *E. nitens*, assim como dos ácidos ursólico e betulínico, em células do cancro da mama triplo negativo e em células não-tumorais epiteliais de mama. Como referido no Capítulo 5, os resultados aqui descritos fornecem pistas novas e relevantes sobre o modo de ação dos compostos da casca de eucalipto e abrem novas perspetivas de investigação que sustentam o seu futuro desenvolvimento na área da terapia anticancro.

keywords

Eucalyptus nitens outer bark extract; betulinic and ursolic acids; triple negative breast cancer; non-tumor breast epithelial cells; cell metabolism; metabolomics; nuclear magnetic resonance spectroscopy.

abstract

Agro-industrial exploitation of eucalyptus for pulp production generates large amounts of biomass residues, particularly bark. *Eucalyptus* spp. barks are a rich source of several triterpenoids, mostly triterpenic acids (TAs). TAs have been demonstrated to modulate numerous signaling pathways involved in carcinogenesis, which may be closely linked to cellular metabolic reprogramming. Given the limited information on the metabolic modulatory activity of eucalyptus bark compounds, the work performed in this thesis aimed at comprehensively assessing the metabolic effects of a lipophilic *E. nitens* outer bark extract and two TAs (betulinic and ursolic acids) in triple negative breast cancer (TNBC) and non-tumor breast cells. Integrative NMR metabolomics of cell culture media, intracellular polar metabolites and cellular lipids was used for that purpose. Chapter 1 introduces some general aspects on breast cancer, such as subtype classification and therapeutic options, and informs on current uses of plant-derived natural products in anticancer therapy, focusing on TAs. Then, the main metabolic dysregulations known to be associated with breast cancer are reviewed, as well as current knowledge on metabolic modulation by TAs and other isoprenoids. Finally, the metabolomics approach is presented, together with a brief state of the art on its applications in the study of breast cancer cells and their metabolic responses to plant-derived natural products. In Chapter 2, the basal metabolic activity and composition of the two cell types used in this work (MDA-MB-231 TNBC cells and MCF-10A non-tumor epithelial cells) are thoroughly described. Based on consumption and excretion patterns, together with analysis of polar endometabolome and lipid composition, metabolic pathway differences were inferred and correlated with the high demand of TNBC cells for macromolecular biosynthesis, energy production and redox control. Chapter 3 addresses the effects of a lipophilic *E. nitens* outer bark extract on the metabolism of MDA-MB-231 and MCF-10A cells. Incubation of TNBC cells with this extract (15 µg/mL) strongly affected the cellular metabolome. Several pathways appeared to be modulated towards mitochondrial respiration enhancement, as evidenced by significantly increased NAD^+/NADH ratios in treated cells. Downregulation of choline kinase (ChoK-α) expression and the content of phosphocholine, often regarded as a marker of breast cancer aggressiveness, was also observed. In MCF-10A epithelial cells, the lipophilic *E. nitens* outer bark extract had an overall milder impact, characterized by intensification of glycolysis and no effect on the cells lipid composition. The metabolic responses of TNBC cells and breast epithelial cells to betulinic acid (BA) and ursolic acid (UA) (abundant TAs present on the lipophilic *E. nitens* outer bark extract) are presented in Chapter 4. In MDA-MB-231 cells, BA was suggested to induce upregulation of glycolytic and TCA cycle activity, together with hydrolysis of neutral lipids and buildup of membrane phospholipids. UA effects were less pronounced upon 48h incubation, but after a recovery period in fresh growth medium, downregulation of glycolysis and decreased ATP levels were observed. In MCF-10A cells, both TAs appeared to reprogram glucose metabolism towards glycogen degradation, intensification of glycolysis, upregulation of the hexosamine biosynthetic pathway, membrane degradation and formation of lipid droplets, likely to scavenge otherwise-toxic lipid species. Overall, this thesis is believed to significantly contribute to advance knowledge on the metabolic modulatory activity of a lipophilic *E. nitens* bark extract, as well as of ursolic and betulinic pure acids, in TNBC and non-tumor breast epithelial cells. As outlined in the final Chapter 5, the new findings reported provide remarkable insight into the mode of action of eucalyptus bark compounds and open new research perspectives to support their future development in the field of anticancer therapy.

Publications resulting from the work carried out within this thesis

Full paper: **Guerra AR**, Duarte IF, Duarte MF. (2018) Targeting tumor metabolism with plant-derived natural products: emerging trends in cancer therapy, Journal of Agricultural and Food Chemistry, 66 (41), pp 10663–10685. DOI: 10.1021/acs.jafc.8b04104.

Abstract: **Guerra AR,** Soares B, Guerreiro O, Ramos P, Oliveira H, Silvestre A, Freire C, Duarte MF: Anti-tumoral activity of lipophilic Eucalyptus bark extracts, enriched on triterpenic acids, against breast cancer cells. Planta Med 2014; 80 - SL41. DOI: 10.1055/s-0034-1394529.

Manuscripts submitted to International Journals:

Full paper: **Guerra AR**, Soares BIG, Oliveira H, Freire CSR, Silvestre AJD, Duarte MF, Duarte IF. NMR metabolomics reveals different metabolic modulatory activity of a lipophilic Eucalyptus outer bark extract on human tumor and non-tumor breast epithelial cells (*submitted*).

Full paper: **Guerra AR**, Paulino A, Castro M, Oliveira H, Duarte MF, Duarte IF. Metabolic effects of triterpenic acids on triple negative breast cancer and non-tumor breast epithelial cells as viewed by NMR metabolomics (*submitted*).

Other publications related to this work

Book chapter: **Guerra AR**, Duarte MF, Duarte IF. (2019) Por que é que a reprogramação do metabolismo tumoral por meio de fitoquímicos poderá ser útil no tratamento do cancro. Bioquímica e Bem-estar, Coimbra MA (ed.), Edições Afrontamento e Departamento de Biologia da Universidade de Aveiro (*in press*).

Book chapter: **Guerra AR**, Duarte IF, Duarte MF. (2017). O Papel dos fitoquímicos na prevenção e tratamento do cancro da mama. Capitulo 4 p. 63-74. Bioquimica e Bem-Estar, Coimbra MA (ed.), Edições Afrontamento e Departamento de Biologia da Universidade de Aveiro. ISBN: 978-972-36.

Full paper: **Guerra AR**, Duarte IF, Duarte MF. (2016) Role of isoprenoid compounds on angiogenic regulation: opportunities and challenges. Current Medicinal Chemistry, Volume 23 DOI:10.2174/0929867323666160217123822.

Book chapter: Silva FS, Soares B, Calçada C, **Guerra AR**, Pereira-Wilson C, Lima CF, Freire CSR, Silvestre AJD, Duarte MF. New valorization strategies for Eucalyptus spp. bark extracts. Wastes: Solutions, Treatments and Opportunities. Vilarinho, Castro & Russo (eds) 2015 Taylor & Francis Group, London, ISBN: 978-1-138-02882-1 (Hardback).

Full paper: Domingues RMA, **Guerra AR**, Duarte M, Freire CSR, Neto CP, Silva CMS, Silvestre AJD. (2014) Bioactive triterpenic acids: From agroforestry biomass residues, to promising therapeutic tools. Mini-Reviews in Organic Chemistry. DOI: 10.2174/1570193X113106660001.

Abstract: **Guerra AR**, Neyton S, Duarte MF. Role of triterpenic acids on thrombin regulation and PAR1 signaling. Planta Med 2014; 80 - P1L113. DOI: 10.1055/s-0034-1394770.

Contents

List of abbreviations and symbols

1D	one-dimensional
2D	two-dimensional
ACC	acetyl-CoA carboxylase
ADP	adenosine diphosphate
AH	aconitase
AMP	adenosine monophosphate
ATM	ataxia-telangiectasia-mutated
ATP	adenosine triphosphate
BA	betulinic acid
BARD1	BRCA1-associated ring domain
BCAA	branched chain amino acids
BSA	bovine serum albumin
CDDO	2-cyano-3,12-dioxooleana-1,9-dien-28-oic imidazolide
CEs	cholesteryl esters
CHEK2	checkpoint kinase 2
Cho	choline
ChoK	choline kinase
CoA	coenzyme A
COSY	correlation spectroscopy
Cr	creatine
DMAPP	dimethylallyl diphosphate
DMEM	Dulbecco's modified Eagle's medium
DMSO	dimethyl sulfoxide
DNA	deoxyribonucleic acid
ECL	enhanced chemiluminescence
EDTA	ethylenediaminetetraacetic acid
ER	estrogen receptor
FA	fatty acid
FAO	fatty acid oxidation
FAS	fatty acid synthase
FBS	fetal bovine serum
FDA	food and drug administration
FH	fumarate hydratase
FID	free induction decay
FT	Fourier transformation
GAC	glutaminase C
GLUTs	glucose transporters
GPC	glycerophosphocholine
GPI	glucose-6-phosphate isomerase
GPLs	glycerophospholipids
GSH	reduced glutathione
GSSG	oxidised glutathione
HBP	hexosamine biosynthetic pathway
HCC	hepatocellular carcinoma
HER	human epidermal growth factor receptor
HIF	hypoxia-inducible factor
HK	hexokinases
HMDB	human metabolome database
HMGCR	3-hydroxy-3-methylglutaryl-CoA reductase

HRMAS	high resolution magic angle spinning
HSQC	heteronuclear single quantum correlation
IC_{50}	half maximal inhibitory concentration
IDH	isocitrate dehydrogenase
IPP	isopentenyl pyrophosphate
*J*res	*J* resolved
KGA	kidney type glutaminase
LV	latent variable
MCT	monocarboxylate transporters
MDH1	malate dehydrogenase 1
MFS	major facilitator superfamily
m-Ino	*myo*-inositol
MMPs	matrix metalloproteinases
MRN	MRE11–RAD50–NBS1
mRNA	messenger ribonucleic acid
MS	mass spectrometry
mtDNA	mitochondrial DNA
MTT	3-(4,5-dimethylthiazol-2-yl)-2,5-diphenyltetrazolium bromide
MVA	multivariate analysis
NAD^+	nicotinamide adenine dinucleotide
NADH	nicotinamide adenine dinucleotide, in the reduced form
NMR	nuclear magnetic resonance
OA	oleanolic acid
OXPHOS	*oxidative phosphorylation*
PBS	phosphate buffered saline
PC	phosphocholine
PCA	principle component analysis
PCr	phosphocreatine
PDC	pyruvate dehydrogenase complex
PDHX	pyruvate dehydrogenase protein X
PDKs	pyruvate dehydrogenase kinases
PEP	phosphoenolpyruvate
PFK	phosphofructokinase
PFKFB	6-phosphofructo-2-kinase/fructose-2,6-bisphosphatases
PHGDH	phosphoglycerate dehydrogenase
PK	pyruvate kinases
PLS-DA	partial least squares-discriminant analysis
PMSF	phenylmethylsulfonyl fluoride
PPP	pentose phosphate pathway
PR	progesterone receptor
PTC	phosphatidylcholine
PTE	phosphatidylethanolamine
PUFA	polyunsaturated fatty acids
RIPA	radioimmunoprecipitation assay
RNase	ribonuclease
SCD	stearoyl-CoA desaturase
SDH	succinate dehydrogenase
SDS	sodium dodecyl sulfate
SGLTs	sodium-dependent glucose co-transporters

SM	sphingomyelin
TA	triterpenic acid
TCA	tricarboxylic acid
TG	triglycerides
TMS	tetramethylsilane
TNBC	triple-negative breast cancer
TOCSY	total correlation spectroscopy
TSP	3-trimethylsilylpropionic acid
UA	ursolic acid
UDP	uridine diphosphate
UDP-GalNAc	UDP-N-acetyl-galactosamine
UDP-Glc	UDP-Glucose
UDP-GlcNAc	UDP-N-acetylglucosamine
UFA	unsaturated fatty acids
UMP	uridine monophosphate
UTP	uridine triphosphate
UV	unit variance
VEGF	vascular endothelial growth factor
VEGFR	vascular endothelial growth factor receptor
VIP	variable importance to the projection

List of Figures

List of Tables

Chapter 1

INTRODUCTION

Parts of this chapter have been published in two review papers:

1) Guerra AR, Duarte IF, Duarte MF. (2018) Targeting tumor metabolism with plant-derived natural products: emerging trends in cancer therapy, *Journal of Agricultural and Food Chemistry*, 66 (41), pp 10663–10685. DOI: 10.1021/acs.jafc.8b04104.

2) Guerra AR, Duarte IF, Duarte MF. (2016) Role of isoprenoid compounds on angiogenic regulation: opportunities and challenges. *Current Medicinal Chemistry*, Volume 23 DOI:10.2174/0929867323666160217123822.

and 2 book chapters:

1) Guerra AR, Duarte MF, Duarte IF. (2019) Por que é que a reprogramação do metabolismo tumoral por meio de fitoquímicos poderá ser útil no tratamento do cancro. Bioquímica e Bem-estar, Coimbra MA (ed.), Edições Afrontamento e Departamento de Biologia da Universidade de Aveiro (*in press*).

2) Guerra AR, Duarte IF, Duarte MF. (2017). O Papel dos fitoquímicos na prevenção e tratamento do cancro da mama. Capitulo 4 p. 63-74. Bioquimica e Bem-Estar, Coimbra MA (ed.), Edições Afrontamento e Departamento de Biologia da Universidade de Aveiro. ISBN: 978-972-36.

1.1. Breast cancer

Breast cancer remains one of the most prevalent cancers in the world, with over 2 million women diagnosed in 2018 (25% of all cancers) [1]. In the European Union, breast cancer has the highest healthcare costs of all cancers (€ 6,73 billions), and accounts for 13% of all cancer-related healthcare costs [2]. Moreover, breast cancer-related deaths in people within working age, in 2008, represented an economic loss of €7 billion, just in Europe [3]. Although breast cancer mortality has been consistently decreasing in developed countries over the last three decades, due to major advances in screening, diagnosis and treatment [4], mitigation of the social and economic burden associated with this disease remains an enormous challenge. The development of safer and more effective therapies is particularly relevant in this respect, given the highly heterogeneous nature of breast cancer and the dreadful side-effects of most current treatments.

1.1.1. Epidemiology and risk factors

Breast cancer is the second most common cancer worldwide and the most frequent among women [1]. Furthermore, breast cancer incidence (Figure 1.1) has been rapidly increasing in most countries in transition, likely indicating changes in reproductive patterns combined with social and economic development issues [1, 5].

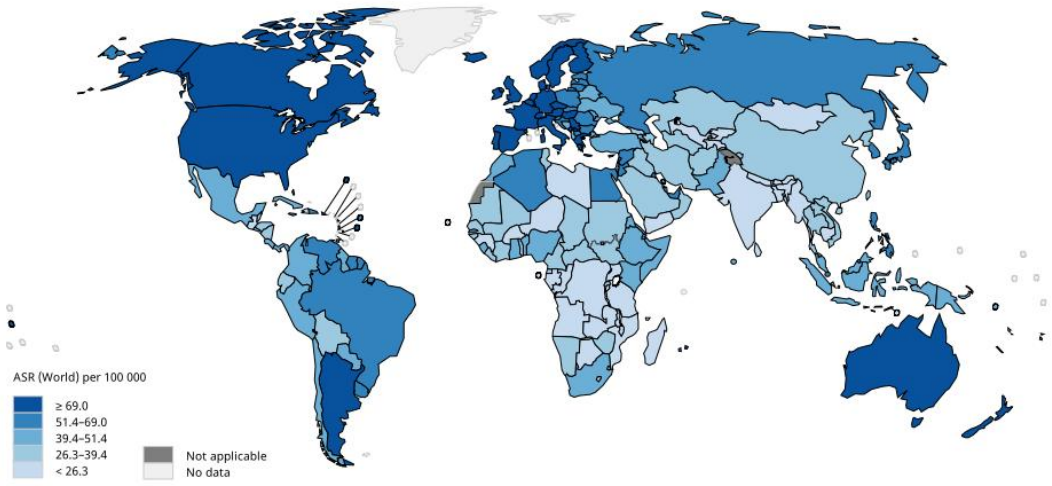

Figure 1.1. Estimated age-standardized incidence rates (per 100 000; all ages), according to GLOBOCAN 2018 (World Health Organization / International Agency for Research on Cancer, http://gco.iarc.fr/today, accessed on 20/10/2019).

In Portugal, breast cancer represents by far the cancer with the highest incidence rate among women (Figure 1.2) [1]. Although mortality has been

decreasing since the 1990s, cancer age-adjusted incidence rates are expected to rise [6-9].

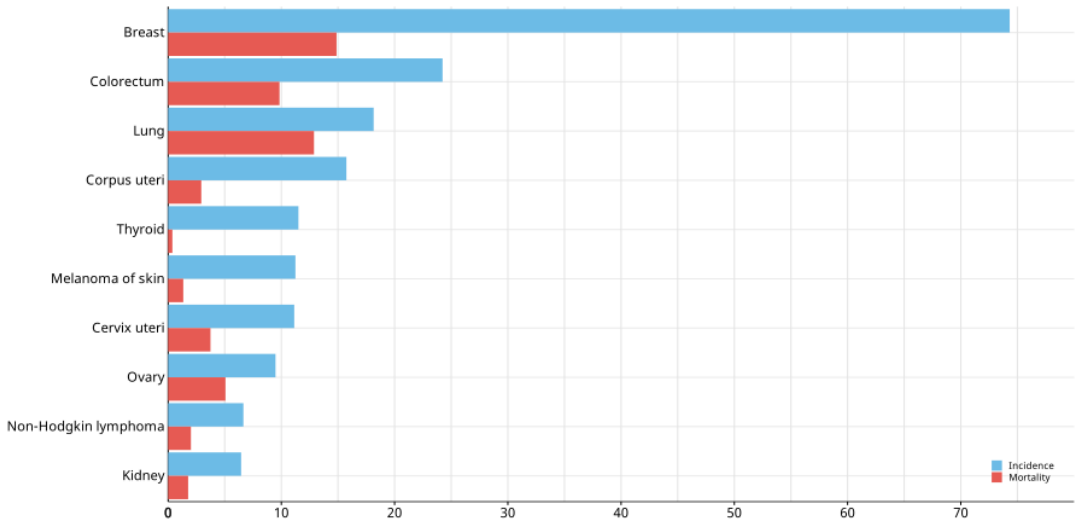

Figure 1.2. Estimated age-standardized incidence and mortality rates of female cancer types in Portugal (per 100 000; all ages), according to GLOBOCAN 2018 (World Health Organization / International Agency for Research on Cancer, http://gco.iarc.fr/today, accessed on 20/10/2019).

Epidemiologic studies revealed several risk factors that have a well-documented effect in breast cancer. The multifactorial etiology of this disease is clearly perceptible by the list of possible influencing factors. Table 1.1 presents a summary of the main risk factors for breast cancer.

Table 1.1. Summary of risk factors for breast cancer.

Age		Risk increases with age [10]
Gender		Predominantly diagnosed in women [7]
Reproductive factors	**Early menarche**	Older age at menarche associated with decreased risk [11]
	Late menopause	Each year delay corresponds to a 3% risk increase [12]
	Age of first birth	Parity at an older age positively associated with cancers that express either estrogen or progesterone receptors [13]

Table 1.1. (cont.)

Reproductive factors	**Parity**	Parous women have an overall lower risk of luminal A breast cancer compared with women who have never given birth, and an increased risk of triple negative tumors [11]
	Breastfeeding	Relative risk reduction of 4.3% for every 12 months of breast-feeding [13]
Exogenous hormones	**Contraceptive hormones**	Consistently associated with increased risk in triple negative subtype. Decreased risk for luminal A subtype [11]
	Hormone replacement	Higher risk in hormone replacement therapy users [14]
Genetic factors	**Mutations in high penetrance genes (BRCA1,BRCA2, TP53, CDH1, PTEN, STK11)**	Increased breast cancer risk by more than 4-fold [15]
	Mutations in moderate penetrance genes (CHEK2, PALB2, ATM, BARD1, MRN complex, RAD51 and paralogs)	Associated with a 2-fold to 4-fold increased risk [15, 16]
	Polymorphism in low penetrance *loci*	Less than 2-fold increased risk [15, 16]
History of benign breast disease		Increased risk of developing breast cancer [17]
Lifestyle	**Alcohol**	Increased risk of developing luminal A breast cancer and HER2-overexpressing breast cancer [11]
	Physical Activity	Physical activity, particularly in adulthood, decreases the risk of developing breast cancer [18]
	Weight	Elevated body mass index among pre-menopausal woman is associated with a decreased risk for luminal A and increased risk for triple negative breast cancer [11]
Radiation exposure		Higher risk [14]

1.1.2. Breast cancer classification

Breast cancer encompasses a heterogeneous group of diseases, with distinct morphological features, immunohistochemical profiles and unique histopathological subtypes that account for the different outcomes and treatment responses [19]. Therefore, precise classification of breast cancers into clinically pertinent subtypes is extremely important to provide adequate treatment options.

The traditional approach to breast cancer classification includes clinicopathological variables, such as tumor size, lymph node involvement or tumor grade, and classical immunohistochemistry markers, such as estrogen receptors (ER), progesterone receptors (PR) and human epidermal growth factor receptor 2 (HER2) status [20]. ERs (ERα and ERβ) are members of the steroid receptor superfamily that mediate the effect of estrogen [21]. Estrogens may exert their effect in breast carcinogenesis acting as initiators (DNA mutations mediated by estrogen metabolites) or as promoters, inducing growth of transformed cells [22]. These receptors bind as dimers to the estrogen response element and regulate estrogen-responsive genes [22]. On the other hand, HER2 belongs to the four membrane tyrosine kinases family and its activation relies on the heterodimerization with another family member or self-homodimerization when expressed at very high levels [20]. Activation of HER2 promotes dimerization and transphosphorylation of its extracellular domains, which can interact with several signaling pathways, and regulate different cellular processes directly related with carcinogenesis (proliferation, survival, differentiation, invasion) [20].

In the last decades, the development of high-throughput platforms for gene expression analysis has allowed the reshape of the breast cancer classification system through the assessment of its diversity at the molecular level. The simultaneous expression analysis of thousands of genes in a single experiment using cDNA microarrays was crucial for the identification of distinct molecular tumor classes. Diverse studies showed that consistent variations in growth rate, activity of certain signaling pathways and tumors composition could be reflected in the expression of certain genes and also in the clinical outcome [23-33]. Although different studies employ different nomenclature or number of categories, breast cancer molecular classification comprises three main subtypes: i) ER positive or luminal-like subtype, which expresses genes that encode typical proteins of luminal epithelial cells; ii) HER2 overexpressing subtype, associated with the gene

amplification of the HER2 proto-oncogene; and iii) basal-like breast carcinomas [34].

The luminal molecular subtype is the most common subtype, accounting for approximately two-thirds of all breast cancers and is characterized by expression of ER, PR and ER responsive genes and other genes that encode typical proteins of luminal epithelial cells [35]. This group can be further classified into luminal-A and luminal-B subtypes, with luminal-A representing the majority of all breast cancer cases [36]. The main differences between the luminal subgroups rely on the increased expression of proliferation-related genes in luminal-B breast carcinomas and decreased expression of ER-related genes [23, 37]. Moreover, luminal-B tumors are usually HER2-positive (up to 6% are negative for both HER2 and ER) and present a worse prognostic and higher relapse rates than luminal-A breast cancers [20, 34, 36]. HER2 overexpressing subtype comprises tumors characterized by high expression of the HER2 gene and other genes associated with the HER2 pathway and are usually negative or express lower levels of ER [38]. Representing about 15-20% of breast cancer subtypes, these tumors have high proliferation rates and display poor prognosis [36]. Basal-like breast carcinomas, which include some transcript characteristics found in basal cells and others related with a subset of normal luminal cells, represent 10-20% of all breast cancer cases [39]. This tumor subtype is more aggressive than other subtypes, characterized by a high proliferation rate, high histological grade and poor prognosis [40]. The terms basal-like and triple negative breast cancer (TNBC) are often used interchangeably, however the term basal-like subtype is derived from gene expression and microarray analysis, and TNBC from immunohistochemical classification and thus, is used in the clinical practice [41].

Triple negative breast cancers (TNBC) are invasive breast cancers which lack the expression of ER, PR and HER2 overexpression/HER2 gene amplification, and represent 80% of all base-like breast carcinomas [39, 42]. This group is highly heterogeneous, with complex genomes and high levels of genetic instability, which results in elevated rates of relapses and poor clinical outcome [43, 44]. TNBC is often diagnosed at a younger age and requires adjuvant chemotherapy to improve survival [44]. Therefore, the development of new and effective therapeutic strategies for this breast cancer subtype is extremely important, particularly in a scenario of limited therapeutic options.

1.1.3. Breast cancer therapy

Although breast cancer mortality has been decreasing in the last decades, available therapeutic approaches remain insufficient to address clinical challenges. The clinical translation of the molecular mechanisms underlying complex biological events in breast cancer development and progression has proven to be a difficult task. In TNBC, despite major advances in understanding tumor biology, the therapeutic options remained virtually unchanged for the last decade [45].

The establishment of a therapeutic regimen in breast cancer involves a multidisciplinary management plan. Tumor characteristics such as molecular subtype or locoregional tumor load, host conditions (e.g. age, menopausal status, comorbidities), and also the patient preference are key points to establish treatment [46]. Classical primary breast cancer therapies involve a surgical approach, radiotherapy, systemic adjuvant chemotherapy and hormonal therapy. However, each breast cancer subtype has specific recommendations for systemic adjuvant therapies [47]. Luminal like tumors are recommended to be treated with endocrine therapy alone (luminal A) or chemotherapy followed by endocrine therapy (luminal B). Depending on stage, HER2 positive breast cancers can be treated with chemotherapy plus trastuzumab, and endocrine therapy should be added if positive for ER or PgR, or both [47]. TNBC patients do not benefit from endocrine therapy or trastuzumab, due to the lack of targetable features. Chemotherapy is, therefore, the basis of systemic treatment and is recommended to include an anthracycline and a taxane [47, 48]. In patients with known BRCA mutation, platinium-based chemotherapy should be also considered [47]. In early-stage breast cancer, or in patients for whom surgery is temporarily contraindicated, anthracycline and taxane-based neoadjuvant chemotherapy results in higher rates of pathologic complete response in TNBC and improves survival outcomes [49]. Nevertheless, TNBC remains associated with a higher risk of early relapse, with a decrease in survival during the first 3-5 years after diagnosis, high rates of metastases and poorer overall survival compared to other subtypes [50-54]. Moreover, patients undergoing chemotherapy regimens often experience dreadful short- and long-term side-effects [55]. Hence, the disclosure of actionable targets is a key aspect for the development of new targeted therapies for TNBC [56, 57].

1.2. Natural products in anticancer therapy

Natural products have historically driven pharmaceutical industry into discovery of new drugs, although their use as lead compounds has declined in the last two-three decades, mainly due to limited compatibility with the high throughput screening and fragment-based approaches used in pharmaceutical companies [58]. Indeed, isolation of suitable quantities from complex natural mixtures is often a major problem and laboratorial synthesis can include a series of laborious and time-consuming steps. In recent years, the interest in these compounds has however re-emerged, partially due to the disappointing results of large screening collections of synthetic molecules, but most of all, due to their broad range of pharmacophores and high degree of stereochemistry. Actually, the number of publications related to the anticancer activity of natural products increased more than 3 times in the last decade (2008-2018) (Figure 1.3).

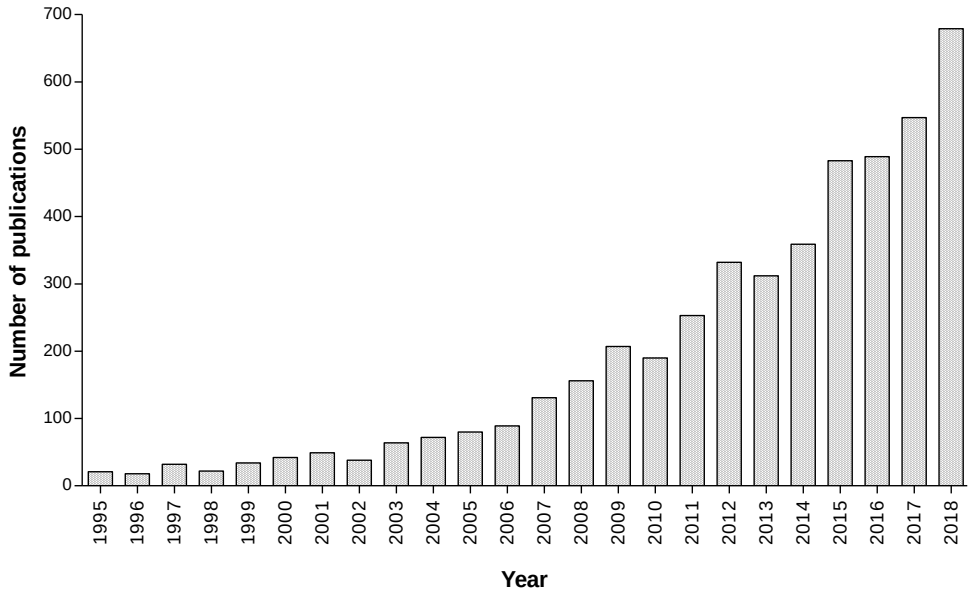

Figure 1.3. Evolution of the number of publications (1995-2018) with the keywords in search topics “anticancer” and “natural products” of Web of Science (2019 October).

Such high structural diversity, together with remarkable biological activities and well-known bioavailability and tolerability (as many are dietary components), make plant-derived natural compounds exquisitely suitable candidates for development of novel therapeutic agents. The establishment of natural products-inspired libraries may allow the transposition of significant characteristics to more adaptable synthetic molecules. Furthermore, novel bioinformatics approaches are providing new tools to predict natural products molecular targets, turning drug discovery from natural products a more efficient process [59, 60]. In cancer

chemotherapy field, natural product-inspired drugs represent a considerable number of anti-tumor agents in the market [61]. Also, several plant-derived compounds are being extensively studied for their anticancer activity in a broad range of cancer models, of which some have reached clinical trials [62]. One promising advantage is that such compounds could be used *per se*, or combined with standard therapies, which can potentially reduce undesired side-effects. Additionally, many plant-derived molecules have been shown to modulate diverse pathways involved in carcinogenic processes, hitting multiple targets and offering increased chances of success.

Diverse plant-natural compounds have reached clinical trials for breast cancer with promising results (e.g. [63-65]). Taxol is a remarkable example of a successful cancer drug isolated in 1966 from *Taxus brevifolia* bark, and currently used in breast cancer treatment [66]. Several new taxane formulations have been developed since approval in 1992 by the Food and Drug Administration (FDA) and these compounds continue to be essential in the treatment of several malignancies [67]. Taxanes are microtubule-stabilizing agents that function primarily by interfering with spindle microtubule dynamics causing cell cycle arrest and subsequently apoptosis. In TNBC, international guidelines recommend the use of taxanes in any setting of the disease [68]. Therefore, plant-derived compounds could represent valuable starting points for the development and discovery of more selective and efficient breast cancer therapies.

1.3. Triterpenic acids (TAs)

Isoprenoids represent one of the largest classes of phytochemicals in the plant kingdom [69], which can also be produced by some animals and microbial species [70, 71]. In the literature, the terms “terpene”, “isoprenoid” and “terpenoid” are frequently used interchangeably, and encompass the entire class derived from the five-carbon precursors isopentenyl pyrophosphate (IPP), and its isomer dimethylallyl diphosphate (DMAPP) [72]. In plants, isoprenoids are secondary metabolites produced in flowers, fruits or roots, and act as important mediators on the defense from insects, pathogens or other plants [73]. Isoprenoids have a vast structural and chemical diversity [69], being generally classified according to the number of five-carbon building blocks into monoterpenoids (C10), sesquiterpenoids (C15), diterpenoids (C20), triterpenoids (C30) and tetraterpenoids (C40) [74].

Triterpenoids are one of the most numerous and diverse groups of plant secondary metabolites. These compounds are ubiquitously distributed and include cyclic and acyclic 30-carbon precursors like squalenes, lanostanes, fusidanes, dammaranes, euphanes, lupanes, oleananes, ursanes, hopanes, tetranortriterpenoids, quassinoids, among others [75, 76]. Most of these compounds are merged 6-6-6-5 tetracyclic, 6-6-6-6-5 or 6-6-6-6-6 pentacyclic structures, although acyclic, monocyclic, bicyclic, tricyclic and hexacyclic triterpenoids have also been isolated from other sources [77]. Triterpenoids, particularly those with lupane, ursane and oleanane backbone structures, such as betulinic (3β-hydroxy-lup-20-en-28-oic, BA), ursolic (3β-hydroxyurs-12-en-28-oic, UA) and oleanolic (3β-hydroxyolean-12-en-28-oic, OA) acids (Figure 1.4), have attracted high interest particularly in regard to their pharmacological potential [78-81]. Even though these acids are triterpenoid structures, the "triterpenic acid" (TA) denomination is most often used throughout the literature; for that reason, it will be adopted in the present work.

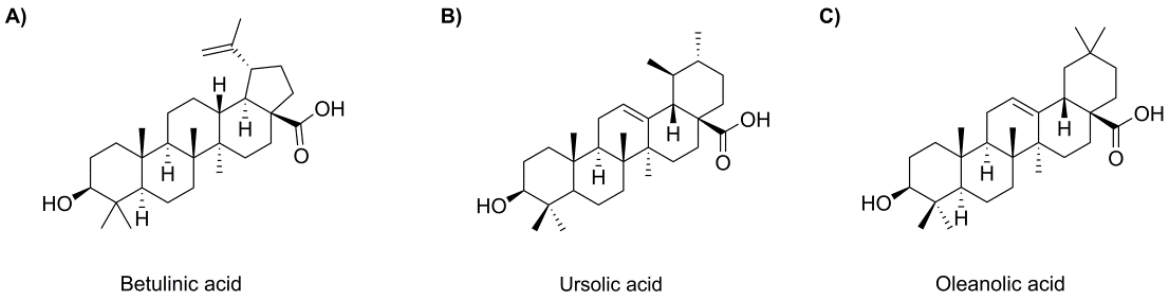

Figure 1.4. Chemical structures of some of the most common triterpenic acids from plants: betulinic (A), ursolic (B) and oleanolic (C) acids.

1.3.1. *Eucalyptus* ssp. bark as a natural source of TAs

Eucalyptus species are the most important fiber source for pulp and paper production in Southwest Europe [82]. These species have high tolerance to environmental stress and fast growth in short rotation plantations, tolerate a wide range of soils and have excellent pulping and bleaching abilities [83]. Although native to Australia, *Eucalyptus* spp. have been introduced in more than 90 countries, with plantations occupying, in 2008, around 19 million hectares worldwide [83, 84]. In Portugal, *Eucalyptus* spp. were introduced in the second half of the 19th century as an ornamental tree, but due to their characteristics, they have become the main planted pulpwood species [85, 86]. In fact, *Eucalyptus* spp. are

predominant in terms of Portuguese forest area (about 844.000 ha) [87]. The dominant species in Portugal is *Eucalyptus globulus*, however there is an increasing quantity of *Eucalyptus nitens* [88]. *E. nitens* (Figure 1.5) adapts better to colder climate conditions, has a fast development rate, and is also more resistant to pests and diseases [89].

The agro-industrial exploitation of *Eucalyptus* wood for pulp and paper production generates large amounts of biomass residues, particularly bark [90-92]. *Eucalyptus* spp. barks are removed from the tree logs before processing and represent 11-15% of the stem dry, which corresponds to 20 tons of product for each 100 tons of produced pulp [90, 93]. In Portugal, bark residues are used for energy production by the pulp and paper industry, indeed, in 2016, these residues represented about 10% of the total energy consumed [86]. However, bark differs chemically from wood due to the higher proportion of ash and extractives, which could be directed to further valorization with the extraction of high-value components prior to burn [94].

Eucalyptus spp. outer bark is an abundant source of several triterpenoids, mostly TAs. In particular, the outer barks of *Eucalyptus* species generally used in plantations from temperate and Mediterranean regions (particularly *E.globulus* and *E. nitens*) present remarkably high TA content [91, 92]. The outer bark of *E. nitens* contains 21.6 g/Kg of TAs, mainly from the lupane (betulinic acid, 6.6 g/kg of outer bark fraction) and oleanane-type acids (oleanolic acid together with 3-acetyloleanolic acid) [91]. This group of compounds is very high priced in the market, and their availability is still quite limited. Therefore, the use of agroforestry and food industry biomass residues, available in large quantities and with low commercial value, as a source of TAs emerges as an exceptional opportunity. Moreover, the development of new applications for these compounds, namely in nutraceutical or pharmaceutical domains, will represent an important contribution for the valorization of this natural resource.

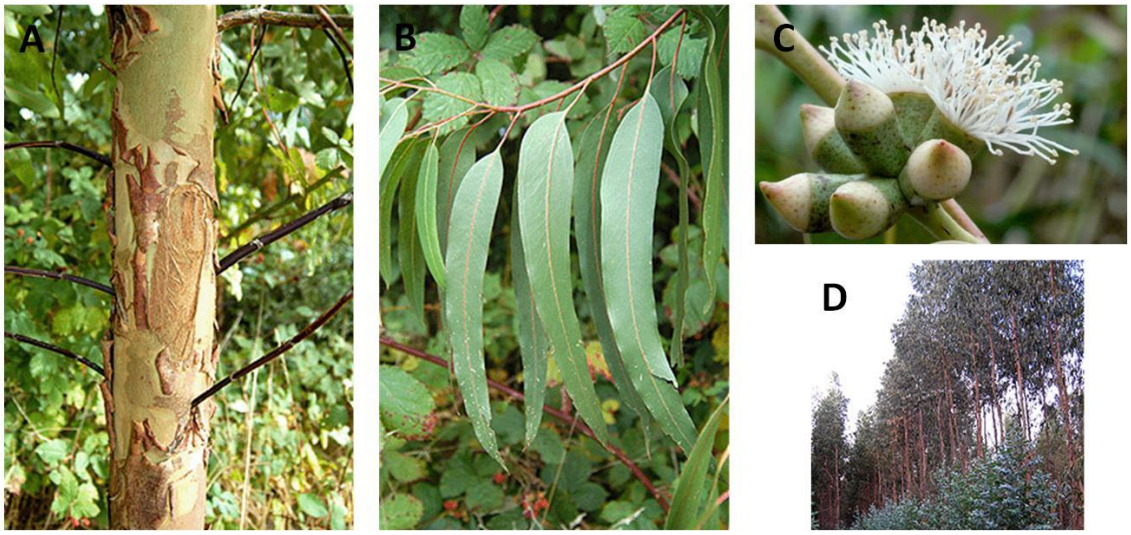

Figure 1.5. *Eucalyptus nitens* tree: (A) bark (B) leaves (C) flowers and (D) overall aspect. Source: New Zealand Plant Conservation Network website and Virginia Tech Department of Forest Resources and Environmental Conservation.

1.3.2. TAs and breast cancer treatment

Over the past 20 years, numerous studies have highlighted the antitumoral potential of triterpenoids. Particularly, the lupane, ursane and oleanane-type structures have been associated to a broad spectrum of pharmacological activities including antioxidant, pro-apoptotic, antiangiogenic and anti-inflammatory, sparking renewed interest with regard to their potential in cancer treatment [95-97]. Notably, some pentacyclic triterpenoids, or their semi-synthetic derivatives, have made their way into clinical trials, although the underlying molecular mechanisms in cancer cells are still object of study [98]. Current knowledge on the biological activity in breast cancer of the two TAs studied in this thesis (betulinic and ursolic acids) is briefly summarized below.

Betulinic Acid (BA)

The effect of BA on breast cancer cells was tested *in vitro* in several breast cancer cell lines (MCF7, SKBR3, MDA-MB-231, MDL13E, BT474, T47D, BT483, BT549 and ZR-75-1), having shown strong ability to decrease cell viability [99, 100]. Subsequent studies further demonstrated that BA could suppress proliferation and migration in diverse breast cancer cell lines in a dose-dependent manner [101-116]. *In vivo*, BA treatment applied to murine models of breast cancer produced a decrease in tumor size and weight [103, 104, 114, 116, 117]. Several studies showed that BA induces apoptosis in breast cancer, both *in vitro* and *in vivo*, via

intrinsic pathway [102-105, 109, 110, 113-115]. BA treatment has also been reported to arrest cell cycle in G2/M phase in MDA-MB-231 breast cancer cells and to significantly facilitate G2/M arrest induced by taxol in MDA-MB-231 and MCF-7 cells [104, 114]. Other studies revealed that BA direct targets include topoisomerase, specificity protein transcription factors (Sp), estrogen signaling, vascular endothelial growth factor receptor (VEGFR) and matrix metalloproteinases (MMPs) [101, 102, 104, 107, 116, 118].

Ursolic Acid (UA)

The potent antiproliferative effect of UA towards several breast cancer cell lines has been well-documented [99, 112, 119-129]. Other studies have reported the ability of this TA to decrease tumor size and weight in murine breast cancer models [130, 131]. Moreover, both intrinsic and extrinsic apoptotic pathways seem to be induced by UA [121, 124, 127, 131, 132]. UA also caused G0/G1 cell cycle arrest in both *in vitro* and *in vivo* models of breast cancer [119, 129, 131]. Other reported targets of UA in breast cancer include the Akt pathway, glucocorticoid receptor, estrogen signaling, breast cancer resistance protein (BCRP/ABCG2), vascular endothelial growth factor (VEGF) and matrix MMPs [107, 121, 123, 129, 131, 133].

1.4. Breast cancer metabolism

The continuous evolution of cell biology research has expanded our understanding of cancer as a complex and diverse set of diseases. Nevertheless, a number of common traits that support tumor formation, growth and metastasis have been described, as thoroughly revisited by Hanahan & Weinberg [134, 135]. Particularly, it has become evident that tumor initiation and progression strongly rely on the reprogramming of cell metabolism, mainly to support increased needs for ATP generation and macromolecules biosynthesis, as well as to maintain a tight control of redox balance.

The initial observation of Otto Warburg describing the ability of cancer cells to carry out aerobic glycolysis, a phenomenon known as the “Warburg effect” [136], is currently recognized as a small part of all metabolic rearrangements undertaken

by cells in oncogenesis. Indeed, tumor cells have been found to display a range of alterations in intracellular metabolic pathways and in metabolic interactions with the microenvironment, to opportunistically modulate nutrient uptake and to drive changes in gene regulation [137]. Differences between the metabolic profile of breast cancer cells and normal breast tissues have been demonstrated in numerous studies [138-140]. As summarized in Figure 1.6, breast cancer typically remodel crucial pathways of their metabolic network, such as glycolysis, the TCA cycle, amino acid, nucleotide and/or lipid metabolisms [141]. Also, specific metabolic dysregulations in breast cancer are thought to reflect tumor heterogeneity [142], potentially giving insight into the underlying causes of this heterogeneity and/or novel therapeutic targets.

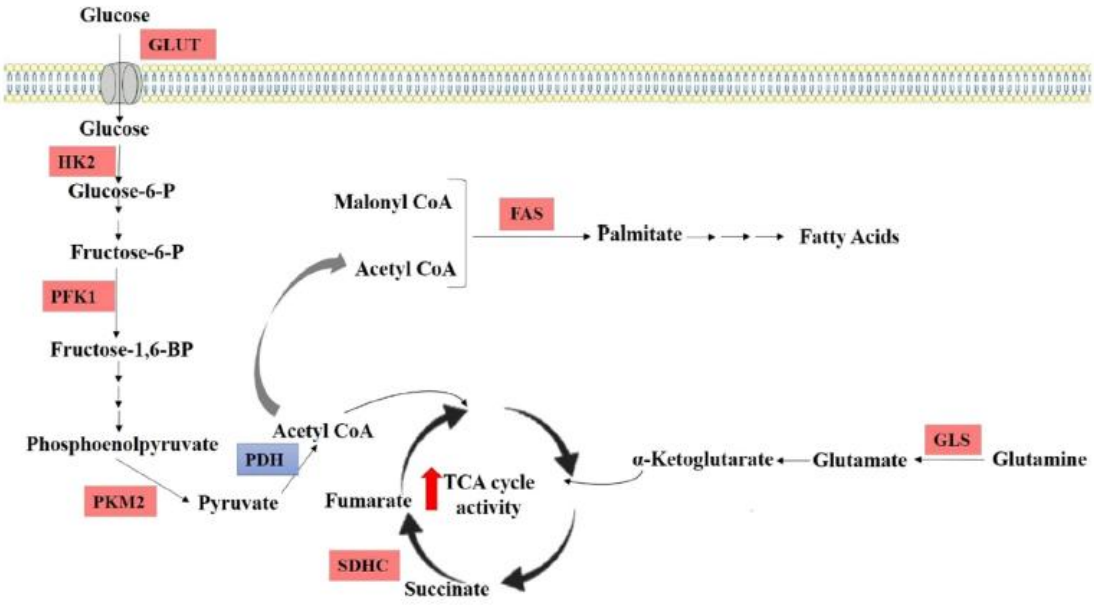

Figure 1.6. Overview of metabolic reprogramming in breast cancer cells. Main changes in glucose metabolism comprise overexpression of the glucose transporter (GLUT) and of the glycolytic enzymes hexokinase 2 (HK2), phosphofructokinase 1 (PFK1) and pyruvate kinase M2 (PKM2); TCA cycle alterations include decreased expression of the enzyme pyruvate dehydrogenase (PDH) and overexpression of the succinate dehydrogenase complex (SDHC); other metabolic shifts in relation to normal cell metabolism comprise increased glutamine consumption, together with increased expression of glutaminase (GLS), increased lipid synthesis and expression/activity of fatty acid synthase (FAS). The proteins overexpressed/decreased in BC are highlighted in red/blue, respectively. Reprinted from Dias *et al*. [141].

1.4.1. Overview of altered metabolic pathways and targets in breast cancer

Glucose is the most abundant nutrient in blood and the primary substrate for mammalian cells' metabolism [137]. The transport of glucose across the cell membrane is mediated by two classes of hexose transporters: the sodium-dependent glucose co-transporters (SGLTs) and the family of glucose transporters (GLUTs). GLUTs are part of the major facilitator superfamily (MFS) and despite their many isoforms, they possess a similar transmembrane anatomy [143, 144]. These membrane transporters isoforms differ mainly on substrate recognition and most have a tissue-specific distribution. The expression of each GLUT is dependent on the tissue metabolic requirements and also on hormonal regulation [145]. Class I facilitative glucose transporters encompass the classical transporters GLUT1-4 [146]. GLUT1 is the most widely distributed isoform, and is frequently overexpressed in cancer, including in breast cancer, being correlated with poor overall survival [147]. Furthermore, overexpression of GLUT1 in TNBC has been associated with a more glycolytic profile [148]. Poorly differentiated breast tumors (grade 2 and 3) also presented significantly higher expression of GLUT1 and GLUT 3 mRNA and protein levels, compared to well differentiated tumors (grade 1) [149].

While differentiated non-proliferating cells obtain most of their energy through oxidative phosphorylation in the mitochondria, tumor cells typically display intensified glycolytic flux and lactate production, which constitute an advantage for rapid energy generation, biomass accumulation, redox maintenance and facilitation of tumor invasion [150, 151]. Enhanced glygolytic activity in breast cancer has been observed both in human cancer tissues and in tumor cell lines [138, 152-154].

Several isoforms of rate-limiting glycolytic enzymes have been found differentially expressed in tumor cells. Among hexokinases (HK), which phosphorylate glucose to glucose-6-phosphate within the first committed (irreversible) step of glycolysis, HK2 has been reported to be highly expressed in malignant cells, in contrast with HK1, abundantly expressed in normal tissues [155, 156]. Immunohistochemical study of untreated primary breast cancer tissues revealed a wide expression of HK2 [157, 158]. Furthermore, HK2 was found to be fundamental in tumor initiation and maintenance in mouse models of HER2-driven breast cancer, while HK1 expression did not change significantly [159]. Recently, HK2 was found to be upregulated in human breast cancer tissues, and Proviral

Insertion in Murine Lymphomas 2 (PIM2) was indicated as a novel regulator of HK2 [160].

Another important glycolytic checkpoint is the conversion of fructose 6-phosphate to fructose 1,6-bisphosphate by phosphofructokinase (PFK). PFK can be activated by AMP/ADP and inhibited by ATP, citrate, long-chain fatty acids and lactate. PFK1 can be activated by oncogenes or the hypoxia-inducible factor (HIF)-1α, and its activity has been reported to be increased in malignant cells [161]. Moreover, triggering Akt phosphorylation could potentially release PFK from ATP inhibition, leading to enzyme activation [162]. On the other hand, fructose-2,6-bisphosphate is the most effective allosteric activator of PFK, suggesting upregulation of enzyme activity to be dependent on high levels of fructose-2,6-bisphosphate in cancer cells [163]. Hennipman and colleagues reported for the first time the increase in PFK activity in breast cancer tissues, in comparison to benign breast disease and normal breast tissues [164]. Later, in breast cancer tissues, PFK1 was found to be in an actin-enriched fraction and its activity was significantly increased compared with control tissues [165]. PFK-L expression, an isoform of PFK1, was also shown to be correlated with aggressiveness and glycolytic efficiency in breast cancer cells [166]. Moreover, the total PFK1 protein levels were found to be increased, and this was accompanied by differential PFK1 isoenzyme expression patterns between human breast cancer and paracancer tissues [167].

The production and degradation of fructose-2,6-bisphosphate is, in turn, supported by a family of bifunctional enzymes, the 6-phosphofructo-2-kinase/fructose-2,6-bisphosphatases (PFKFB), more specifically PFKFB3. PFKFB3 is often overexpressed in human cancers and has an important role in cell proliferation through regulation of cell cycle [163]. Immunohistochemistry analysis revealed that PFKFB3 levels were upregulated in human HER2+ breast cancer and that its inhibition restrained glucose metabolism and the growth of HER2-driven breast tumors [168]. Recently, immunohistochemistry confirmed that PFKFB3 was highly expressed in breast cancer tissues and this elevated expression correlated with poor overall survival [169]. The proliferation, migration and invasion of MDA-MB-231 and MDA-MB-468 breast cancer cells were inhibited by the suppression of PFKFB3. Moreover, suppression of this enzyme resulted in restrained breast tumor xenograft growth in nude mice [169].

In the last committed step of glycolysis, pyruvate kinases (PK) catalyze the conversion of phosphoenolpyruvate (PEP) to pyruvate, with concomitant production

of ATP. There are four mammalian PK isoenzymes - PKL, PKR, PKM1 and PKM2 - with distinctive tissue expression. PKM1 and PKM2 are encoded by the same gene through alternative splicing, and their relative expression in cells relates to the preference for either glycolysis or oxidative phosphorylation [170]. While normal adult cells preferentially express PKM1, rapid proliferating tumor cells and non-malignant proliferating cells abundantly express PKM2 [171]. Accumulating evidence suggests that elevated PKM2 expression in breast cancer is associated with worse survival in breast cancer patients and correlates with lymph node metastasis [172].

Other branches diverting from glycolysis and implicated in cancer are the serine biosynthesis pathway, through which non-essential amino acids are generated, and the subsequent one-carbon metabolism cycle, required for methylation reactions, as well as for purine and glutathione (GSH) biosynthesis [173]. Some tumor cells show amplification or overexpression of phosphoglycerate dehydrogenase (PHGDH), which catalyzes the first step in the serine biosynthesis pathway. Hence, its inhibition could selectively target tumor cells with upregulated *de novo* serine biosynthesis [174]. In ER-negative breast cancers, PHGDH protein levels were found to be elevated in 70% of analyzed samples [175]. Moreover, ER-negative human breast cancer cells lines were also reported to overexpress PHGDH [176]. In human breast tissues and cell lines, high PHGDH expression was also associated with TNBC [177, 178].

In addition to glucose, glutamine is another crucially important substrate for tumor cell growth and metabolism. This non-essential amino acid not only supplies nitrogen for the biosynthesis of other amino acids, nucleic acids and hexosamines, as it is metabolized *via* the tricarboxylic acid (TCA) cycle, replenishing depleted intermediates and contributing to energy generation [151, 179]. Furthermore, glutamine is an alternative carbon donor to lipid synthesis, *via* reductive carboxylation to citrate, and is involved in the synthesis of GSH, an important antioxidant in cells [179]. Breast cancer molecular subtypes have different glutamine requirements: luminal-type cells are more glutamine independent, while TNBC cells lines are highly dependent on glutamine for growth and survival, being susceptible to glutamine-targeting therapeutics [180-182]. Hence, glutamine metabolism is an appealing therapeutic target, and drug strategies are being specially directed to the inhibition of glutaminase, the enzyme responsible for the conversion of glutamine to glutamate [183]. Immunohistochemical analysis of breast

tumor tissues revealed that glutamine metabolism-related proteins, including glutaminase are differentially expressed according to breast cancer molecular subtype [184]. Particularly, HER2-type breast cancer exhibited the highest glutamine metabolic activity, with the exception of tumoral glutaminase 1 expression, which was higher in TNBC than in other molecular subtypes [184]. Moreover, in TNBC tumor tissues, glutaminase expression was associated with poor disease-free survival in TNBC patients presenting lymph node metastasis and high levels of tumor-infiltrating lymphocytes [185]. Recently, splice variants of the glutaminase gene, kidney type glutaminase (KGA) and glutaminase C (GAC) were described as essential for TNBC survival and proliferation, besides being necessary for TNBC xenografts growth [186].

Promotion of pyruvate mitochondrial oxidation, modulation of TCA cycle enzymes and interference with respiratory chain complexes have also been exploited as possible therapeutic targets [183]. Actually, in breast cancer tumors and cell lines, mutations in mitochondrial DNA (mtDNA), including those affecting respiratory complex I and OXPHOS, were already observed [187, 188]. The pyruvate dehydrogenase complex (PDC), which is responsible for converting pyruvate into acetyl-CoA (required for the TCA cycle, *de novo* lipogenesis and protein acetylation), is negatively regulated by pyruvate dehydrogenase kinases (PDKs). These enzymes are typically overexpressed in cancer cells, often as a result of HIF activation, partially explaining their diminished mitochondrial function [189, 190]. Interestingly, pyruvate dehydrogenase protein X (PDHX), a structural component of PDC, was found to have lower expression levels in breast tumor samples, and was associated with low patient survival [191].

TCA cycle reactions are catalyzed by multiple enzymes which can either be mutated or deregulated in malignant tissues. Indeed, some drugs targeting TCA cycle enzymes, such as aconitase (AH), isocitrate dehydrogenase (IDH), fumarate hydratase (FH) or succinate dehydrogenase (SDH) are currently under investigation [192]. In human breast cancer tissues, SDHA (a subunit of SDH complex) presented high-level expression in HER2 subtype breast cancers and lower expression levels in luminal A subtype [193]. In BRCA1-transfected TNBC cells, overexpression of SDHC gene was observed with concomitant succinate decrease, resulting in glycolysis downregulation (by HIF1α degradation) and increased ATP production (as a consequence of TCA cycle and OXPHOS activation) [194].

Rapidly proliferating cells have increased demand for lipids and steroids, in order to sustain the production of phospholipid bilayers and signaling molecules. Increased fatty acid (FA) synthesis and upregulated membrane lipids were observed in breast cancer tissues [195]. Furthermore, decreased levels of free FA were also detected, suggesting newly synthetized FA to be promptly employed in membrane phospholipids production [138]. The balance between lipogenesis and FA utilization seems to be dependent on tumor subtypes, as shown in breast cancer tissues and cell lines [196, 197]. MDA-MB-231 TNBC cells appear to preferentially incorporate FA into storage triacylglycerols, while luminal cells divert FA into mitochondrial oxidation [197]. Fatty acid synthase (FAS) is a key enzyme in lipogenesis, which catalyzes the terminal steps of *de novo* fatty acid synthesis [198]. Many cancer cells have shown overexpression of this enzyme, hence several inhibitors have been developed, and their efficacy assessed in preclinical models [199]. In breast cancer tissues and cells, FAS expression was higher in the HER2-positive subtype and lower in TNBC [178, 200].

Alterations in choline metabolism generally accompany breast cancer progression, in association with phospholipid metabolism [142, 201]. Several studies have reported an increase of choline metabolites in breast cancer tumors (reviewed in [202, 203]). Moreover, increased levels of phosphocholine were associated with ER- breast tumours of histological grade 3 [195]. Choline kinase α (ChoK-α), which catalyzes the conversion of choline to phosphocholine, has been held responsible for the elevated phosphocholine levels in breast cancer [201]. Patient-derived tumor breast specimens revealed a high expression and activity of this enzyme in 39% of tumoral samples [204]. Furthermore, increased ChoK-α activity was found to be associated with ER-negative breast tumors [204], and amplification of its expression was correlated with invasion and drug resistance in breast cancer cells [205].

1.4.2. Metabolic modulation of cancer cells by TAs and other isoprenoids

Targeting tumor cell metabolism to achieve therapeutic benefit in cancer treatment has been continuously harnessing increased interest. From the discovery and clinical success of anti-folate drugs in the early twentieth century, to the nucleoside analogues a few years later, antimetabolites have been used for

decades in the treatment of several types of cancer [206, 207]. Their considerable success offered the proof-of-concept for this type of therapies. Currently, diverse metabolic targets are being exploited, and several metabolism-targeted drugs are being tested, both in preclinical cancer models and in clinical studies [183, 192, 208-210]. Many plant-derived molecules have been shown to modulate diverse pathways involved in carcinogenic processes, hitting multiple targets and offering increased chances of success. A particular interesting feature is the recognizably strong interconnection between tumor-specific signaling pathways and metabolic adaptations [211]. Hence, significant efforts have been recently conducted to elucidate how plant-derived natural compounds may act as modulators of tumor cell metabolism and, in this way, exert anticancer activity.

The high structural diversity and promising biological activities of plant-derived isoprenoids, including as anticancer drugs, underline their enormous potential for drug discovery. With a view to achieve improved understanding of the role of metabolism in the anticancer activity of plant-derived isoprenoids, several studies have investigated how these compounds affect major energetic and biosynthetic pathways in tumor cells. Table 1.2 and Figure 1.7 offer a concise view of this subject, also reviewed by us in [212], while the main findings obtained for betulinic and ursolic acids (the TAs studied in this thesis) are described in more detail below.

Betulinic acid (BA) has been widely studied for its antitumoral potential in multiple cancer models, but few works have addressed its ability to modulate cellular metabolism. Pandita and colleagues have studied the combination of dietary molecules, such as BA, with gemcitabine, a common chemotherapeutic drug, in pancreatic cancer cells and their impact on a key glycolytic enzyme, PKM2 [213]. The results showed that BA was able to decrease PKM2 protein level in the PANC-1 cell line, although PKM2 activity increased with treatment. On the contrary, PKM2 activity decreased in treated MIA PaCa-2 cells. The combination of BA with gemcitabine produced a similar, enhanced effect, demonstrating that this triterpenoid could effectively potentiate gemcitabine cytotoxicity in human pancreatic cancer cell lines [213]. In a breast cancer cell line (SK-BR-3), BA treatment resulted in decreased PKM2 protein abundance and lactate level [129]. Furthermore, BA decreased the protein levels of HK and PKM2 in the MCF-7 cell line, modulating the glycolytic pathway [129]. Finally, in cervical cancer cells (HeLa cells), BA was shown to inhibit the activity of stearoyl-CoA desaturase (SCD)-1, an

enzyme involved in *de novo* fatty acid synthesis [214]. This resulted in an increased incorporation of saturated fatty acids in cardiolipin, inducing mitochondria to undergo ultrastructural changes and ultimately leading to cell death.

Recent work has addressed the role of ursolic acid (UA) in the glycolytic activity of breast cancer cells [129]. This triterpenic acid could decrease intracellular ATP levels in MCF-7, MDA-MB-231 and SK-BR-3 cells, whereas intracellular lactate decreased only in MCF-7 and SK-BR-3 cells, as compared to untreated controls. The HK2 protein level was found to be lower in MDA-MB-231 and SK-BR-3 cells and the effects observed were attributed to diminished Akt signaling [129]. Previously, an ursolic acid derivative, US597, used in conjunction with 2-DG, was found to target both apoptosis and glycolysis to induce death of hepatocellular carcinoma (HCC) (HepG2) cells [215]. US597 could reduce HK activity, and the combination of the two compounds resulted in synergetic inhibition. Additionally, US597 diminished intracellular ATP levels, and lactate production (this latter change being observed in combination with 2-DG) [215].

In conclusion, plant-derived compounds can offer innovative and effective solutions for the development of new chemotherapeutic drugs targeting cancer cell metabolism. Further understanding of their impact on specific metabolic pathways is therefore an important research line to be pursued. In this respect, the metabolomics approach is particularly relevant, as it can reveal unanticipated metabolic effects and help shedding light into the complex mechanisms through which natural compounds interact with tumor cells.

Table 1.2. Effects of isoprenoids on energetic and biosynthetic metabolic pathways of different human tumor cells.

Compound	Tumor cells	Metabolic effects	Reference
Andrographolide	Leukemia (MV-4-11, NB4)	↓FAS, acetyl-CoA carboxylase 1 (ACC1) protein level ↑ Stromal interaction molecule 1 (STIM1) protein level ↓ Several fatty acid contents (oleic acid, stearic acid, palmitoleic acid, palmitic acid)	[216]
Betulinic acid	Breast (SK-BR-3)	↓ Lactate production ↓PKM2 protein level	[129]
	Breast (MCF-7)	↓ HK2, PKM2 protein level	
	Cervical (HeLa cells)	↓ SCD-1 activity ↑ Incorporation of saturated fatty acids in cardiolipin	[214]
	Pancreatic (MIA PaCa-2)	↓ PKM2 activity	[213]
	Pancreatic (PANC-1)	↓PKM2 protein level ↑PKM2 activity	
Cacalol	Breast (MCF-7, MDA-MB-231)	↓FAS mRNA level ↓FAS protein level	[217]
Celastrol	Cervical (HeLa cells)	Glycolysis Citrate cycle Amino acid metabolism Protein biosynthesis	[218]
Artimisinin derivatives *Dihydroartemisinin*	Lung (A549, PC-9)	↓ GLUT1 protein level ↓ Glucose uptake; ATP generation, lactate production	[219]
	Lung (H1975)	Inhibits GLUT1 translocation to cytoplasmatic membrane ↓ Glucose uptake, ATP generation, lactate production	[220]
Artesunate	Colon (HCT-116)	↓ Acyl-CoA Synthetase Long Chain Family Member 5 (ACSL5), 3-hydroxyacyl-CoA dehydrogenase (HADH), FAS protein levels	[221]
Galbanic acid	Lung (A549)	↓ GLUT1 mRNA level ↓ Enolase 1 (ENO1) mRNA level	[222]
	Ovarian (NIH:OVCAR-3)	↓ GLUT1 mRNA level ↓ ENO1 mRNA level	
Geraniol	Breast (MCF-7)	↓ 3-hydroxy-3-methylglutaryl-CoA reductase (HMGCR) activity	[223]
	HCC (HepG2)	↓ HMGCR activity	[224]
	HCC (HepG2)	↓ HMGCR mRNA level and protein level Fatty acid metabolism ↓Mevalonate pathway ↓ PC synthesis	[225]
	Prostate (PC-3)	↑ p-ACC protein level	[226]
Geranylgeranoic acid	HCC (Huh-7)	↑ Fructose 6-phosphate ↓ Fructose 1,6-diphosphate ↑ Spermine ↓ Spermidine	[227]
Ginsenoside 20(S)-Rg3	Ovarian (SK-OV-3, 3AO)	↓ GLUT1 mRNA level ↓ Glucose uptake; lactate production ↓HK2, PKM2 mRNA and protein level ↓ LDH, PDK, PFK mRNA level	[228]

Table 1.2. (cont.)

Compound	Tumor cells	Metabolic effects	Reference
Oleanolic acid	Breast (MCF-7)	↓ Glucose uptake, lactate production	[229, 230]
	Breast (MCF-7)	↑p- ACC1, p-HMGCR protein level ↓FAS protein level ↓ *de novo* fatty acid synthesis	[230]
	High salt induced breast cancer cells (MDA-MB-231)	↓ Glucose uptake; lactate production ↓ HK, PKM2, LDHA protein level ↓PK activity	[231]
	Prostate (PC-3)	↓ PKM2 protein level ↑ PKM1 protein level ↑ PK activity	[229]
	Prostate (PC-3)	↑p- ACC1, p-HMGCR protein level ↓FAS protein level ↓ *de novo* Fatty acid synthesis	[230]
Oleanolic acid derivative *CDDO-Im*	Liposarcoma cells (LiSa-2)	↓FAS mRNA level ↓FAS protein level ↓ *de novo* fatty acid synthesis	[232]
Oridonin	Colon (SW480)	↓ GLUT1, Monocarboxylate transporter 1 (MCT1) mRNA and protein level ↓ Glucose uptake; lactate export ↑ ATP generation	[233]
	Colon (SW480, SW620)	↓FAS mRNA level ↓FAS protein level ↓ Palmitic acid, stearic acid	[234]
	Uveal melanoma (OCM-1, MUM2B)	↓FAS protein level	[235]
Pomolic Acid	Breast (MCF-7)	↓FAS protein level ↑ p-ACC1 protein level ↓ *de novo* Fatty acid synthesis	[236]
Pristimerin	Breast (SK-BR-3)	↓FAS protein level ↓FAS activity	[237]
Pseudolaric acid B	Lung (A549)	↑ GLUT1 protein level ↑ Glucose uptake, ATP generation, lactate production ↑HK-2 protein level	[238]
Tanshinone IIA	Gastric (AGS)	↓ Glucose-6-phosphate isomerase (GPI), LDHB, Malate dehydrogenase 1 (MDH1) ↑ Phosphoenolpyruvate carboxykinase 2	[239]
	Esophageal (Ec109)	↓PKM2 mRNA and protein level	[240]
Tanshinone IIA derivative *Acetyltanshinone IIA*	Breast cancer cells (MDA-MB-453, SK-BR-3)	↓FAS, p- ACL protein level ↑ p-ACC protein level	[241]
Thymoquinone	Pancreatic (MIA PaCa-2)	↑PKM2 activity	[213]
	Pancreatic (PANC-1)	↓PKM2 protein level ↓PKM2 activity	
Ursolic acid	Breast (MCF-7, MDA-MB-231, SK-BR-3)	↓ ATP generation ↓ PKM2	[129]
	Breast (MCF-7, SK-BR-3)	↓ lactate production	
	Breast (MDA-MB-231, SK-BR-3)	↓ HK2 protein level	
Ursolic acid derivative *US597*	HCC (HepG2)	↓ HK activity ↓ ATP generation	[215]

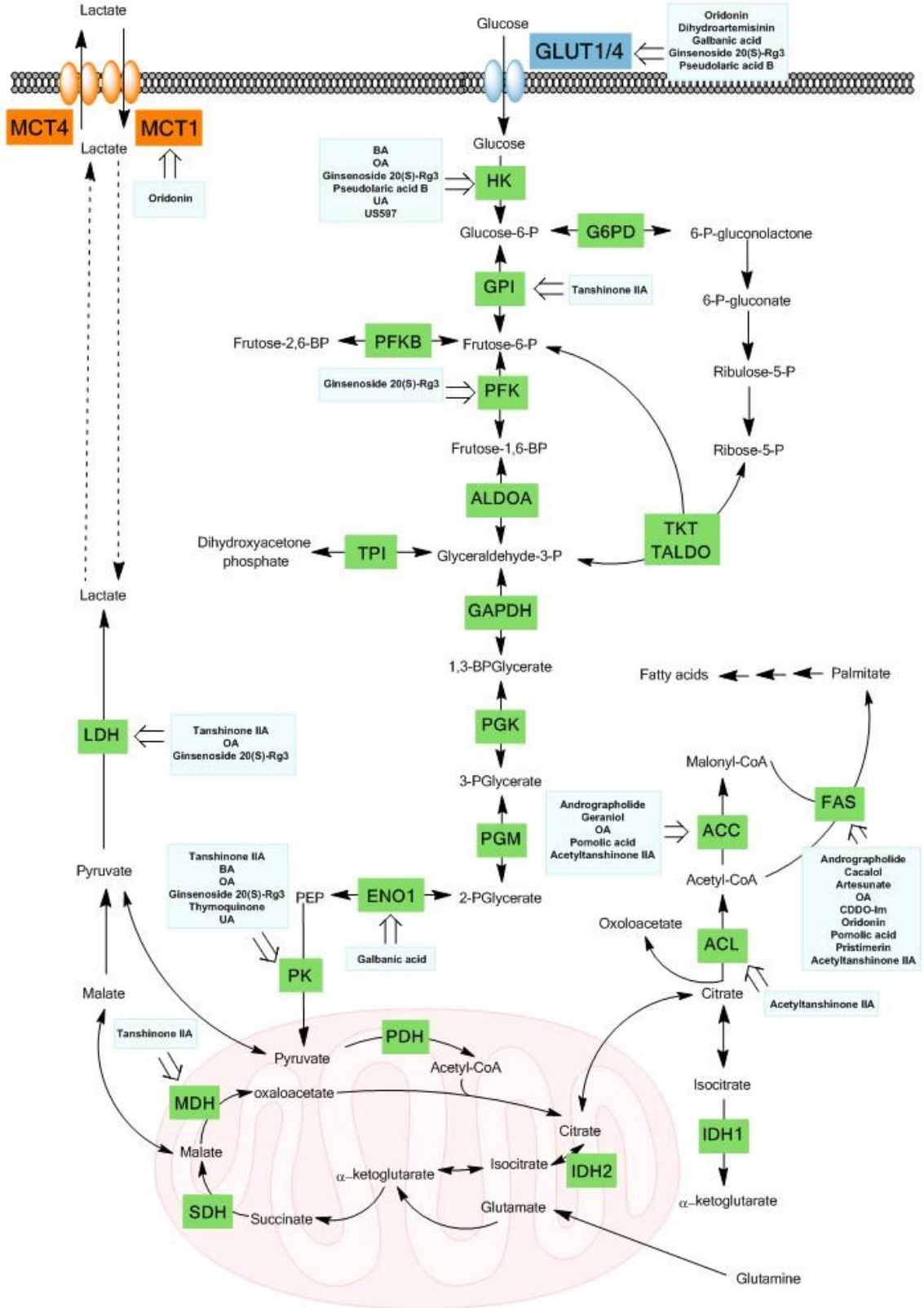

Figure 1.7. Schematic overview of main metabolic targets of isoprenoids in tumor cells (as listed in Table 1.2). Adapted from Guerra *et al.* [212].

1.5. Metabolomics in breast cancer research

Metabolomics can be regarded as the systematic measurement of low molecular weight compounds (up to 2 kDa) which are involved in chemical reactions taking place in biological systems and/or that arise from xenobiotic, dietary or other exogenous sources [242]. The set of metabolites of a certain biological matrix (cells, tissues, biofluids, or whole organisms), designated as the metabolome, is closely interconnected with the genome and the proteome levels, acting both as downstream products and modulators of their activity [243]. As such, variations in the cellular metabolome closely reflect cells phenotypic and functional features and represent a useful window into their biochemical behavior. The field of cancer research is one where metabolomics has been more intensely applied to address multiple challenges, such as identifying new disease biomarkers, monitoring treatment responses or supporting mechanistic understanding of cancer-related processes [244]. The metabolomics study of breast cancer includes an extensive body of literature, recently reviewed by MacCartney *et al*. [245]. The aim of this section, rather than giving a comprehensive view of metabolomics applications in breast cancer research, is to focus on the aspects that are particularly relevant within the scope of this thesis, namely, the metabolic profiling of breast cancer cells and their responses to plant-derived natural compounds.

1.5.1. Overview of the metabolomics approach and methods

The typical metabolomics workflow (Figure 1.8) comprises experimental design, sample collection and treatment, data acquisition, data processing and biological interpretation [242]. The first stage is concerned with formulating the scientific questions that one wants to address and defining the experimental strategy to be used. For instance, it includes choosing between untargeted or targeted metabolomics (the latter being focused on specific metabolites of interest) and selecting appropriate sample matrices together with adequate controls. Sample collection and treatment should then proceed under rigorously established and reproducible protocols in order to minimize unwanted variability. Regarding sample analysis, the two main techniques employed in metabolomics for data acquisition are mass spectrometry (MS)-based methods (usually coupled to a chromatographic technique) and nuclear magnetic resonance (NMR) spectroscopy. By using highly advanced and reliable instrumentation, both techniques are suitable for the analysis

of complex biological samples, each presenting its own advantages and limitations [246]. In fact, they are highly complementary and new hybrid approaches have shown promising potential in metabolome comprehensive studies [247]. MS-based methods are generally more sensitive than NMR, allowing for the detection of metabolites at concentrations in the pM – nM range. On the other hand, this drastically increases the complexity of the data gathered, posing great challenges in terms of metabolite identification and quantification. The greatest downside of NMR is its inherent low sensitivity, which limits the set of detectable metabolites to those present in the µM – mM range. But this technique also offers important advantages, such as the high reproducibility, the non-destructive character and the quantitative nature. Moreover, NMR allows the direct analysis of tissues and cells (without prior extraction procedures), the use of stable isotope labels to trace metabolic pathways and it can even be used *in vivo* [248].

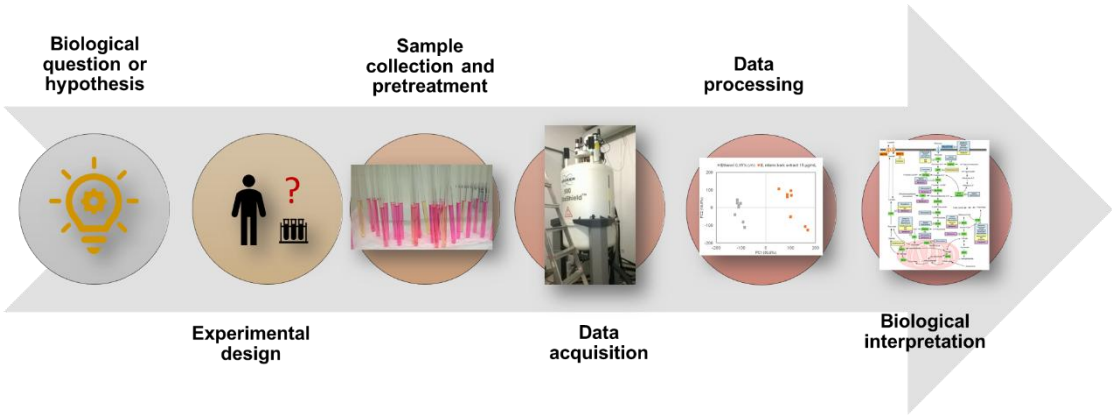

Figure 1.8. Typical metabolomics workflow.

In this thesis, liquid state ^{1}H NMR was the method employed to analyze cell medium supernatants and cell extracts. This technique allows for the detection of virtually all ^{1}H-containing molecules above a certain concentration threshold (> µM) based on the fact that protons are NMR-active nuclei, i.e., they possess a nuclear spin number (I = ½), which confers them magnetic properties useful to observe spectral signals [249]. In particular, under the influence of a static magnetic field (B0) and a second oscillating magnetic field (B_1), protons will absorb energy and then relax back to equilibrium, at a rate dependent on their chemical environment. This generates an oscillating signal in the detection coil - the observed free induction decay (FID), which is then converted into a frequency domain spectrum by Fourier transformation (FT). Nuclei with different chemical environments

(electronic cloud or chemical neighborhood) will resonate at slightly different frequencies, resulting in different positions of the NMR frequency scale. The frequency values are converted into dimensionless values called chemical shifts (δ), expressed in parts per million and calibrated by a signal from a reference compound, to ensure that the chemical shifts are independent of B_0 and data acquired at different field strengths can be directly compared. Moreover, ^{1}H NMR signals present typical splitting patterns (multiplicities) due to interaction with neighboring nuclei via scalar (*J)* coupling. Hence, the ^{1}H NMR spectrum of a molecule can be regarded as a signature of its chemical identity. Another important property of ^{1}H NMR spectra is that the area under a signal is directly proportional to the number of nuclei that originate that signal, making the technique inherently quantitative.

^{1}H NMR spectra of complex biological samples (like cell extracts) typically comprise hundreds of signals arising from several tens of different metabolites. For the unambiguous identification of these metabolites, two-dimensional (2D) NMR methods are required. Briefly, these methods rely on the acquisition of a set of 1D spectra (each FID having a *t*2 acquisition time) under incrementation of a *t*1 evolution delay. The spectrum obtained after performing FT on both *t*1 and *t*2 data is a 2D map, where spectral information is spread into two dimensions [249]. Correlation spectroscopy (COSY) and total correlation spectroscopy (TOCSY) are homonuclear shift-correlation experiments, commonly used in metabolomics studies, where spin-spin through bond correlations appear as cross peaks, symmetrically positioned around the plot diagonal. Hence, in each compound, scalar coupled protons (distanced by 2-3 bonds in the case of COSY or up to 5-6 bonds in the case of TOCSY) are part of a spin system. The detection of spin systems from different compounds helps to resolve and annotate overlapping resonances. The heteronuclear single quantum coherence (HSQC) experiment is also very useful for assignment of complex mixtures, as it provides information on the single bond connectivity between ^{1}H and ^{13}C atoms. Finally, in the *J* resolved (*J*res) experiment, *J*-coupling information is separated from chemical shifts, meaning that the ^{1}H spectrum is presented in the horizontal dimension and the coupling pattern of each signal is displayed in the vertical dimension.

NMR metabolomics typically generates complex datasets that require appropriate data pre-processing procedures and statistical methods, such as multivariate analysis (MVA). These tools are generally applied in order to reduce data complexity, maximize information recovery, discriminate between sample classes and

highlight the variables important for classification [250]. Principal Component Analysis (PCA) is an unsupervised method (no *a priori* information about sample classes), which converts the original variables into a set of uncorrelated (orthogonal) new variables, called principal components (PCs, PC1, PC2, ..., PCn), thereby defining a lower n-dimensional space to represent the data. In this way, the original data matrix is decomposed into a scores matrix (containing information of the position of the samples in the new lower n-dimensional space) and a loadings matrix (which represents the way in which original variables contribute to the scores). The visualization of PCA results, particularly of the scores scatter plots, helps to identify outliers and grouping trends in the dataset. Another MVA method widely used in metabolomics is Projection to Latent Structures – Discriminant Analysis (PLS-DA). In this supervised method, the new latent variables (LVs) are iteratively obtained to model both the data matrix X and its correlation with Y (a second matrix containing information on sample class), so that the first LV maximizes class discrimination.

1.5.2. NMR metabolic profiling of breast cancer tissues and cells

NMR metabolomic studies of breast tissue samples revealed markedly different metabolic profiles between tumor and non-tumor samples, including consistent upregulation of metabolites like glycine, taurine, phosphocholine and lactate [251-256]. A particularly promising approach used direct tissue analysis by High Resolution Magic Angle Spinning (HRMAS) NMR to identify resection margins during breast cancer surgery [257]. The main biomarkers identified for this purpose were choline-containing compounds, with tumor tissue containing significantly higher amounts of phosphocholine. Metabolic differences between breast cancer subtypes, as defined by well-established classifiers, such as the ER, PR and HER2 status, were also reported. In general, ER and PR negative tumors were characterized by higher quantities of glycine, taurine and phosphocholine than samples from receptor-positive patients [258]. Another study combining gene expression microarrays and HRMAS NMR spectroscopy could identify 3 subgroups of luminal A breast cancer with different glycolytic activity [259]. Gene ontologies related to the extracellular matrix were correlated to *myo*-inositol and taurine, while cell cycle-related genes correlated mostly to choline. Distinct metabolic profiles for basal- and luminal-like breast cancer have also been reported [260] Data analysis showed higher concentrations of glycerophosphocholine than phosphocholine in basal-like tumor, which could be in part explained by lower choline kinase

expression and increased phosphatidylcholine degradation in the more aggressive subtype. TNBC was also successfully discriminated from breast cancer positive for ER, PR and HER2 receptors, based on metabolite profiles obtained by HRMAS NMR spectroscopy [261]. Choline levels were reported to be more elevated in TNBC, probably in association with increased cell proliferation and oncogenic signaling. Furthermore, glutamate levels were higher in TNBC samples while glutamine levels were lower, suggesting glutamine-dependent cell growth and upregulated glutaminolysis.

NMR metabolic profiling of cultured breast cells has also been successfully employed to investigate altered metabolic pathways in breast cancer. Although cell lines provide a limited perspective about the complex tumor mass and its microenvironment, working with cultured cells enables better control of external variables, higher homogeneity within sample groups, and simpler experimental implementation. Only a few studies have focused on the comparison between the metabolic composition of breast tumor and non-tumor cell lines. Maria and co-workers have employed HRMAS to analyze the metabolic profiles of epithelial MCF-10A cells and two cancer cell lines (MCF7 and MDA-MB-231) [262]. However, due to the relatively low spectral resolution obtained and the high degree of spectral overlap with macromolecule signals, the number of metabolites detected in each cell line was very small (6 to 15). The metabolic profiles of the cell lines used in this thesis (MCF-10A and MDA-MB-231) were also briefly compared in a study addressing the effects of dichloroacetate and allopurinol on cell metabolism [263]. Differences in lactate, glutamine, glycine and alanine were highlighted as the main differences underlying the responses to the pharmacological agents tested. Finally, another relevant work made use of stable isotope resolved metabolomics to probe different energy producing and anabolic pathways in one primary breast and three breast cancer cell lines, but the specific comparison between MCF-10A and MDA-MB-231 was not carried out [264].

1.5.3. Metabolomics studies of the effects of plant-derived natural compounds on breast cancer cells

Up to now, few studies have been performed to study the effect of plant-natural products on breast cancer cells metabolism by metabolomics. Jäger and co-workers employed a metabolomics analysis based on high-throughput liquid chromatography-based mass spectrometry to explore the metabolic effects of resveratrol on MCF-7 and MDA-MB-231 breast cancer cell lines [265]. Results showed a noticeable increase in the synthesis of serotonin, kynurenine, and spermindine in both cell lines, representative of a strong interaction of resveratrol with cellular biogenic amine metabolism. Moreover, increased levels of arachidonic acid, and its metabolite 12S-HETE were found, which could have been released from cell membrane phospholipids after activation of phospholipase A2 and subsequent metabolism by 12-lipoxygenase. Bayet-Robert and co-workers have also analyzed metabolomic responses of MCF-7 and MDA-MB-231 breast cancer cells to curcumin alone, and MCF-7 cells to curcumin in cotreatment with docetaxel using ^{1}H NMR spectroscopy [266]. Results showed glutathione metabolism, lipid/phospholipid metabolism, and glucose utilization as prominent targets of curcumin. Metabolic profiling via gas chromatography-mass spectrometry (GC-MS) of the breast cancer cell line MCF-7 and the non-tumorigenic breast cell line MCF-12A exposed to genistein revealed changes in sphingolipid metabolism [267]. The metabolic alterations induced by genistein, daidzein and a soy seed extract were also evaluated in MCF-7 and MDA-MB-231 breast cancer cells, using a global metabolomic approach [268]. In MCF-7 estrogen positive cells, the increase in the intracellular levels of 6-phosphogluconate and ribose 5-phosphate, upon exposure to the isoflavones, suggested the upregulation of the pentose phosphate pathway (PPP), whereas for MDA-MB-231 TNBC cells glutamine uptake was significantly restricted. Furthermore, a targeted metabolomics approach was used to investigate the impact of genistein and daidzein on the formation of estrogen metabolites in MCF-7 cells [269]. Recently, resveratrol impact on steroid metabolism, in human MDA-MB-231 MCF-7 breast cancer cells, was also assessed [270].

1.6. Scope and aims of this thesis

The agro-industrial exploitation of eucalyptus for pulp and paper production generates large amounts of biomass residues, especially bark. Their refinement to value-added compounds with potential application in other sectors, for instance in the pharmaceutical industry, contributes to a sustainable circular-economy. *Eucalyptus nitens* (*E. nitens*) outer bark is an abundant source of several bioactive compounds, especially triterpenic acids (TAs), with reported anticancer activity in several cellular and animal models, including in breast cancer. Triple negative breast cancer (TNBC) is the breast cancer subtype for which available therapeutic options are more limited, raising the need for new alternative and/or adjuvant therapies, such as natural-based products.

Cell metabolism is an important facet of cancer onset and progression, and metabolic modulation by pharmacological agents represents a promising approach to aid anticancer treatment. However, current information on the metabolic effects of plant-derived natural compounds is still very limited, and improved knowledge in this field could provide a more comprehensive understanding of their modes of action, at the cellular and molecular level.

The work developed in this thesis aimed at comprehensively assessing the metabolic effects of a lipophilic *E. nitens* outer bark extract and two TAs (betulinic and ursolic acids) towards TNBC and non-tumor breast epithelial cells. Specific research aims were:

i) to achieve a detailed characterization of the metabolic activity and composition of the breast cell models used, through integrative NMR metabolomics of cell culture media, intracellular polar metabolites and cellular lipids;

ii) to identify and interpret the alterations induced by a *E. nitens* bark extract in the metabolome of non-tumor and tumor breast cells;

iii) to identify and interpret the alterations induced by betulinic and ursolic acids in the metabolome of non-tumor and tumor breast cells;

iv) to highlight the differences between non-tumor and tumor cellular responses and correlate them with the cells basal metabolic activity and composition;

v) to propose hypotheses about metabolic targets and pathways modulated by the *E. nitens* bark extract and the two TAs tested, that may improve current understanding of their modes of action and potentiate their further development in natural product-based anticancer therapy.

1.7. References

1. Bray, F., Ferlay, J., Soerjomataram, I., Siegel, R.L., Torre, L.A.and Jemal, A., (2018). Global cancer statistics 2018: GLOBOCAN estimates of incidence and mortality worldwide for 36 cancers in 185 countries. *Ca: Cancer Journal for Clinicians*, 68(6), 394-424.

2. Luengo-Fernandez, R., Leal, J., Gray, A.and Sullivan, R., (2013). Economic burden of cancer across the European Union: a population-based cost analysis. *The lancet oncology*, 14(12), 1165-1174.

3. Hanly, P., Soerjomataram, I.and Sharp, L., (2015). Measuring the societal burden of cancer: The cost of lost productivity due to premature cancer-related mortality in Europe. *International Journal of Cancer*, 136(4), E136-E145.

4. Carioli, G., Malvezzi, M., Rodriguez, T., Bertuccio, P., Negri, E.and La Vecchia, C., (2017). Trends and predictions to 2020 in breast cancer mortality in Europe. *Breast*, 36 89-95.

5. DeSantis, C.E., Bray, F., Ferlay, J., Lortet-Tieulent, J., Anderson, B.O.and Jemal, A., (2015). International variation in female breast cancer incidence and mortality rates. *Cancer Epidemiology Biomarkers & Prevention*, 24(10), 1495-1506.

6. Pinheiro, P.S., TyczyÅ„ski, J.E., Bray, F., Amado, J., Matos, E.and Parkin, D.M., (2003). Cancer incidence and mortality in Portugal. *European Journal of Cancer*, 39(17), 2507-2520.

7. Ferlay, J., Steliarova-Foucher, E., Lortet-Tieulent, J., Rosso, S., Coebergh, J.W.W., Comber, H., Forman, D.and Bray, F., (2013). Cancer incidence and mortality patterns in Europe: estimates for 40 countries in 2012. *European Journal of Cancer*, 49(6), 1374-1403.

8. Ferlay, J., Soerjomataram, I., Dikshit, R., Eser, S., Mathers, C., Rebelo, M., Parkin, D.M., Forman, D.and Bray, F., (2015). Cancer incidence and mortality worldwide: sources, methods and major patterns in GLOBOCAN 2012. *International Journal of Cancer*, 136(5), E359-86.

9. de Lacerda, G.F., Kelly, S.P., Bastos, J., Castro, C., Mayer, A., Mariotto, A.B.and Anderson, W.F., (2018). Breast cancer in Portugal: Temporal trends and age-specific incidence by geographic regions. *Cancer Epidemiology*, 54 12-18.

10. Vogel, V.G., Bland, K.I., Copeland, E.M., Klimberg, V.S.and Gradishar, W.J., *15 - Epidemiology of Breast Cancer*, in *The Breast (Fifth Edition)*. 2018, Elsevier. p. 207-218.e4.

11. Barnard, M.E., Boeke, C.E.and Tamimi, R.M., (2015). Established breast cancer risk factors and risk of intrinsic tumor subtypes. *Biochimica Et Biophysica Acta-Reviews on Cancer*, 1856(1), 73-85.

12. Beral, V., Bull, D., Pirie, K., Reeves, G., Peto, R., Skegg, D., LaVecchia, C., Magnusson, C., Pike, M.C., Thomas, D., *et al.*, (2012). Menarche, menopause, and breast cancer risk: individual participant meta-analysis, including 118 964 women with breast cancer from 117 epidemiological studies. *Lancet Oncology*, 13(11), 1141-1151.

13. Anderson, K.N., Schwab, R.B.and Martinez, M.E., (2014). Reproductive risk factors and breast cancer subtypes: a review of the literature. *Breast Cancer Research and Treatment*, 144(1), 1-10.

14. Feng, Y.X., Spezia, M., Huang, S.F., Yuan, C.F., Zeng, Z.Y., Zhang, L.H., Ji, X.J., Liu, W., Huang, B., Luo, W.P., Liu, B., Lei, Y., Du, S., Vuppalapati, A., Luu, H.H., Haydon, R.C., He, T.C.and Ren, G.S., (2018). Breast cancer development and progression: Risk factors, cancer stem cells, signaling pathways, genomics, and molecular pathogenesis. *Genes & Diseases*, 5(2), 77-106.

15. Kleibl, Z. and Kristensen, V.N., (2016). Women at high risk of breast cancer: Molecular characteristics, clinical presentation and management. *Breast*, 28 136-144.

16. Gomez-Flores-Ramos, L., Alvarez-Gomez, R.M., Villarreal-Garza, C., Wegman-Ostrosky, T.and Mohar, A., (2017). Breast cancer genetics in young women: What do we know? *Mutation Research-Reviews in Mutation Research*, 774 33-45.

17. Ferrara, A., (2011). Benign breast disease. *Radiologic Technology*, 82(5), 447M-62M.

18. Peterson, L.L. and Ligibel, J.A., (2018). Physical activity and breast Cancer: an opportunity to improve outcomes. *Current Oncology Reports*, 20(7).

19. Provenzano, E., Ulaner, G.A.and Chin, S.F., (2018). Molecular classification of breast Cancer. *Pet Clinics*, 13(3), 325-338.

20. Yersal, O. and Barutca, S., (2014). Biological subtypes of breast cancer: Prognostic and therapeutic implications. *World Journal of Clinical Oncology*, 5(3), 412-24.

21. Nilsson, S., Makela, S., Treuter, E., Tujague, M., Thomsen, J., Andersson, G., Enmark, E., Pettersson, K., Warner, M.and Gustafsson, J.A., (2001). Mechanisms of estrogen action. *Physiological Reviews*, 81(4), 1535-1565.

22. De Marchi, T., Foekens, J.A., Umar, A.and Martens, J.W., (2016). Endocrine therapy resistance in estrogen receptor (ER)-positive breast cancer. *Drug Discov Today*, 21(7), 1181-8.

23. Sorlie, T., Perou, C.M., Tibshirani, R., Aas, T., Geisler, S., Johnsen, H., Hastie, T., Eisen, M.B., van de Rijn, M., Jeffrey, S.S., Thorsen, T., Quist, H., Matese, J.C., Brown, P.O., Botstein, D., Lonning, P.E.and Borresen-Dale, A.L., (2001). Gene expression patterns of breast carcinomas distinguish tumor subclasses with clinical implications. *Proceedings of the National Academy of Sciences of the United States of America*, 98(19), 10869-74.

24. Sotiriou, C., Neo, S.Y., McShane, L.M., Korn, E.L., Long, P.M., Jazaeri, A., Martiat, P., Fox, S.B., Harris, A.L.and Liu, E.T., (2003). Breast cancer classification and prognosis based on gene expression profiles from a population-based study. *Proceedings of the National Academy of Sciences of the United States of America*, 100(18), 10393-10398.

25. Abd El-Rehim, D.M., Ball, G., Pinder, S.E., Rakha, E., Paish, C., Robertson, J.F.R., Macmillan, D., Blamey, R.W.and Ellis, I.O., (2005). High-throughput protein expression analysis using tissue microarray technology of a large well-characterised series identifies biologically distinct classes of breast cancer confirming recent cDNA expression analyses. *International Journal of Cancer*, 116(3), 340-350.

26. Fan, C., Oh, D.S., Wessels, L., Weigelt, B., Nuyten, D.S.A., Nobel, A.B., van't Veer, L.J.and Perou, C.M., (2006). Concordance among gene-expression-based predictors for breast cancer. *New England Journal of Medicine*, 355(6), 560-569.

27. Hu, Z.Y., Fan, C., Oh, D.S., Marron, J.S., He, X.P., Qaqish, B.F., Livasy, C., Carey, L.A., Reynolds, E., Dressler, L., *et al.*, (2006). The molecular portraits of breast tumors are conserved across microarray platforms. *Bmc Genomics*, 7, 96.

28. Gatza, M.L., Lucas, J.E., Barry, W.T., Kim, J.W., Wang, Q.L., Crawford, M.D., Datto, M.B., Kelley, M., Mathey-Prevot, B., Potti, A.and Nevins, J.R., (2010). A pathway-based classification of human breast cancer. *Proceedings of the National Academy of Sciences of the United States of America*, 107(15), 6994-6999.

29. Lehmann, B.D., Bauer, J.A., Chen, X., Sanders, M.E., Chakravarthy, A.B., Shyr, Y.and Pietenpol, J.A., (2011). Identification of human triple-negative breast cancer subtypes and preclinical models for selection of targeted therapies. *Journal of Clinical Investigation*, 121(7), 2750-2767.

30. Curtis, C., Shah, S.P., Chin, S.F., Turashvili, G., Rueda, O.M., Dunning, M.J., Speed, D., Lynch, A.G., Samarajiwa, S., Yuan, Y.Y., *et al.*, (2012). The genomic and transcriptomic architecture of 2,000 breast tumors reveals novel subgroups. *Nature*, 486(7403), 346-352.

31. Koboldt, D.C., Fulton, R.S., McLellan, M.D., Schmidt, H., Kalicki-Veizer, J., McMichael, J.F., Fulton, L.L., Dooling, D.J., Ding, L., Mardis, E.R., *et al.*, (2012). Comprehensive molecular portraits of human breast tumours. *Nature*, 490(7418), 61-70.

32. Dai, X.F., Chen, A.and Bai, Z.H., (2014). Integrative investigation on breast cancer in ER, PR and HER2-defined subgroups using mRNA and miRNA expression profiling. *Scientific Reports*, 4, 6566.

33. Gnant, M., Filipits, M., Greil, R., Stoeger, H., Rudas, M., Bago-Horvath, Z., Mlineritsch, B., Kwasny, W., Knauer, M., Singer, C., *et al.*, (2014). Predicting distant recurrence in receptor-positive breast cancer patients with limited clinicopathological risk: using the PAM50 Risk of Recurrence score in 1478 postmenopausal patients of the ABCSG-8 trial treated with adjuvant endocrine therapy alone. *Annals of Oncology*, 25(2), 339-345.

34. Dai, X.F., Li, T., Bai, Z.H., Yang, Y.K., Liu, X.X., Zhan, J.L.and Shi, B.Z., (2015). Breast cancer intrinsic subtype classification, clinical use and future trends. *American Journal of Cancer Research*, 5(10), 2929-2943.

35. Ignatiadis, M. and Sotiriou, C., (2013). Luminal breast cancer: from biology to treatment. *Nature Reviews Clinical Oncology*, 10(9), 494-506.

36. Eroles, P., Bosch, A., Perez-Fidalgo, J.A.and Lluch, A., (2011). Molecular biology in breast cancer: intrinsic subtypes and signaling pathways. *Cancer Treat Reviews*, 38(6), 698-707.

37. Sorlie, T., Tibshirani, R., Parker, J., Hastie, T., Marron, J.S., Nobel, A., Deng, S., Johnsen, H., Pesich, R., Geisler, S., Demeter, J., Perou, C.M., Lonning, P.E., Brown, P.O., Borresen-Dale, A.L.and Botstein, D., (2003). Repeated observation of breast tumor subtypes in independent gene expression data sets. *Proceedings of the National Academy of Sciences of the United States of America*, 100(14), 8418-8423.

38. Staaf, J., Ringner, M., Vallon-Christersson, J., Jonsson, G., Bendahl, P.O., Holm, K., Arason, A., Gunnarsson, H., Hegardt, C., Agnarsson, B.A., Luts, L., Grabau, D., Ferno, M., Malmstrom, P.O., Johannsson, O.T., Loman, N., Barkardottir, R.B.and Borg, A., (2010). Identification of subtypes in human epidermal growth factor receptor 2--positive breast cancer reveals a gene signature prognostic of outcome. *Journal of Clinical Oncology*, 28(11), 1813-20.

39. Gusterson, B. and Eaves, C.J., (2018). Basal-like Breast Cancers: From Pathology to Biology and Back Again. *Stem Cell Reports*, 10(6), 1676-1686.

40. Neophytou, C., Boutsikos, P.and Papageorgis, P., (2018). Molecular mechanisms and emerging therapeutic targets of Triple-Negative Breast Cancer metastasis. *Frontiers in Oncology*, 8, 31.

41. Alluri, P. and Newman, L.A., (2014). Basal-like and triple-negative breast cancers: searching for positives among many negatives. *Surgical Oncology Clinics of North America*, 23(3), 567-77.

42. Pareja, F., Geyer, F.C., Marchio, C., Burke, K.A., Weigelt, B.and Reis-Filho, J.S., (2016). Triple-negative breast cancer: the importance of molecular and histologic subtyping, and recognition of low-grade variants. *Npj Breast Cancer*, 2, 16036.

43. Abramson, V.G., Lehmann, B.D., Ballinger, T.J.and Pietenpol, J.A., (2015). Subtyping of Triple-Negative Breast Cancer: Implications for therapy. *Cancer*, 121(1), 8-16.

44. Geyer, F.C., Pareja, F., Weigelt, B., Rakha, E., Ellis, I.O., Schnitt, S.J.and Reis, J.S., (2017). The spectrum of Triple-Negative Breast disease high- and low-grade lesions. *American Journal of Pathology*, 187(10), 2139-2151.

45. Telli, M.L. and Sledge, G.W., (2015). The future of breast cancer systemic therapy: the next 10 years. *Journal of Molecular Medicine-Jmm*, 93(2), 119-125.

46. Harbeck, N. and Gnant, M., (2017). Breast cancer. *Lancet*, 389(10074), 1134-1150.

47. Coates, A.S., Winer, E.P., Goldhirsch, A., Gelber, R.D., Gnant, M., Piccart-Gebhart, M., Thurlimann, B.and Senn, H.J., (2015). Tailoring therapies--improving the management of early breast cancer: St Gallen International Expert Consensus on the Primary Therapy of Early Breast Cancer 2015. *Annals of Oncology*, 26(8), 1533-46.

48. Foulkes, W.D., Smith, I.E.and Reis, J.S., (2010). Triple-Negative Breast Cancer. *New England Journal of Medicine*, 363(20), 1938-1948.

49. Liedtke, C., Mazouni, C., Hess, K.R., Andre, F., Tordai, A., Mejia, J.A., Symmans, W.F., Gonzalez-Angulo, A.M., Hennessy, B., Green, M., Cristofanilli, M., Hortobagyi, G.N.and Pusztai, L., (2008). Response to neoadjuvant therapy and long-term survival in patients with triple-negative breast cancer. *Journal of Clinical Oncology*, 26(8), 1275-1281.

50. Voduc, K.D., Cheang, M.C.U., Tyldesley, S., Gelmon, K., Nielsen, T.O.and Kennecke, H., (2010). Breast cancer subtypes and the risk of local and regional relapse. *Journal of Clinical Oncology*, 28(10), 1684-1691.

51. Montagna, E., Bagnardi, V., Rotmensz, N., Viale, G., Renne, G., Cancello, G., Balduzzi, A., Scarano, E., Veronesi, P., Luini, A., Zurrida, S., Monti, S., Mastropasqua, M.G., Bottiglieri, L., Goldhirsch, A.and Colleoni, M., (2012). Breast cancer subtypes and outcome after local and regional relapse. *Annals of Oncology*, 23(2), 324-U299.

52. Fernandez, A.G., Chabrera, C., Font, M.G., Fraile, M., Gonzalez, S., Barco, I., Gonzalez, C., Cirera, L., Veloso, E., Lain, J.M., Pessarrodona, A.and Gimenez, N., (2013). Differential survival and recurrence patterns of patients operated for breast cancer according to the new immunohistochemical classification: analytical survey from 1997 to 2012. *Tumor Biology*, 34(4), 2349-2355.

53. Minicozzi, P., Bella, F., Toss, A., Giacomin, A., Fusco, M., Zarcone, M., Tumino, R., Falcini, F., Cesaraccio, R., Candela, G., La Rosa, F., Federico, M.and Sant, M., (2013). Relative and disease-free survival for breast cancer in relation to subtype: a population-based study. *Journal of Cancer Research and Clinical Oncology*, 139(9), 1569-1577.

54. Wu, X., Baig, A., Kasymjanova, G., Kafi, K., Holcroft, C., Mekouar, H., Carbonneau, A., Bahoric, B., Sultanem, K.and Muanza, T., (2016). Pattern of local recurrence and distant metastasis in breast cancer by molecular subtype. *Cureus*, 8(12), e924.

55. Tao, J.J., Visvanathan, K.and Wolff, A.C., (2015). Long term side effects of adjuvant chemotherapy in patients with early breast cancer. *Breast*, 24 S149-S153.

56. Lebert, J.M., Lester, R., Powell, E., Seal, M.and McCarthy, J., (2018). Advances in the systemic treatment of triple-negative breast cancer. *Current Oncology*, 25 S142-S150.

57. Rida, P., Ogden, A., Ellis, I.O., Varga, Z., Wolff, A.C., Traina, T.A., Hatzis, C., Palmer, J.R., Ambrosone, C.B., Lehmann, B.D., Nanda, R., Montgomery Rice, V., Brawley, O.W., Torres, M.A., Rakha, E.and Aneja, R., (2018). First international TNBC conference meeting report. *Breast Cancer Research and Treatment*, 169(3), 407-412.

58. Harvey, A.L., Edrada-Ebel, R.and Quinn, R.J., (2015). The re-emergence of natural products for drug discovery in the genomics era. *Nature Reviews Drug Discovery*, 14(2), 111-129.

59. Rodrigues, T., Reker, D., Schneider, P.and Schneider, G., (2016). Counting on natural products for drug design. *Nature Chemistry*, 8(6), 531-541.

60. Romano, J.D. and Tatonetti, N.P., (2019). Informatics and computational methods in natural product drug discovery: A review and perspectives. *Frontiers in Genetics*, 10, 368.

61. Newman, D.J. and Cragg, G.M., (2016). Natural products as sources of new drugs from 1981 to 2014. *Journal of Natural Products*, 79(3), 629-661.

62. Butler, M.S., Robertson, A.A.B.and Cooper, M.A., (2014). Natural product and natural product derived drugs in clinical trials. *Natural Product Reports*, 31(11), 1612-1661.

63. Bayet-Robert, M., Kwiatkowski, F., Leheurteur, M., Gachon, F., Planchat, E., Abrial, C., Mouret-Reynier, M.A., Durando, X., Barthomeuf, C.and Chollet, P., (2010). Phase I dose escalation trial of docetaxel plus curcumin in patients with advanced and metastatic breast cancer. *Cancer Biology & Therapy*, 9(1), 8-14.

64. Miller, J.A., Lang, J.E., Ley, M., Nagle, R., Hsu, C.H., Thompson, P.A., Cordova, C., Waer, A.and Chow, H.H., (2013). Human breast tissue disposition and bioactivity of limonene in women with early-stage breast cancer. *Cancer Prevention Research (Philadelphia)*, 6(6), 577-84.

65. Crew, K.D., Ho, K.A., Brown, P., Greenlee, H., Bevers, T.B., Arun, B., Sneige, N., Hudis, C., McArthur, H.L., Chang, J., Rimawi, M., Cornelison, T.L., Cardelli, J., Santella, R.M., Wang, A., Lippman, S.M.and Hershman, D.L., (2015). Effects of a green tea extract, Polyphenon E, on systemic biomarkers of growth factor signalling in women with hormone receptor-negative breast cancer. *Journal of Human Nutrition and Dietetics*, 28(3), 272-82.

66. McGrogan, B.T., Gilmartin, B., Camey, D.N.and McCann, A., (2008). Taxanes, microtubules and chemoresistant breast cancer. *Biochimica Et Biophysica Acta-Reviews on Cancer*, 1785(2), 96-132.

67. Wani, M.C. and Horwitz, S.B., (2014). Nature as a remarkable chemist: a personal story of the discovery and development of Taxol. *Anti-Cancer Drugs*, 25(5), 482-487.

68. Mustacchi, G. and De Laurentiis, M., (2015). The role of taxanes in triple-negative breast cancer: literature review (vol 9, pg 4303, 2015). *Drug Design Development and Therapy*, 9 5669-5669.

69. Wang, G., Tang, W.and Bidigare, R., *Terpenoids As Therapeutic Drugs and Pharmaceutical Agents*, in *Natural Products*, L. Zhang and A. Demain, Editors. 2005, Humana Press. p. 197-227.

70. Paduch, R., Kandefer-Szerszen, M., Trytek, M.and Fiedurek, J., (2007). Terpenes: substances useful in human healthcare. *Archivum Immunologiae et Therapiae Experimentalis*, 55(5), 315-27.

71. Parikh, N.R., Mandal, A., Bhatia, D., Siveen, K.S., Sethi, G.and Bishayee, A., (2014). Oleanane triterpenoids in the prevention and therapy of breast cancer: current evidence and future perspectives. *Phytochemistry Reviews*, 13(4), 793-810.

72. Withers, S.T. and Keasling, J.D., (2007). Biosynthesis and engineering of isoprenoid small molecules. *Applied Microbiology and Biotechnology*, 73(5), 980-90.

73. Gershenzon, J. and Dudareva, N., (2007). The function of terpene natural products in the natural world. *Nature Chemical Biology*, 3(7), 408-414.

74. Domingues, R.M.A., Guerra, A.R., Duarte, M., Freire, C.S.R., Neto, C.P., Silva, C.M.S.and Silvestre, A.J.D., (2014). Bioactive triterpenic acids: from agroforestry biomass residues to promising therapeutic tools. *Mini-Reviews in Organic Chemistry*, 11(3), 382-399.

75. Connolly, J.D. and Hill, R.A., (2008). Triterpenoids. *Natural Product Reports*, 25(4), 794-830.

76. Hill, R.A. and Connolly, J.D., (2012). Triterpenoids. *Natural Product Reports*, 29(7), 780-818.

77. Xu, R., Fazio, G.C.and Matsuda, S.P.T., (2004). On the origins of triterpenoid skeletal diversity. *Phytochemistry*, 65(3), 261-291.

78. Peron, G., Marzaro, G.and Dall'Acqua, S., (2018). Known triterpenes and their derivatives as scaffolds for the development of new therapeutic agents for cancer. *Current Medicinal Chemistry*, 25(10), 1259-1269.

79. Teng, H., Yuan, B.Y., Gothai, S., Arulselvan, P., Song, X.J.and Chen, L., (2018). Dietary triterpenes in the treatment of type 2 diabetes: To date. *Trends in Food Science & Technology*, 72 34-44.

80. Xiao, S.L., Tian, Z.Y., Wang, Y.F., Si, L.L., Zhang, L.H.and Zhou, D.M., (2018). Recent progress in the antiviral activity and mechanism study of pentacyclic triterpenoids and their derivatives. *Medicinal Research Reviews*, 38(3), 951-976.

81. Xu, G.B., Xiao, Y.H., Zhang, Q.Y., Zhou, M.and Liao, S.G., (2018). Hepatoprotective natural triterpenoids. *European Journal of Medicinal Chemistry*, 145 691-716.

82. Lamberg, J.-A., Ojala, J., Peltoniemi, M.and Särkkä, T., *The Evolution of Global Paper Industry 1800-2050: A Comparative Analysis*. Vol. 17. 2012: Springer Science & Business Media.

83. Leslie, A.D., Mencuccini, M.and Perks, M., (2012). The potential for Eucalyptus as a wood fuel in the UK. *Applied Energy*, 89(1), 176-182.

84. Iglesias-Trabado, G. and Wilstermann, D., (2008). Eucalyptus universalis, global cultivated eucalypt forests map 2008. *GIT Forestry Consulting™ EUCALYPTOLOGICS: Information Resources on Eucalyptus Cultivation Worldwide, http://www.git-forestry.com*.

85. Silva-Pando, F.J. and Pino-Perez, R., (2016). Introduction of eucalyptus into Europe. *Australian Forestry*, 79(4), 283-291.

86. CELPA , A.d.I.P., *2016 - Boletim Estatístico da Indústria Papeleira Portuguesa*. 2017: Lisbon.

87. Instituto da Conservação da Natureza e das Florestas, I.P., *IFN6 – Principais resultados – relatório sumário*. 2019.

88. Perez-Cruzado, C., Merino, A.and Rodriguez-Soalleiro, R., (2011). A management tool for estimating bioenergy production and carbon sequestration in Eucalyptus globulus and Eucalyptus nitens grown as short rotation woody crops in north-west Spain. *Biomass & Bioenergy*, 35(7), 2839-2851.

89. Gonzalez-Garcia, M., Hevia, A., Majada, J.and Barrio-Anta, M., (2013). Above-ground biomass estimation at tree and stand level for short rotation plantations of Eucalyptus nitens (Deane & Maiden) Maiden in Northwest Spain. *Biomass & Bioenergy*, 54 147-157.

90. Domingues, R.M.A., Sousa, G.D.A., Freire, C.S.R., Silvestre, A.J.D.and Neto, C.P., (2010). Eucalyptus globulus biomass residues from pulping industry as a source of high value triterpenic compounds. *Industrial Crops and Products*, 31(1), 65-70.

91. Domingues, R.M.A., Patinha, D.J.S., Sousa, G.D.A., Villaverde, J.J., Silva, C.M., Freire, C.S.R., Silvestre, A.J.D.and Neto, C.P., (2011). Eucalyptus biomass residues from agro-forest and pulping industries as sources of high-value triterpenic compounds. *Cellulose Chemistry and Technology*, 45(7-8), 475-481.

92. Domingues, R.M.A., Sousa, G.D.A., Silva, C.M., Freire, C.S.R., Silvestre, A.J.D.and Neto, C.P., (2011). High value triterpenic compounds from the outer barks of several Eucalyptus species cultivated in Brazil and in Portugal. *Industrial Crops and Products*, 33(1), 158-164.

93. Quilhó, T. and Pereira, H., (2001). Within and between-tree variation of bark content and wood density of Eucalyptus globulus in commercial plantations. *IAWA Journal*, 22(3), 255-265.

94. Neiva, D.M., Araújo, S., Gominho, J., Carneiro, A.d.C.and Pereira, H., (2018). Potential of Eucalyptus globulus industrial bark as a biorefinery feedstock: Chemical and fuel characterization. *Industrial Crops and Products*, 123 262-270.

95. Laszczyk, M.N., (2009). Pentacyclic triterpenes of the lupane, oleanane and ursane group as tools in cancer therapy*. Planta Medica*, 75(15), 1549-1560.

96. Rufino-Palomares, E.E., Perez-Jimenez, A., Reyes-Zurita, F.J., Garcia-Salguero, L., Mokhtari, K., Herrera-Merchan, A., Medina, P.P., Peragon, J.and Lupianez, J.A., (2015). Anti-cancer and anti-angiogenic properties of various natural pentacyclic tri-terpenoids and some of their chemical derivatives*. Current Organic Chemistry*, 19(10), 919-947.

97. Salvador, J.A.R., Leal, A.S., Valdeira, A.S., Goncalves, B.M.F., Alho, D.P.S., Figueiredo, S.A.C., Silvestre, S.M.and Mendes, V.I.S., (2017). Oleanane-, ursane-, and quinone methide friedelane-type triterpenoid derivatives: Recent advances in cancer treatment*. European Journal of Medicinal Chemistry*, 142 95-130.

98. Ghante, M.H. and Jamkhande, P.G., (2019). Role of Pentacyclic Triterpenoids in Chemoprevention and Anticancer Treatment: An overview on targets and underling mechanisms*. Journal of Pharmacopuncture*, 22(2), 55-67.

99. Amico, V., Barresi, V., Condorelli, D., Spatafora, C.and Tringali, C., (2006). Antiproliferative terpenoids from almond hulls (Prunus dulcis): Identification and structure-activity relationships*. Journal of Agricultural and Food Chemistry*, 54(3), 810-814.

100. Kessler, J.H., Mullauer, F.B., de Roo, G.M.and Medema, J.P., (2007). Broad in vitro efficacy of plant-derived betulinic acid against cell lines derived from the most prevalent human cancer types*. Cancer Letters*, 251(1), 132-45.

101. Bar, F.M.A., Khanfar, M.A., Elnagar, A.Y., Liu, H., Zaghloul, A.M., Badria, F.A., Sylvester, P.W., Ahmad, K.F., Raisch, K.P.and El Sayed, K.A., (2009). Rational design and semisynthesis of betulinic acid analogues as potent topoisomerase inhibitors*. Journal of Natural Products*, 72(9), 1643-1650.

102. Liu, X.Y., Jutooru, I., Lei, P., Kim, K., Lee, S.O., Brents, L.K., Prather, P.L.and Safe, S., (2012). Betulinic acid targets YY1 and ErbB2 through cannabinoid receptor-dependent disruption of microRNA-27a:ZBTB10 in breast cancer*. Molecular Cancer Therapeutics*, 11(7), 1421-1431.

103. Damle, A.A., Pawar, Y.P.and Narkar, A.A., (2013). Anticancer activity of betulinic acid on MCF-7 tumors in nude mice*. Indian Journal of Experimental Biology*, 51(7), 485-491.

104. Mertens-Talcott, S.U., Noratto, G.D., Li, X.R., Angel-Morales, G., Bertoldi, M.C.and Safe, S., (2013). Betulinic acid decreases ER-negative breast cancer cell growth in vitro and in Vivo: Role of Sp Transcription Factors and MicroRNA-27a:ZBTB10*. Molecular Carcinogenesis*, 52(8), 591-602.

105. Sun, Y.F., Song, C.K., Viemstein, H., Unger, F.and Liang, Z.S., (2013). Apoptosis of human breast cancer cells induced by microencapsulated betulinic acid from sour jujube fruits through the mitochondria transduction pathway*. Food Chemistry*, 138(2-3), 1998-2007.

106. Hussein-Al-Ali, S.H., Arulselvan, P., Fakurazi, S.and Hussein, M.Z., (2014). The in vitro therapeutic activity of betulinic acid nanocomposite on breast cancer cells (MCF-7) and normal fibroblast cell (3T3)*. Journal of Materials Science*, 49(23), 8171-8182.

107. Kim, H.I., Quan, F.S., Kim, J.E., Lee, N.R., Kim, H.J., Jo, S.J., Lee, C.M., Jang, D.S.and Inn, K.S., (2014). Inhibition of estrogen signaling through depletion of estrogen receptor alpha by ursolic acid and betulinic acid from Prunella vulgaris var. lilacina*. Biochemical and Biophysical Research Communications*, 451(2), 282-287.

108. Park, S.Y., Kim, H.J., Kim, K.R., Lee, S.K., Lee, C.K., Park, K.K.and Chung, W.Y., (2014). Betulinic acid, a bioactive pentacyclic triterpenoid, inhibits skeletal-related events induced by breast cancer bone metastases and treatment*. Toxicology and Applied Pharmacology*, 275(2), 152-162.

109. Tiwari, R., Puthli, A., Balakrishnan, S., Sapra, B.K.and Mishra, K.P., (2014). Betulinic acid-induced cytotoxicity in human breast tumor cell lines MCF-7 and T47D and its modification by tocopherol*. Cancer Investigation*, 32(8), 402-408.

110. Hsu, R.J., Hsu, Y.C., Chen, S.P., Fu, C.L., Yu, J.C., Chang, F.W., Chen, Y.H., Liu, J.M., Ho, J.Y.and Yu, C.P., (2015). The triterpenoids of Hibiscus syriacus induce apoptosis and inhibit cell migration in breast cancer cells. *Bmc Complementary and Alternative Medicine*, 15.

111. Bebenek, E., Chrobak, E., Wietrzyk, J., Kadela, M., Chrobak, A., Kusz, J., Ksiazek, M., Jastrzebska, M.and Boryczka, S., (2016). Synthesis, structure and cytotoxic activity of acetylenic derivatives of betulonic and betulinic acids. *Journal of Molecular Structure*, 1106 210-219.

112. Mishra, T., Arya, R.K., Meena, S., Joshi, P., Pal, M., Meena, B., Upreti, D.K., Rana, T.S.and Datta, D., (2016). Isolation, Characterization and anticancer potential of cytotoxic triterpenes from Betula utilis bark. *Plos One*, 11(7), e0159430.

113. Eyong, K.O., Bairy, G., Eno, A.A., Taube, J., Hull, K.G., Folefoc, G., Foyet, H.S.and Romo, D., (2017). Triterpenoids from the stem bark of Vitellaria paradoxa (Sapotaceae) and derived esters exhibit cytotoxicity against a breast cancer cell line. *Medicinal Chemistry Research*, 27(1), 268-277.

114. Cai, Y.L., Zheng, Y.F., Gu, J.Y., Wang, S.Q., Wang, N., Yang, B.W., Zhang, F.X., Wang, D.M., Fu, W.J.and Wang, Z.Y., (2018). Betulinic acid chemosensitizes breast cancer by triggering ER stress-ediated apoptosis by directly targeting GRP78. *Cell Death & Disease*, 9.

115. Gao, Y., Ma, Q., Ma, Y.B., Ding, L., Xu, X.L., Wei, D.F., Wei, L.and Zhang, J.W., (2018). Betulinic acid induces apoptosis and ultrastructural changes in MDA-MB-231 breast cancer cells. *Ultrastructural Pathology*, 42(1), 49-54.

116. Zeng, A.Q., Yu, Y., Yao, Y.Q., Yang, F.F., Liao, M., Song, L.J., Li, Y.L., Yu, Y., Li, Y.J., Deng, Y.L., Yang, S.P., Zeng, C.J., Liu, P., Xie, Y.M., Yang, J.L., Zhang, Y.W., Ye, T.H.and Wei, Y.Q., (2018). Betulinic acid impairs metastasis and reduces immunosuppressive cells in breast cancer models. *Oncotarget*, 9(3), 3794-3804.

117. Yang, W.S., Chadalapaka, G., Cho, S.G., Lee, S.O., Jin, U.H., Jutooru, I., Choi, K., Leung, Y.K., Ho, S.M., Safe, S.and Kim, K.H., (2014). The transcriptional repressor ZBTB4 regulates EZH2 through a microRNA-ZBTB4-specificity protein signaling axis. *Neoplasia*, 16(12), 1059-1069.

118. Tzenov, Y.R., Andrews, P., Voisey, K., Gai, L., Carter, B., Whelan, K., Popadiuk, C.and Kao, K.R., (2016). Selective estrogen receptor modulators and betulinic acid act synergistically to target ER alpha and SP1 transcription factor dependent Pygopus expression in breast cancer. *Journal of Clinical Pathology*, 69(6), 518-526.

119. Es-Saady, D., Simon, A., Jayat-Vignoles, C., Chulia, A.J.and Delage, C., (1996). MCF-7 cell cycle arrested at G1 through ursolic acid, and increased reduction of tetrazolium salts. *Anticancer Research*, 16(1), 481-6.

120. He, X.J. and Liu, R.H., (2007). Triterpenoids isolated from apple peels have potent antiproliferative activity and may be partially responsible for apple's anticancer activity. *Journal of Agricultural and Food Chemistry*, 55(11), 4366-4370.

121. Kassi, E., Sourlingas, T.G., Spiliotaki, M., Papoutsi, Z., Pratsinis, H., Aligiannis, N.and Moutsatsou, P., (2009). Ursolic acid triggers apoptosis and Bcl-2 downregulation in MCF-7 breast cancer cells. *Cancer Investigation*, 27(7), 723-733.

122. Qamar, K.A., Dar, A., Siddiqui, B.S., Kabir, N., Aslam, H., Ahmed, S., Erum, S., Habib, S.and Begum, S., (2010). Anticancer activity of Ocimum basilicum and the effect of ursolic acid on the cytoskeleton of MCF-7 human breast cancer cells. *Letters in Drug Design & Discovery*, 7(10), 726-736.

123. Yeh, C.T., Wu, C.H.and Yen, G.C., (2010). Ursolic acid, a naturally occurring triterpenoid, suppresses migration and invasion of human breast cancer cells by modulating c-Jun N-terminal kinase, Akt and mammalian target of rapamycin signaling. *Molecular Nutrition & Food Research*, 54(9), 1285-95.

124. Kim, K.H., Seo, H.S., Choi, H.S., Choi, I., Shin, Y.C.and Ko, S.G., (2011). Induction of apoptotic cell death by ursolic acid through mitochondrial death pathway and extrinsic death receptor pathway in MDA-MB-231 cells*. Archives of Pharmacal Research*, 34(8), 1363-1372.

125. Shan, J.Z., Xuan, Y.Y., Ruan, S.Q.and Sun, M., (2011). Proliferation-inhibiting and apoptosis-inducing effects of ursolic acid and oleanolic acid on multi-drug resistance cancer cells in vitro*. Chinese Journal of Integrative Medicine*, 17(8), 607-611.

126. Gu, G.W., Barone, I., Gelsomino, L., Giordano, C., Bonofiglio, D., Statti, G., Menichini, F., Catalano, S.and Ando, S., (2012). Oldenlandia diffusa extracts exert antiproliferative and apoptotic effects on human breast cancer cells through ER alpha/Sp1-mediated p53 activation*. Journal of Cellular Physiology*, 227(10), 3363-3372.

127. Wang, J.S., Ren, T.N.and Xi, T., (2012). Ursolic acid induces apoptosis by suppressing the expression of FoxM1 in MCF-7 human breast cancer cells*. Medical Oncology*, 29(1), 10-15.

128. Mazumder, K., Tanaka, K.and Fukase, K., (2013). Cytotoxic activity of ursolic acid derivatives obtained by isolation and oxidative derivatization*. Molecules*, 18(8), 8929-8944.

129. Lewinska, A., Adamczyk-Grochala, J., Kwasniewicz, E., Deregowska, A.and Wnuk, M., (2017). Ursolic acid-mediated changes in glycolytic pathway promote cytotoxic autophagy and apoptosis in phenotypically different breast cancer cells*. Apoptosis*, 22(6), 800-815.

130. Singletary, K., MacDonald, C.and Wallig, M., (1996). Inhibition by rosemary and carnosol of 7,12 dimethylbenz[alpha]anthracene (DMBA)-induced rat mammary tumorigenesis and in vivo DMBA-DNA adduct formation*. Cancer Letters*, 104(1), 43-48.

131. De Angel, R.E., Smith, S.M., Glickman, R.D., Perkins, S.N.and Hursting, S.D., (2010). Antitumor effects of ursolic acid in a mouse model of postmenopausal breast cancer*. Nutrition and Cancer-an International Journal*, 62(8), 1074-1086.

132. Zhao, C., Yin, S.T., Dong, Y.H., Guo, X., Fan, L.H., Ye, M.and Hu, H.B., (2013). Autophagy-dependent EIF2AK3 activation compromises ursolic acid-induced apoptosis through upregulation of MCL1 in MCF-7 human breast cancer cells*. Autophagy*, 9(2), 196-207.

133. Tan, K.W., Li, Y., Paxton, J.W., Birch, N.P.and Scheepens, A., (2013). Identification of novel dietary phytochemicals inhibiting the efflux transporter breast cancer resistance protein (BCRP/ABCG2)*. Food Chemistry*, 138(4), 2267-2274.

134. Hanahan, D. and Weinberg, R.A., (2000). The hallmarks of cancer*. Cell*, 100(1), 57-70.

135. Hanahan, D. and Weinberg, R.A., (2011). Hallmarks of cancer: The next generation*. Cell*, 144(5), 646-674.

136. Warburg, O., Posener, K.and Negelein, E., (1924). On the metabolism of carcinoma cells*. Biochemische Zeitschrift*, 152 309-344.

137. Pavlova, N.N. and Thompson, C.B., (2016). The emerging hallmarks of cancer metabolism*. Cell Metabolism*, 23(1), 27-47.

138. Budczies, J., Denkert, C., Muller, B.M., Brockmoller, S.F., Klauschen, F., Gyorffy, B., Dietel, M., Richter-Ehrenstein, C., Marten, U., Salek, R.M., Griffin, J.L., Hilvo, M., Oresic, M., Wohlgemuth, G.and Fiehn, O., (2012). Remodeling of central metabolism in invasive breast cancer compared to normal breast tissue - a GC-TOFMS based metabolomics study*. Bmc Genomics*, 13, 334.

139. More, T.H., RoyChoudhury, S., Christie, J., Taunk, K., Mane, A., Santra, M.K., Chaudhury, K.and Rapole, S., (2018). Metabolomic alterations in invasive ductal carcinoma of breast: A comprehensive metabolomic study using tissue and serum samples*. Oncotarget*, 9(2), 2678-2696.

140. Tayyari, F., Gowda, G.A.N., Olopade, O.F., Berg, R., Yang, H.H., Lee, M.P., Ngwa, W.F., Mittal, S.K., Raftery, D.and Mohammed, S.I., (2018). Metabolic profiles of triple-negative and luminal A breast cancer subtypes in African-American identify key metabolic differences*. Oncotarget*, 9(14), 11677-11690.

141. Dias, A.S., Almeida, C.R., Helguero, L.A.and Duarte, I.F., (2019). Metabolic crosstalk in the breast cancer microenvironment. *European Journal of Cancer*, 121 154-171.

142. Tan, J. and Le, A., (2018). Breast cancer metabolism. *Heterogeneity of Cancer Metabolism*, 1063 83-93.

143. Adekola, K., Rosen, S.T.and Shanmugam, M., (2012). Glucose transporters in cancer metabolism. *Current Opinion in Oncology*, 24(6), 650-4.

144. Mueckler, M. and Thorens, B., (2013). The SLC2 (GLUT) family of membrane transporters. *Molecular Aspects of Medicine*, 34(2-3), 121-38.

145. Szablewski, L., (2013). Expression of glucose transporters in cancers. *Biochimica et Biophysica Acta*, 1835(2), 164-9.

146. Navale, A.M. and Paranjape, A.N., (2016). Glucose transporters: physiological and pathological roles. *Biophysical Reviews*, 8(1), 5-9.

147. Wang, J., Ye, C., Chen, C., Xiong, H., Xie, B., Zhou, J., Chen, Y., Zheng, S.and Wang, L., (2017). Glucose transporter GLUT1 expression and clinical outcome in solid tumors: a systematic review and meta-analysis. *Oncotarget*, 8(10), 16875-16886.

148. Choi, J., Jung, W.H.and Koo, J.S., (2013). Metabolism-related proteins are differentially expressed according to the molecular subtype of invasive breast cancer defined by surrogate immunohistochemistry. *Pathobiology*, 80(1), 41-52.

149. Krzeslak, A., Wojcik-Krowiranda, K., Forma, E., Jozwiak, P., Romanowicz, H., Bienkiewicz, A.and Brys, M., (2012). Expression of GLUT1 and GLUT3 glucose transporters in endometrial and breast cancers. *Pathology & Oncology Research*, 18(3), 721-728.

150. Heiden, M.G.V., Cantley, L.C.and Thompson, C.B., (2009). Understanding the Warburg effect: The metabolic requirements of cell proliferation. *Science*, 324(5930), 1029-1033.

151. Cantor, J.R. and Sabatini, D.M., (2012). Cancer cell metabolism: One hallmark, many faces. *Cancer Discovery*, 2(10), 881-898.

152. Brauer, H.A., Makowski, L., Hoadley, K.A., Casbas-Hernandez, P., Lang, L.J., Roman-Perez, E., D'Arcy, M., Freemerman, A.J., Perou, C.M.and Troester, M.A., (2013). Impact of tumor microenvironment and epithelial phenotypes on metabolism in breast cancer. *Clinical Cancer Research*, 19(3), 571-585.

153. Willmann, L., Schlimpert, M., Halbach, S., Erbes, T., Stickeler, E.and Kammerer, B., (2015). Metabolic profiling of breast cancer: Differences in central metabolism between subtypes of breast cancer cell lines. *Journal of Chromatography B-Analytical Technologies in the Biomedical and Life Sciences*, 1000 95-104.

154. Lanning, N.J., Castle, J.P., Singh, S.J., Leon, A.N., Tovar, E.A., Sanghera, A., MacKeigan, J.P., Filipp, F.V.and Graveel, C.R., (2017). Metabolic profiling of triple-negative breast cancer cells reveals metabolic vulnerabilities. *Cancer & Metabolism*, 5(6).

155. Rempel, A., Bannasch, P.and Mayer, D., (1994). Differences in expression and intracellular distribution of hexokinase isoenzymes in rat liver cells of different transformation stages. *Biochimica et Biophysica Acta (BBA) - Gene Structure and Expression*, 1219(3), 660-668.

156. Pedersen, P.L., Mathupala, S., Rempel, A., Geschwind, J.F.and Ko, Y.H., (2002). Mitochondrial bound type II hexokinase: a key player in the growth and survival of many cancers and an ideal prospect for therapeutic intervention. *Biochimica et Biophysica Acta*, 1555(1-3), 14-20.

157. Gudnason, V., Ingvarsson, S., Jonasdottir, A., Andresdottir, V.and Egilsson, V., (1984). Isoenzyme pattern and subcellular-localization of hexokinases in human-breast cancer and nonpathological breast-tissue. *International Journal of Cancer*, 34(1), 63-66.

158. Brown, R.S., Goodman, T.M., Zasadny, K.R., Greenson, J.K.and Wahl, R.L., (2002). Expression of hexokinase II and Glut-1 in untreated human breast cancer. *Nuclear Medicine and Biology*, 29(4), 443-453.

159. Patra, K.C., Wang, Q., Bhaskar, P.T., Miller, L., Wang, Z.B., Wheaton, W., Chandel, N., Laakso, M., Muller, W.J., Allen, E.L., Jha, A.K., Smolen, G.A., Clasquin, M.F., Robey, R.B.and Hay, N., (2013). Hexokinase 2 Is required for tumor initiation and maintenance and its systemic deletion is therapeutic in mouse models of cancer. *Cancer Cell*, 24(2), 213-228.

160. Yang, T.T., Ren, C., Qiao, P.Y., Han, X., Wang, L., Lv, S.J., Sun, Y.H., Liu, Z.J., Du, Y.and Yu, Z.H., (2018). PIM2-mediated phosphorylation of hexokinase 2 is critical for tumor growth and paclitaxel resistance in breast cancer. *Oncogene*, 37(45), 5997-6009.

161. Yalcin, A., Telang, S., Clem, B.and Chesney, J., (2009). Regulation of glucose metabolism by 6-phosphofructo-2-kinase/fructose-2,6-bisphosphatases in cancer. *Experimental and Molecular Pathology*, 86(3), 174-9.

162. Scatena, R., Bottoni, P., Pontoglio, A., Mastrototaro, L.and Giardina, B., (2008). Glycolytic enzyme inhibitors in cancer treatment. *Expert Opinion on Investigational Drugs*, 17(10), 1533-45.

163. Lincet, H. and Icard, P., (2014). How do glycolytic enzymes favour cancer cell proliferation by nonmetabolic functions? *Oncogene*, 34(29), 3751-9.

164. Hennipman, A., Smits, J., Vanoirschot, B., Vanhouwelingen, J.C., Rijksen, G., Neyt, J.P., Vanunnik, J.A.M.and Staal, G.E.J., (1987). Glycolytic-enzymes in breast-cancer, benign breast disease and normal breast-tissue. *Tumor Biology*, 8(5), 251-263.

165. El-Bacha, T., de Freitas, M.S.and Sola-Penna, M., (2003). Cellular distribution of phosphofructokinase activity and implications to metabolic regulation in human breast cancer. *Molecular Genetics and Metabolism*, 79(4), 294-299.

166. Zancan, P., Sola-Penna, M., Furtado, C.M.and Da Silva, D., (2010). Differential expression of phosphofructokinase-1 isoforms correlates with the glycolytic efficiency of breast cancer cells. *Molecular Genetics and Metabolism*, 100(4), 372-378.

167. Wang, G.N., Xu, Z.L., Wang, C.H., Yao, F., Li, J.J., Chen, C.and Sun, S.R., (2013). Differential phosphofructokinase-1 isoenzyme patterns associated with glycolytic efficiency in human breast cancer and paracancer tissues. *Oncology Letters*, 6(6), 1701-1706.

168. O'Neal, J., Clem, A., Reynolds, L., Dougherty, S., Imbert-Fernandez, Y., Telang, S., Chesney, J.and Clem, B.F., (2016). Inhibition of 6-phosphofructo-2-kinase (PFKFB3) suppresses glucose metabolism and the growth of HER2+ breast cancer. *Breast Cancer Research and Treatment*, 160(1), 29-40.

169. Peng, F., Li, Q., Sun, J.Y., Luo, Y., Chen, M.and Bao, Y., (2018). PFKFB3 is involved in breast cancer proliferation, migration, invasion and angiogenesis. *International Journal of Oncology*, 52(3), 945-954.

170. He, X., Du, S., Lei, T., Li, X., Liu, Y., Wang, H., Tong, R.and Wang, Y., (2017). PKM2 in carcinogenesis and oncotherapy. *Oncotarget*, 8(66), 110656-110670.

171. Dayton, T.L., Jacks, T.and Vander Heiden, M.G., (2016). PKM2, cancer metabolism, and the road ahead. *EMBO Reports*, 17(12), 1721-1730.

172. Yang, Y.M., Wu, K., Liu, Y.L., Shi, L., Tao, K.X.and Wang, G.B., (2017). Prognostic significance of metabolic enzyme pyruvate kinase M2 in breast cancer A meta-analysis. *Medicine*, 96(46), e8690.

173. Yang, M. and Vousden, K.H., (2016). Serine and one-carbon metabolism in cancer. *Nature Reviews Cancer*, 16(10), 650-662.

174. Locasale, J.W., (2013). Serine, glycine and one-carbon units: cancer metabolism in full circle. *Nature Reviews Cancer*, 13(8), 572-83.

175. Possemato, R., Marks, K.M., Shaul, Y.D., Pacold, M.E., Kim, D., Birsoy, K., Sethumadhavan, S., Woo, H.K., Jang, H.G., Jha, A.K., *et al.*, (2011). Functional genomics reveal that the serine synthesis pathway is essential in breast cancer. *Nature*, 476(7360), 346-U119.

176. Chen, J.Y., Chung, F., Yang, G.Z., Pu, M.Y., Gao, H., Jiang, W., Yin, H., Capka, V., Kasibhatla, S., Laffitte, B., Jaeger, S., Pagliarini, R., Chen, Y.Y.and Zhou, W.L., (2013). Phosphoglycerate dehydrogenase is dispensable for breast tumor maintenance and growth. *Oncotarget*, 4(12), 2502-2511.

177. Locasale, J.W., Grassian, A.R., Melman, T., Lyssiotis, C.A., Mattaini, K.R., Bass, A.J., Heffron, G., Metallo, C.M., Muranen, T., Sharfi, H., *et al.*, (2011). Phosphoglycerate dehydrogenase diverts glycolytic flux and contributes to oncogenesis. *Nature Genetics*, 43(9), 869-U79.

178. Kim, S.K., Jung, W.H.and Koo, J.S., (2014). Differential expression of enzymes associated with serine/glycine metabolism in different breast cancer subtypes. *Plos One*, 9(6), e101004.

179. Michalak, K.P., Mackowska-Kedziora, A., Sobolewski, B.and Wozniak, P., (2015). Key roles of glutamine pathways in reprogramming the cancer metabolism. *Oxidative Medicine and Cellular Longevity*, 2015 964321.

180. Kung, H.N., Marks, J.R.and Chi, J.T., (2011). Glutamine synthetase is a genetic determinant of cell type-specific glutamine independence in breast epithelia. *Plos Genetics*, 7(8), e1002229.

181. Timmerman, L.A., Holton, T., Yuneva, M., Louie, R.J., Padro, M., Daemen, A., Hu, M., Chan, D.A., Ethier, S.P., van 't Veer, L.J., Polyak, K., McCormick, F.and Gray, J.W., (2013). Glutamine sensitivity analysis identifies the xCT antiporter as a common triple-negative breast tumor therapeutic target. *Cancer Cell*, 24(4), 450-465.

182. Gross, M.I., Demo, S.D., Dennison, J.B., Chen, L., Chernov-Rogan, T., Goyal, B., Janes, J.R., Laidig, G.J., Lewis, E.R., Li, J., MacKinnon, A.L., Parlati, F., Rodriguez, M.L.M., Shwonek, P.J., Sjogren, E.B., Stanton, T.F., Wang, T.T., Yang, J.F., Zhao, F.and Bennett, M.K., (2014). Antitumor activity of the glutaminase inhibitor CB-839 in triple-negative breast cancer. *Molecular Cancer Therapeutics*, 13(4), 890-901.

183. Martinez-Outschoorn, U.E., Peiris-Pages, M., Pestell, R.G., Sotgia, F.and Lisanti, M.P., (2017). Cancer metabolism: a therapeutic perspective. *Nature Reviews Clinical Oncology*, 14(1), 11-31.

184. Kim, S., Kim, D.H., Jung, W.H.and Koo, J.S., (2013). Expression of glutamine metabolism-related proteins according to molecular subtype of breast cancer. *Endocrine-Related Cancer*, 20(3), 339-348.

185. Kim, J.Y., Heo, S.H., Choi, S., Song, I.H., Park, I.A., Kim, Y.A., Park, H.S., Park, S.Y., Bang, W.S., Gong, G.and Lee, H.J., (2017). Glutaminase expression is a poor prognostic factor in node-positive triple-negative breast cancer patients with a high level of tumor-infiltrating lymphocytes. *Virchows Archiv*, 470(4), 381-389.

186. Lampa, M., Arlt, H., He, T., Ospina, B., Reeves, J., Zhang, B.L., Murtie, J., Deng, G.J., Barberis, C., Hoffmann, D., Cheng, H., Pollard, J., Winter, C., Richon, V., Garcia-Escheverria, C., Adrian, F., Wiederschain, D.and Srinivasan, L., (2017). Glutaminase is essential for the growth of triple-negative breast cancer cells with a deregulated glutamine metabolism pathway and its suppression synergizes with mTOR inhibition. *Plos One*, 12(9), e0185092.

187. Imanishi, H., Hattori, K., Wada, R., Ishikawa, K., Fukuda, S., Takenaga, K., Nakada, K.and Hayashi, J.I., (2011). Mitochondrial DNA mutations regulate metastasis of human breast cancer cells. *Plos One*, 6(8), e23401.

188. Santidrian, A.F., Matsuno-Yagi, A., Ritland, M., Seo, B.B., LeBoeuf, S.E., Gay, L.J., Yagi, T.and Felding-Habermann, B., (2013). Mitochondrial complex I activity and NAD(+)/NADH balance regulate breast cancer progression. *Journal of Clinical Investigation*, 123(3), 1068-1081.

189. McFate, T., Mohyeldin, A., Lu, H., Thakar, J., Henriques, J., Halim, N.D., Wu, H., Schell, M.J., Tsang, T.M., Teahan, O., Zhou, S., Califano, J.A., Jeoung, N.H., Harris, R.A.and Verma, A., (2008). Pyruvate dehydrogenase complex activity controls metabolic and malignant phenotype in cancer cells. *Journal of Biological Chemistry*, 283(33), 22700-8.

190. Zimmer, A.D., Walbrecq, G., Kozar, I., Behrmann, I.and Haan, C., (2016). Phosphorylation of the pyruvate dehydrogenase complex precedes HIF-1-mediated effects and pyruvate dehydrogenase kinase 1 upregulation during the first hours of hypoxic treatment in hepatocellular carcinoma cells. *Hypoxia (Auckl)*, 4 135-145.

191. Eastlack, S.C., Dong, S.L., Ivan, C.and Alahari, S.K., (2018). Suppression of PDHX by microRNA-27b deregulates cell metabolism and promotes growth in breast cancer. *Molecular Cancer*, 17(1), 100.

192. Luengo, A., Gui, D.Y.and Vander Heiden, M.G., (2017). Targeting metabolism for cancer therapy. *Cell Chemical Biology*, 24(9), 1161-1180.

193. Kim, S., Kim, D.H., Jung, W.H.and Koo, J.S., (2013). Succinate dehydrogenase expression in breast cancer. *Springerplus*, 2(1), 299.

194. Privat, M., Radosevic-Robin, N., Aubel, C., Cayre, A., Penault-Llorca, F., Marceau, G., Sapin, V., Bignon, Y.J.and Morvan, D., (2014). BRCA1 induces major energetic metabolism reprogramming in breast cancer cells. *Plos One*, 9(7), e102438.

195. Hilvo, M., Denkert, C., Lehtinen, L., Muller, B., Brockmoller, S., Seppanen-Laakso, T., Budczies, J., Bucher, E., Yetukuri, L., Castillo, S., Berg, E., Nygren, H., Sysi-Aho, M., Griffin, J.L., Fiehn, O., Loibl, S., Richter-Ehrenstein, C., Radke, C., Hyotylainen, T., Kallioniemi, O., Iljin, K.and Oresic, M., (2011). Novel theranostic opportunities offered by characterization of altered membrane lipid metabolism in breast cancer progression. *Cancer Research*, 71(9), 3236-3245.

196. Tang, X.H., Lin, C.C., Spasojevic, I., Iversen, E.S., Chi, J.T.and Marks, J.R., (2014). A joint analysis of metabolomics and genetics of breast cancer. *Breast Cancer Research*, 16(4), 415.

197. Balaban, S., Lee, L.S., Varney, B., Aishah, A., Gao, Q.Q., Shearer, R.F., Saunders, D.N., Grewal, T.and Hoy, A.J., (2018). Heterogeneity of fatty acid metabolism in breast cancer cells underlies differential sensitivity to palmitate-induced apoptosis. *Molecular Oncology*, 12(9), 1623-1638.

198. Flavin, R., Peluso, S., Nguyen, P.L.and Loda, M., (2010). Fatty acid synthase as a potential therapeutic target in cancer. *Future Oncology*, 6(4), 551-62.

199. Liu, Q., Luo, Q., Halim, A.and Song, G., (2017). Targeting lipid metabolism of cancer cells: A promising therapeutic strategy for cancer. *Cancer Letters*, 401 39-45.

200. Jin, Q.R., Yuan, L.X., Boulbes, D., Baek, J.M., Wang, Y.N., Gomez-Cabello, D., Hawke, D.H., Yeung, S.C., Lee, M.H., Hortobagyi, G.N., Hung, M.C.and Esteva, F.J., (2010). Fatty acid synthase phosphorylation: a novel therapeutic target in HER2-overexpressing breast cancer cells. *Breast Cancer Research*, 12(6), R96.

201. Katz-Brull, R., Seger, D., Rivenson-Segal, D., Rushkin, E.and Degani, H., (2002). Metabolic markers of breast cancer: Enhanced choline metabolism and reduced choline-ether-phospholipid synthesis. *Cancer Research*, 62(7), 1966-1970.

202. Glunde, K., Penet, M.F., Jiang, L., Jacobs, M.A.and Bhujwalla, Z.M., (2015). Choline metabolism-based molecular diagnosis of cancer: an update. *Expert Review of Molecular Diagnostics*, 15(6), 735-747.

203. Haukaas, T.H., Euceda, L.R., Giskeodegard, G.F.and Bathen, T.F., (2017). Metabolic portraits of breast cancer by HR MAS MR spectroscopy of intact tissue samples. *Metabolites*, 7(2), E18.

204. de Molina, A.R., Gutierrez, R., Ramos, M.A., Silva, J.M., Silva, J., Bonilla, F., Sanchez, J.J.and Lacal, J.C., (2002). Increased choline kinase activity in human breast carcinomas: clinical evidence for a potential novel antitumor strategy. *Oncogene*, 21(27), 4317-4322.

205. Shah, T., Wildes, F., Penet, M.F., Winnard, P.T., Glunde, K., Artemov, D., Ackerstaff, E., Gimi, B., Kakkad, S., Raman, V.and Bhujwalla, Z.M., (2010). Choline kinase overexpression increases invasiveness and drug resistance of human breast cancer cells. *NMR in Biomedicine*, 23(6), 633-642.

206. Farber, S., Diamond, L.K., Mercer, R.D., Sylvester, R.F.and Wolff, J.A., (1948). Temporary remissions in acute leukemia in children produced by folic acid antagonist, 4-aminopteroyl-glutamic acid (aminopterin). *New England Journal of Medicine*, 238(23), 787-793.

207. Heidelberger, C., Chaudhuri, N.K., Danneberg, P., Mooren, D., Griesbach, L., Duschinsky, R., Schnitzer, R.J., Pleven, E.and Scheiner, J., (1957). Fluorinated Pyrimidines, a new class of tumour-inhibitory compounds. *Nature*, 179(4561), 663-666.

208. Vander Heiden, M.G., (2011). Targeting cancer metabolism: a therapeutic window opens. *Nature Reviews Drug Discovery*, 10(9), 671-684.

209. Galluzzi, L., Kepp, O., Vander Heiden, M.G.and Kroemer, G., (2013). Metabolic targets for cancer therapy. *Nature Reviews Drug Discovery*, 12(11), 829-846.

210. Bobrovnikova-Marjon, E. and Hurov, J.B., *Targeting Metabolic Changes in Cancer: Novel Therapeutic Approaches*, in *Annual Review of Medicine, Vol 65*. 2014. p. 157-170.

211. Cairns, R.A., Harris, I.S.and Mak, T.W., (2011). Regulation of cancer cell metabolism. *Nature Reviews Cancer*, 11(2), 85-95.

212. Guerra, A.R., Duarte, M.F.and Duarte, I.F., (2018). Targeting tumor metabolism with plant-derived natural products: emerging trends in cancer therapy. *Journal of Agricultural and Food Chemistry*, 66(41), 10663-10685.

213. Pandita, A., Kumar, B., Manvati, S., Vaishnavi, S., Singh, S.K.and Bamezai, R.N., (2014). Synergistic combination of gemcitabine and dietary molecule induces apoptosis in pancreatic cancer cells and down regulates PKM2 expression. *Plos One*, 9(9), e107154.

214. Potze, L., Di Franco, S., Grandela, C., Pras-Raves, M.L., Picavet, D.I., van Veen, H.A., van Lenthe, H., Mullauer, F.B., van der Wel, N.N., Luyf, A., van Kampen, A.H.C., Kemp, S., Everts, V., Kessler, J.H., Vaz, F.M.and Medema, J.P., (2015). Betulinic acid induces a novel cell death pathway that depends on cardiolipin modification. *Oncogene*, 35(4), 427-437.

215. Wang, J.C., Jiang, Z., Xiang, L.P., Li, Y.F., Ou, M.R., Yang, X., Shao, J.W., Lu, Y.S., Lin, L.F., Chen, J.Z., Dai, Y.and Jia, L., (2014). Synergism of ursolic acid derivative US597 with 2-deoxy-D-glucose to preferentially induce tumor cell death by dual-targeting of apoptosis and glycolysis. *Scientific Reports*, 4, 5006.

216. Chen, X., Zhang, J.B., Yuan, L.X., Lay, Y.F., Wong, Y.K., Lim, T.K., Ong, C.S., Lin, Q.S., Wang, J.G.and Hua, Z.C., (2017). Andrographolide suppresses MV4-11 cell proliferation through the inhibition of FLT3 signaling, fatty acid synthesis and cellular iron uptake. *Molecules*, 22(9), e1444.

217. Liu, W., Furuta, E., Shindo, K., Watabe, M., Xing, F., Pandey, P.R., Okuda, H., Pai, S.K., Murphy, L.L., Cao, D.L., Mo, Y.Y., Kobayashi, A., Iiizumi, M., Fukuda, K., Xia, B.and Watabe, K., (2011). Cacalol, a natural sesquiterpene, induces apoptosis in breast cancer cells by modulating Akt-SREBP-FAS signaling pathway. *Breast Cancer Research and Treatment*, 128(1), 57-68.

218. Hu, Y., Qi, Y., Liu, H., Fan, G.and Chai, Y., (2013). Effects of celastrol on human cervical cancer cells as revealed by ion-trap gas chromatography-mass spectrometry based metabolic profiling. *Biochimica et Biophysica Acta*, 1830(3), 2779-89.

219. Mi, Y.J., Geng, G.J., Zou, Z.Z., Gao, J., Luo, X.Y., Liu, Y., Li, N., Li, C.L., Chen, Y.Q., Yu, X.Y.and Jiang, J., (2015). Dihydroartemisinin inhibits glucose uptake and cooperates with

glycolysis inhibitor to induce apoptosis in non-small cell lung carcinoma cells. *Plos One*, 10(3), e0120426.

220. Jiang, J., Geng, G., Yu, X., Liu, H., Gao, J., An, H., Cai, C., Li, N., Shen, D., Wu, X., Zheng, L., Mi, Y.and Yang, S., (2016). Repurposing the anti-malarial drug dihydroartemisinin suppresses metastasis of non-small-cell lung cancer via inhibiting NF-kappaB/GLUT1 axis. *Oncotarget*, 7(52), 87271-87283.

221. Chen, X., Wong, Y.K., Lim, T.K., Lim, W.H., Lin, Q.S., Wang, J.G.and Hua, Z.C., (2017). Artesunate activates the intrinsic apoptosis of HCT116 cells through the suppression of fatty acid synthesis and the NF-kappa B pathway. *Molecules*, 22(8), E1272.

222. Eskandani, M., Abdolalizadeh, J., Hamishehkar, H., Nazemiyeh, H.and Barar, J., (2015). Galbanic acid inhibits HIF-1 alpha expression via EGFR/HIF-1 alpha pathway in cancer cells. *Fitoterapia*, 101 1-11.

223. Duncan, R.E., Lau, D., El-Sohemy, A.and Archer, M.C., (2004). Geraniol and beta-ionone inhibit proliferation, cell cycle progression, and cyclin-dependent kinase 2 activity in MCF-7 breast cancer cells independent of effects on HMG-CoA reductase activity. *Biochemical Pharmacology*, 68(9), 1739-47.

224. Polo, M.P. and de Bravo, M.G., (2006). Effect of geraniol an fatty-acid and mevalonate metabolism in the human hapatoma cell line Hep G2. *Biochemistry and Cell Biology-Biochimie Et Biologie Cellulaire*, 84(1), 102-111.

225. Crespo, R., Villegas, S.M., Abba, M.C., de Bravo, M.G.and Polo, M.P., (2013). Transcriptional and posttranscriptional inhibition of HMGCR and PC biosynthesis by geraniol in 2 Hep-G2 cell proliferation linked pathways. *Biochemistry and Cell Biology-Biochimie Et Biologie Cellulaire*, 91(3), 131-139.

226. Kim, S.H., Park, E.J., Lee, C.R., Chun, J.N., Cho, N.H., Kim, I.G., Lee, S., Kim, T.W., Park, H.H., So, I.and Jeon, J.H., (2012). Geraniol induces cooperative interaction of apoptosis and autophagy to elicit cell death in PC-3 prostate cancer cells. *International Journal of Oncology*, 40(5), 1683-90.

227. Iwao, C. and Shidoji, Y., (2015). Upregulation of energy metabolism-related, p53-target TIGAR and SCO2 in HuH-7 cells with p53 mutation by geranylgeranoic acid treatment. *Biomedical Research*, 36(6), 371-81.

228. Li, J., Liu, T., Zhao, L., Chen, W., Hou, H., Ye, Z.and Li, X., (2015). Ginsenoside 20(S)Rg3 inhibits the Warburg effect through STAT3 pathways in ovarian cancer cells. *International Journal of Oncology,* 46(2), 775-81.

229. Liu, J., Wu, N., Ma, L.N., Liu, M., Liu, G., Zhang, Y.Y.and Lin, X.K., (2014). Oleanolic acid suppresses aerobic glycolysis in cancer cells by switching pyruvate kinase type M isoforms. *Plos One*, 9(3), 91606.

230. Liu, J., Zheng, L.H., Wu, N., Ma, L.N., Zhong, J.T., Liu, G.and Lin, X.K., (2014). Oleanolic acid induces metabolic adaptation in cancer cells by activating the AMP-activated protein kinase pathway. *Journal of Agricultural and Food Chemistry*, 62(24), 5528-5537.

231. Amara, S., Zheng, M.and Tiriveedhi, V., (2016). Oleanolic acid inhibits high salt-induced exaggeration of Warburg-like metabolism in breast cancer cells. *Cell Biochemistry and Biophysics*, 74(3), 427-434.

232. Hughes, D.T., Martel, P.M., KinlaU, W.B.and Eisenberg, B.L., (2008). The synthetic triterpenoid CDDO-Im inhibits fatty acid synthase expression and has anti proliferative and proapoptotic effects in human liposarcoma cells. *Cancer Investigation*, 26(2), 118-127.

233. Yao, Z., Xie, F., Li, M., Liang, Z., Xu, W., Yang, J., Liu, C., Li, H., Zhou, H.and Qu, L.H., (2017). Oridonin induces autophagy via inhibition of glucose metabolism in p53-mutated colorectal cancer cells. *Cell Death and Disease*, 8(2), e2633.

234. Kwan, H.Y., Yang, Z., Fong, W.F., Hu, Y.M., Yu, Z.L.and Hsiao, W.L., (2013). The anticancer effect of oridonin is mediated by fatty acid synthase suppression in human colorectal cancer cells. *Journal of Gastroenterology*, 48(2), 182-92.

235. Gu, Z., Wang, X., Qi, R., Wei, L., Huo, Y., Ma, Y., Shi, L., Chang, Y., Li, G.and Zhou, L., (2015). Oridonin induces apoptosis in uveal melanoma cells by upregulation of Bim and downregulation of Fatty Acid Synthase. *Biochemical and Biophysical Research Communications*, 457(2), 187-93.

236. Youn, S.H., Lee, J.S., Lee, M.S., Cha, E.Y., Thuong, P.T., Kim, J.R.and Chang, E.S., (2012). Anticancer properties of pomolic acid-induced AMP-activated protein kinase activation in MCF7 human breast cancer cells. *Biological & Pharmaceutical Bulletin*, 35(1), 105-110.

237. Lee, J.S., Yoon, I.S., Lee, M.S., Cha, E.Y., Thuong, P.T., Diep, T.T.and Kim, J.R., (2013). Anticancer activity of pristimerin in epidermal growth factor receptor 2-positive SKBR3 human breast cancer cells. *Biological & Pharmaceutical Bulletin*, 36(2), 316-325.

238. Yao, G.D., Yang, J., Li, X.X., Song, X.Y., Hayashi, T., Tashiro, S.I., Onodera, S., Song, S.J.and Ikejima, T., (2017). Blocking the utilization of glucose induces the switch from senescence to apoptosis in pseudolaric acid B-treated human lung cancer cells in vitro. *Acta Pharmacologica Sinica*, 38(10), 1401-1411.

239. Lin, L.L., Hsia, C.R., Hsu, C.L., Huang, H.C.and Juan, H.F., (2015). Integrating transcriptomics and proteomics to show that tanshinone IIA suppresses cell growth by blocking glucose metabolism in gastric cancer cells. *Bmc Genomics*, 16, 41.

240. Zhang, H.S., Zhang, F.J., Li, H., Liu, Y., Du, G.Y.and Huang, Y.H., (2016). Tanshinone A inhibits human esophageal cancer cell growth through miR-122-mediated PKM2 down-regulation. *Archives of Biochemistry and Biophysics*, 598 50-6.

241. Guerram, M., Jiang, Z.Z., Yousef, B.A., Hamdi, A.M., Hassan, H.M., Yuan, Z.Q., Luo, H.W., Zhu, X.and Zhang, L.Y., (2015). The potential utility of acetyltanshinone IIA in the treatment of HER2-overexpressed breast cancer: Induction of cancer cell death by targeting apoptotic and metabolic signaling pathways. *Oncotarget*, 6(26), 21865-21877.

242. Cheng, J., Lan, W., Zheng, G.and Gao, X., *Metabolomics: A high-throughput platform for metabolite profile exploration*, in *Computational Systems Biology*. 2018, Springer. p. 265-292.

243. Rinschen, M.M., Ivanisevic, J., Giera, M.and Siuzdak, G., (2019). Identification of bioactive metabolites using activity metabolomics. *Nature Reviews Molecular Cell Biology*, 20(6), 353-367.

244. Kaushik, A.K. and DeBerardinis, R.J., (2018). Applications of metabolomics to study cancer metabolism. *Biochimica Et Biophysica Acta-Reviews on Cancer*, 1870(1), 2-14.

245. McCartney, A., Vignoli, A., Biganzoli, L., Love, R., Tenori, L., Luchinat, C.and Di Leo, A., (2018). Metabolomics in breast cancer: A decade in review. *Cancer Treatment Reviews*, 67 88-96.

246. Emwas, A.H., Roy, R., McKay, R.T., Tenori, L., Saccenti, E., Gowda, G.A.N., Raftery, D., Alahmari, F., Jaremko, L., Jaremko, M.and Wishart, D.S., (2019). NMR Spectroscopy for Metabolomics Research. *Metabolites*, 9(7), E123.

247. Bingol, K. and Bruschweiler, R., (2015). Two elephants in the room: new hybrid nuclear magnetic resonance and mass spectrometry approaches for metabolomics. *Current Opinion in Clinical Nutrition and Metabolic Care*, 18(5), 471-7.

248. Markley, J.L., Bruschweiler, R., Edison, A.S., Eghbalnia, H.R., Powers, R., Raftery, D.and Wishart, D.S., (2017). The future of NMR-based metabolomics. *Current Opinion in Biotechnology*, 43 34-40.

249. Zerbe, O. and Jurt, S., *Applied NMR spectroscopy for chemists and life scientists*, 2013, John Wiley & Sons.

250. Trygg, J., Holmes, E.and Lundstedt, T., (2007). Chemometrics in metabonomics. *Journal of Proteome Research*, 6(2), 469-479.

251. Gribbestad, I.S., Fjosne, H.E., Haugen, O.A., Nilsen, G., Krane, J., Petersen, S.B.and Kvinnsland, S., (1993). In-vitro proton NMR-spectroscopy of extracts from human breast-tumors and noninvolved breast-tissue. *Anticancer Research*, 13(6A), 1973-1980.

252. Mackinnon, W.B., Barry, P.A., Malycha, P.L., Gillett, D.J., Russell, P., Lean, C.L., Doran, S.T., Barraclough, B.H., Bilous, M.and Mountford, C.E., (1997). Fine-needle biopsy specimens of benign breast lesions distinguished from invasive cancer ex vivo with proton MR spectroscopy. *Radiology*, 204(3), 661-666.

253. Cheng, L.L., Chang, I.W., Smith, B.L.and Gonzalez, R.G., (1998). Evaluating human breast ductal carcinomas with high-resolution magic-angle spinning proton magnetic resonance spectroscopy. *Journal of Magnetic Resonance*, 135(1), 194-202.

254. Mountford, C.E., Somorjai, R.L., Malycha, P., Gluch, L., Lean, C., Russell, P., Barraclough, B., Gillett, D., Himmelreich, U., Dolenko, B., Nikulin, A.E.and Smith, I.C.P., (2001). Diagnosis and prognosis of breast cancer by magnetic resonance spectroscopy of fine-needle aspirates analysed using a statistical classification strategy. *British Journal of Surgery*, 88(9), 1234-1240.

255. Sitter, B., Lundgren, S., Bathen, T.F., Halgunset, J., Fjosne, H.E.and Gribbestad, I.S., (2006). Comparison of HR MAS MR spectroscopic profiles of breast cancer tissue with clinical parameters. *NMR in Biomedicine*, 19(1), 30-40.

256. Li, M., Song, Y., Cho, N., Chang, J.M., Koo, H.R., Yi, A., Kim, H., Park, S.and Moon, W.K., (2011). An HR-MAS MR metabolomics study on breast tissues obtained with core needle biopsy. *Plos One*, 6(10), e25563.

257. Bathen, T.F., Geurts, B., Sitter, B., Fjosne, H.E., Lundgren, S., Buydens, L.M., Gribbestad, I.S., Postma, G.and Giskeodegard, G.F., (2013). Feasibility of MR metabolomics for immediate analysis of resection margins during breast cancer surgery. *Plos One*, 8(4), e61578.

258. Giskeodegard, G.F., Grinde, M.T., Sitter, B., Axelson, D.E., Lundgren, S., Fjosne, H.E., Dahl, S., Gribbestad, I.S.and Bathen, T.F., (2010). Multivariate modeling and prediction of breast cancer prognostic factors using MR metabolomics. *Journal of Proteome Research*, 9(2), 972-979.

259. Borgan, E., Sitter, B., Lingjaerde, O.C., Johnsen, H., Lundgren, S., Bathen, T.F., Sorlie, T., Borresen-Dale, A.L.and Gribbestad, I.S., (2010). Merging transcriptomics and metabolomics - advances in breast cancer profiling. *Bmc Cancer*, 10, 628.

260. Moestue, S.A., Borgan, E., Huuse, E.M., Lindholm, E.M., Sitter, B., Borresen-Dale, A.L., Engebraaten, O., Maelandsmo, G.M.and Gribbestad, I.S., (2010). Distinct choline metabolic profiles are associated with differences in gene expression for basal-like and luminal-like breast cancer xenograft models. *Bmc Cancer*, 10, 433.

261. Cao, M.D., Lamichhane, S., Lundgren, S., Bofin, A., Fjosne, H., Giskeodegard, G.F.and Bathen, T.F., (2014). Metabolic characterization of triple negative breast cancer. *Bmc Cancer*, 14, 941.

262. Maria, R.M., Altei, W.F., Andricopulo, A.D., Becceneri, A.B., Cominetti, M.R., Venancio, T.and Colnago, L.A., (2015). Characterization of metabolic profile of intact non-tumor and tumor breast cells by high-resolution magic angle spinning nuclear magnetic resonance spectroscopy. *Analytical Biochemistry*, 488 14-18.

263. Lefort, N., Brown, A., Lloyd, V., Ouellette, R., Touaibia, M., Culf, A.S.and Cuperlovic-Culf, M., (2014). H-1 NMR metabolomics analysis of the effect of dichloroacetate and allopurinol on breast cancers. *Journal of Pharmaceutical and Biomedical Analysis*, 93 77-85.

264. Lane, A.N., Tan, J., Wang, Y.L., Yan, J., Higashi, R.M.and Fan, T.W.M., (2017). Probing the metabolic phenotype of breast cancer cells by multiple tracer stable isotope resolved metabolomics. *Metabolic Engineering*, 43 125-136.

265. Jager, W., Gruber, A., Giessrigl, B., Krupitza, G., Szekeres, T.and Sonntag, D., (2011). Metabolomic analysis of resveratrol-induced effects in the human breast cancer cell lines MCF-7 and MDA-MB-231. *OMICS*, 15(1-2), 9-14.

266. Bayet-Robert, M. and Morvan, D., (2013). Metabolomics reveals metabolic targets and biphasic responses in breast cancer cells treated by curcumin alone and in association with docetaxel. *Plos One*, 8(3), e57971.

267. Engel, N., Lisec, J., Piechulla, B.and Nebe, B., (2012). Metabolic profiling reveals sphingosine-1-phosphate kinase 2 and lyase as key targets of (phyto-)estrogen action in the breast cancer cell line MCF-7 and not in MCF-12A. *Plos One*, 7(10), e47833.

268. Uifalean, A., Schneider, S., Gierok, P., Ionescu, C., Iuga, C.A.and Lalk, M., (2016). The impact of soy isoflavones on MCF-7 and MDA-MB-231 breast cancer cells using a global metabolomic approach. *International Journal of Molecular Sciences*, 17(9), e1443.

269. Poschner, S., Maier-Salamon, A., Zehl, M., Wackerlig, J., Dobusch, D., Pachmann, B., Sterlini, K.L.and Jager, W., (2017). The impacts of Genistein and Daidzein on estrogen conjugations in human breast cancer cells: A targeted metabolomics approach. *Frontiers in Pharmacology*, 8, 699.

270. Poschner, S., Maier-Salamon, A., Zehl, M., Wackerlig, J., Dobusch, D., Meshcheryakova, A., Mechtcheriakova, D., Thalhammer, T., Pachmann, B.and Jager, W., (2018). Resveratrol inhibits key steps of steroid metabolism in a human estrogen-receptor positive breast cancer model: Impact on cellular proliferation. *Frontiers in Pharmacology*, 9(742).

Chapter 2

NMR METABOLIC PROFILING OF TRIPLE NEGATIVE BREAST CANCER AND NON-TUMOR BREAST EPITHELIAL CELLS

Abstract

The present work provides a comprehensive perspective of the main metabolic differences between triple negative breast cancer (TNBC) cells (MDA-MB-231) and breast epithelial cells (MCF-10A), using a high resolution Nuclear Magnetic Resonance (NMR) metabolomics approach. Integrated analysis of the cells exometabolome with polar intracellular and lipid composition revealed major differences between TNBC and epithelial cells, with the former being characterized by: upregulated glycolytic and TCA cycle activity, relatively lower mitochondrial respiration and energetic pool, active hexosamine biosynthetic pathway, high phosphocholine content, redox imbalance with decreased levels of the endogenous antioxidant glutathione, and enrichment in neutral lipids (likely forming cytosolic droplets). These differences reflect the reprogrammed metabolic network of MDA-MB-231 breast cancer cells to meet their high demand for macromolecular biosynthesis, energy production and redox homeostasis. By providing information on preferred metabolic pathways of both cancer and epithelial breast cells, this work is important to support anticancer drug screening and development.

Keywords: Triple negative breast cancer; Cell metabolism; Metabolomics; Nuclear Magnetic Resonance (NMR) spectroscopy; Metabolic profile

2.1. Introduction

Breast cancer remains one of the most prevalent cancers worldwide, with over 2 million women diagnosed only in 2018 (1 in 4 cancer cases among women) [1]. Advances in breast cancer screening and treatment have decreased overall mortality [2], however the heterogeneous nature of breast cancer and the dreadful side-effects of treatments continue to raise a pressing need to provide safer and more effective therapies. The most aggressive breast cancer subtypes are basal-like breast carcinomas, which include some molecular features found in basal cells and others related with a subset of normal luminal cells, and represent 10-20% of all breast cancer cases [3, 4]. Triple negative breast cancers (TNBC) represent, in turn, 80% of base-like breast carcinomas and are defined as invasive breast cancers which lack the expression of estrogen receptor (ER), progesterone receptor (PR), and human epidermal growth factor receptor 2 (HER2) overexpression/HER2 gene amplification [3, 5]. This highly heterogeneous sub-group, with complex genomes and high levels of genetic instability, presents elevated rates of relapses and poor clinical outcome [6, 7].

Tumor initiation and progression strongly rely on the reprogramming of cell metabolism [8]. Therefore, targeting tumor cell metabolism to achieve therapeutic benefit in cancer treatment has been harnessing increased interest and research efforts. TNBC heterogeneity in combination with the lack of targeted therapies poses a major challenge for the development of effective treatments. Innovative approaches, such as metabolomics, may potentially aid breast cancer screening, tumor characterization and prediction of treatment response, enabling the development of more adequate treatment options [9]. Cell culture metabolomics represents a valid and convenient tool to complement data obtained from whole organism studies [10, 11]. Indeed, although tumor cell models are a limited representation of *the in vivo* tumor environment, they allow for a focused study of molecular alterations and the underlying biochemical mechanisms, under controlled conditions which reduce the confounding influence of inter-individual variability. In fact, this reduction in uncontrolled variability can uncover more subtle metabolic changes, which in turn can be correlated with data from other ‘omic’ approaches, such as genomics and proteomics [11]. High resolution Nuclear Magnetic Resonance (NMR) spectroscopy is an insightful, highly reproducible analytical technique for metabolomics, which can give both qualitative and quantitative information on a wide-range of metabolites [12]. In cancer cell studies, NMR-based metabolomics has proven to be particularly useful to uncover perturbed metabolic pathways, based on relative or absolute data on intra- or extra-cellular metabolite

levels [13]. Furthermore, the insights provided into disease biochemistry support the use of NMR spectroscopy in drug testing and development [14].

In this work, we used NMR metabolomics to investigate the basal metabolic activity and composition of a TNBC cell line (MDA-MB-231) and a non-tumorigenic epithelial cell line (MCF-10A). The variations in the intracellular and extracellular metabolome were assessed by ^{1}H NMR spectroscopy of cell extracts (aqueous and organic) and of cell culture media, respectively.

2.2. Materials and Methods

2.2.1. Chemicals

Dulbecco's Modified Eagle Medium (DMEM), DMEM/F12 medium and trypsin (0.5 g/L) / EDTA (0.2 g/L) were purchased from Biowest (Nuaillé, France). Horse serum, human epidermal growth factor, human insulin, hydrocortisone, cholera toxin sodium phosphate monobasic (NaH_2PO_4), sodium phosphate dibasic (Na_2HPO_4) and deuterium oxide containing 3-(trimethylsilyl)propionic-2,2,3,3-d_4 acid, sodium salt (D_2O/TSP, 99.9 atom % D, 0.75 wt. % TSP) were obtained from Sigma-Aldrich (St. Louis, MO, USA). Fetal bovine serum (FBS) was purchased from Gibco (Grand Island, NY, USA). D_2O (99.96%) and deuterated chloroform with 0.03% tetramethylsilane (TMS) were obtained from Euriso-top (Saint-Aubin, France). Methanol was purchased from Merk (Darmstadt, Germany) and chloroform was acquired from Normapur (VWR, Radnor, PA, USA).

2.2.2. Cell culture

The human breast cancer cell line MDA-MB-231 and the immortalized normal breast epithelial cell line MCF-10A were purchased from American Type Cell Culture (ATCC, Manassas, VA, USA). MDA-MB-231 cells were cultured in DMEM supplemented with 10% (v/v) heat-inactivated FBS. MCF-10A cells were cultured in DMEM/F12 medium, supplemented with 5% (v/v) heat-inactivated horse serum, human epidermal growth factor (20 ng/ml), human insulin (10 µg/ml), hydrocortisone (100 ng/ml) and cholera toxin (0.1 nM). The cells were maintained at 37ºC in a 5% CO_2 humidified atmosphere. For routine subculturing, cells were trypsinized with a trypsin

(0.5 g/L)/EDTA (0.2 g/L) solution and suspended in fresh growth medium before platting.

2.2.3. Sample collection and preparation for NMR analysis

MDA-MB-231 and MCF-10A cells were seeded onto 10 cm diameter Petri dishes at a density of 6 x 10^5 cells/mL and allowed to recover overnight. Then, cell culture medium was replaced by fresh complete medium and cells were incubated for 48h. Four independent assays with duplicates were performed, giving a total of eight replicate samples per cell type. Cell extracts were prepared according to Carrola *et al*. [15]. Briefly, medium was collected and centrifuged (1000*g*, 5min) and the supernatant stored at -80ºC until analysis. Culture medium without cells was placed under the same conditions and collected. Cells were washed 4 times with ice-cold PBS and 650 μL of cold methanol 80% (v/v) was added for quenching. Cells were scraped off the dish and vortexed in microcentrifuge tubes containing 0.5 mm glass beads. Next, chloroform (260 μL) and water (220 μL) were added to samples, each addition being followed by vortexing. Finally, after centrifugation (2000*g*, 15 min), aqueous and organic phases were collected and transferred to new vials. Aqueous extracts were dried under vacuum and organic extracts under a stream of nitrogen gas. All samples were stored at -80ºC. For NMR analyses, dried aqueous extracts were reconstituted in 600 μL of deuterated phosphate buffer (100 mM, pH 7.4) containing 0.1 mM TSP, while organic extracts were reconstituted in deuterated chloroform containing 0.03% TMS. As for medium samples, 540 μL of thawed medium were mixed with 60 μL of D_2O containing 0.25% TSP. 550 μL of each sample were transferred into 5 mm NMR tubes.

2.2.4. NMR data acquisition and processing

^{1}H NMR spectra of all samples were acquired on a Bruker Avance III HD 500 NMR spectrometer (University of Aveiro, Portuguese NMR Network) operating at 500.13 MHz for ^{1}H observation using a 5 mm TXI probe. Standard 1D spectra (Bruker pulse programs 'noesypr1d', with water suppression, for medium samples and aqueous extracts, and 'zg' for organic extracts) were recorded with a 7002.8 Hz spectral width, 32 k data points, a 2 s relaxation delay and 512 scans. Spectral processing comprised exponential multiplication with 0.3 Hz line broadening, zero filling to 64 k data points, manual phasing, baseline correction, and chemical shift calibration to the TSP or TMS signal at 0 ppm. 2D ^{1}H-^{1}H total correlation (TOCSY) spectra, ^{1}H-^{13}C heteronuclear single quantum correlation (HSQC) spectra and *J*-resolved spectra were also

registered for selected samples to assist spectral assignment. The main acquisition and processing parameters for these experiments are provided in Supplementary Table S2.1. Metabolites were identified mainly with support of 2D spectra and the spectral databases BBIOREFCODE-2-0-0 (Bruker Biospin, Rheinstetten, Germany) and HMDB [16].

2.2.5. Multivariate analysis and spectral integration of NMR spectra

Spectra were normalized by total spectral area, to compensate for differences in cell numbers, and scaled to unit variance, giving equal variance to all variables. PCA was then applied in the SIMCA-P 11.5 software (Umetrics, Umeå, Sweden) and the results were visualized through scores scatter plots. Selected signals in the normalized 1D spectra were integrated using the AmixViewer software 3.9.15 (Bruker BioSpin, Rheinstetten, Germany). The percentage of variation and respective error for aqueous and organic extracts were calculated for each metabolite, in cancer cells relatively to epithelial controls. The statistical significance of the differences was assessed using the two-sample *t* test (confidence level 95%).

2.3. Results

2.3.1. Cells metabolic activity assessed by NMR analysis of culture media

Variations in cell-conditioned medium composition offer useful data on metabolic cellular activity. Figure 2.1 shows representative ^{1}H NMR spectra of MDA-MB-231-conditioned medium and of acellular culture medium incubated under the same conditions (48h). Figure 2.2 presents typical examples of the corresponding 2D spectra used for spectral assignment. The full list of metabolites detected in complete culture medium upon incubation of both MDA-MB-231 and MCF-10A cells is presented in Supplementary Table S2.2.

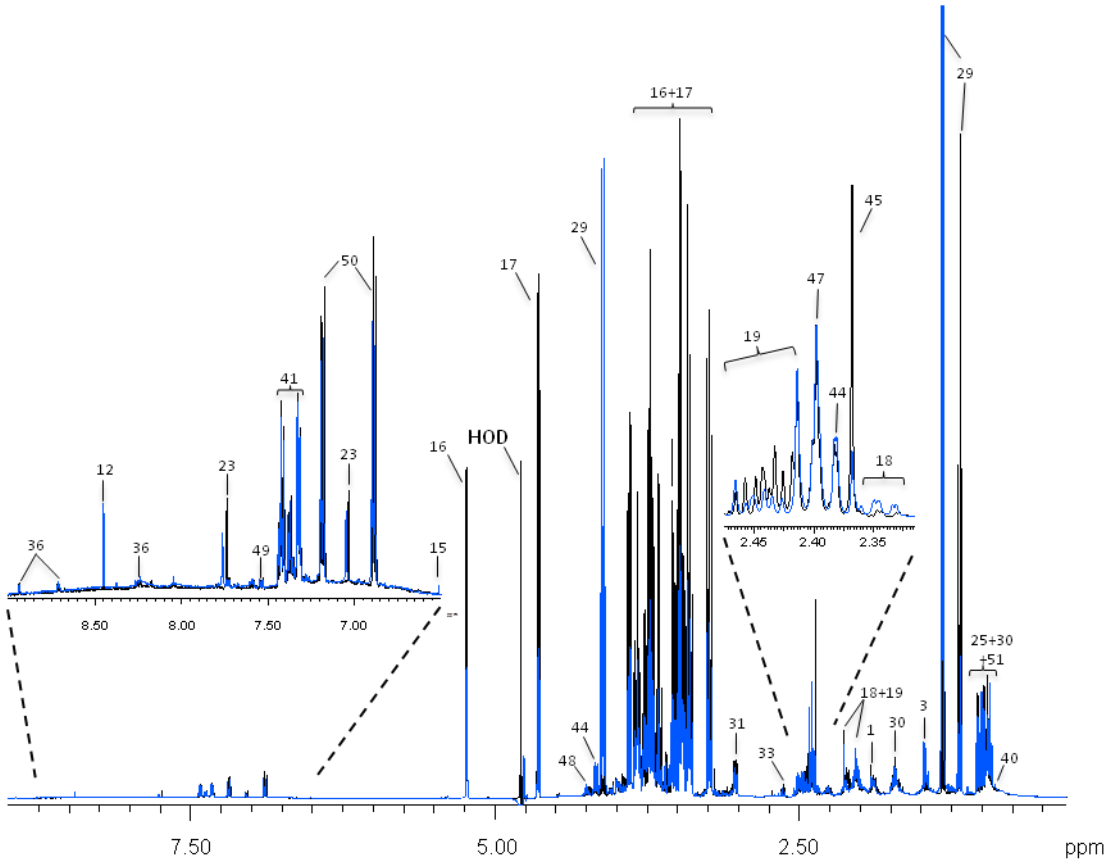

Figure 2.1. ^{1}H NMR spectra of culture media: DMEM acellular medium (black) and supernatant from MDA-MB-231 breast tumor cells grown for 48h (blue). Signals are numbered according to Supplementary Table S2.2.

NMR signal integration enabled the analysis and quantification of substrate utilization and metabolite production/excretion in culture medium upon cell incubation relative to acellular culture medium (Figure 2.3). The main substrates consumed by MDA-MB-231 TNBC cells were pyruvate, glucose and choline, together with smaller consumptions of some amino acids (e.g. leucine). Lactate was by far the main metabolite excreted, followed by formate, glutamate, 2-oxoisovalerate, fumarate, alanine and citrate. On the other hand, MCF-10A epithelial cells showed a marked utilization of several amino acids, including glutamine, branched chain amino acids (leucine, isoleucine, valine) and aromatic amino acids (phenylalanine and tyrosine), as well as acetate and pyruvate, while showing smaller glucose consumption. In terms of metabolites secreted into the culture medium, MCF-10A cells released lactate, although to a much lower extension than MDA-MB-231 cancer cells, together with isobutyrate, 1-methylnicotinamide, 3-hydroxyisovalerate and fumarate, among others (Figure 2.3).

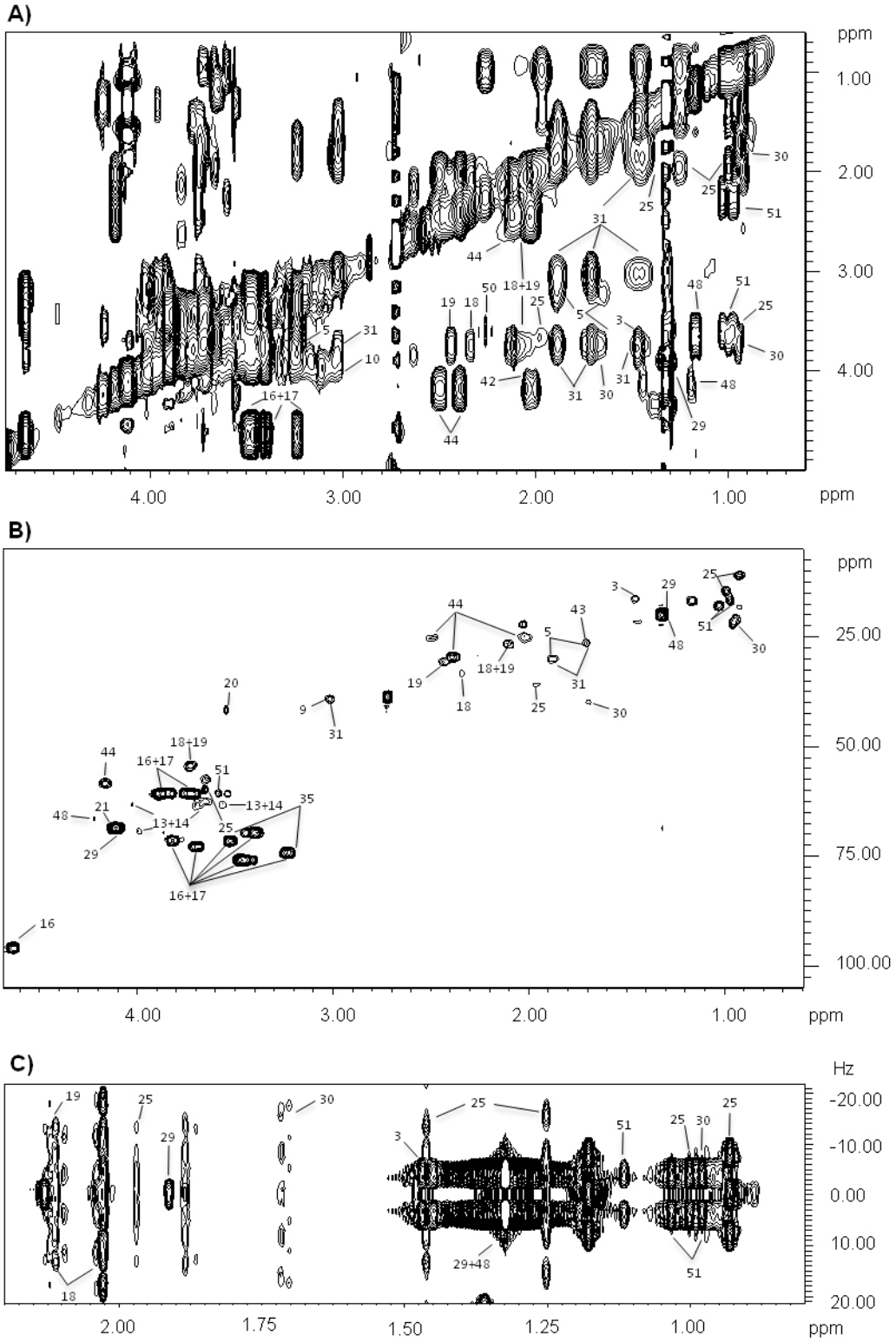

Figure 2.2. Expansions of 2D NMR spectra of MDA-MB-231 cells-conditioned medium: **A)** ^{1}H-^{1}H TOCSY, **B)** ^{1}H-^{13}C HSQC, **C)** *J*-resolved. Signals are numbered according to Supplementary Table S2.2.

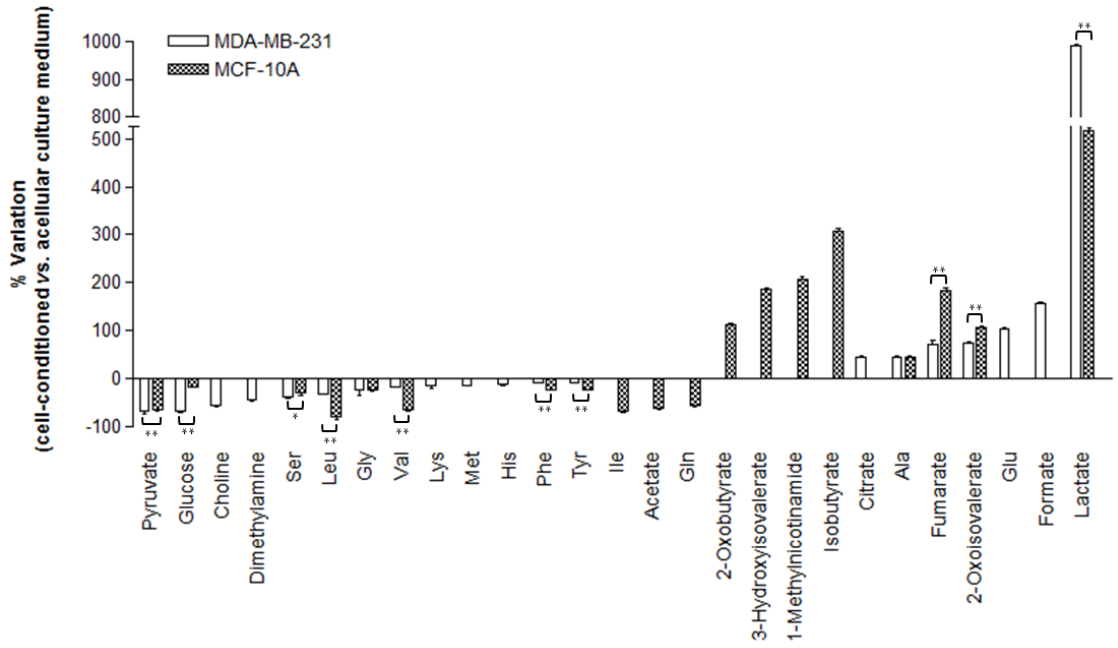

Figure 2.3. Variations in metabolites consumed (negative bars) and excreted (positive bars) by MCF-10A and MDA-MB-231 breast cells, as assessed by comparison between 48h cells-conditioned media and acellular culture media. ***P*-value < 0.01; **P*-value < 0.05. Three-letter code used for amino acids.

2.3.2. Intracellular polar metabolites of epithelial and tumor cells

Typical ^{1}H NMR spectra of aqueous extracts from both cell lines are shown in Figure 2.4. Two-dimensional (2D) spectra (^{1}H-^{1}H TOCSY, ^{1}H-^{13}C HSQC, and *J*-resolved) were recorded for selected samples of both cell types and, together with some spiking experiments and comparison to spectral databases, allowed the identification of 60 intracellular polar compounds (Supplementary Table S2.3). Example 2D spectra are shown in Figure 2.5 for an MDA-MB-231 aqueous extract.

Metabolites identified in the low-frequency region (δ 0-3 ppm) comprised several amino acids (e.g. branched chain amino acids, alanine, arginine, aspartate, glutamate, glutamine), organic acids (e.g. lactate, acetate, pyruvate, succinate) and a ketone body (3-hydroxybutyrate). In the mid-frequency region (δ 3-5.5 ppm), the spectra of cellular aqueous extracts showed resonances of several other intercellular metabolites, such as choline, phosphocholine (PC) and glycerophosphocholine (GPC), creatine, phosphocreatine, myo-inositol, reduced glutathione (GSH), glucose-1-phosphate and glucose. Finally, in the high frequency region (δ 5.5-10 ppm), intracellular aromatic amino acids (e.g. tyrosine, histidine), organic acids (fumarate and formate), nucleotides and derivatives (e.g. ATP, UTP) were identified.

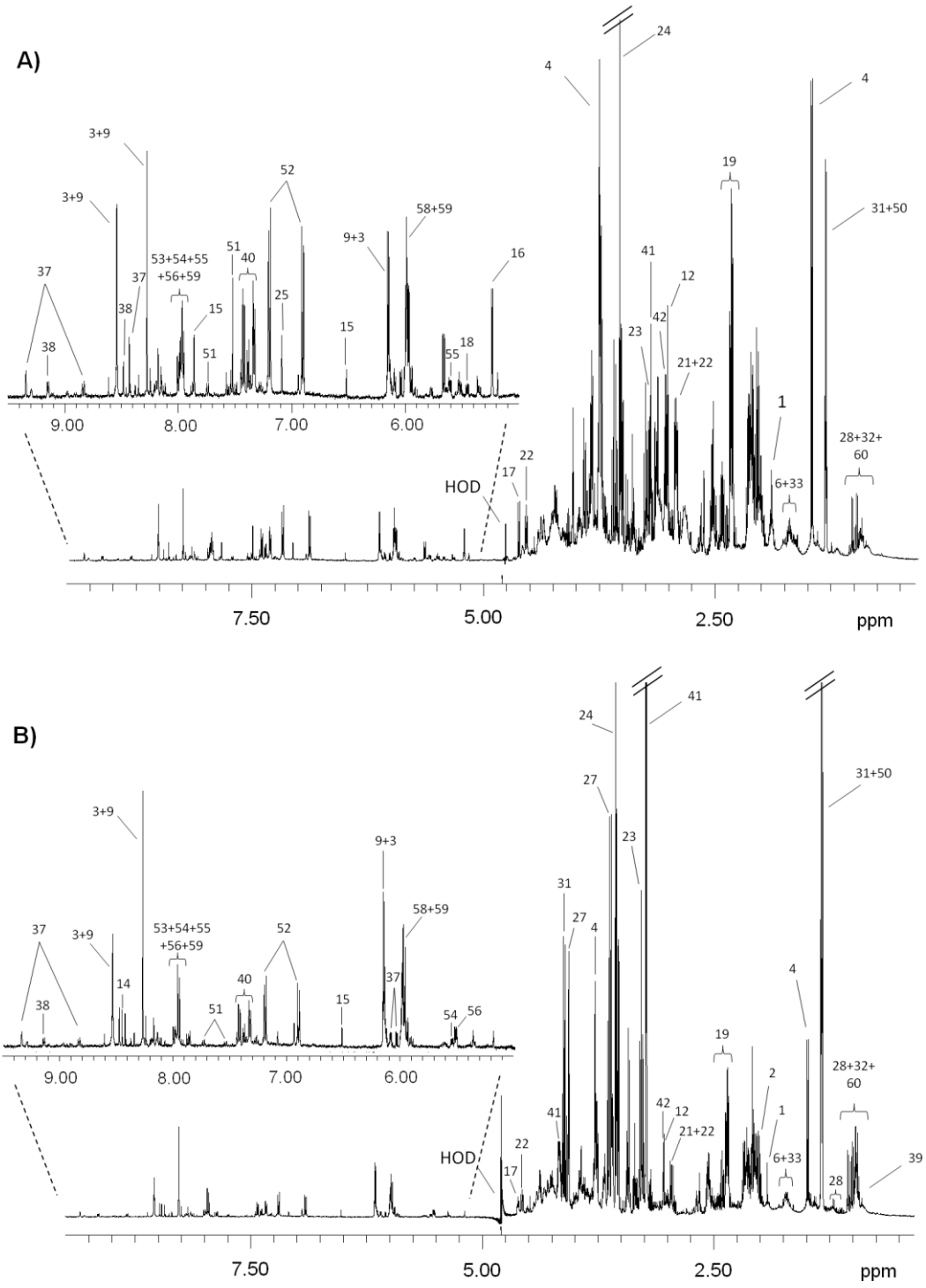

Figure 2.4. ^{1}H NMR spectra of aqueous extracts from **A)** MCF-10A and **B)** MDA-MB-231 breast cells. Signals are numbered according to Supplementary Table S2.3.

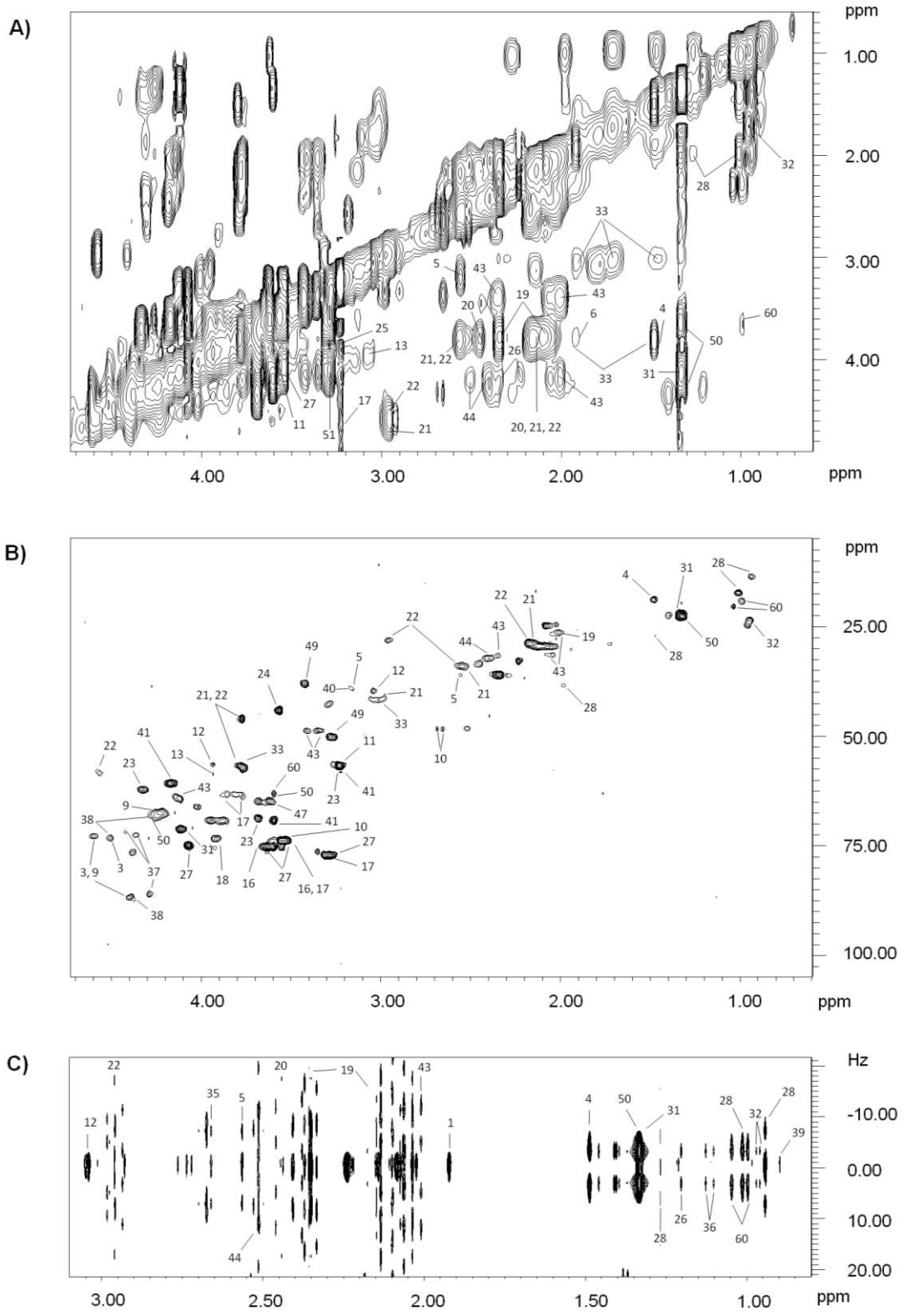

Figure 2.5. Expansions of 2D NMR spectra of aqueous extracts from MDA-MB-231 breast tumor cells: **A)** ^{1}H-^{1}H TOCSY, **B)** ^{1}H-^{13}C HSQC, **C)** *J*-resolved. Signals are numbered according to Supplementary Table S2.3.

Although most metabolites were present in both cell lines, the profiles of MDA-MB-231 tumor and MCF-10A epithelial cells showed significant quantitative differences. In order to explore grouping trends, principal component analysis (PCA) was applied to the spectra. The resulting PCA scores scatter plot (Figure 2.6A) displays a clear separation between the two groups, indicating consistent differences in MDA-MB-231 and MCF-10 aqueous extracts profiles. Spectral integration of individual metabolites then allowed a detailed investigation of the magnitude of those changes. The results obtained regarding variations of intracellular aqueous metabolites in MDA-MB-231 relative to MCF-10A cells are shown in Figure 2.6B.

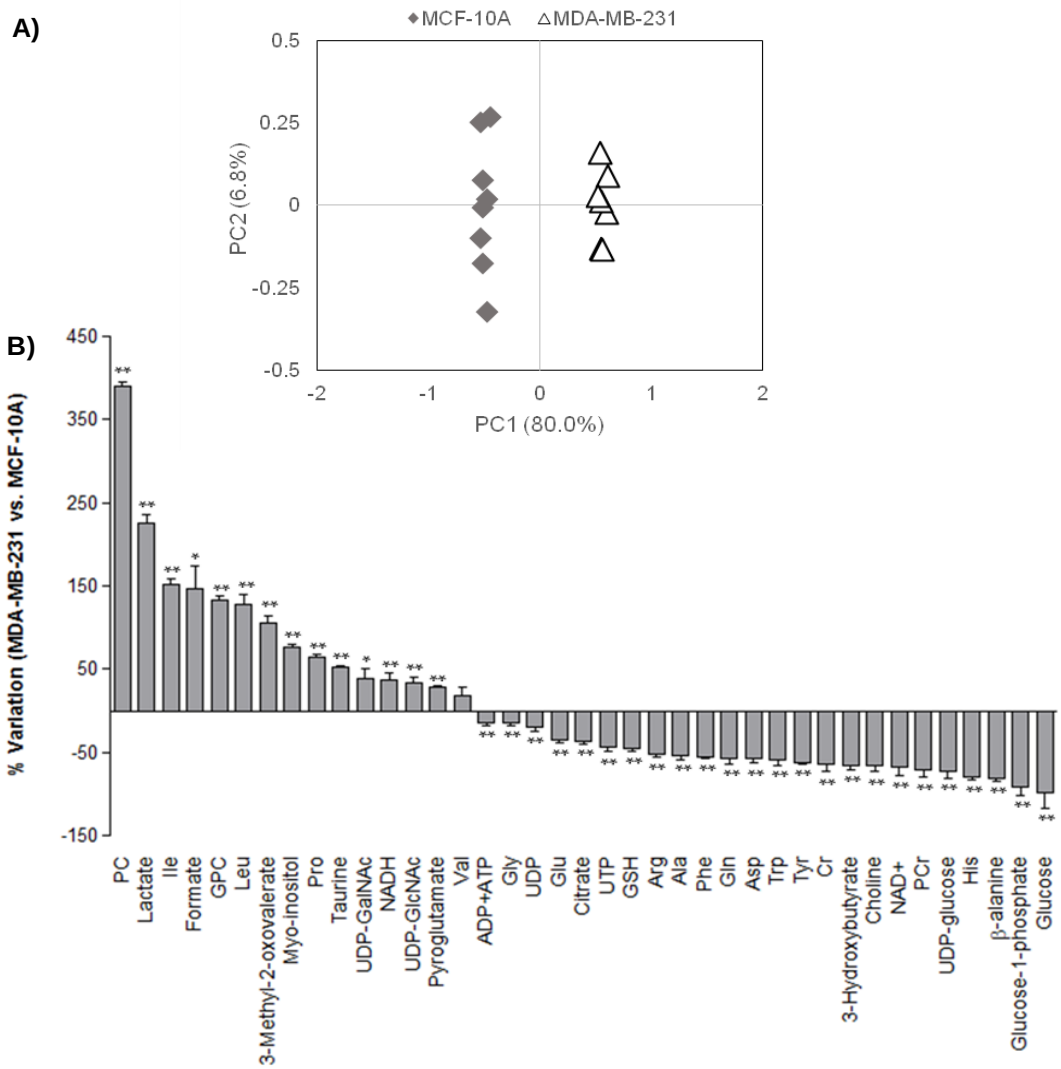

Figure 2.6. **A)** Scores scatter plot obtained by PCA of ^{1}H NMR spectra from aqueous extracts of MCF-10A and MDA-MB-231 breast cells, **B)** Variation of intracellular aqueous metabolites in MDA-MB-231 tumor cells relative to MCF-10A epithelial cells. * *P*-value < 0.05. Three-letter code used for amino acids. PC, phosphocholine; GPC, glycerophosphocholine; UDP-GalNAc, UDP-N-acetyl-galactosamine; UDP-GlcNAc, UDP-N-acetyl-glucosamine; UDP-Glc, UDP-Glucose; Cr, creatine; PCr, phosphocreatine; GSH, reduced glutathione; m-Ino, myo-inositol.

Compared to non-tumor cells, the intracellular composition of TNBC cells was characterized, among others, by: i) high levels of phosphocholine and glycerophoscholine, together with reduced choline content, ii) increased lactate and decreased glucose levels, iii) decreased levels of citrate and of several amino acids (except for proline and branched chain amino acids), iv) lower NAD+ to NADH ratio, v) reduced levels of ADP+ATP, creatine and phosphocreatine, vi) increased content of UDP-N-acetyl glucosamine/galactosamine, together with lower levels of UDP and UTP, vii) decreased levels of UDP-glucose and glucose-1-phosphate.

2.3.3. Lipid composition of epithelial and tumor cells

Characterization of the cellular lipid pool was performed through the NMR analysis of organic extracts. Figure 2.7 presents characteristic ^{1}H NMR spectra of organic extracts from MCF-10A and MDA-MB-231 breast cells, while examples of 2D experiments (^{1}H-^{1}H TOCSY, ^{1}H-^{13}C HSQC, and *J*-resolved) are displayed in Figure 2.8. In spite of the high degree of overlap between structurally similar lipids, such as fatty acyl chains incorporated in several lipid species, it was possible to identify signals which are characteristic of different lipid classes, such as triglycerides, phospholipids (including phosphatidylcholine, phosphatidylethanolamine, sphingomyelin and plasmalogen lipids), cholesterol and cholesterol esters. Moreover, the degree of fatty acyl (FA) chain unsaturation and the relative amounts of polyunsaturated fatty acids could be assessed based on specific signal ratios. Supplementary Table S2.4 lists the different lipid species identified and their respective NMR resonances.

Multivariate analysis (Figure 2.9A) of lipid profiles revealed an obvious separation between the two cell lines, reflecting the distinctive features of MDA-MB-231 and MCF-10 cellular lipid composition. As shown in Figure 2.9B, MDA-MB-231 TNBC cells presented higher abundance of neutral lipids, particularly cholesteryl esters and triglycerides, relative to MCF-10A epithelial cells. Moreover, in terms of FA composition, MDA-MB-231 cells were found to contain more polyunsaturated fatty acids (PUFA), and lower relative contribution of linoleic acid to the PUFA pool. Finally, the cancer cell line had a lower relative amount of plasmalogen phospholipids.

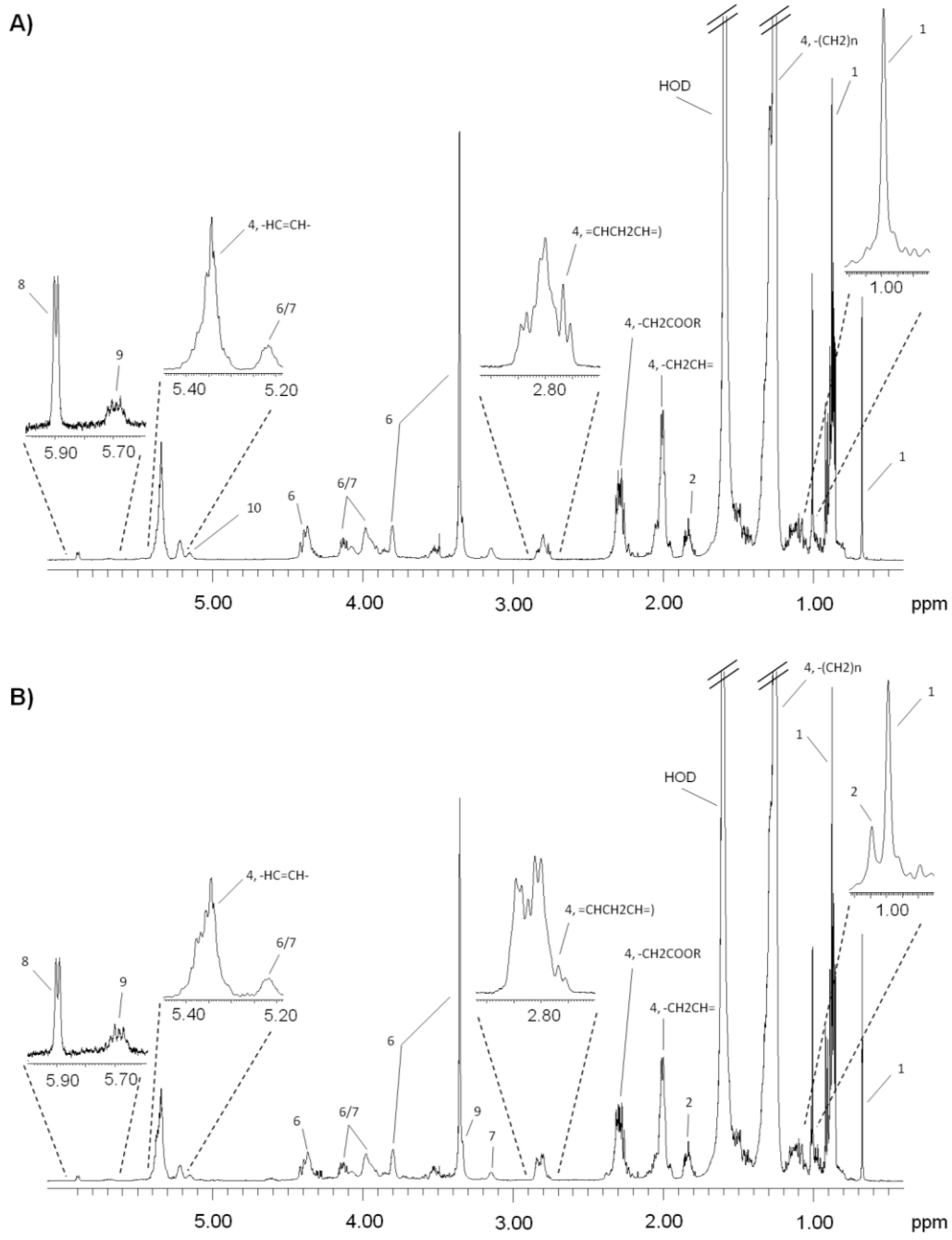

Figure 2.7. ^{1}H NMR spectra of organic extracts from **A)** MCF-10A and **B)** MDA-MB-231 breast cells. Signals are numbered according to Supplementary Table S2.4.

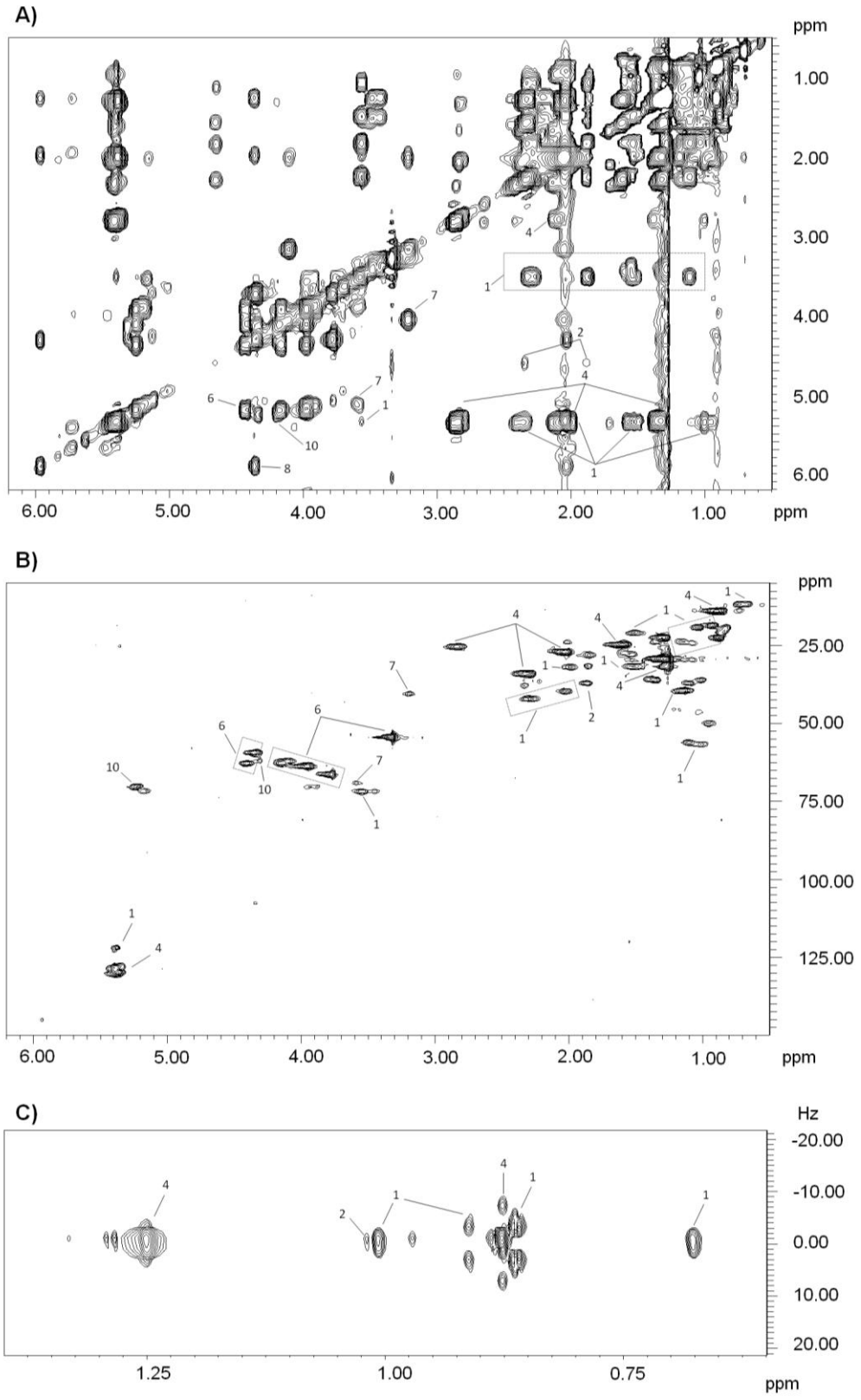

Figure 2.8. Expansions of 2D ^{1}H NMR spectra of an organic extract from MDA-MB-231 breast tumor cells: **A)** ^{1}H-^{1}H TOCSY, **B)** ^{1}H-^{13}C HSQC, **C)** *J*-resolved. Signals are numbered according to Supplementary Table S2.4.

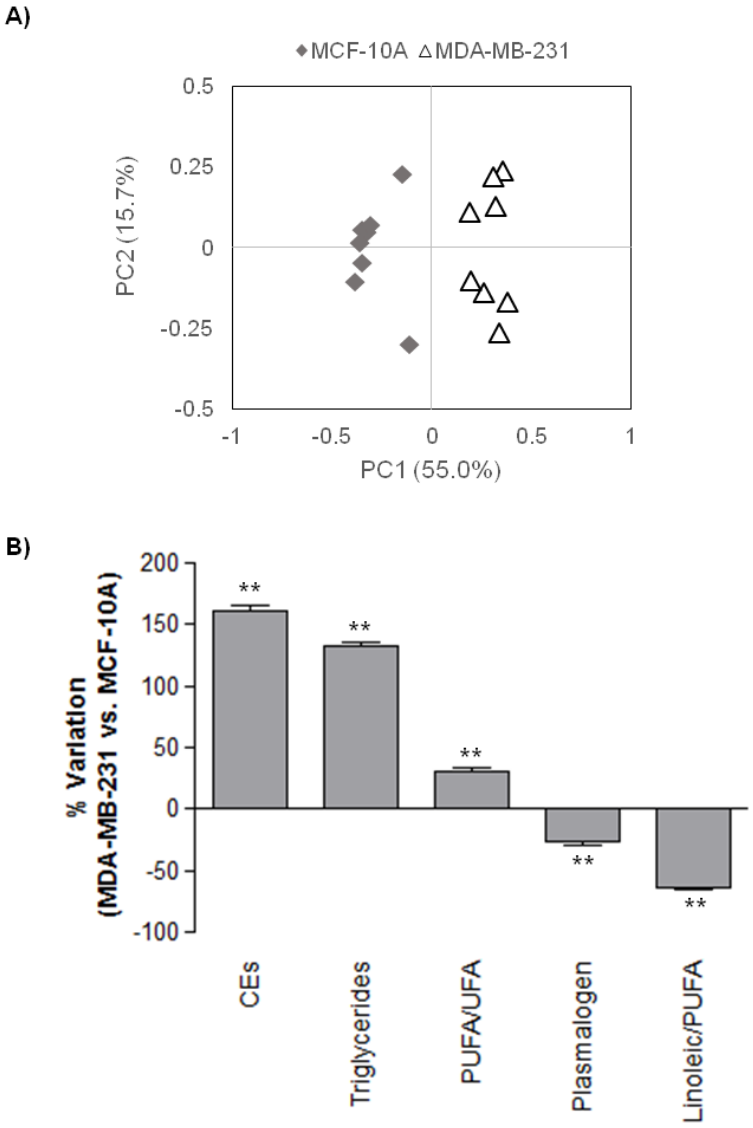

Figure 2.9. A) Scores scatter plot obtained by PCA of ^{1}H NMR spectra from organic extracts of MCF-10A and MDA-MB-231 breast cells, **B)** Variation of lipid species in MDA-MB-231 tumor cells relative to MCF-10A epithelial cells. ***P*-value < 0.01; CEs, cholesteryl esters; PUFA, polyunsaturated fatty acyl chains; UFA, unsaturated fatty acyl chains.

2.4. Discussion

Cell metabolomics is a powerful tool in the study of cellular processes and in preclinical drug testing. Characterization of the metabolic status of a given cell line allows a better understanding of cell biochemical pathways and may provide clues for identification of molecular targets. The present study reports a comprehensive comparative characterization of the metabolic profiles of MDA-MB-231 TNBC cells and

epithelial MCF-10A breast cells, based on integrated NMR metabolomics of culture medium supernatants, aqueous and organic cell extracts.

In our model of MDA-MB-231 TNBC cells, glucose was one of the most consumed metabolites, being rapidly utilized, as corroborated by its lower intracellular levels, compared with breast epithelial cells. Previous studies have demonstrated that the MDA-MB-231 cell line has a high rate of glucose uptake and turnover, when compared to non-cancerous breast cell lines [17-19]. Additionally, lactate was the most extensively excreted metabolite and intracellular lactate content was much higher in MDA-MB-231 breast cancer cells relative to the MCF-10A epithelial cell line. Hence, these results confirm that the MDA-MB-231 cell line displays a classical Warburg effect (high glucose uptake and conversion into lactate), characteristic of TNBC [20] and of most cancer cells [21]. Pyruvate was also extensively consumed, in agreement with the previous observation that MDA-MB-231 breast cancer cells rapidly proliferate in the presence of exogenous pyruvate, which fuels the mitochondrial TCA cycle to support rapid cell growth [22]. Increased intracellular NADH (a major product of glycolysis and the TCA cycle) together with decreased NAD^+ levels, in MDA-MB-231 cells compared with MCF-10A cells, further support enhanced glycolysis and TCA cycle. This is possibly accompanied by downregulated oxidative phosphorylation, as also suggested by decreased ATP pools in the cancer cells. The upregulation of the TCA cycle could also account for the observed intracellular decreases of citrate and aspartate. Moreover, decreased citrate could also reflect its use in fatty acid synthesis, as previously observed in TNBC tumor tissues [23].

The increase in glycolysis is typically accompanied by an increase of its intermediary metabolites, which in turn may fuel different biosynthetic pathways. In our TNBC cell model, intracellular glucose-1-phosphate and UDP-glucose levels were lower than in normal epithelial cells. Glucose-1-phosphate can be derived from the glycolytic intermediate glucose-6-phosphate and be converted into UDP-glucose, which is then a substrate for glycogen synthesis. Also, fructose-6-phosphate, another glycolytic intermediate, may fuel the hexosamine biosynthetic pathway (HBP) producing both UDP-N-acetylglucosamine (UDP-GlcNAc) and its derivative UDP-N-acetylgalactosamine (UDP-GalNAc), which are important substrates for protein glycosylation, known to be highly altered in cancer [24]. In the intracellular metabolome of MDA-MB-231 cells, both these metabolites were increased comparatively to MCF-10A cells, while precursor nucleotides (UDP and UTP) were decreased, suggesting an upregulated HBP. In line with this observation, UDP-GlcNAc was found to be increased in breast cancer tissues, as a result of upregulation of the enzymes involved in its synthesis [25].

Glutamine is a key substrate for cancer cells proliferation and progression. This amino acid is not only required for the synthesis of nucleotides, non-essential amino acids and fatty acids, as it is also involved in redox balance [26]. In this work, MDA-MB-231 cells displayed lower intracellular levels of glutamine and glutamate compared with epithelial breast cells, suggesting active glutaminolysis. Concordantly, MDA-MB-231 cells have been found to exhibit a phenotype of glutamine addiction [27], which has been generally associated with increased energetic requirements [19, 28-31]. In addition, human TNBC tissues have been reported to present elevated expression of glutamine metabolic enzymes [32].

Tumors also take up branched chained amino acids for protein synthesis or for energy purposes [33]. Both cells lines consumed leucine and valine from the culture medium, and MCF-10A also consumed isoleucine. At the intracellular level, branched-chained amino acids, proline and taurine were increased in MDA-MB-231 cells, while most amino acids showed decreased levels in TNBC cells, relative to breast epithelial cells. The high demand for energy production might explain their reduced concentrations in cancer cells. Differences in amino acid metabolism between MDA-MB-231 and MCF-10A cells were also found in earlier studies [17-19, 28, 30, 31, 34, 35]. Intracellular ADP+ATP levels were lower in MDA-MB-231 cells relative to the epithelial cell line, which likely reflects the preference of cancer cells for glycolysis, with the concomitant downregulation of oxidative phosphorylation, a more efficient pathway for energy production. Moreover, MDA-MB-231 cells displayed lower levels of creatine and phosphocreatine, which may relate to their role in the phosphocreatine-creatine kinase shuttle as an ATP buffering system [36].

Another noticeable difference in the endometabolome of TNBC cells, relative to epithelial breast cells, regarded the levels of reduced glutathione (GSH). Glutathione is an antioxidant tripeptide found in almost all cells, that plays a major role as a free radical scavenger and detoxifying agent [37]. Our results showed that MDA-MB-231 breast cancer cells contained lower GSH levels than MCF-10A cells, in agreement with previous reports comparing TNBC cells to non-transformed cells [35]. This may relate to the high production of reactive oxygen species typically observed in cancer cells and the use of glutathione pools in the control of redox homeostasis.

The two cell lines showed considerable differences in metabolites relating to lipid metabolism. For instance, 3-hydroxybutyrate was lower in TNBC cells relative to epithelial MCF-10A cells. This metabolite arises from the β-oxidation of fatty acids (FAO), when excess acetyl-CoA is not processed by the TCA cycle but is used instead for ketone body production [38]. Hence decreased 3-hydroxybutyrate levels in MDA-

MB-231 cells could reflect downregulated FAO. The intracellular levels of choline metabolites, involved in membrane-related phospholipid metabolism, were also significantly different between MDA-MB-231 and MDA-10A cells. The former contained lower levels of choline and higher levels of phosphocholine (PC) and glycerophosphocholine (GPC). Altered choline metabolism has been reported by others in the MDA-MB-231 cell line [17, 28, 29]. In particular, choline kinase (ChoK) has been found upregulated in TNBC, resulting in accumulation of PC [39-41] and significantly altered phospholipid metabolism (reviewed in [42]). The NMR analysis of cells organic extracts further revealed important differences in their lipid composition. MDA-MB-231 cells showed higher levels of triglycerides and cholesteryl esters than MCF-10A cells. These neutral lipids are found in cytosolic lipid droplets, typically abundant in cancer cells [43]. Interestingly, in breast cancer tissue samples, the intratumor accumulation of cholesteryl esters has been associated with proliferation and aggressive potential [44].

In conclusion, to our knowledge, this study represents the most detailed description of the basal metabolic activity of MDA-MB-231 and MCF-10A cells. The untargeted NMR metabolomics approach used here provided an integrative perspective of metabolic reprogramming in TNBC cells to support their energetic and biosynthetic needs. This knowledge is fundamental to understand cellular responses to external stimuli, thus representing useful background information in drug screening and development.

2.5. References

1. Bray, F., Ferlay, J., Soerjomataram, I., Siegel, R.L., Torre, L.A.and Jemal, A., (2018). Global cancer statistics 2018: GLOBOCAN estimates of incidence and mortality worldwide for 36 cancers in 185 countries. *Ca: Cancer Journal for Clinicians*, 68(6), 394-424.

2. Carioli, G., Malvezzi, M., Rodriguez, T., Bertuccio, P., Negri, E.and La Vecchia, C., (2017). Trends and predictions to 2020 in breast cancer mortality in Europe. *Breast*, 36 89-95.

3. Gusterson, B. and Eaves, C.J., (2018). Basal-like breast cancers: from pathology to biology and back again. *Stem Cell Reports*, 10(6), 1676-1686.

4. Neophytou, C., Boutsikos, P.and Papageorgis, P., (2018). Molecular mechanisms and emerging therapeutic targets of triple-negative breast cancer metastasis. *Frontiers in Oncology*, 8, 31.

5. Pareja, F., Geyer, F.C., Marchio, C., Burke, K.A., Weigelt, B.and Reis-Filho, J.S., (2016). Triple-negative breast cancer: the importance of molecular and histologic subtyping, and recognition of low-grade variants. *Npj Breast Cancer*, 2, 16036.

6. Abramson, V.G., Lehmann, B.D., Ballinger, T.J.and Pietenpol, J.A., (2015). Subtyping of triple-negative breast cancer: Implications for therapy. *Cancer*, 121(1), 8-16.

7. Geyer, F.C., Pareja, F., Weigelt, B., Rakha, E., Ellis, I.O., Schnitt, S.J.and Reis, J.S., (2017). The spectrum of triple-negative breast disease high- and low-grade lesions. *American Journal of Pathology*, 187(10), 2139-2151.

8. Fouad, Y.A. and Aanei, C., (2017). Revisiting the hallmarks of cancer. *American Journal of Cancer Research*, 7(5), 1016-1036.

9. Wishart, D.S., (2016). Emerging applications of metabolomics in drug discovery and precision medicine. *Nature Reviews Drug Discovery*, 15(7), 473-484.

10. Duarte, I.F., Lamego, I., Rocha, C.and Gil, A.M., (2009). NMR metabonomics for mammalian cell metabolism studies. *Bioanalysis*, 1(9), 1597-1614.

11. Cuperlovic-Culf, M., Barnett, D.A., Culf, A.S.and Chute, I., (2010). Cell culture metabolomics: applications and future directions. *Drug Discovery Today*, 15(15-16), 610-621.

12. Markley, J.L., Bruschweiler, R., Edison, A.S., Eghbalnia, H.R., Powers, R., Raftery, D.and Wishart, D.S., (2017). The future of NMR-based metabolomics. *Current Opinion in Biotechnology*, 43 34-40.

13. Hollinshead, K.E.R., Williams, D.S., Tennant, D.A.and Ludwig, C., (2016). Probing cancer cell metabolism using NMR spectroscopy. *Tumor Microenvironment: Study Protocols*, 899 89-111.

14. Halama, A., (2014). Metabolomics in cell culture - a strategy to study crucial metabolic pathways in cancer development and the response to treatment. *Archives of Biochemistry and Biophysics*, 564 100-109.

15. Carrola, J., Bastos, V., de Oliveira, J.M.P.F., Oliveira, H., Santos, C., Gil, A.M.and Duarte, I.F., (2016). Insights into the impact of silver nanoparticles on human keratinocytes metabolism through NMR metabolomics. *Archives of Biochemistry and Biophysics*, 589 53-61.

16. Wishart, D.S., Feunang, Y.D., Marcu, A., Guo, A.C., Liang, K., Vazquez-Fresno, R., Sajed, T., Johnson, D., Li, C.R., Karu, N., Sayeeda, Z., *et al.*, (2018). HMDB 4.0: the human metabolome database for 2018. *Nucleic Acids Research*, 46(D1), D608-D617.

17. Maria, R.M., Altei, W.F., Andricopulo, A.D., Becceneri, A.B., Cominetti, M.R., Venancio, T.and Colnago, L.A., (2015). Characterization of metabolic profile of intact non-tumor and tumor breast cells by high-resolution magic angle spinning nuclear magnetic resonance spectroscopy*. Analytical Biochemistry*, 488 14-18.

18. Willmann, L., Schlimpert, M., Halbach, S., Erbes, T., Stickeler, E.and Kammerer, B., (2015). Metabolic profiling of breast cancer: Differences in central metabolism between subtypes of breast cancer cell lines*. Journal of Chromatography B-Analytical Technologies in the Biomedical and Life Sciences*, 1000 95-104.

19. Gowda, G.A.N., Barding, G.A., Dai, J., Gu, H.W., Margineantu, D.H., Hockenbery, D.M.and Raftery, D., (2018). A metabolomics study of BPTES altered metabolism in human breast cancer cell lines*. Frontiers in Molecular Biosciences*, 5, 49.

20. Elia, I., Schmieder, R., Christen, S.and Fendt, S.M., (2015). Organ-specific cancer metabolism and its potential for therapy*. Handbook of Experimental Pharmacology*, 233 321-53.

21. Isidoro, A., Casado, E., Redondo, A., Acebo, P., Espinosa, E., Alonso, A.M., Cejas, P., Hardisson, D., Fresno Vara, J.A., Belda-Iniesta, C., Gonzalez-Baron, M.and Cuezva, J.M., (2005). Breast carcinomas fulfill the Warburg hypothesis and provide metabolic markers of cancer prognosis*. Carcinogenesis*, 26(12), 2095-2104.

22. Diers, A.R., Broniowska, K.A., Chang, C.F.and Hogg, N., (2012). Pyruvate fuels mitochondrial respiration and proliferation of breast cancer cells: effect of monocarboxylate transporter inhibition*. Biochemical Journal*, 444(3), 561-71.

23. Kanaan, Y.M., Sampey, B.P., Beyene, D., Esnakula, A.K., Naab, T.J., Ricks-Santi, L.J., Dasi, S., Day, A., Blackman, K.W., Frederick, W., Copeland, R.L., Sr., Gabrielson, E.and Dewitty, R.L., Jr., (2014). Metabolic profile of triple-negative breast cancer in African-American women reveals potential biomarkers of aggressive disease*. Cancer Genomics Proteomics*, 11(6), 279-94.

24. Akella, N.M., Ciraku, L.and Reginato, M.J., (2019). Fueling the fire: emerging role of the hexosamine biosynthetic pathway in cancer*. Bmc Biology*, 17(1), 52.

25. Oikari, S., Kettunen, T., Tiainen, S., Hayrinen, J., Masarwah, A., Sudah, M., Sutela, A., Vanninen, R., Tammi, M.and Auvinen, P., (2018). UDP-sugar accumulation drives hyaluronan synthesis in breast cancer*. Matrix Biology*, 67, 63-74.

26. Geck, R.C. and Toker, A., (2016). Nonessential amino acid metabolism in breast cancer*. Advances in Biological Regulation*, 62 11-17.

27. Kung, H.N., Marks, J.R.and Chi, J.T., (2011). Glutamine synthetase is a genetic determinant of cell type-specific glutamine independence in breast epithelia*. Plos Genetics*, 7(8), e1002229.

28. Cuperlovic-Culf, M., Chute, I.C., Culf, A.S., Touaibia, M., Ghosh, A., Griffiths, S., Tulpan, D., Leger, S., Belkaid, A., Surette, M.E.and Ouellette, R.J., (2011). H-1 NMR metabolomics combined with gene expression analysis for the determination of major metabolic differences between subtypes of breast cell lines*. Chemical Science*, 2(11), 2263-2270.

29. Belkaid, A., Cuperlovic-Culf, M., Touaibia, M., Ouellette, R.J.and Surette, M.E., (2016). Metabolic effect of estrogen receptor agonists on breast cancer cells in the presence or absence of carbonic anhydrase inhibitors*. Metabolites*, 6(2), E16.

30. Peterson, A.L., Walker, A.K., Sloan, E.K.and Creek, D.J., (2016). Optimized method for untargeted metabolomics analysis of MDA-MB-231 breast cancer cells*. Metabolites*, 6(4), E30.

31. Winnike, J.H., Stewart, D.A., Pathmasiri, W., McRitchie, S.L.and Sumner, S.J., (2018). Stable Isotope-Resolved Metabolomic Differences between hormone-responsive and triple-negative breast cancer cell lines*. International Journal of Breast Cancer*, 2018, 2063540.

32. Kim, S., Kim, D.H., Jung, W.H.and Koo, J.S., (2013). Expression of glutamine metabolism-related proteins according to molecular subtype of breast cancer. *Endocrine-Related Cancer*, 20(3), 339-348.

33. Ananieva, E.A. and Wilkinson, A.C., (2018). Branched-chain amino acid metabolism in cancer. *Current Opinion in Clinical Nutrition and Metabolic Care*, 21(1), 64-70.

34. Lanning, N.J., Castle, J.P., Singh, S.J., Leon, A.N., Tovar, E.A., Sanghera, A., MacKeigan, J.P., Filipp, F.V.and Graveel, C.R., (2017). Metabolic profiling of triple-negative breast cancer cells reveals metabolic vulnerabilities. *Cancer & Metabolism*, 5(6).

35. Beatty, A., Fink, L.S., Singh, T., Strigun, A., Peter, E., Ferrer, C.M., Nicolas, E., Cai, K.Q., Moran, T.P., Reginato, M.J., Rennefahrt, U.and Peterson, J.R., (2018). Metabolite profiling reveals the glutathione biosynthetic pathway as a therapeutic target in triple-negative breast cancer. *Molecular Cancer Therapeutics*, 17(1), 264-275.

36. Bessman, S.P. and Geiger, P.J., (1981). Transport of energy in muscle - the phosphorylcreatine shuttle. *Science*, 211(4481), 448-452.

37. Bansal, A. and Simon, M.C., (2018). Glutathione metabolism in cancer progression and treatment resistance. *Journal of Cell Biology*, 217(7), 2291-2298.

38. Kadochi, Y., Mori, S., Fujiwara-Tani, R., Luo, Y., Nishiguchi, Y., Kishi, S., Fujii, K., Ohmori, H.and Kuniyasu, H., (2017). Remodeling of energy metabolism by a ketone body and medium-chain fatty acid suppressed the proliferation of CT26 mouse colon cancer cells. *Oncology Letters*, 14(1), 673-680.

39. Glunde, K., Jie, C.and Bhujwalla, Z.M., (2004). Molecular causes of the aberrant choline phospholipid metabolism in breast cancer. *Cancer Research*, 64(12), 4270-4276.

40. Gadiya, M., Mori, N., Cao, M.D., Mironchik, Y., Kakkad, S., Gribbestad, I.S., Glunde, K., Krishnamachary, B.and Bhujwalla, Z.M., (2014). Phospholipase D1 and choline kinase-alpha are interactive targets in breast cancer. *Cancer Biology & Therapy*, 15(5), 593-601.

41. He, M.W., Guo, S.and Li, Z.L., (2015). In situ characterizing membrane lipid phenotype of breast cancer cells using mass spectrometry profiling. *Scientific Reports*, 5, 11298.

42. Iorio, E., Caramujo, M.J., Cecchetti, S., Spadaro, F., Carpinelli, G., Canese, R.and Podo, F., (2016). Key players in choline metabolic reprograming in triple-negative breast cancer. *Frontiers in Oncology*, 6, 205.

43. Welte, M.A. and Gould, A.P., (2017). Lipid droplet functions beyond energy storage. *Biochimica Et Biophysica Acta-Molecular and Cell Biology of Lipids*, 1862(10), 1260-1272.

44. de Gonzalo-Calvo, D., Lopez-Vilaro, L., Nasarre, L., Perez-Olabarria, M., Vazquez, T., Escuin, D., Badimon, L., Barnadas, A., Lerma, E.and Llorente-Cortes, V., (2015). Intratumor cholesteryl ester accumulation is associated with human breast cancer proliferation and aggressive potential: a molecular and clinicopathological study. *Bmc Cancer*, 15, 460.

Supplementary information to Chapter 2

Table S2.1. Main parameters used for the acquisition and processing of 500 MHz 1D ^{1}H and 2D NMR spectra of culture media, aqueous extracts, and organic extracts, of MDA-MB-231 and MCF-10A cells.

1D spectra	**Culture medium**	**Aqueous extracts**	**Organic extracts**
Acquisition parameters			
Pulse program[a]	*noesypr1d*	*noesypr1d*	*zg*
FID data points, TD	32768	32768	32768
Number of scans	512	512	512
Spectral width (ppm)	14.0019	14.0019	14.0019
Relaxation delay, RD (s)	4	4	4
Mixing time, t_m (ms)	100	100	
Processing parameters			
Window function	Exponential	Exponential	Exponential
Spectrum data points, SI	65536	65536	65536
Line broadening, LB (Hz)	0.30	0.30	0.30
2D spectra	**Culture medium/Aqueous extracts/Organic extracts**		
Acquisition parameters			
Experiments	^{1}H- ^{1}H TOCSY	^{1}H- ^{13}C HSQC	*J*-resolved
Pulse program[a]	*dipsi2phpr*	*hsqcetgp*	*jresgpprqf*
FID data points [F1]	128/128/256	128/200	40/80/80
FID data points [F2]	4096	2048	4096/16384/8192
Number of scans	80/200/80	128/360/256	80/128/80
Spectral width [F1] (ppm)	16.0214/16.0214/ 16.0214	14.0019/14.0019/ 184.9971	0.0868
Spectral width [F2] (ppm)	14.0019/16.0214/ 14.0019	165.6393/165.6393/ 14.0019	12.6549/16.0214/ 12.6549
Relaxation delay, RD (s)	2	2	2
Mixing time, D9 (ms)	70		
Processing parameters			
Window function	qsine/qsine	qsine/qsine	sine
Spectrum data points [F1], SI	2048	1024	128
Spectrum data points [F2], SI	4096	1024	16384
Line broadening [F1], LB (Hz)	0.30		0.30
Line broadening [F2], LB (Hz)			0.30

[a]Bruker library

Table S2.2. Assignment of resonances in the NMR spectra of culture media from MDA-MB-231 and MCF-10A breast cells. Multiplicity: s, singlet; d, doublet; t, triplet; m, multiplet; dd, double of doublets.

No.	Compound	δ ^{1}H in ppm (multiplicity/ assignment)/ δ ^{13}C in ppm	Cell type	
			MDA-MB-231	MCF-10A
1	Acetate	1.91 (s, β-CH_3)	✓	✓
2	N-acetylaspartate	2.01 (s, CH_3); 2.48 (dd, β-CH_2); 2.68 (dd, β'-CH_2); 4.38 (dd, α-CH)	✓	✓
3	Alanine (Ala)	1.48 (d, β-CH_3)/16.25; 3.79 (q, α-CH)	✓	✓
4	Allantoin	5.40 (s, CH)	✓	
5	Arginine (Arg)	1.72 (m, γ-CH_2)/26.50; 1.92 (m, β-CH_2)/30.12; 3.24 (t, δ-CH_2); 3.77 (α-CH)	✓	✓
6	Aspartate (Asp)	2.66 (dd, β-CH); 3.91 (dd, α-CH)	✓	✓
7	Citrate	2.54 (d, α, β-CH_2); 2.70 (d, α', β'-CH_2)	✓	✓
8	Choline	3.21 (s, $N(CH_3)_3$); 3.52 (m, CH_2(NH)); 4.08 (m, CH_2(OH))/58.32	✓	✓
9	Creatine	3.03 (s, CH_3)/39.19; 3.92 (s, CH_2)/56.2	✓	✓
10	Cysteine (Cys)	3.03 (m, β-CH_2); 3.92 (dd, α-CH)	✓	✓
11	Dimethylamine	2.72 (s, CH_3)	✓	
12	Formate	8.45 (s, CH)	✓	
13	α-Frutose	3.65 (m, C1H)/ 62.36; 3.88 (m, C6H)/69.47; 4.00 (m, C4H)/69.08; 4.03 (dd, C5H)/63.02; 4.11 (m, C3H)/74.94	✓	✓
14	β-Frutose	3.57 (m, C1H)/63.02; 3.78 (m, C6H)/67.32; 3.80 (m, C5H); 4.11 (m, C3H)	✓	✓
15	Fumarate	6.51 (s, CH)	✓	✓
16	α-Glucose	3.40 (m, C4H)/69.58; 3.53 (dd, C2H)/71.35; 3.71 (m, C3H)/72.61; 3.82 (m, C6H)/60.51; 3.83 (m, C5H) /71.22; 5.23 (d, C1H)/92.00	✓	✓
17	β-Glucose	3.24 (dd, C2H)/74.31; 3.45 (m, C4H)/69.58; 3.47 (m, C5H)/75.70; 3.50 (t, C3H)/75.53; 3.73 (m, C6H)/60.66; 3.89 (dd, C6'H)/60.65; 4.64 (d, C1H)/95.77	✓	✓

Table S2.2 (cont.)

No.	Compound	δ ^{1}H in ppm (multiplicity/ assignment)/ δ ^{13}C in ppm	Cell type	
			MDA-MB-231	MCF-10A
18	Glutamate (Glu)	2.03 (m, β-CH); 2.11 (m, β'-CH)/26.57; 2.35 (m, γ-CH_2)/33.28; 3.73 (t, α-CH)/53.81	✓	✓
19	Glutamine (Gln)	2.11 (m, β-CH_2)/26.65; 2.44 (m, γ-CH_2)/30.70; 3.75 (t, α-CH)/54.30	✓	✓
20	Glycine (Gly)	3.55 (s, α-CH_2)/41.65	✓	✓
21	3-Hidroxybutyrate	1.18 (d, γ-CH_3); 2.30 (dd, half α-CH_2); 2.42 (dd, half α-CH_2); 4.11 (m, β-CH)/68.40	✓	
22	3-Hydroxyisovalerate	1.26 (s, βCH_3)/27.84; 2.38 (s, αCH_2)		✓
23	Histidine (His)	3.20 (m, β-CH_2); 7.05 (s, C4H, ring); 7.76 (s, C2H, ring); 8.05 (s, C2H, ring)	✓	✓
24	Isobutyrate	1.08 (d, CH_3); 2.40 (m, α-CH)		✓
25	Isoleucine (Ile)	0.93 (t, δ-CH_3)/11.03; 1.01 (d, β'-CH_3)/14.56; 1.25 (m, γ-CH_2); 1.47 (m, γ'-CH_2); 1.97 (m, β-CH)/35.93; 3.66 (d, α-CH)/59.76	✓	✓
26	2-Ketobutyrate	1.06 (t, α-CH)		✓
27	Ketoleucine	0.93 (d, δ-CH_3); 2.63 (d, β-CH_2)	✓	✓
28	α-Ketovaline	1.12 (d, γ-CH 3); 3.02 (m, β-CH)	✓	✓
29	Lactate	1.32 (d, β-CH_3)/19.91; 4.11 (q, α-CH)/68.41	✓	✓
30	Leucine (Leu)	0.95 (d, δ-CH_3)/21.42; 1.00 (d, δ'-CH_3); 1.62 (m, γ-CH); 1.70 (m, β-CH 2)/29.84; 3.73 (t, α-CH)/54.39	✓	✓
31	Lysine (Lys)	1.45 (m, γ-CH_2)/21.47; 1.72 (m, δ-CH_2)/26.48; 1.88 (m, β-CH_2)/30.06; 3.02 (t, ε-CH_2)/29.31; 3.82 (t, α-CH)	✓	✓
32	Mannose	3.55 (t, C3H), 3.83 (m, C4H)/71.28; 3.94 (m, C2H); 5.19 (d, C6H)		✓
33	Methionine (Met)	2.13 (s, β-CH_2); 2.18 (t, β-CH_2); 2.64 (t, γ-CH_2); 3.84 (t, α-CH)	✓	✓
34	1-Methylnicotinamide	4.49 (s, NCH_3); 8.90 (d, C4H ring); 8.98 (d, C6H ring); 9.28 (s, C2H ring)		✓
35	*myo*-Inositol	3.24 (t, C5H)/74.10; 3.53 (C1H, C3H)/71.34; 3.63 (dd, C4H, C6H); 4.01 (t, C2H)	✓	✓

Table S2.2 (cont.)

No.	Compound	δ ^{1}H in ppm (multiplicity/ assignment)/ δ ^{13}C in ppm	Cell type	
			MDA-MB-231	MCF-10A
35	*myo*-Inositol	3.24 (t, C5H)/74.10; 3.53 (C1H, C3H)/71.34; 3.63 (dd, C4H, C6H); 4.01 (t, C2H)	✓	✓
36	Niacinamide	7.59 (dd, N5, ring); 8.25 (dd, N4, ring); 8.71 (dd, N6, ring); 8.94 (s, N2, ring)	✓	
37	2-Oxobutyrate	1.06 (t, CH2)		✓
38	2-Oxoisoleucine	0.85 (t, δ-CH_3); 1.08 (d, β'-CH_3); 1.45 (m, γ-CH_2); 1.72 (m, γ'-CH_2); 2.93 (m, β-CH)	✓	✓
39	2-Oxoisovalerate	1.12 (d, CH_3); 3.03 (m, β-CH)	✓	✓
40	Pantothenate	0.89 (s, CH_3); 0.92 (s, CH_3); 2.41 (t, α-CH_2); 3.38 (d, CH_2); 3.43 (q, β-CH_2); 3.52 (d, CH_2); 3.97 (s, CH)	✓	✓
41	Phenylalanine (Phe)	3.11 (m, β-CH); 3.28 (dd, β'-CH); 3.97 (m, α-CH); 7.32 (d, C2H, C6H, ring); 7.38 (d, C4H, ring); 7.42 (t, C3H, C5H, ring)	✓	✓
42	Proline (Pro)	2.02 (m, γ-CH_2); 2.07 (m, β-CH); 2.34 (m, β'-CH); 3.33 (dt, δ-CH); 3.41 (dt, δ'-CH); 4.13 (dd, α-CH)	✓	✓
43	Putrescine	1.71(m, CH_2)/26.42; 3.03 (t, CH_2)		✓
44	Pyroglutamate	2.03 (m, β-CH_2)/24.89; 2.40 (m, γ-CH_2)/29.67; 2.50 (m, β'-CH_2)/25.29; 4.17 (dd, α-CH)/58.31	✓	✓
45	Pyruvate	2.37 (s, β-CH_3)	✓	✓
46	Serine (Ser)	3.83 (dd, α-CH); 3.93 (m, β-CH_2)	✓	✓
47	Succinate	2.40 (s, CH_2)	✓	✓
48	Threonine (Thr)	1.32 (d, γ-CH_3)/19.90; 3.56 (d, α-CH); 4.25 (m, β-CH)/66.41	✓	✓
49	Tryptophan (Trp)	3.47 (dd, β'-CH); 4.08 (dd, α-CH)/58.32; 7.28 (t, C6H, ring); 7.32 (s, C2H, ring)/128.85; 7.54 (d, C7H, ring); 7.73 (d, C4H,ring)	✓	✓
50	Tyrosine	3.03 (m, β'-CH); 3.19 (m, β-CH); 3.91 (m, α-CH); 6.89 (d, C3H, C5H, ring); 7.19(d, C2H, C6H, ring)	✓	✓
51	Valine (Val)	0.98 (d, γ-CH_3)/16.61; 1.03 (d, γ'-CH_3)/17.84; 2.28 (m, β-CH)/29.20; 3.60 (d, α-CH)/60.50	✓	✓

Table S2.3. Assignment of resonances in the NMR profile of aqueous extracts from MCF-10A and MDA-MB-231 cells. Multiplicity: s, singlet; d, doublet; t, triplet; m, multiplet; dd, double of doublets; br, broad signal.

No.	Compound	δ ^{1}H in ppm (multiplicity/ assignment)/ δ ^{13}C in ppm	Cell type	
			MDA-MB-231	MCF-10A
1	Acetate	1.92 (s; β-CH_3)	✓	✓
2	N-Acetylaspartate	2.01 (s, CH_3); 2.48 (dd, β-CH_2); 2.68 (dd, β'-CH_2); 4.38 (dd, α-CH)	✓	✓
3	ADP	4.21 (m, C5'H, ribose); 4.38 (m, C4'H, ribose)/86.25; 4.50 (m, C2'H, ribose)/72.96; 6.14 (d, C1'H, ribose)/89.49; 8.28 (s, C8, ring); 8.54(s, C2, ring)	✓	✓
4	Alanine	1.48 (d, β-CH_3)/18.47; 3.78 (q, α-CH)	✓	✓
5	β-Alanine	2.56 (t, β-CH_2)/36.00; 3.17 (t, α-CH_2)/39.18	✓	✓
6	Arginine	1.65 (m, γ-CH_2); 1.92 (m, β-CH_2); 3.23 (t, δ-CH_2); 3.76 (α-CH_3)	✓	✓
7	Asparagine	2.85 (dd, β-CH_3); 2.95 (dd, β'-CH_3); 3.99 (dd, α-CH)	✓	✓
8	Aspartate	2.70 (dd, β-CH); 2.80 (dd, β'-CH); 3.90 (dd, α-CH)	✓	✓
9	ATP	4.23 (m, C5'H, ribose)/67.34; 4.29 (m, C5''H, ribose); 4.38 (m, C4'H, ribose)/86.25; 4.59 (m, C2'H, ribose)/72.59; 6.14 (d, C1'H, ribose)/89.49;8.28 (s, C2, ring); 8.54 (s, NH, ring)	✓	✓
10	Citrate	2.53 (d, CH_3)/48.07; 2.65 (d, α', β'-CH_2)/48.33	✓	✓
11	Choline	3.21 (s, N(CH_3)$_3$)/56.53; 3.52 (m, CH_2 (NH)); 4.05 (m, CH_2(OH))	✓	✓
12	Creatine	3.03 (s, CH_3)/39.62; 3.92 (s, CH_2)/56.35	✓	✓
13	Cysteine	3.09 (m, β-CH2); 3.94 (dd, α-CH)/58.74	✓	✓
14	Formate	8.46 (s, CH)	✓	✓
15	Fumarate	6.52 (s, CH)	✓	✓
16	α-Glucose	3.41 (m, C4H); 3.54 (dd, C2H)/73.63; 3.67 (m, C3H)/75.19; 3.81 (m, C6H)/63.11; 3.85 (m, C5H)/63.11; 5.23 (d, C1H)	✓	✓
17	β-Glucose	3.28 (dd, C2H)/76.83; 3.41 (m, C4H); 3.47 (m, C5H); 3.48 (t, C3H); 3.76 (m, C6H)/63.11; 3.85 (dd C6'H)/63.11; 4.65 (d, C1H)	✓	✓

Table S2.3. (cont.)

No.	Compound	δ ^{1}H in ppm (multiplicity/ assignment)/ δ ^{13}C in ppm	Cell type	
			MDA-MB-231	MCF-10A
18	Glucose-1-phosphate	3.40 (t, C4H); 3.49 (m, C2H); 3.77 (m, C3H); 3.75 (m, C6H); 3.86 (m C6'H); 3.91 (m, C5'H)/73.20; 5.46 (dd, C1H)	✓	✓
19	Glutamate	2.00 (m, β-CH_2)/26.35; 2.13 (m, β'-CH_2); 2.34 (m, γ-CH_2); 3.75 (α CH);	✓	✓
20	Glutamine	2.11 (m (m, β-CH_2); 2.45 (m, γ-CH_2); 3.78 (t, α-CH)	✓	✓
21	Glutathione, oxidised (GSSG)	2.16 (m, β-CH_2 , Glu)/28.95; 2.55 (m, γ-CH_2 , Glu)/23.95; 3.00 (m, β-CH_2, Cys)/41.60; 3.30 (m, β-CH_2 , Cys')/41.15; 3.77 (α-CH, Gly)/45.97; 3.76 (α-CH, Glu)/56.85; 4.74 (m, α-CH, Cys)/55.17	✓	✓
22	Glutathione, reduced (GSH)	2.16 (m, β-CH_2, Glu)/28.83; 2.54 (m, γ-CH_2, Glu)/33.91; 2.95 (m, β-CH_2, Cys)/28.14; 3.77 (α-CH, Gly)/45.97; 3.78 (α-CH, Glu)/56.8; 4.56 (m, α-CH, Cys)/58.30; 8.35 (NH, Gly)	✓	✓
23	Glycerophosphocholine (GPC)	3.23 (s, N(CH_3)3)/56.72; 3.68 (β'-CH_2(N))/68.52; 4.32 (m, α'-CH_2(P)/61.97	✓	✓
24	Glycine	3.56 (s, α-CH_2)/43.98	✓	✓
25	Histidine	3.27 (m, β-CH_2); 3.99(dd αCH); 7.08 (s, C4H, ring); 7.84 (s, C2H, ring)	✓	✓
26	3-Hydroxybutyrate	1.08 (d, γ-CH_3); 2.28 (dd, CH_2); 2.42 (dd, CH_2); 4.14 (m, CH)	✓	✓
27	*myo*-Inositol	3.27 (t, C5H)/77.01; 3.54 (C1H, C3H)/73.71; 3.61 (dd, C4H, C6H)/75.00; 4.07 (t, C2H)/74.85	✓	✓
28	Isoleucine	0.94 (t, δ-CH_3)/13.58; 1.00 (d, β'-CH_3)/17.26; 1.27 (m, γ-CH_2)/27.33; 1.47 (m, γ'-CH_2)/27.01; 1.97 (m, β-CH)/38.33	✓	✓
29	α-Ketoglutarate	2.44 (t, β-CH_2); 3.00 (t, γ-CH_2)	✓	✓
30	Ketoleucine	0.92 (d, δ-CH_3); 2.10 (m, γ-CH); 2.61 (d, β-CH_2)	✓	✓
31	Lactate	1.32 (d, β-CH_3)/22.60; 4.10 (m, α-CH)/71.09	✓	✓
32	Leucine	0.95 (d, δ-CH_3)/23.47; 0.96 (d, δ'-CH_3)/24.61; 1.69 (m, γ-CH)/42.48;1.72 (m, β-CH 2); 3.73 (t, α-CH)	✓	✓

Table S2.3. (cont.)

No.	Compound	δ ^{1}H in ppm (multiplicity/ assignment)/ δ ^{13}C in ppm	Cell type	
			MDA-MB-231	MCF-10A
33	Lysine	1.49 (m, γ-CH_2); 1.72 (m, δ-CH_2)/28.86; 1.90 (m, β-CH_2); 3.00 (t, ε-CH_2)/41.57; 3.76 (t, α-CH)/57.10	✓	✓
34	Malate	2.38 (dd, β'-CH); 2.67 (dd, β-CH); 4.30 (dd, α-CH)	✓	✓
35	Methionine	2.13 (s, β-CH_2); 2.16 (t, β-CH_2); 2.61 (t, γ-CH_2); 3.85 (t, α-CH)	✓	✓
36	3-Methyl-2-oxovalerate	0.90(t, δ-CH_3), 1.10 (d, β'-CH_3), 1.45(m, γ-CH), 1.70 (m, γ'-CH_2), 2.95 (m, β-CH)	✓	✓
37	NAD^+	4.28 (m, A5')/85.91; 4.36 (m, A4')/72.35; 4.38 (m, A4'/N5'); 4.42 (dd, N3')/ 72.64; 4.50 (m, A3'); 4.55 (m, N2'); 6.04 (d, N1'); 6.09 (d, A1'); 8.18 (s, A2); 8.20 (N5); 8.43 (s, A8); 8.84 (d, N4); 9.15 (d, N6); 9.34 (s, N2)	✓	✓
38	NADH	2.70 (m, N4); 4.08 (br. s., N2'); 4.17 (m, N4'); 4.21 (d, N3'); 4.25 (m, A5')/67.70; 4.40 (m, A4')/86.32; 4.50 (m, A3')/73.18; 4.75 (N5); 5.98 (dd, N6); 6.12 (d, A1'); 6.95 (d, N2); 8.23 (s, A2), 8.48 (s, A8)	✓	✓
39	Pantothenate	0.90 (s, CH_3); 0.94 (s, CH_3); 2.42 (t, α-CH_2); 3.38 (d, CH_2); 3.43 (q, β-CH_2); 3.50 (d, CH_2); 3.98 (s, CH)	✓	✓
40	Phenlyalanine	3.16 (m, β-CH)/ 38.27; 3.29 (dd, β'-CH); 3.99 (m, α-CH)/56.67; 7.32 (d, C2H, C6H, ring)/131.95; 7.39 (d, C4H, ring); 7.41 (t, C3H, C5H, ring)/131.70	✓	✓
41	Phosphocholine (PC)	3.22 (s, N(CH_3)3)/56.72; 3.59 (m, N-CH_2)/69.00; 4.16 (m, PO_3 - CH_2)/60.67	✓	✓
42	Phosphocreatine	3.04 (s, CH_3); 3.95 (s, CH_2)	✓	✓
43	Proline	1.99 (m, γ-CH_2)/26.35; 2.05 (m, β-CH)/31.44; 2.34 (m, β'-CH)/31.54; 3.34 (dt, δ-CH)/48.61; 3.40 (dt, δ'-CH)/38.78; 4.13 (dd, α-CH)/63.93	✓	✓
44	Pyroglutamate	2.00 (m, β-CH_2); 2.40 (m, γ-CH_2)/32.27; 2.51 (m, β'-CH 2); 4.17 (dd, α-CH)	✓	✓
45	Pyruvate	2.36 (s, β-CH_3)	✓	✓

Table S2.3. (cont.)

No.	Compound	δ ^{1}H in ppm (multiplicity/ assignment)/ δ ^{13}C in ppm	Cell type	
			MDA-MB-231	MCF-10A
46	Serine	3.84 (dd, α-CH); 3.97 (m, β-CH_2)	✓	✓
47	Sorbitol	3.62 (m, C1H/C4H/C6H)/54.67, 3.73(d, C6H), 3.77 (m, C3H), 3.81 (d, C1H), 3.83 (m, C2H/C5H)	✓	✓
48	Succinate	2.41 (s, CH_2)	✓	✓
49	Taurine	3.27 (t, S-CH_2)/50.10; 3.42 (t, N-CH_2)/38.05	✓	✓
50	Threonine	1.32 (d, γ-CH_3)/22.62; 3.60 (d, α-CH)/62.97; 4.23 (m, β-CH)/67.27	✓	✓
51	Tryptophan	3.28 (dd, β-CH); 3.48 (dd, β'-CH); 4.01 (dd, α-CH); 7.21 (t, C5H, ring); 7.29 (t, C6H, ring); 7.32 (s, C2H, ring); 7.55 (d, C7H, ring); 7.74 (d, C4H,ring)	✓	✓
52	Tyrosine	3.06 (m, β'-CH); 3.19 (m, β-CH); 3.94 (m, α-CH); 6.90 (d, C3H, C5H, ring); 7.20 (d, C2H, C6H, ring)	✓	✓
53	UDP	4.26 (m, C5'H, ribose); 4.30 (m, C4'H, ribose); 4.38 (t, C2'H, ribose); 5.95 (s, C1'H, ribose); 5.97 (d, C6, ring); 8.00 (d, C5, ring)	✓	✓
54	UDP-N-acetyl-galactosamine (UDP-GalNAc)	5.56 (dd, C1'')	✓	✓
55	UDP-Glucose (UDP-Glc)	5.60 (dd, C1'');	✓	✓
56	UDP-N-acetyl-glucosamine (UDP-GlcNAc)	5.52 (dd, C1'')	✓	✓
58	UMP	3.99 (m, C5'H, ribose); 4.24 (m, C4'H, ribose); 4.41 (t, C2'H, ribose); 5.98 (m, C1'H, ribose/C6, ring); 8.12 (d, C5, ring)	✓	✓
59	UTP	4.25 (m, C4'H, ribose); 4.26 (m, C5'H, ribose); 4.43 (t, C2'H, ribose); 5.95 (s, C1'H, ribose); 5.97 (d, C6, ring); 7.98 (d, C5, ring)	✓	✓
60	Valine	0.99 (d, γ-CH_3)/19.21; 1.03 (d, γ'-CH_3)/20.48; 2.26 (m, β-CH); 3.59 (d, α-CH)/62.98	✓	✓

Table S2.4. Assignment of resonances in the NMR profile of organic extracts from MDA-MB-231 cells and MCF-10A. Multiplicity: s, singlet; d, doublet; t, triplet; m, multiplet; dd, double of doublets.

No.	Compound	δ ^{1}H in ppm (multiplicity/ assignment)/ δ ^{13}C in ppm	Cell type	
			MDA-MB-231	MCF-10A
1	Cholesterol	0.69 (s, CH_3-18)/11.84; 0.85 (d, CH_3-26)/22.54; 0.89 (d, CH_3-27)/22.54; 0.89(d, CH_3-21)/18.54; 0.92 (m, CH-9)/50.02; 0.98 (m, CH-14)/56.92; 0.99 (s, CH_3-19)/19.21; 1.06 (s, CH-15)/24.26; 1.06 (m, CH_2-1)/37.15; 1.07 (m, CH-17)/56.07; 1.11 (m, CH_2-24)/39.45; 1.12 (m, CH_2-23)/23.71; 1.32 (m, CH-20)/35.90; 1.47 (m, CH_2-11)/20.94; 1.49 (m, CH_2-2)/31.67; 1.50 (m, CH-25)/27.82; 1.94 (t, CH_2-7)/31.94; 1.97 (t, CH_2-7')/31.94; 1.98 (CH_2-12)/39.63; 2.00 (CH_2-12)/39.58; 2.26 (m, CH_2-4')/42.17; 3.51 (m, CH-3)/71.68; 5.33 (m, CH-6)/121.65	✓	✓
2	Cholesterol ester	1.02 (s, CH_3-19); 1.83 (m, CH_2-2); 1.84 (m, CH_2-1)/37.10; 2.31 (m, CH_2-4'); 4.61 (m, CH-3)	✓	✓
3	Diglycerides	3.73, 4.28 (glyceryl CH_2 *sn*1/*sn*3); 5.08 (glyceryl CH *sn*2)	✓	✓
4	Fatty acyl chains (mainly in phospholipids)	0.87 (t, $CH_3(CH_2)_n$)/13.98; 1.27 (m, $(CH_2)_n$)/22.54/29.55/31.71; 1.57 (m, -CH_2 -CH_2CO)/24.80; 2.03 (m, -CH_2CH=)/27.07; 2.28 (m, -CH_2COOR)/34.06; 2.80 (t, =CHCH_2CH=)/25.50; 5.35 (m, -HC=CH-)/129.03	✓	✓
5	Free fatty acids	0.98 (t, CH_3 $(CH_2)_n$); 1.61 (m, -CH_2-CH_2CO); 2.05 (m, -CH_2CH=); 2.35 (t, -CH_2COOH); 2.76 (t, =CHCH_2CH=)	✓	✓
6	Phosphatidylcholine (PTC)	3.30 (s, $N(CH_3)_3$)/54.44; 3.75 (CH_2N)/66.45; 3.92 (glyceryl CH_2 *sn*3)/63.70; 4.38 (glyceryl CH_2 *sn*1)/62.77; 4.31 (CH_2-OP)/59.33; 5.19 (glyceryl CH *sn*2)/70.27	✓	✓
7	Phosphatidylethanol-amine (PTE, diacyl form)	3.15 (s, CH_2 -N)/40.46; 3.55 (glyceryl CH_2 *sn*1)/69.05; 3.92 (glyceryl CH_2 sn3)/63.58; 4.11 (CH_2 -OP)/62.66; 5.19 (glyceryl CH sn2)/70.24	✓	✓
8	PTE plasmalogen (PTE, plasmenyl form)	1.27 ($(CH_2)_n$); 2.00 (-CH=CH-CH_2); 3.90 (glyceryl CH_2 *sn*3); 4.32 (glyceryl CH_2 *sn*1); 5.90 (-CH=CH-)	✓	✓
9	Sphingomyelin (SM)	3.33 (s, $N(CH_3)_3$); 5.45 (-CH=CH-); 5.67 (-CH=CH-)	✓	✓
10	Triglycerides (TG)	4.13, 4.27 (dd, glyceryl CH_2 *sn*1/*sn*3)/61.93; 5.19 (glyceryl CH *sn*2)/70.26	✓	✓

Chapter 3

METABOLIC EFFECTS OF A EUCALYPTUS BARK LIPOPHILIC EXTRACT ON TRIPLE NEGATIVE BREAST CANCER AND NON-TUMOR BREAST EPITHELIAL CELLS

Part of this chapter is included in the manuscript entitled “NMR metabolomics reveals different metabolic modulatory activity of a lipophilic Eucalyptus outer bark extract on human tumor and non-tumor breast epithelial cells”, co-authored by A.R. Guerra, B.I.G. Soares, C.S.R. Freire, A.J.D. Silvestre, M.F. Duarte and I.F. Duarte (*submitted*).

Abstract

In this work, untargeted NMR metabolomics was used to unveil the impact of a Eucalyptus (*E. nitens*) lipophilic outer bark extract on the metabolism of TNBC and epithelial breast cells. Integrative analysis of culture medium, intracellular polar metabolites and cellular lipids provided a comprehensive picture of cells metabolic adaptations, which enabled several hypotheses about the metabolic targets and pathways affected to be proposed. One of the most marked effects upon 48h incubation of MDA-MB-231 breast cancer cells with the *E. nitens* extract (15 µg/mL) comprised enhancement of the NAD^+/NADH ratio, likely reflecting a shift to mitochondrial respiration, which appeared to be fueled by oxidation of fatty acids resulting from hydrolysis of neutral lipids (triglycerides and cholesteryl esters), and/or by amino acids possibly arising from autophagic protein degradation. Contrastingly, in MCF-10A breast epithelial cells, the *E. nitens* extract appeared to intensify glycolysis and the TCA cycle (resulting in decreased NAD^+/NADH ratio) and had no effect on the cells lipid composition. This knowledge contributes to improve current understanding of the biological activity of *E. nitens* lipophilic outer bark extracts, and is potentially useful to promote their development in the field of TNBC anticancer therapy.

Keywords: *Eucalyptus nitens* bark extracts; Triterpenic acids; Triple negative breast cancer; NMR metabolomics; Cell metabolism; NAD^+/NADH ratio

3.1. Introduction

Several plant-derived natural compounds have been demonstrated to exert potent anticancer activity by modulating multiple pathways involved in carcinogenesis and tumor progression [1]. Triterpenic acids (TAs), specifically with the lupane, ursane and oleanane-type structures, have been connected with an extensive range of pharmacological activities including antioxidant, pro-apoptotic, antiangiogenic and anti-inflammatory, sparking renewed interest with regard to their potential in cancer treatment [2-5]. Eucalyptus spp. outer barks are abundant biomass residues from the pulp and paper industry, and a generous source of several triterpenoids, mostly TAs [6, 7]. In particular, lipophilic extracts of *E. nitens* outer bark were found to contain 21.6 g/Kg of TAs, mainly from the ursane (ursolic acid – UA, 3.5 g/kg of bark fraction), lupane (betulinic acid - BA, 6.6 g/kg of bark fraction), and oleanane-type acids (oleanolic acid – OA, 7.3 g/kg of bark fraction together with 3-acetyloleanolic acid) [6]. These plant extracts were also demonstrated to have interesting biological activities, being able to modulate the proliferation and viability of breast cancer cells [8]. However, their possible development as anticancer natural products requires a deeper understanding of their mode of action at the cellular and molecular level.

Metabolic rewiring is considered one of cancer hallmarks, which accompanies tumorigenesis and actively contributes to tumor progression, namely through epigenetic regulation, the production of oncometabolites, and the crosstalk with non-cancer cells in the tumor microenvironment [9]. Based on this knowledge, the modulation of metabolic enzymes and pathways in cancer cells has been intensively explored as a therapeutic strategy to aid tumor regression and/or eradication [10]. In particular, there has been great interest in assessing the impact of plant extracts and plant-derived natural compounds (phytochemicals) on tumor cell metabolism, as they potentially hit multiple targets, thus offering increased chances of success [5]. At the same time, the pleiotropic effects of plant extracts and phytochemicals are particularly difficult to characterize by conventional single-targeted biochemical assays. By allowing the simultaneous detection of numerous cellular metabolites, untargeted metabolic profiling (metabolomics) offers a powerful approach to gain comprehensive insight into changes in different metabolic pathways upon exposure to pharmacological agents [11]. Despite some remarkable advances, triple negative breast cancer (TNBC) pharmacological therapies are still limited and have not significantly improved survival in patients [12]. The high degree of TNBC heterogeneity, together with its high resistance to conventional

chemotherapy and the lack of targeted therapies represent a major challenge in TNBC management and make the search for alternative and/or adjuvant therapies a chiefly important goal [13].

In this work, nuclear magnetic resonance (NMR) metabolomics has been employed to assess how an Eucalyptus lipophilic bark extract, with a well-characterized chemical composition [14], affects the metabolism of breast cancer cells, specifically the TNBC MDA-MB-231 cell line, in comparison to the effects produced in non-cancer MCF-10A breast epithelial cells. Cell culture medium supernatants were analyzed together with aqueous and organic cell extracts to obtain a complete and integrated view of changes in the cells metabolome. This approach is expected to provide new insight into the biological activity and metabolic targets of the *E. nitens* extract, in both cancer and normal cells, and, in a broader sense, to assess the potential of this raw-material as a source of compounds capable of acting as an adjuvant treatment for breast cancer, particularly TNBC.

3.2. Materials and Methods

3.2.1. Preparation and analysis of *Eucalyptus nitens* outer bark extract

Eucalyptus nitens barks were randomly sampled from a clone plantation as previously described [7]. Before extraction, the outer bark was separated by hand and grounded to a granulometry lower than 2 mm. Outer bark samples where then extracted with dichloromethane as described elsewhere [15]. *E. nitens* lipophilic extract was analyzed by gas chromatography-mass spectrometry, as previously reported [14]. The extract contained TAs and other less abundant components, such as fatty acids, aliphatic alcohols and sterols. The most abundant pentacyclic triterpenoids in the extract were betulinic acid (BA) (20.02 ± 0.90 mg/g of total extract), betulonic acid (14.72 ± 0.69 mg/g of total extract), oleanolic acid (10.71 ± 0.56 mg/g of total extract) and ursolic acid (9.90 ± 0.63 mg/g of total extract) [14]. The extract was further dissolved in absolute ethanol (Carlo Erba Reagents, Milan, Italy), to a final concentration of 10 mg/mL for the following assays and stored at -20ºC.

3.2.2. Cell culture

The human TNBC MDA-MB-231 cell line and the immortalized normal breast epithelial MCF-10A cell line were obtained from American Type Cell Culture (ATCC, Manassas, VA, USA). MDA-MB-231 cells were cultured in Dulbecco's Modified Eagle Medium (DMEM) (Biowest, Nuaillé, France) supplemented with 10% (v/v) heat-inactivated fetal bovine serum (FBSi) (Gibco, MA, USA). MCF-10A cells were cultured in DMEM/F12 medium (Biowest, Nuaillé, France), supplemented with 5% (v/v) heat-inactivated horse serum (Sigma-Aldrich, MO, USA), human epidermal growth factor (20 ng/ml), human insulin (10 µg/ml), hydrocortisone (100 ng/ml) and cholera toxin (0.1 nM) (Sigma-Aldrich, St. Louis, MO, USA). The same lot of FBS and horse serum was used in all experiments. The cells were maintained at 37ºC in a 5% CO_2 humidified atmosphere (C150, Binder GmbH, Tuttlingen, Germany). Before confluence, the cells were washed with phosphate buffered saline (PBS), harvested with the addition of a trypsin (0.5 g/L) / EDTA (0.2 g/L) (Biowest, Nuaillé, France) solution and suspended in fresh growth medium before platting.

3.2.3. Cell viability assay

Cells were seeded in 96-well plates at 2 x 10^5 cells/mL and allowed to adhere for 24h. Then, cells were incubated with *E. nitens* outer bark extract (0.01-25 µg/mL), for 24h, 48h and 72h. Vehicle solvent control cells received ethanol (0.15% (v/v)). Cell viability was estimated by 3-(4,5-dimethylthiazol-2-yl)-2,5-diphenyltetrazolium bromide (MTT) assay as previously described [16]. Briefly, 20 µL of MTT (Calbiochem, California, USA) stock solution was added to each well (final concentration 0.5 mg/mL), followed by an incubation period of 4h. A DMSO/ethanol (1:1) solution was then added to dissolve the formed formazan crystals, followed by a spectrophotometric determination at 570 nm (MultiSkan FC, ThermoScientific, Rochester, USA). Results were expressed as the percentage of cell viability relative to control (cells with vehicle solvent). IC_{50}, defined as the concentration necessary to cause 50% inhibition of cell viability, was calculated using GraphPad Prism 5.0 (GraphPad Prism Software Inc., San Diego, USA), by plotting the percentage of cell viability as a function of sample concentration logarithm. Triplicates were performed in three independent experiments for each treatment.

3.2.4. Cell cycle analysis by flow cytometry

MDA-MB-231 and MCF-10A cells were seeded in six-well plates at a density of 4 x 10^5 cells/mL and cultured for 24h at 37ºC. In this and the following assays, cells were treated with concentrations that reduced approximately 50% of cell viability. MDA-MB-231 cells were treated with 15 µg/mL and MCF-10A cells with 0.25 µg/mL of *E. nitens* lipophilic outer bark extract, for 48h. Vehicle solvent control cells received ethanol (0.15% (v/v)). After incubation, cells were collected, washed with PBS and fixed with 85% cold ethanol. Cell pellets were collected again by centrifugation at 300*g* for 5 min at 4°C and resuspended in PBS. Cells were then treated with RNase (50 µg/mL) (Sigma-Aldrich, MO, USA) and propidium iodide staining solution (50 µg/mL) (Sigma-Aldrich, MO, USA) and incubated for at least 20 min at room temperature, in the dark. Propidium iodide-stained cells were analyzed on a Coulter EPICS XL (Beckman Coulter, Hialeah, FL, USA) flow cytometer. The results were acquired using the SYSTEM II software (version 3.0 Beckman-Coulter®). Four replicates were performed for each treatment, and for each sample, at least 5000 nuclei were acquired. Analysis of cell cycle distribution was performed using the FlowJo software (Tree Star, Ashland, OR, USA).

3.2.5. Cell exposure for metabolomics assays

MDA-MB-231 and MCF-10A cells were seeded at a density of 6 x 10^5 cells/mL onto 10 cm diameter Petri dishes and allowed to adhere for 24h. Then, the medium was replaced by fresh complete medium containing 15 µg/mL or 0.25 µg/mL of *E. nitens* lipophilic outer bark extract, for MDA-MB-231 and MCF-10A cells, respectively. Vehicle solvent control cells received ethanol (0.15% (v/v)). The cells were incubated for 48h. Four independent experiments with duplicates were performed for each treatment.

3.2.6. Sample collection and preparation for NMR analysis

Culture medium was collected and centrifuged (1000*g*, 5min) and the supernatant stored at -80ºC until analysis. Culture medium without cells, placed under the same conditions, was also collected. Cells were washed 4 times with PBS and extracted with methanol (Merk (Darmstadt, Germany)):chloroform (Normapur (VWR, Radnor, PA, USA)):water (1:1:0.7) according to Carrola *et al*. [17]. The resulting aqueous and organic phases were collected and dried (under vacuum or under a stream of nitrogen gas, respectively). All samples were stored at

-80ºC. Dried aqueous extracts were reconstituted in 600 µL of deuterated phosphate buffer (100 mM, pH7.4) containing 0.1 mM 3-trimethylsilylpropionic acid (TSP-d_4, Sigma-Aldrich, St. Louis, MO, USA) and organic extracts were reconstituted in deuterated chloroform containing 0.03% tetramethylsilane (TMS, Euriso-top, Saint-Aubin, France). As for medium samples, 540 µL of thawed medium were mixed with 60 µL of D_2O containing 0.25% TSP-d_4 (Euriso-top, Saint-Aubin, France). 550 µL of each sample were transferred into 5 mm NMR tubes.

3.2.7. NMR data acquisition and processing

^{1}H NMR spectra of all samples were acquired on a Bruker Avance III HD 500 NMR spectrometer (University of Aveiro, Portuguese NMR Network) operating at 500.13 MHz for ^{1}H observation, using a 5 mm TXI probe. Standard 1D spectra (Bruker pulse programs 'noesypr1d' for medium samples and aqueous extracts, and 'zg' for organic extracts) were recorded with a 7002.8 Hz spectral width, 32 k data points, a 2 s relaxation delay and 512 scans. Spectral processing comprised exponential multiplication with 0.3 Hz line broadening, zero filling to 64 k data points, manual phasing, baseline correction, and chemical shift calibration to the TSP or TMS signal at 0 ppm. 2D ^{1}H-^{1}H total correlation (TOCSY) spectra, ^{1}H-^{13}C heteronuclear single quantum correlation (HSQC) spectra and *J*-resolved spectra were also registered for selected samples to assist spectral assignment. The main acquisition and processing parameters for these experiments are provided in Supplementary Table S2.1. Metabolites were identified with the support of 2D spectra (Figure 2.2; Figure 2.5; Figure 2.8) and the spectral reference databases BBIOREFCODE-2-0-0 (Bruker Biospin, Rheinstetten, Germany) and HMDB [18].

3.2.8. Multivariate analysis and spectral integration of NMR spectra

Spectra were normalized by total spectral area, to compensate for differences in cell numbers, and scaled to Unit Variance (UV), giving equal variance to all variables. Principal Component Analysis (PCA) and Partial Least Squares Discriminant Analysis (PLS-DA) were then applied in the SIMCA-P 11.5 software (Umetrics, Umeå, Sweden), with a sevenfold internal cross validation, from which Q^2 and R^2 values, respectively reflecting predictive capability and explained variance, were extracted. PLS-DA loadings plots were back-transformed by multiplying the loading weight w by the standard deviation of each variable and colored according to variable importance to the projection (VIP) using the R statistical software version 3.4.1. (R Core Team (2017). R: A language and

environment for statistical computing. R Foundation for Statistical Computing, Vienna, Austria. http://www.R-project.org/). Selected signals in the normalized 1D spectra were integrated using the AmixViewer software (version 3.9.14, Bruker BioSpin, Rheinstetten, Germany) and normalized by the total spectral area. The magnitude of each metabolite change was assessed through the percentage of variation (and its respective error) in exposed samples relatively to controls, and through the effect size (ES) adjusted for small sample numbers (and respective standard error) [19]. Metabolite variations with absolute ES greater than 0.8 were expressed in a heatmap**,** colored as a function of the percentage of variation, employing the R software version 3.4.1. Moreover, the statistical significance of the difference between the means of two groups (control and exposed) was assessed using the two-sample t-test.

3.2.9. Immunoblot analysis

MDA-MB-231 cells were seeded at a density of 6 x 10^5 cells/mL and incubated for 24h at 37ºC. Then, cells were treated with medium containing 15 µg/mL of *E. nitens* lipophilic outer bark extract. Vehicle solvent control cells received ethanol (0.15% (v/v)). After 48h of incubation, cells were harvest and extracted with ice cold cell RIPA buffer (1% NP-40 in 150 mM NaCl, 50 mM Tris-HCl (pH 8), 2 mM EDTA) containing 1 mM PMSF, phosphatase inhibitors (20 mM NaF, 20 mM $Na_2V_3O_4$) and protease inhibitor cocktail (Roche, Mannheim, Germany). Total protein concentration was determined by the Lowry method [20], using BSA as a protein standard. Cell lysates were run in a SDS-polyacrilamide gel and then electroblotted to nitrocellulose membranes (Amersham Biosciences, Buckinghamshire, UK). Nitrocellulose membranes were blocked with 5% (w/v) of nonfat dry milk and the immunoblots exposed to primary antibody against Choline kinase (ChoK) α (1:100) (sc-376489; Santa Cruz Biotechnology Inc., Dallas, USA); Glutaminase (1:10000) (ab156876; Abcam, Cambridge, UK) and β-actin (1:1500) (sc-47778; Santa Cruz Biotechnology Inc., Dallas, USA), overnight at 4ºC. Bands were visualized via chemiluminescence using the respective horseradish peroxidase–conjugated secondary antibody, and developed with ECL reagents (Amersham Biosciences, Buckinghamshire, UK). Signal intensity was quantified using NIH ImageJ software.

3.2.10. Statistical analysis

For sections 3.2.3, 3.2.4 and 3.2.9, all parameters measured were analyzed using the PROC GLM option of SAS (SAS Institute Inc., Cary, NC, USA). Where differences existed, the source of the differences at $P < 0.05$ significance level was identified by all pairwise multiple comparison procedures via the Tukey's test.

3.3. Results

3.3.1. Impact of *E. nitens* lipophilic outer bark extract on cell viability

In order to evaluate the inhibitory potential of *E. nitens* lipophilic outer bark extract towards the viability of MDA-MB-231 breast cancer cells and MCF-10A breast epithelial cells, dose-response curves were determined through the MTT assay at different incubation times (24, 48 and 72h). The viability of MDA-MB-231 cells exposed to the *E. nitens* lipophilic outer bark extract decreased in a dose- and time-dependent manner (Figure 3.1A). While at 24h incubation, cell viability was not significantly altered, at 48h and 72h, it showed a significant decrease, as observed by the IC_{50} values (Table 3.1). Human breast epithelial MCF-10A cells were more sensitive to the same *E. nitens* extract, significantly decreasing viability at extract concentrations as low as 0.01 µg/mL (Figure 3.1B). The resulting IC_{50} values were lower than 0.5 µg/mL for all tested incubation times (Table 3.1). Moreover, there was no significant difference ($P>0.05$) between the IC_{50} values determined for 24h, 48h and 72h. Based on these results, concentrations close to the 48h IC_{50} values found for each cell type were selected for subsequent assays, namely 15 µg/mL and 0.25 µg/mL *E. nitens* lipophilic outer bark extract for MDA-MB-231 and MCF-10A cells, respectively.

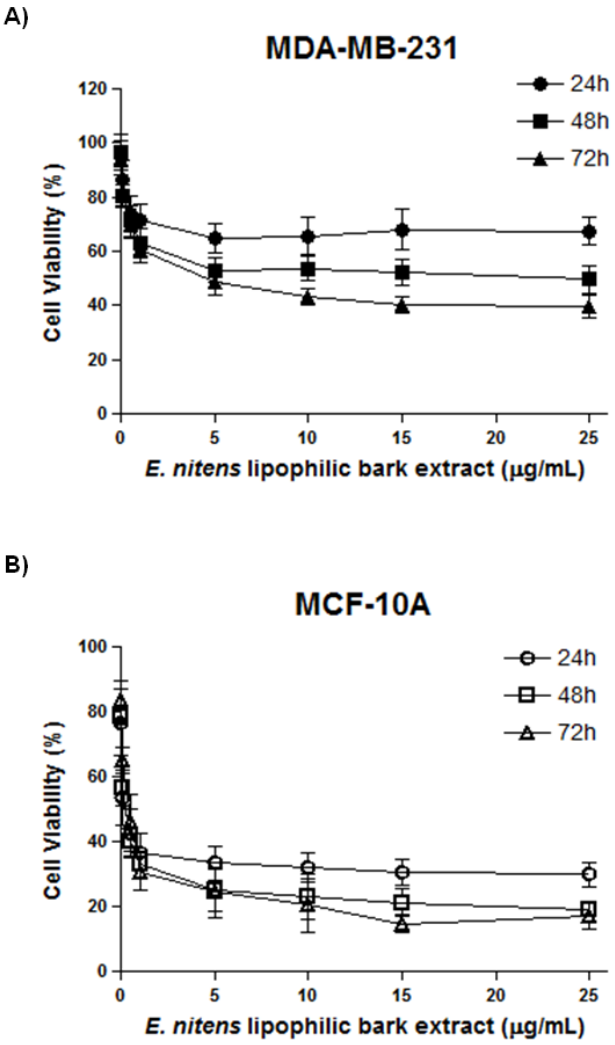

Figure 3.1. Effect of *Eucalyptus nitens* lipophilic bark extract on the viability of A) MDA-MB-231 and B) MCF-10A cells. Cells were treated with increasing concentrations of *E. nitens* lipophilic bark extract for 24, 48 and 72h and cell viability was measured by the MTT assay. Data represent the mean ± standard deviation of three independent experiments.

Table 3.1. IC_{50} values regarding cell viability inhibition by *Eucalyptus nitens* lipophilic outer bark extract on the MDA-MB-231 and MCF-10A cell lines, as determined through the MTT assay.

Cell line	IC_{50} (µg/mL)[1]		
	24h	48h	72h
MDA-MB-231	no effect	11.35±2.97[a]	6.29±1.30[b]
MCF-10A	0.41±0.23[c]	0.31±0.08[c]	0.40±0.14[c]

[1] Each value is expressed as mean ± standard deviation. Three independent experiments were carried out. Means marked with different letters are statistically different (*P*-value <0.05).

3.3.2. Effect of *E. nitens* lipophilic outer bark extract on the cell cycle of MDA-MB-231 and MCF-10A cells

Flow cytometry was applied to gain further insight into the inhibitory effects of *E. nitens* lipophilic outer bark extract, upon analysis of MDA-MB-231 and MCF-10A cells distribution through cell cycle phases (G0/G1, S and G2 phases) (Figure 3.2).

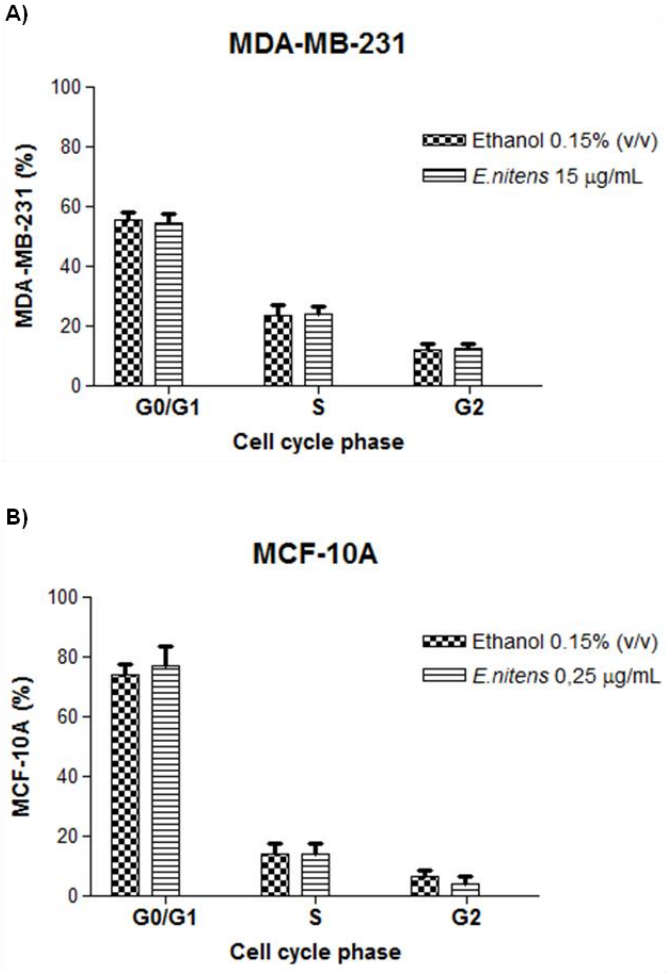

Figure 3.2. Cell cycle phase distribution of A) MDA-MB-231 and B) MCF-10A cells, treated with 15 µg/mL and 0.25 µg/mL *E. nitens* lipophilic bark extract, respectively, after 48h-incubations. Ethanol was the solvent control. Each column and bar represents, respectively, the mean and the standard deviation. Four replicates were performed.

The 48h-treatment of MDA-MB-231 breast cancer cells with 15 µg/mL *E. nitens* lipophilic outer bark extract did not cause significant changes (P>0.05) on G0/G1, S or G2 cell cycle phases. Similarly, MCF-10A epithelial cells did not present significant changes on cell phase distribution upon incubation with 0.25 µg/mL *E. nitens* lipophilic bark extract for 48h.

3.3.3. Metabolic variations induced by *E. nitens* lipophilic outer bark extract on the metabolome of MDA-MB-231 and MCF-10 breast cells

The metabolic effects of the *E. nitens* lipophilic outer bark extract on breast cancer and epithelial cells were evaluated upon 48h incubations with 15 μg/mL and 0.25 μg/mL, for MDA-MB-231 and MCF-10A cells, respectively. Profiling of the cells exometabolome was performed through NMR analysis of culture medium supernatants, while variations in the intracellular metabolic composition were assessed through analysis of aqueous and organic cell extracts.

3.3.3.1. Extracellular metabolic changes induced by *E. nitens* lipophilic outer bark extract

In order to assess whether incubation of breast cells with the *E. nitens* extract affected their consumption and excretion patterns, metabolite variations in cell-conditioned medium relative to acellular culture medium were assessed in untreated control cells, and in cells incubated with the *E. nitens* extract. The results are shown in Figures 3.3 and 3.4 for MDA-MB-231 and MCF-10A cells, respectively.

In regard to MDA-MB-231 cancer cells, there were no significant differences in the amounts of metabolites consumed or excreted between control and *E. nitens*-treated cells (Figure 3.3). Both control and treated cells consumed mainly pyruvate, glucose, choline and several amino acids from the culture medium, while excreting citrate, alanine, fumarate, 2-oxoisvalerate, glutamate, formate and lactate, to similar extent.

Contrastingly, the exometabolome of MCF-10A epithelial cells was greatly affected by incubation with the *E. nitens* extract (Figure 3.4). Compared to control cells, treated cells significantly consumed more pyruvate, glutamine, serine and glucose, and excreted more alanine and lactate. On the other hand, treated cells reduced the consumption of branched chain amino acids (BCAA), glycine and phenylalanine, as well as the excretion of isobutyrate and other short chain fatty acids resulting from branched chain amino acids (BCAA) catabolism (2-oxoisovalerate, 2-oxobutyrate, 3-hydroxyisovalerate).

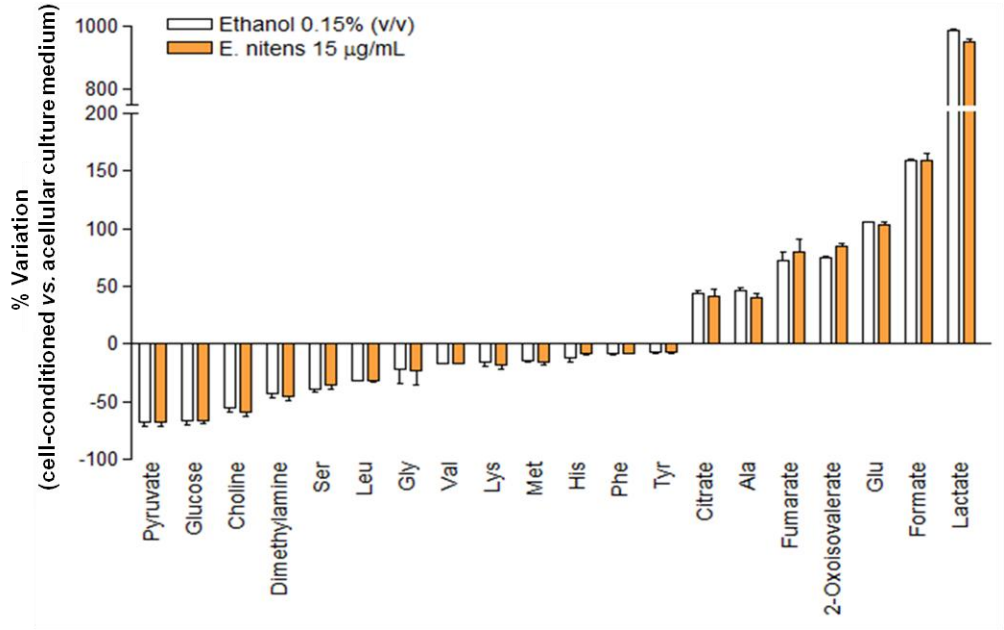

Figure 3.3. Variations in metabolites consumed (negative bars) and excreted (positive bars) by MDA-MB-231 breast cancer cells, under control conditions and upon treatment with 15 µg/mL of *E. nitens* lipophilic outer bark extract, as assessed by comparison between acellular culture media and 48h cells-conditioned media. Ethanol was the solvent control. Three-letter code used for amino acids.

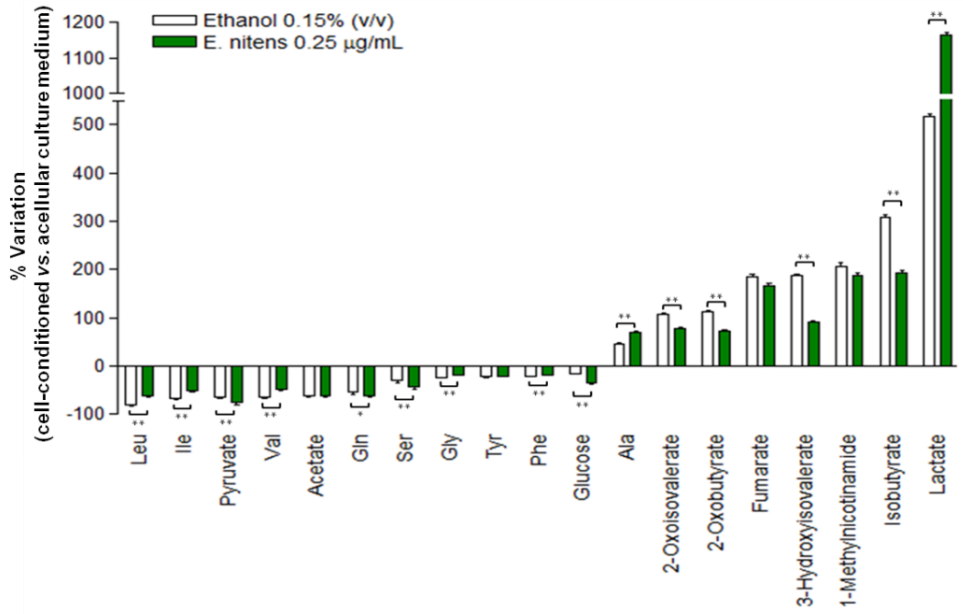

Figure 3.4. Variations in metabolites consumed (negative bars) and excreted (positive bars) by MCF-10A epithelial breast cells, under control conditions and upon treatment with 0.25 µg/mL of *E. nitens* lipophilic bark extract, as assessed by comparison between acellular culture media and 48h cells-conditioned media. Ethanol was the solvent control. ***P*-value < 0.01; **P*-value < 0.05. Three-letter code used for amino acids.

3.3.3.2. Intracellular metabolic changes induced by *E. nitens* lipophilic outer bark extract

The ^{1}H NMR spectra of cell aqueous extracts showed contributions from about 60 metabolites, identified based on matching sample data to spectral data recorded in-house for standard compounds and/or deposited in other available databases (Supplementary Table S2.3.). As a first approach to assess the changes in the cells endometabolome upon incubation with the *E. nitens* extract, multivariate analysis was applied to the spectral datasets collected for each cell type. The results are shown in Figure 3.5 and Figure 3.6, for MDA-MB-231 and MCF-10A cells, respectively. In the case of cancer cells, the two sample groups (control and *E. nitens*-treated cells) were clearly separated in the scores scatter plot generated by PCA (Figure 3.5A) and discriminated through PLS-DA with high explained variance (R^2Y 0.99) and predictive power (Q^2 0.96) (Figure 3.5B). The corresponding LV1 loadings (Figure 3.5C) suggested that the main variations responsible for group discrimination included, among others, increased levels of glycerophosphocholine and several amino acids (e.g. BCAA and glutamine) in treated cells (negative LV1 scores and loadings), together with relative higher levels of metabolites such as phosphocholine, glutathione and glutamate in untreated controls (positive LV1 scores and loadings).

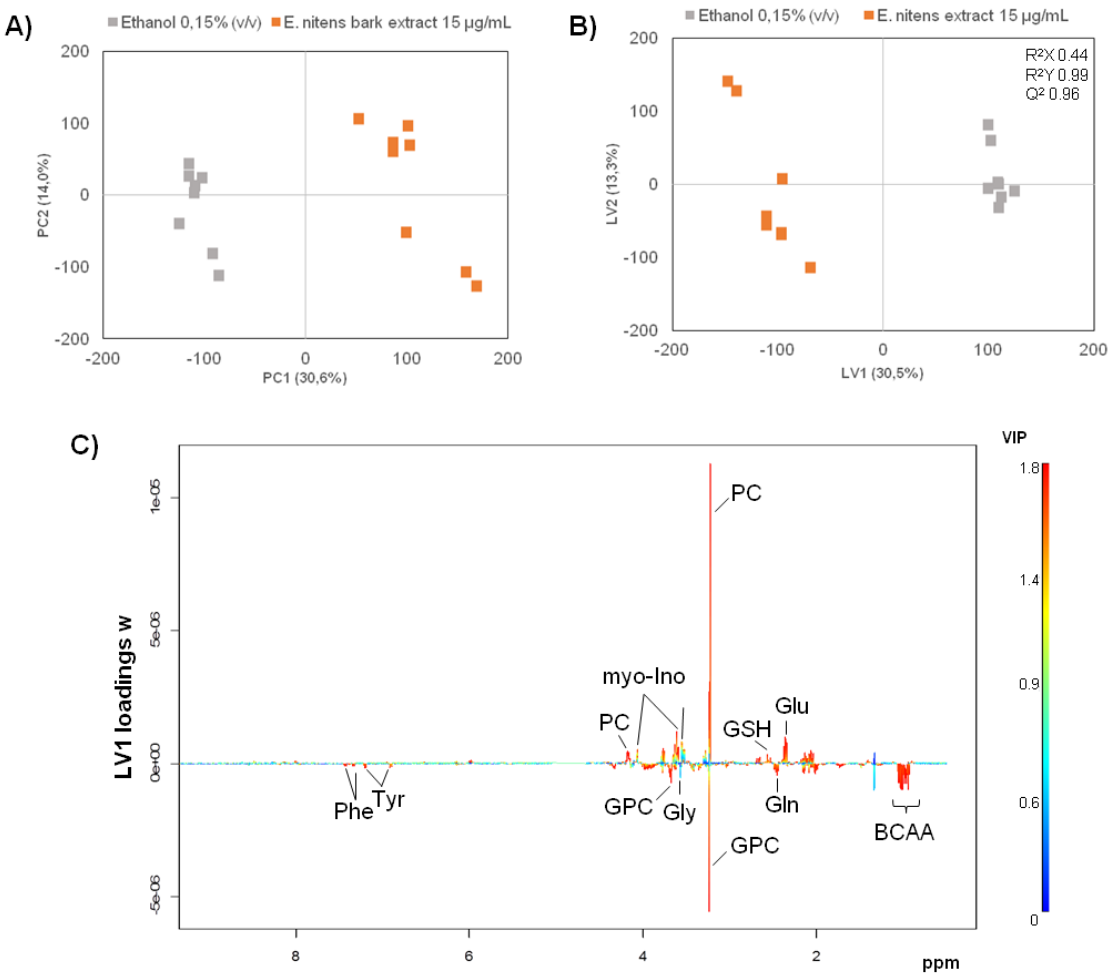

Figure 3.5. Multivariate analysis of ^{1}H NMR spectra from aqueous extracts of MDA-MB-231 control cells and cells exposed to *E. nitens* lipophilic outer bark extract: A) PCA; B) PLS-DA scores scatter plots and C) LV1 loadings w, coloured as a function of variable importance to the projection (VIP). BCAA, branched chain amino acids; Three letter code used for amino acids; GSH, reduced glutathione; PC, phosphocholine; GPC, glycerophosphocholine; myo-Ino, myo-inositol.

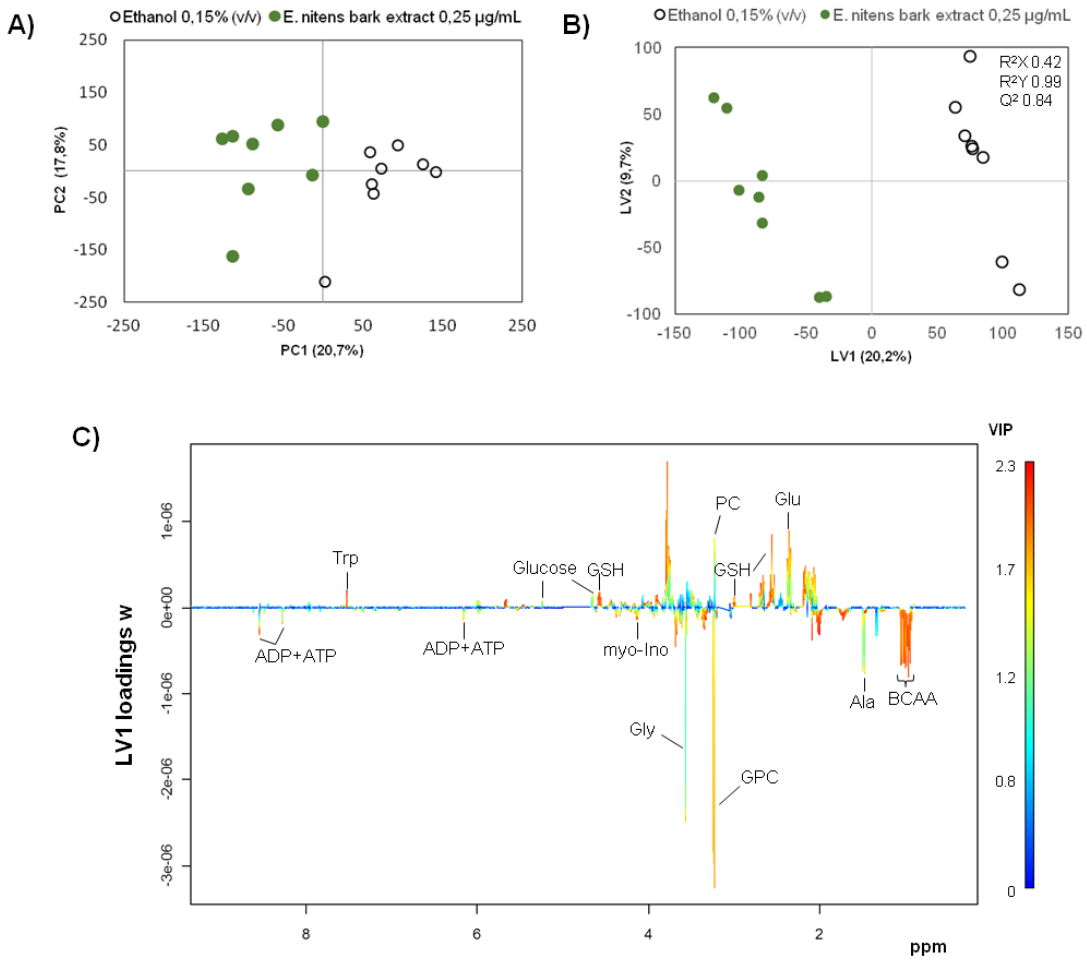

Figure 3.6. Multivariate analysis of ^{1}H NMR spectra from aqueous extracts of MCF-10A control cells and cells exposed to *E. nitens* lipophilic outer bark extract: A) PCA; B) PLS-DA scores scatter plots and C) LV1 loadings w, coloured as a function of variable importance to the projection (VIP). BCAA, branched chain amino acids; Three letter code used for amino acids; GSH, reduced glutathione; PC, phosphocholine; GPC, glycerophosphocholine; myo-Ino, myo-inositol.

Incubation with the *E. nitens* extract also induced pronounced changes in the intracellular metabolic profile of epithelial MCF-10A breast cells, as shown by the good separation between sample groups achieved through PCA and PLS-DA multivariate analyses (Figure 3.6A and 3.6B). Inspection of PLS-DA loadings (Figure 3.6C) suggested the *E. nitens* metabolic signature in epithelial cells to comprise both common and different features compared to the effects produced in cancer cells (Figure 3.5C).

Spectral integration of individual metabolites was then employed to perform a more detailed analysis of the *E. nitens*-induced variations in both cell types. The results are presented in full in Supplementary Table S3.1 and summarized in the form of a heatmap colour-coded according to the percentage of variation relatively to respective controls (Figure 3.7).

Both cell types displayed significant increases in the sugar derivatives uridine diphosphate-N-acetylglucosamine/galactosamine (UDP-GlcNAc and UDP-GalNAc), which, in the case of MCF-10A cells, were accompanied by decreases in glucose and glucose-1-phosphate. The TCA cycle intermediates citrate and fumarate were also affected, decreasing significantly in both cell types, although more extensively in cancer cells. Additionally, formate was seen to decrease only in cancer cells.

The *E. nitens* extract extensively modulated the levels of intracellular amino acids, especially in MDA-MB-231 cells. In particular, *E. nitens*-treated cancer cells displayed large increases (> 60%) in nine amino acids (proline, histidine, BCAA and aromatic amino acids), mild increases (< 25%) in three others (aspartate, alanine and glycine) and a ~50% decrease in glutamate. As for MCF-10A epithelial cells, decreases were noted for glutamate and aspartate, while glutamine levels remained unchanged. Moreover, several other amino acids increased in *E. nitens*-treated epithelial cells, similarly to what was observed for cancer cells (although with different magnitudes). On the other hand, significant variations in the amino acid derivatives creatine and phosphocreatine were observed only in cancer cells, with the former increasing and the latter decreasing upon incubation with the *E. nitens* extract.

The levels of several nucleotides were altered in *E. nitens*-treated cells compared to untreated controls. In particular, uridine nucleotides (UMP, UDP and UTP) greatly decreased in MDA-MB-231-treated cells, while a moderate decrease in UTP was observed in MCF-10A-treated cells. Additionally, higher overall levels of ATP were found in *E. nitens*-treated MCF-10A cells, whereas MDA-MB-231 cells showed only a mild non-significant increase in ATP. Another particularly interesting difference in cellular responses to the *E. nitens* extract regarded the levels of NAD^+ and NADH. While the NAD^+ to NADH ratio decreased when epithelial cells were incubated with the *E. nitens* extract, it increased considerably in *E. nitens*-exposed cancer cells (relatively to respective controls). Other intracellular effects of the *E. nitens* extracts comprised increases in choline and glycerophosphocholine together with decreases in phosphocholine (both cell types), decreases in glutathione (both cell types) and myo-inositol (cancer cells only) and increases in taurine (Figure 3.7).

Within the intracellular metabolic effects described above, we have then looked closer at variations where metabolite ratios in MDA-MB-231 cells treated with the *E. nitens* extract approached those found in MCF10-A epithelial cells, as these could reflect a reversal of the malignant metabotype. The main results of this comparison are shown in Figure 3.8. The NAD^+/NADH ratio was lower in control

MDA-MB-231 cells and, upon treatment with the *E. nitens* extract, it recovered to levels found in epithelial cells. On the other hand, the glutamate/glutamine and the phosphocholine/choline ratios were greatly enhanced in tumor cells compared to epithelial cells, and decreased significantly upon exposure of MDA-MB-231 cells to the *E. nitens* extract.

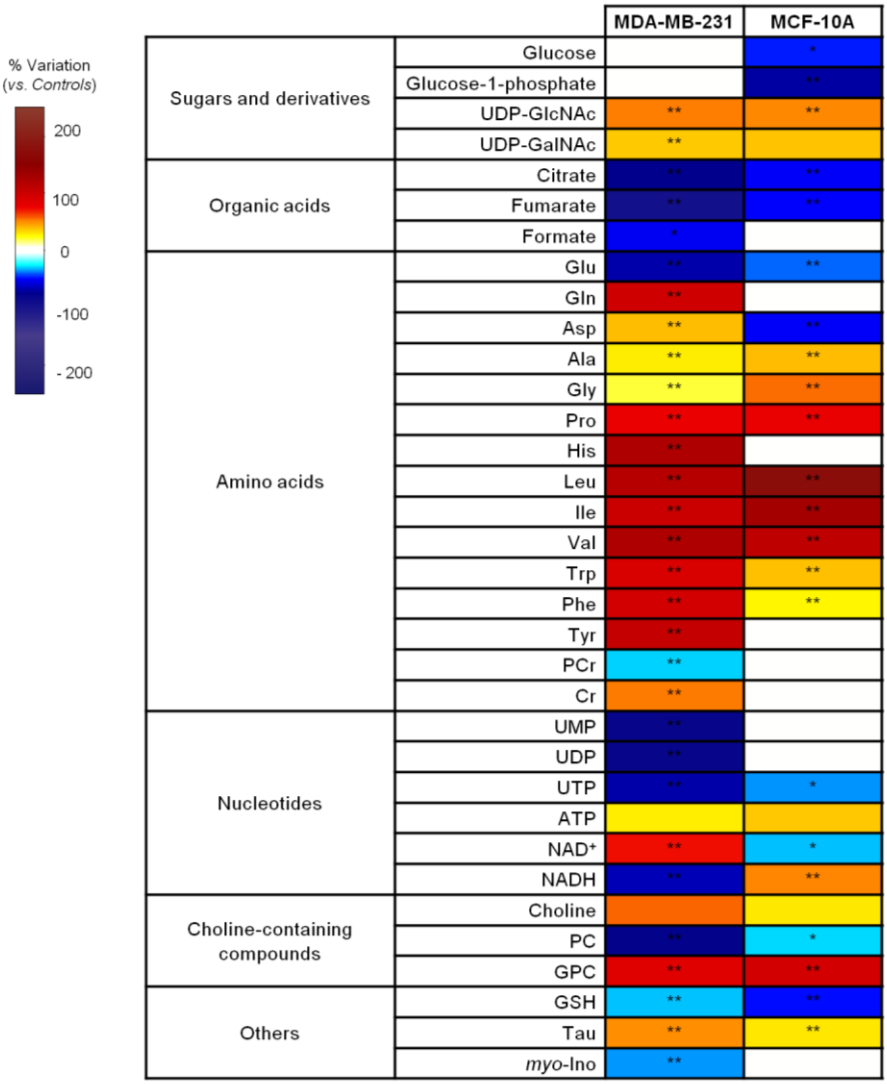

Figure 3.7. Heatmap of the main metabolite variations in aqueous extracts from MDA-MB-231 and MCF-10 cells exposed, respectively, to 15 µg/mL and 0.25 µg/mL of *E. nitens* lipophilic outer bark extract, colored according to % variation in relation to controls. * *P*-value <0.05, ** *P*-value < 0.01. Three letter code used for amino acids; Cr, creatine; PCr, phosphocreatine; ATP, adenosine triphosphate; NAD^+/NADH , nicotinamide adenine dinucleotide/reduced form; GSH, reduced glutathione; PC, phosphocholine; GPC, glycerophosphocholine; UMP/UDP/UTP, uridine mono/di/triphosphate; UDP-GalNAc, UDP-N-acetyl-galactosamine; UDP-GlcNAc, UDP-N-acetyl-glucosamine.

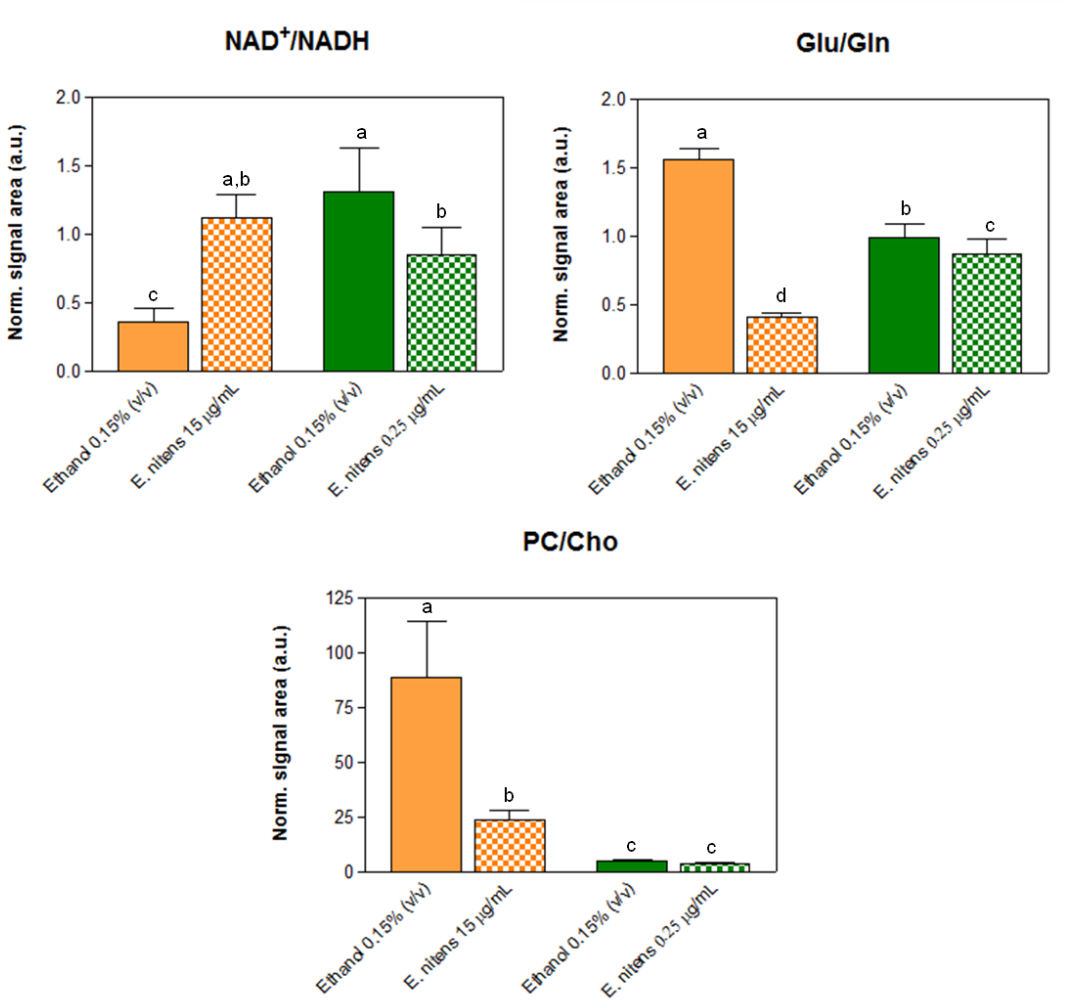

Figure 3.8. Selected metabolite ratios in aqueous extracts of MDA-MB-231 (orange) and MCF-10A cells (green) exposed, respectively, to 15 µg/mL and 0.25 µg/mL of *E. nitens* lipophilic outer bark extract. Means marked with different letters are statistically different (*P*-value <0.05). Three letter code used for amino acids; NAD^+/NADH , nicotinamide adenine dinucleotide/reduced form; PC, phosphocholine.

To assess *E. nitens*-induced changes in the cellular lipid composition, cell organic extracts were also analyzed by ^{1}H NMR spectroscopy. Interestingly, the NMR-detected lipid composition of MCF-10A epithelial cells remained unaffected upon 48h incubation with the *E. nitens* extract, as realized through visual spectral comparison and multivariate analysis (results not shown). In contrast, *E. nitens*-treated MDA-MB-231 cells displayed several alterations in their lipidic profile, compared to untreated controls. This was visible through multivariate analysis of spectral data (Figure 3.9) and confirmed through spectral integration of representative signals (Figure 3.10). Incubation of breast cancer cells with the *E. nitens* extract caused significant decreases in cholesteryl esters and triglycerides, together with increases in free cholesterol and glycerophospholipids. The ratio of polyunsaturated fatty acyl chains (PUFA) to unsaturated fatty acyl chains (UFA)

also presented a significantly higher level in MDA-MB-231 cells exposed to *E. nitens* lipophilic outer bark extract.

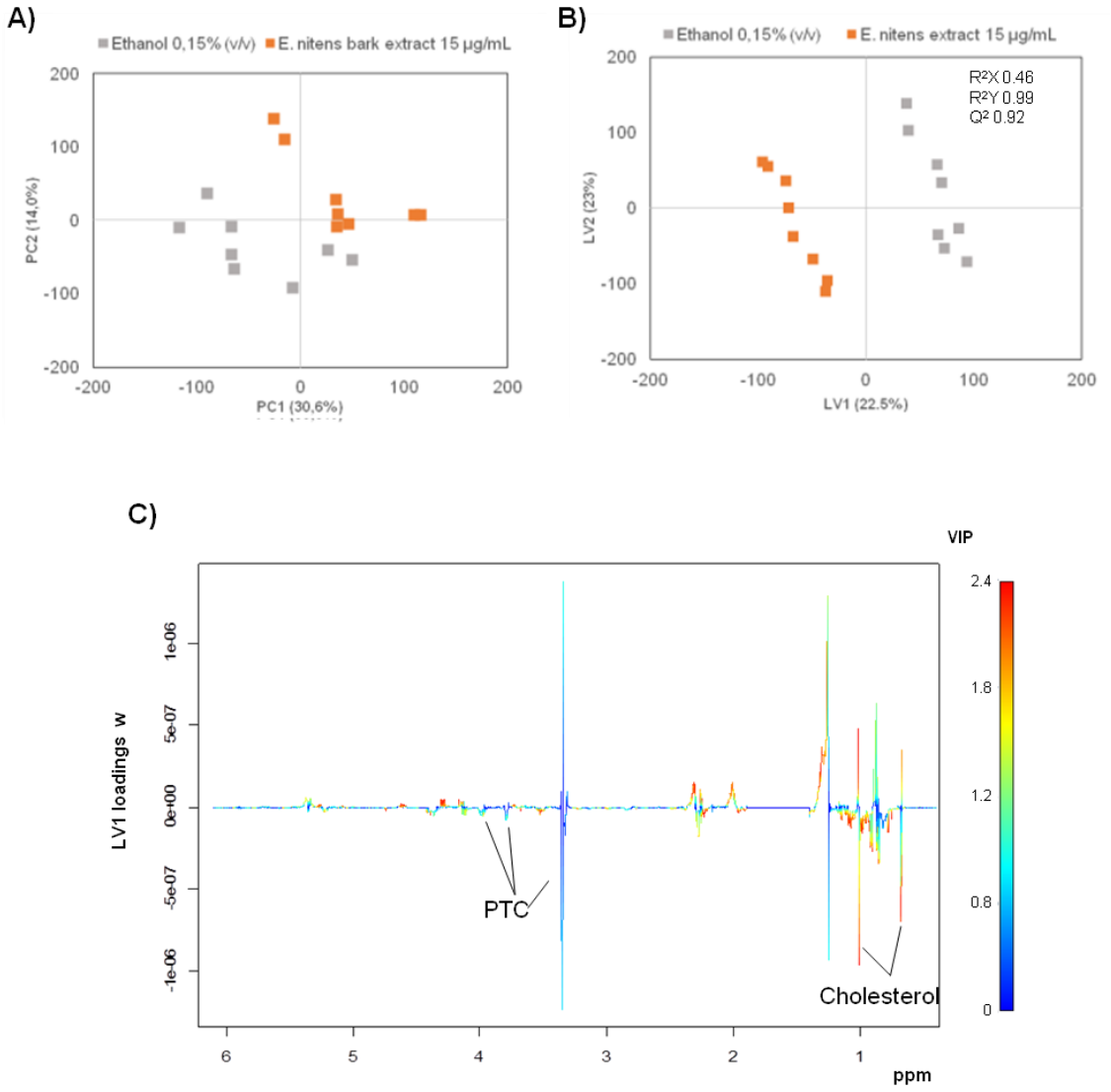

Figure 3.9. Multivariate analysis of ^{1}H NMR spectra from lipophilic extracts of MDA-MB-231 control cells and cells exposed to *E. nitens* lipophilic outer bark extract: A) PCA; B) PLS-DA scores scatter plots and C) LV1 loadings w, coloured as a function of variable importance to the projection (VIP). PTC, phosphatidylcholine.

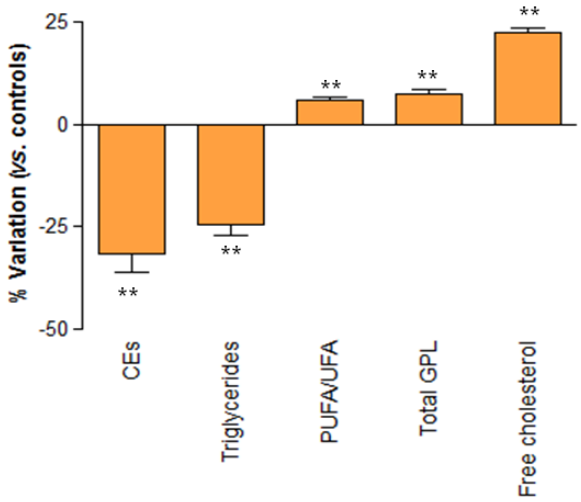

Figure 3.10. Lipid-related variations in organic extracts from MDA-MB-231 breast cancer cells treated for 48h with 15 µg/mL *E. nitens* lipophilic bark extract. Ethanol was the solvent control. ** *P*-value < 0.01. CEs, cholesteryl esters; PUFA, polyunsaturated fatty acyl chains, UFA, unsaturated fatty acyl chains; GPLs, Glycerophospholipids.

3.3.4. Effect of *E. nitens* lipophilic outer bark extract on the expression of selected proteins in MDA-MB-231 cells

The significant decrease in the phosphocholine/choline ratio observed in MDA-MD-231 cells upon incubation with the *E. nitens* extract (Figure 3.8) suggested that the expression of choline kinase (ChoK), the enzyme which catalyzes the first reaction in the Kennedy pathway of phosphatidylcholine biosynthesis [21], could be altered. Indeed, the results presented in Figure 3.11A and 3.11B revealed that incubating MDA-MB-231 cells with the *E. nitens* extract for 48h significantly decreased the relative expression of ChoK-α in these cells, as compared to untreated tumor cells ($P < 0.05$).

Additionally, based on the distinct glutamine to glutamate ratios observed in control and *E. nitens*-treated MDA-MB-231 cells (Figure 3.8), we have hypothesized that the *E. nitens* extract could modulate the expression of glutaminase (GLS), the enzyme responsible for the glutamine to glutamate conversion. Hence, protein expression levels of both splice variants of the GLS gene, kidney type glutaminase (KGA) and glutaminase C (GAC) were analyzed in MDA-MB-231 cells, after 48h treatment with *E. nitens* lipophilic outer bark extract (15 µg/mL) (Figure 3.11C and 3.11D).

The relative expression level of KGA remained unaltered in MDA-MB- 231 cells, after treatment with the extract, in comparison with control tumor cells. For the GAC splice variant, *E. nitens*-treated MDA-MB-231 cells showed a tendency to present a lower protein expression level relative to controls, but this difference was not statistically different ($p > 0.05$).

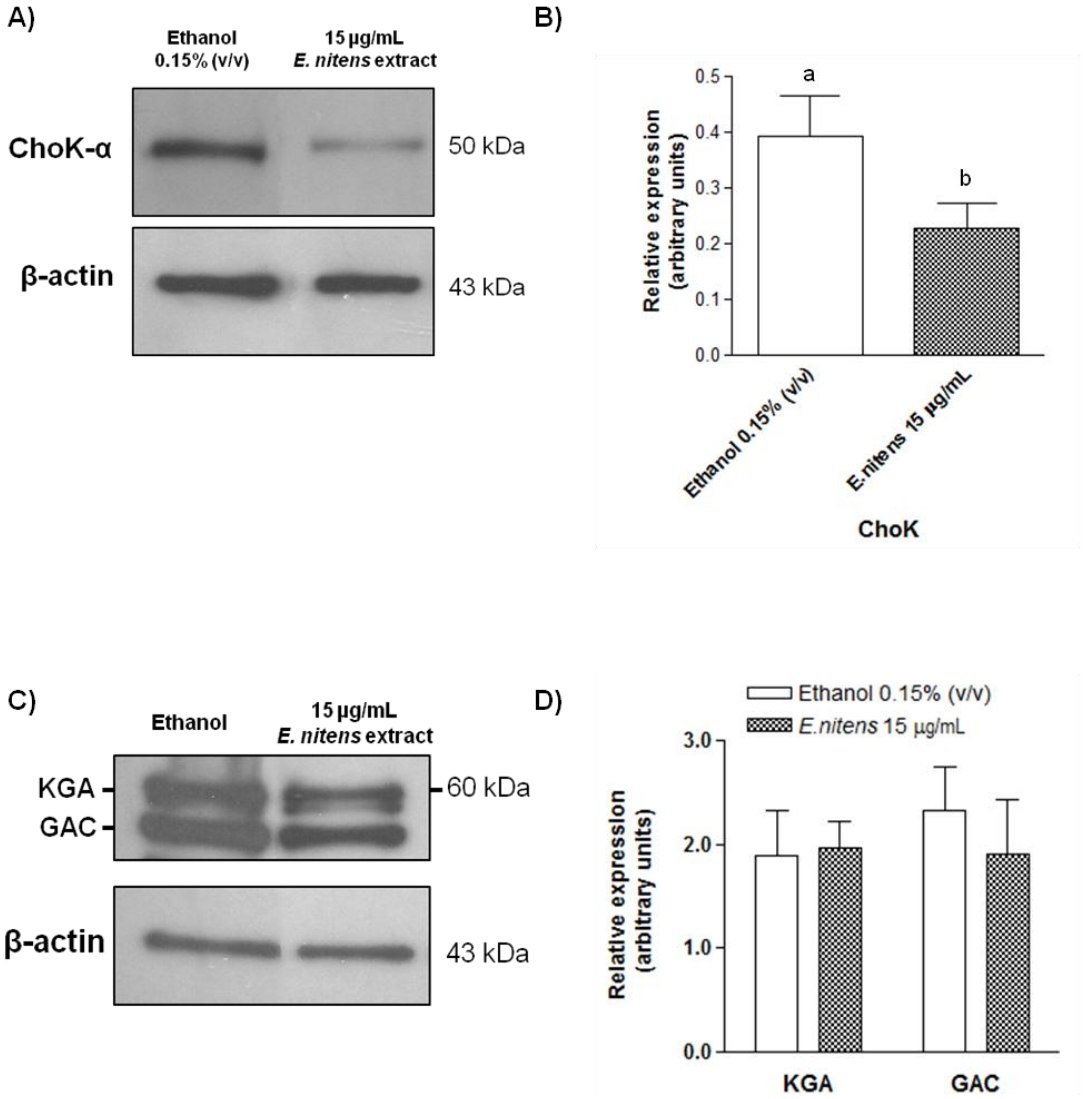

Figure 3.11. Western blot analysis of Choline Kinase-α and Glutaminase splice variants (KGA and GAC) in MDA-MB-231 cells, after 48 h treatments with 15 µg/mL *E. nitens* lipophilic outer bark extract. Ethanol (0.15% (v/v)) was used as solvent control. A) Representative image of ChoK immunoblots; B) Relative ChoK expression determined by analysis of band integrated density and normalization to β-actin. C) Representative image of KGA and GAC immunoblots; D) Relative KGA and GAC expression determined by analysis of band integrated density and normalization to β-actin. Each column and bar respectively represents the mean and the standard deviation of three independent experiments. Columns with different letters are statistically different (*P*-value < 0.05).

3.4. Discussion

The anticancer properties of plant biomass extracts and phytochemicals continues to harness great interest as several of these natural products have the potential to modulate multiple oncogenic pathways, to promote synergistic effects when used in combination with standard therapies and/or to attenuate adverse systemic side effects [22]. The outer bark of *E. nitens* is a widely available source of bioactive compounds, particularly of triterpenic acids [6], whose tumoricidal activity has been demonstrated in several cell models [2-4]. However, the therapeutic potential of the *E. nitens* extracts remains underappreciated and calls for an improved understanding of their mode of action at the cellular and molecular levels. The aims of this work were to assess the potential of a lipophilic *E. nitens* outer bark extract to affect the viability of TNBC cells and to reveal the metabolic alterations associated with the extract's inhibitory action, in both tumor and non-tumor epithelial cells.

Our results demonstrated that the *E. nitens* outer bark extract inhibits the viability of MDA-MB-231 breast cancer cells in a dose- and time-dependent manner. Breast epithelial MCF-10A cells were even more sensitive to the plant extract for all the tested periods. The much higher IC_{50} values found for cancer cells in comparison to epithelial cells are in line with the properties reported for the MDA-MB-231 cell line, namely the high proliferation rate, metastatic ability, resistance to chemotherapeutic drugs and intrinsic resistance to cell death [23, 24]. Obviously, the high cytotoxicity of the *E. nitens* extract towards epithelial cells could represent a limitation, since, within an *in vivo* setting, it is possible that normal tissue could be severely damaged by anticancer effective doses. This is a common problem encountered for anticancer compounds, which may potentially be mitigated through drug-delivery strategies or the use of lower doses able to sensitize/modulate tumor cells rather than killing them directly. For the sake of this study, aimed at comparing the metabolic responses of cancer and epithelial cells to the *E. nitens* extract, concentrations producing the same level of viability inhibition (~50%) in both cell lines were employed in cell cycle and metabolomics assays.

The ability of the *E. nitens* extract to modulate the cell cycle was assessed by flow cytometry analysis of the cells distribution through G0/G1, S and G2 phases. The extract did not produce significant changes in the cell cycle phases of either cancer or epithelial cells, after 48h incubation. Interestingly, the main component of the extract, betulinic acid (20.02 ± 0.90 mg/g extract), was reported to arrest cell cycle in G2/M phase when administered to MDA-MB-231 cells at 5 and 10 μM for 48h, and to significantly facilitate G2/M arrest induced by taxol in MDA-

MB-231 and MCF-7 cells [25, 26]. Ursolic acid (2.5-50µM) also caused G0/G1 cell cycle arrest in *in vitro* models of breast cancer [27-29]. Hence, our results suggest that pure TAs may have a higher impact on the cell cycle of TNBC cells than the TA-rich *E. nitens* extract studied here.

The *E. nitens* extract clearly affected the metabolism of both MDA-MB-231 and MCF-10A cells, as shown by the marked variations in the cells metabolic profiles assessed by ^{1}H NMR spectroscopy. Interestingly, the exometabolome of MCF-10A cells was much more responsive to *E. nitens* exposure than that of MDA-MB-231 cells. On the contrary, the effects produced at the intracellular level, both in aqueous and lipophilic metabolites, were generally more numerous and pronounced in MDA-MB-231 cancer cells. This shows the complementarity of the exo and endometabolome windows and suggests that the two cell types may have different ways of harmonizing metabolite flow and intracellular metabolic composition.

The balance between glycolytic and oxidative metabolism appeared to be strongly modulated by the *E. nitens* extract, as suggested by variations in sugars, TCA cycle intermediates, the nicotinamide adenine dinucleotide redox couple (NAD^+ and NADH), several amino acids and lipids (Figure 3.12). Contrarily to epithelial cells, cancer cells increased NAD^+ and decreased NADH levels upon exposure to the *E. nitens* extract. Low NAD^+/NADH ratios, as observed here for untreated MDA-MB-231 cells (Figure 3.8) are characteristic of cancer cells, due to their high glycolytic activity (glycolysis consumes NAD^+) and/or a defective OXPHOS. Indeed, mitochondrial DNA mutations in genes encoding complex I of the respiratory chain, which catalyzes the first step of NADH oxidation, have been found in different cancer types, including in breast cancer [30-33]. On the other hand, the raise in the NAD^+/NADH ratio in E. nitens-treated cancer cells could reflect a shift towards less glycolytic metabolism and normalization of mitochondrial function, as OXPHOS regenerates NAD^+ in the process of ATP production. Notably, a previous work has established a negative correlation between NAD^+/NADH ratios in MDA-MB-231 cells and their aggressive, malignant phenotype [34, 38]. The authors have shown that by enhancing the cellular NAD^+/NADH ratio, either by altering complex I activity or interfering with NAD^+ synthesis, tumor growth and metastatic activity were inhibited, both *in vitro* and *in vivo*. Hence, it is reasonable to hypothesize that modulation of the NAD^+/NADH intracellular ratio by the *E. nitens* extract could be a key feature of its anticancer activity, possibly through interference with complex I of the respiratory chain, an hypothesis that warrants further investigation in the future.

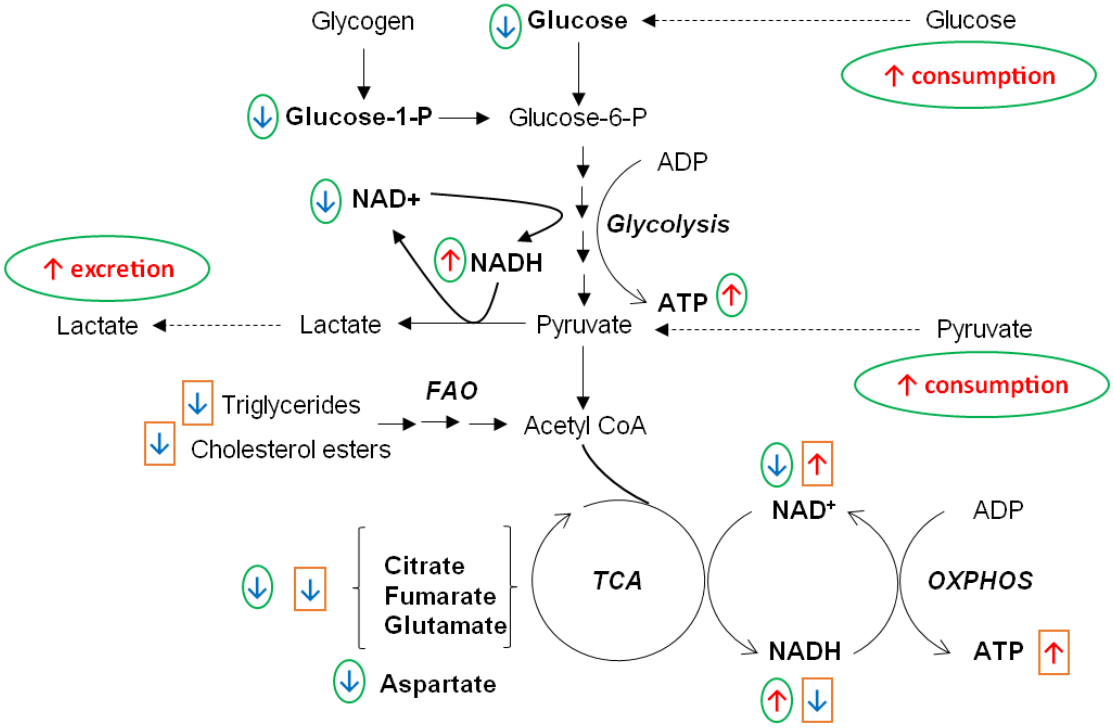

Figure 3.12. Schematic diagram of the putative effects in the glycolytic and oxidative metabolism of *E. nitens* lipophilic outer bark extract in MDA-MB-231 breast cancer and MCF-10A epithelial breast cells. Effects on MDA-MB-231 and MCF-10A cells are represented by orange squares and green circles, respectively.

E. nitens-treated MDA-MB-231 cells further displayed significantly reduced levels of triglycerides and cholesterol esters (Figure 3.10), which could have been hydrolyzed to provide free fatty acids for beta-oxidation, and subsequently generate acetyl-CoA that can be fueled into the TCA cycle. The observed decreases in citrate and fumarate are also consistent with the possible intensification of the TCA cycle, thus providing additional NADH required for OXPHOS. Moreover, glutamate levels decreased concomitantly with a significant increase in glutamine. Glutamine is a key substrate for cancer cells, required not only for biosynthetic pathways (amino acids and nucleic acids production), but also for glutaminolysis, whereby it is converted into glutamate, which in turn may fuel the TCA cycle and energy generation [35]. MDA-MB-231 cells have been found to be glutamine-dependent and to exhibit a phenotype of glutamine addiction [36]. Glutaminase, the enzyme responsible for conversion of glutamine into glutamate was reported to be higher in TNBC than in other breast cancer subtypes and both splice variants of the *GLS* gene, kidney type glutaminase (KGA) and glutaminase C (GAC), were recently reported to be essential for the survival and proliferation of TNBC cells [37]. Thus, based on the decreased glutamate/glutamine ratio in treated cancer cells (Figure

3.8), we have postulated that the *E. nitens* extract could downregulate the expression/activity of glutaminase, thus inhibiting glutaminolysis. However, the immunoblot assays performed to verify this hypothesis were not conclusive, as the GAC splice variant showed only a non-significant decreasing trend in treated MDA-MB-231 cancer cells.

Santidrian and co-workers have also shown that the mechanism linking enhanced complex I activity and NAD^+/NADH levels to reduced aggressiveness of breast cancer cells involved induction of autophagy by regulating mTORC1 signaling [38]. Interestingly, we have found the *E. nitens* extract to induce a pronounced increase in the levels of several amino acids in MDA-MB-231 cells, which could reflect autophagy-related protein degradation [39]. Moreover, autophagy is known to mobilize diverse cellular energy stores in order to provide ATP for various steps of autophagic processes [40]. This could be related to the observed decrease in phosphocreatine and concomitant increase in creatine, which corroborates reprogramming of energy storage and transmission [41].

Regarding MCF-10A cells, the glycolytic-oxidative balance appeared to be modulated by the *E. nitens* extract in a different way, as suggested by the opposing variations in NAD^+ and NADH levels (Figure 3.12). Treated epithelial cells displayed a reduction in the NAD^+/NADH ratio, contrarily to what was observed in cancer cells. Other possibly related variations include increased consumption of extracellular glucose, pyruvate and glutamine, increased excretion of lactate, decreased intracellular levels of glucose, glucose-1-phosphate (possibly arising from glycogen degradation), citrate and fumarate, as well as of the TCA cycle anaplerotic substrates aspartate and glutamate. Taken together, these results suggest that, in MCF-10A cells, the *E. nitens* extract intensified glycolysis and the TCA cycle (NAD^+ consuming pathways). Moreover, intracellular levels of amino acids were affected to a lesser extent, with the exception of branched chain amino acids, for which substantial increases were observed.

The variations in nucleotide sugars and free nucleotides suggest that the *E. nitens* extract modulated the hexosamine biosynthetic pathway (HBP) in both cell types (Figure 3.13). This pathway integrates glucose, fatty acids, amino acids and nucleotides metabolism and produces UDP-N-acetylglucosamine (UDP-GlcNAc) and its derivative UDP-N-acetylgalactosamine (UDP-GalNAc), which are fundamental substrates for several glycosylation reactions [42]. MDA-MB-231 and MCF-10A cells exposed to *E. nitens* lipophilic outer bark extract presented significantly increased levels of both UDP-GlcNAc and its derivative UDP-*N*-

acetylgalactosamine (UDP-GalNAc), suggesting an increased glucose flux through the hexosamine biosynthetic pathway.

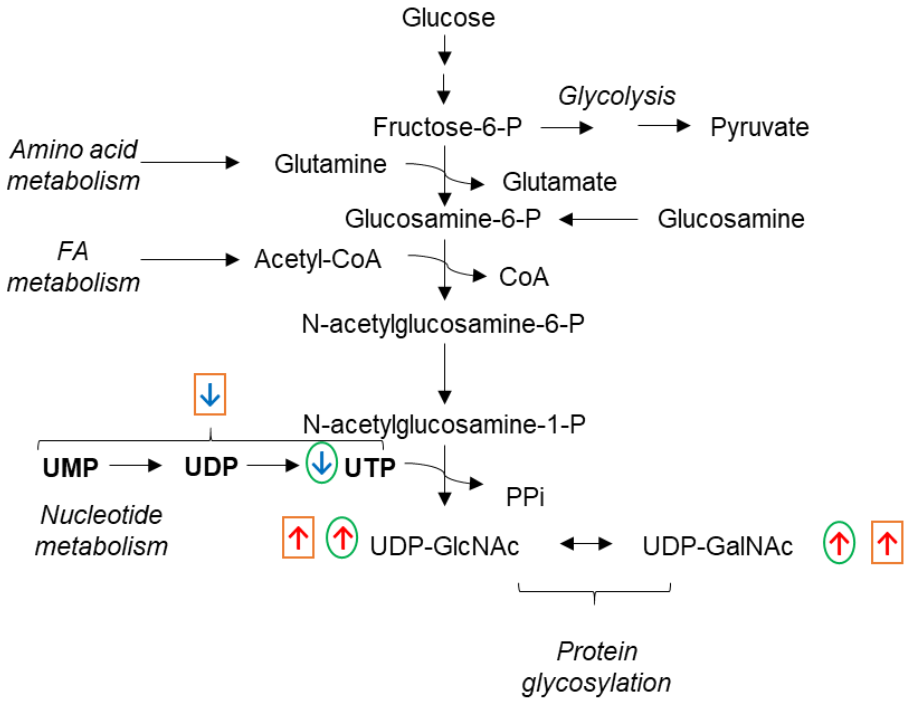

Figure 3.13. Schematic diagram of the putative effects in the hexosamine biosynthetic pathway (HBP) of *E. nitens* lipophilic outer bark extract in MDA-MB-231 breast cancer and MCF-10A epithelial breast cells. Effects on MDA-MB-231 and MCF-10A cells are represented by orange squares and green circles, respectively.

Phospholipid metabolism also seemed to be affected upon exposure of both cell lines to the *E. nitens* extract, as suggested by decreased intracellular levels of phosphocholine (PC) and increased levels of choline (Cho) and glycerophosphocholine (GPC). Alterations in choline metabolism have been thoroughly described in TNBC, both in patients and in experimental models (reviewed in [21]). Upregulation of choline kinase (ChoK-α), which catalyzes the first committed step in phosphatidylcholine (PTC) biosynthesis (Kennedy pathway), has been reported to result in phosphocholine accumulation in TNBC cells/tissues [43-45]. Accordingly, we found a much higher PC/Cho ratio in untreated MDA-MB-231 cells than in MCF-10A cells (Figure 3.8). Interestingly, this ratio decreased considerably upon exposure of TNBC cells to the *E. nitens* extract, becoming closer to the ratio found in epithelial cells. Furthermore, we found that downregulation of ChoK-α protein expression levels in treated MDA-MB-231 cells could help explaining this variation. Additionally, the increase in total glycerophospholipids found in the organic extracts of MDA-MB-231 treated cells (Figure 3.10) suggests

that increased membrane formation could also account for the observed decrease in PC (Figure 3.14).

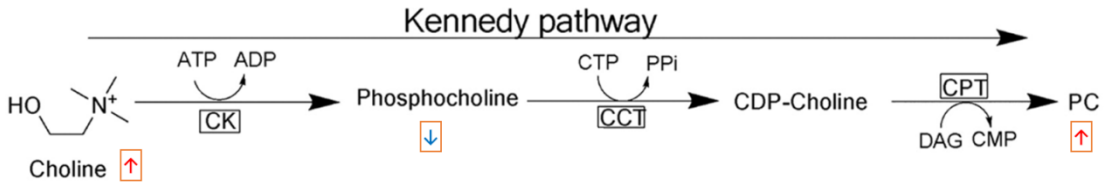

Figure 3.14. Schematic diagram of the putative effects in the Kennedy pathway of *E. nitens* lipophilic outer bark extract in MDA-MB-231 breast cancer cells.

The intracellular levels of the antioxidant tripeptide glutathione (GSH), a key metabolite in cellular redox homeostasis, were seen to decrease in both cell types, suggesting that GSH synthesis/recycling did not compensate its use. Interestingly, taurine a sulfur-containing amino acid that results from cysteine catabolism (a precursor of GSH), was increased in treated cells. Taurine has been demonstrated to induce apoptosis in MDA-MB-231 cells and to inhibit tumor growth in MDA-MB-231 cells-nude mice xenografts [46]. Another effect induced by *E.nitens* lipophilic bark extract in MDA-MB-231 cells was the decrease in myo-inositol levels. This metabolite plays an important role in various cellular processes, including cell growth and survival, and has been found to be significantly increased in triple negative MDA-MB-231 cells [47, 48].

3.5. Conclusion

This work has provided significant novel insight into the metabolic modulation of tumor and non-tumor breast cells induced by a lipophilic *E. nitens* outer bark extract. The integrative analysis of culture medium, intracellular polar metabolites and cellular lipids by ^{1}H NMR metabolomics provided a comprehensive picture of cells metabolic adaptations, which allowed us to generate several hypotheses about the metabolic targets and pathways affected. This knowledge contributes to improve current understanding of the biological activity of this plant extract and is potentially useful to potentiate its development in the field of TNBC natural product-based anticancer therapy.

3.6. References

1. Kaur, P. and Sharma, V., (2018). Prospective plant based anticancer lead molecules. *Current Topics in Medicinal Chemistry*, 18(30), 2567-2583.

2. Laszczyk, M.N., (2009). Pentacyclic triterpenes of the lupane, oleanane and ursane group as tools in cancer therapy. *Planta Medica*, 75(15), 1549-1560.

3. Rufino-Palomares, E.E., Perez-Jimenez, A., Reyes-Zurita, F.J., Garcia-Salguero, L., Mokhtari, K., Herrera-Merchan, A., Medina, P.P., Peragon, J. and Lupianez, J.A., (2015). Anti-cancer and anti-angiogenic properties of various natural pentacyclic triterpenoids and some of their chemical derivatives. *Current Organic Chemistry*, 19(10), 919-947.

4. Salvador, J.A.R., Leal, A.S., Valdeira, A.S., Goncalves, B.M.F., Alho, D.P.S., Figueiredo, S.A.C., Silvestre, S.M.and Mendes, V.I.S., (2017). Oleanane-, ursane-, and quinone methide friedelane-type triterpenoid derivatives: Recent advances in cancer treatment. *European Journal of Medicinal Chemistry*, 142 95-130.

5. Guerra, A.R., Duarte, M.F.and Duarte, I.F., (2018). Targeting tumor metabolism with plant-derived natural products: emerging trends in cancer therapy. *Journal of Agricultural and Food Chemistry*, 66(41), 10663-10685.

6. Domingues, R.M.A., Patinha, D.J.S., Sousa, G.D.A., Villaverde, J.J., Silva, C.M., Freire, C.S.R., Silvestre, A.J.D.and Neto, C.P., (2011). Eucalyptus biomass residues from agro-forest and pulping industries as sources of high-value triterpenic compounds. *Cellulose Chemistry and Technology*, 45(7-8), 475-481.

7. Domingues, R.M.A., Sousa, G.D.A., Silva, C.M., Freire, C.S.R., Silvestre, A.J.D.and Neto, C.P., (2011). High value triterpenic compounds from the outer barks of several Eucalyptus species cultivated in Brazil and in Portugal. *Industrial Crops and Products*, 33(1), 158-164.

8. Guerra, A., Soares, B., Guerreiro, O., Ramos, P., Oliveira, H., Silvestre, A., Freire, C.and Duarte, M.F., (2014). Anti-tumoral activity of lipophilic Eucalyptus bark extracts, enriched on triterpenic acids, against breast cancer cells. *Planta Medica*, 80(16), 1368-1368.

9. Fouad, Y.A. and Aanei, C., (2017). Revisiting the hallmarks of cancer. *American Journal of Cancer Research*, 7(5), 1016-1036.

10. Martinez-Outschoorn, U.E., Peiris-Pages, M., Pestell, R.G., Sotgia, F.and Lisanti, M.P., (2017). Cancer metabolism: a therapeutic perspective. *Nature Reviews Clinical Oncology*, 14(1), 11-31.

11. Wishart, D.S., (2016). Emerging applications of metabolomics in drug discovery and precision medicine. *Nature Reviews Drug Discovery*, 15(7), 473-484.

12. Vojtek, M., Marques, M.P.M., Ferreira, I.M.P.L.V.O., Mota-Filipe, H.and Diniz, C., (2019). Anticancer activity of palladium-based complexes against triple-negative breast cancer. *Drug Discovery Today*, 24(4), 1044-1058.

13. Schneeweiss, A., Denkert, C., Fasching, P.A., Fremd, C., Gluz, O., Kolberg-Liedtke, C., Loibl, S.and Luck, H.J., (2019). Diagnosis and therapy of Triple-Negative Breast Cancer (TNBC) - Recommendations for daily routine practice. *Geburtshilfe Und Frauenheilkunde*, 79(6), 605-617.

14. Parreira, P., Soares, B.I.G., Freire, C.S.R., Silvestre, A.J.D., Reis, C.A., Martins, M.C.L.and Duarte, M.F., (2017). Eucalyptus spp. outer bark extracts inhibit

Helicobacter pylori growth: in vitro studies. *Industrial Crops and Products*, 105 207-214.

15. Freire, C.S.R., Silvestre, A.J.D., Neto, C.P.and Cavaleiro, J.A.S., (2002). Lipophilic extractives of the inner and outer barks of Eucalyptus globulus. *Holzforschung*, 56(4), 372-379.

16. Mosmann, T., (1983). Rapid colorimetric assay for cellular growth and survival - Application to proliferation and cytotoxicity assays. *Journal of Immunological Methods*, 65(1-2), 55-63.

17. Carrola, J., Bastos, V., de Oliveira, J.M.P.F., Oliveira, H., Santos, C., Gil, A.M.and Duarte, I.F., (2016). Insights into the impact of silver nanoparticles on human keratinocytes metabolism through NMR metabolomics. *Archives of Biochemistry and Biophysics*, 589 53-61.

18. Wishart, D.S., Feunang, Y.D., Marcu, A., Guo, A.C., Liang, K., Vazquez-Fresno, R., Sajed, T., Johnson, D., Li, C.R., Karu, N., Sayeeda, Z., *et al.*, (2018). HMDB 4.0: the human metabolome database for 2018. *Nucleic Acids Research*, 46(D1), D608-D617.

19. Berben, L., Sereika, S.M.and Engberg, S., (2012). Effect size estimation: Methods and examples. *International Journal of Nursing Studies*, 49(8), 1039-1047.

20. Lowry, O.H., Rosebrough, N.J., Farr, A.L.and Randall, R.J., (1951). Protein measurement with the folin phenol reagent. *Journal of Biological Chemistry*, 193(1), 265-275.

21. Iorio, E., Caramujo, M.J., Cecchetti, S., Spadaro, F., Carpinelli, G., Canese, R.and Podo, F., (2016). Key players in choline metabolic reprograming in triple-negative breast cancer. *Frontiers in Oncology*, 6, 205.

22. Dutta, S., Mahalanobish, S., Saha, S., Ghosh, S.and Sil, P.C., (2019). Natural products: An upcoming therapeutic approach to cancer. *Food and Chemical Toxicology*, 128 240-255.

23. Smith, L., Watson, M.B., O'Kane, S.L., Drew, P.J., Lind, M.J.and Cawkwell, L., (2006). The analysis of doxorubicin resistance in human breast cancer cells using antibody microarrays. *Molecular Cancer Therapeutics*, 5(8), 2115-2120.

24. Parekh, A., Das, D., Das, S., Dhara, S., Biswas, K., Mandal, M.and Das, S., (2018). Bioimpedimetric analysis in conjunction with growth dynamics to differentiate aggressiveness of cancer cells. *Scientific Reports*, 8(1), 783.

25. Mertens-Talcott, S.U., Noratto, G.D., Li, X.R., Angel-Morales, G., Bertoldi, M.C.and Safe, S., (2013). Betulinic acid decreases ER-negative breast cancer cell growth in vitro and in vivo: Role of Sp transcription factors and microRNA-27a:ZBTB10. *Molecular Carcinogenesis*, 52(8), 591-602.

26. Cai, Y.L., Zheng, Y.F., Gu, J.Y., Wang, S.Q., Wang, N., Yang, B.W., Zhang, F.X., Wang, D.M., Fu, W.J.and Wang, Z.Y., (2018). Betulinic acid chemosensitizes breast cancer by triggering ER stress-ediated apoptosis by directly targeting GRP78. *Cell Death & Disease*, 9(6), 636.

27. Es-Saady, D., Simon, A., Jayat-Vignoles, C., Chulia, A.J.and Delage, C., (1996). MCF-7 cell cycle arrested at G1 through ursolic acid, and increased reduction of tetrazolium salts. *Anticancer Research*, 16(1), 481-486.

28. De Angel, R.E., Smith, S.M., Glickman, R.D., Perkins, S.N.and Hursting, S.D., (2010). Antitumor effects of ursolic acid in a mouse model of postmenopausal breast cancer. *Nutrition and Cancer-an International Journal*, 62(8), 1074-1086.

29. Lewinska, A., Adamczyk-Grochala, J., Kwasniewicz, E., Deregowska, A.and Wnuk, M., (2017). Ursolic acid-mediated changes in glycolytic pathway promote cytotoxic autophagy and apoptosis in phenotypically different breast cancer cells. *Apoptosis*, 22(6), 800-815.

30. Brandon, M., Baldi, P.and Wallace, D.C., (2006). Mitochondrial mutations in cancer. *Oncogene*, 25(34), 4647-4662.

31. Shen, L.J., Wei, J., Chen, T., He, J., Qu, J.C., He, X.M., Jiang, L.X., Qu, Y.M., Fang, H.Z., Chen, G.R., Lu, J.X.and Bai, Y.D., (2011). Evaluating mitochondrial DNA in patients with breast cancer and benign breast disease. *Journal of Cancer Research and Clinical Oncology*, 137(4), 669-675.

32. Mayr, J.A., Meierhofer, D., Zimmermann, F., Feichtinger, R., Kogler, C., Ratschek, M., Schmeller, N., Sperl, W.and Kofler, B., (2008). Loss of complex I due to mitochondrial DNA mutations in renal oncocytoma. *Clinical Cancer Research*, 14(8), 2270-2275.

33. Fendt, L., Niederstatter, H., Huber, G., Zelger, B., Dunser, M., Seifarth, C., Rock, A., Schafer, G., Klocker, H.and Parson, W., (2011). Accumulation of mutations over the entire mitochondrial genome of breast cancer cells obtained by tissue microdissection. *Breast Cancer Research and Treatment*, 128(2), 327-336.

34. Lunetti, P., Di Giacomo, M., Vergara, D., De Domenico, S., Maffia, M., Zara, V., Capobianco, L.and Ferramosca, A., (2019). Metabolic reprogramming in breast cancer results in distinct mitochondrial bioenergetics between luminal and basal subtypes. *Febs Journal*, 286(4), 688-709.

35. Geck, R.C. and Toker, A., (2016). Nonessential amino acid metabolism in breast cancer. *Advances in Biological Regulation*, 62 11-17.

36. Kung, H.N., Marks, J.R.and Chi, J.T., (2011). Glutamine synthetase is a genetic determinant of cell type-specific glutamine independence in breast epithelia. *Plos Genetics*, 7(8), e100229.

37. Lampa, M., Arlt, H., He, T., Ospina, B., Reeves, J., Zhang, B.L., Murtie, J., Deng, G.J., Barberis, C., Hoffmann, D., Cheng, H., Pollard, J., Winter, C., Richon, V., Garcia-Escheverria, C., Adrian, F., Wiederschain, D.and Srinivasan, L., (2017). Glutaminase is essential for the growth of triple-negative breast cancer cells with a deregulated glutamine metabolism pathway and its suppression synergizes with mTOR inhibition. *Plos One*, 12(9), e0185092.

38. Santidrian, A.F., Matsuno-Yagi, A., Ritland, M., Seo, B.B., LeBoeuf, S.E., Gay, L.J., Yagi, T.and Felding-Habermann, B., (2013). Mitochondrial complex I activity and NAD(+)/NADH balance regulate breast cancer progression. *Journal of Clinical Investigation*, 123(3), 1068-1081.

39. Thomas, M., Davis, T., Loos, B., Sishi, B., Huisamen, B., Strijdom, H.and Engelbrecht, A.M., (2018). Autophagy is essential for the maintenance of amino acids and ATP levels during acute amino acid starvation in MDAMB231 cells. *Cell Biochemistry and Function*, 36(2), 65-79.

40. Singh, R. and Cuervo, A.M., (2011). Autophagy in the cellular energetic balance. *Cell Metabolism*, 13(5), 495-504.

41. Yan, Y.B., (2016). Creatine kinase in cell cycle regulation and cancer. *Amino Acids*, 48(8), 1775-1784.

42. Chaiyawat, P., Netsirisawan, P., Svasti, J.and Champattanachai, V., (2014). Aberrant O-GlcNAcylated proteins: New perspectives in breast and colorectal cancer. *Frontiers in Endocrinology (Lausanne)*, 5 193.

43. Glunde, K., Jie, C.and Bhujwalla, Z.M., (2004). Molecular causes of the aberrant choline phospholipid metabolism in breast cancer. *Cancer Research*, 64(12), 4270-4276.

44. Gadiya, M., Mori, N., Cao, M.D., Mironchik, Y., Kakkad, S., Gribbestad, I.S., Glunde, K., Krishnamachary, B.and Bhujwalla, Z.M., (2014). Phospholipase D1 and choline kinase-alpha are interactive targets in breast cancer. *Cancer Biology & Therapy*, 15(5), 593-601.

45. He, M.W., Guo, S.and Li, Z.L., (2015). In situ characterizing membrane lipid phenotype of breast cancer cells using mass spectrometry profiling. *Scientific Reports*, 5, 11298.

46. Zhang, X.L., Lu, H.F., Wang, Y.B., Liu, C.J., Zhu, W.F., Zheng, S.Y.and Wan, F.S., (2015). Taurine induces the apoptosis of breast cancer cells by regulating apoptosis-related proteins of mitochondria. *International Journal of Molecular Medicine*, 35(1), 218-226.

47. Willmann, L., Schlimpert, M., Halbach, S., Erbes, T., Stickeler, E.and Kammerer, B., (2015). Metabolic profiling of breast cancer: Differences in central metabolism between subtypes of breast cancer cell lines. *Journal of Chromatography B-Analytical Technologies in the Biomedical and Life Sciences*, 1000 95-104.

48. Kim, H.Y., Lee, K.M., Kim, S.H., Kwon, Y.J., Chun, Y.J.and Choi, H.K., (2016). Comparative metabolic and lipidomic profiling of human breast cancer cells with different metastatic potentials. *Oncotarget*, 7(41), 67111-67128.

Supplementary information to Chapter 3

Table S3.1. Main metabolite variations in polar extracts of MDA-MB-231 and MCF-10A cells exposed to 15 µg/mL and 0.25 µg/mL *E. nitens* lipophilic outer bark extract, respectively, in relation to controls, expressed as % variation (%var) and respective error (±), effect size (ES) and *P*-value (*P*). The variations with |ES| < 0.8 (or standard error > |ES|, or mean error > |% variation|) were considered null.

		MDA-MB-231	**MCF-10A**
Glucose	*%var*	0	-27.95
	±		13.18
	ES	0	-1.17
	P		0.0272
Glucose-1-phosphate	*%var*	0	-53.80
	±		7.76
	ES		-4.48
	P	0	1.6672E-06
UDP-GlcNAc	*%var*	32.60	30.08
	±	2.22	6.13
	ES	5.96	1.98
	P	5.1E-09	0.0015
UDP-GalNAc	*%var*	19.29	20.14
	±	4.13	9.14
	ES	2.01	0.91
	P	0.0009	0.0741
Citrate	*%var*	-59.43	-31.01
	±	4.82	4.52
	ES	-8.29	-3.84
	P	1.9285E-07	1.0299E-05
Fumarate	*%var*	-83.16	-30.14
	±	7.43	10.45
	ES	-9.06	-1.60
	P	4.19E-10	0.0053
Formate	*%var*	-32.46	0
	±	12.53	
	ES	0.01	0
	P	-1.4612	
Glu	*%var*	-51.27	-21.73
	±	4.46	4.95
	ES	-7.31	-2.33
	P	1.9068E-07	0.0006
Gln	*%var*	86.95	0
	±	2.34	
	ES	12.23	
	P	5.0135E-13	0
Asp	*%var*	21.28	-30.40
	±	2.46	4.44
	ES	3.69	-3.91
	P	2.0607E-05	9.3404E-07
Ala	*%var*	12.94	21.45
	±	1.82	3.52
	ES	3.15	2.60
	P	1.3231E-05	0.0003
Gly	*%var*	8.88	36.07
	±	1.62	2.21
	ES	2.48	6.53
	P	0.0002	4.3563E-08
Pro	*%var*	61.18	63.54
	±	2.14	4.62
	ES	10.34	4.94
	P	8.4222E-12	1.4406E-07

Table S3.1. (cont)

		MDA-MB-231	MCF-10A
His	%var	116.92	0
	±	4.61	
	ES	7.56	
	P	3.86E-10	0
Leu	%var	109.95	221.68
	±	1.68	14.15
	ES	19.99	3.51
	P	2.1706E-11	3.5265E-06
Ile	%var	91.58	125.53
	±	1.73	10.61
	ES	17.20	3.44
	P	1.3502E-13	4.8192E-06
Val	%var	115.71	101.25
	±	2.04	9.94
	ES	16.95	3.20
	P	2.0037E-11	1.0360E-05
Trp	%var	78.05	20.77
	±	5.47	2.35
	ES	4.85	3.78
	P	8.2E-08	2.46E-06
Phe	%var	84.18	11.30
	±	1.77	1.61
	ES	15.81	3.14
	P	3.79E-10	1.87E-05
Tyr	%var	1.92	0
	±	96.60	
	ES	16.03	
	P	3.05E-10	0
PCr	%var	2.91	0
	±	-13.33	
	ES	-2.32	0
	P	0.0002	
Cr	%var	33.12	0
	±	3.36	
	ES	4.00	0
	P	1.9023E-06	
UMP	%var	-69.06	0
	±	17.88	
	ES	-2.79	0
	P	0.0002	
UDP	%var	-69.04	0
	±	6.30	
	ES	-7.92	0
	P	1.23E-09	
UTP	%var	-52.15	7.08
	±	4.85	-18.12
	ES	-6.88	-1.33
	P	7.78E-10	0.0166
ATP	%var	12.67	19.46
	±	6.07	4.56
	ES	0.93	1.84
	P	0.0786	0.0019
NAD^+	%var	57.08	-14.73
	±	7.52	6.59
	ES	2.79	-1.14
	P	4.76E-05	0.0302
NADH	%var	-48.43	7.11
	±	4.21	30.77
	ES	-7.18	1.77
	P	7.08E-10	0.0022
Choline	%var	37.93	13.76
	±	16.85	6.30
	ES	0.89	0.97
	P	0.0856	0.0655

Table S3.1. (cont)

		MDA-MB-231	**MCF-10A**
PC	%var	-62.87	-12.70
	±	5.27	4.71
	ES	-8.22	-1.36
	P	7.4707E-11	0.0135
GPC	%var	72.17	83.65
	±	2.93	12.45
	ES	8.57	2.24
	P	9.9613E-11	0.0014
GSH	%var	-14.62	-29.05
	±	2.88	3.02
	ES	-2.59	-5.32
	P	9.69E-05	2.6307E-08
Tau	%var	29.55	14.01
	±	1.21	2.78
	ES	10.03	2.22
	P	4.9058E-12	0.0006
myo-Ino	%var	-18.00	0
	±	1.43	
	ES	-6.54	0
	P	1.0007E-08	

Chapter 4

METABOLIC EFFECTS OF TRITERPENIC ACIDS ON TRIPLE NEGATIVE BREAST CANCER AND NON-TUMOR BREAST EPITHELIAL CELLS

Part of this chapter is included in the manuscript entitled “Metabolic effects of triterpenic acids on triple negative breast cancer and non-tumor breast epithelial cells as viewed by NMR metabolomics”, co-authored by A.R. Guerra, A. Paulino, M. Castro, H. Oliveira, M.F. Duarte and I.F. Duarte (s*ubmitted*).

Abstract

Plant-derived pentacyclic triterpenic acids (TAs) have gained increasing attention due to their multiple biological activities. Betulinic acid (BA) and ursolic acid (UA) are known to modulate diverse pathways involved in carcinogenic processes, offering increased changes of success in refractory cancers, such as triple negative breast cancer (TNBC). In this work, the metabolic responses of TNBC cells and breast epithelial cells to BA and UA were assessed by NMR metabolomics, with a view to reveal the metabolic modulatory activities of these compounds. In MDA-MB-231 cells, BA was suggested to induce upregulation of glycolysis and the TCA cycle, together with hydrolysis of neutral lipids and buildup of membrane phospholipids. UA effects were less pronounced upon 48h incubation, but after a recovery period in fresh growth medium, downregulation of glycolysis and decreased ATP levels were observed. In MCF-10A cells, both TAs appeared to reprogram glucose metabolism towards glycogen degradation, intensification of glycolysis, upregulation of the hexosamine biosynthetic pathway, membrane degradation and formation of lipid droplets, likely to scavenge otherwise-toxic lipid species. Notably, the markedly different impact produced by either BA or UA in TNBC and breast epithelial cells supports the idea that these compounds are promising candidates for the differential metabolic modulation of tumor cells, potentially targeting their metabolic vulnerabilities.

Keywords: Betulinic acid; Ursolic acid; Triple negative breast cancer; Non-tumor breast epithelial cells; Cell metabolism; NMR metabolomics

4.1. Introduction

Triple negative breast cancer (TNBC) comprises invasive breast tumors which lack the expression of estrogen receptor (ER), progesterone receptor (PR) and human epidermal growth factor receptor type 2 (HER2) overexpression/HER2 gene amplification. There are no effective targeted therapies for TNBC, which represents 10-20% of all breast cancer cases. Chemotherapy remains the only therapeutic option for affected individuals [1-3], and has failed to improve patient survival [4]. Hence, the search for new drugs or adjuvant treatment options remains a pressing challenge in the management of TNBC.

Natural products have historically driven pharmaceutical industry into discovery of new drugs, mainly due to their high structural diversity and remarkable biological activities [5, 6]. Triterpenoids represent a numerous and structurally diverse group of plant secondary metabolites [7]. These compounds include cyclic and acyclic 30-carbon precursors and are ubiquitously distributed in nature. Among triterpenoids, triterpenes with pentacyclic skeletons, such as oleanane, ursane, and lupane carbon skeletons, have gained attention from the biological perspective, sparking renewed interest with regard to their potential in cancer treatment [8-10]. Particularly, betulinic acid (BA) and ursolic acid (UA), which are abundant in birch trees' outer barks (Betula spp.) and across a wide range of plant families [11], have been widely studied for their anti-tumoral potential in multiple cancer models. In particular, they have been shown to modulate diverse pathways involved in carcinogenic processes, offering increased changes of success in refractory cancers [12-17]. A few works have also addressed the impact of these triterpenic acids (TAs) on tumor metabolism, namely on specific glycolytic enzymes and lactate production [6]. However, a more comprehensive picture of their impact on both tumor and non-tumor cell metabolism is still missing.

In our previous work, we have shown that the outer bark of *Eucalyptus nitens* is a rich source of triterpenic acids [18], including BA (6.6 g/kg of bark fraction) and UA (3.5 g/kg). Additionally, a lipophilic *E. nitens* outer bark extract was shown to inhibit the proliferation and viability of TNBC cells and to have a strong, wide-range impact on their metabolism [19]. In particular, our findings indicated that *E. nitens* extract deeply modulated pathways that are crucial to TNBC survival and aggressive phenotype, such as the balance between glycolysis and mitochondrial respiration, and phospholipid metabolism. It is thus important to further assess the bioactivity and metabolic impact of individual components present in the lipophilic *E. nitens* outer bark extract.

The present work aims at assessing the metabolic effects of BA and UA in MDA-MB-231 breast cancer cells (TNBC model), as well as in MCF-10A non-tumor breast epithelial cells. Identification and quantification of changes in the cells exo- and endometabolome were performed through ^{1}H NMR analysis of cell culture medium supernatants, aqueous and organic cell extracts. This approach is expected to provide new insights into the involvement of metabolic reprogramming in cellular responses to these TAs, and will hopefully contribute to advance research on phytochemical-based therapy for TNBC.

4.2. Materials and Methods

4.2.1. Materials

Dulbecco's modified Eagle's medium (DMEM), DMEM/F12 medium and trypsin (5 g/L)-EDTA (2 g/L) were supplied by Biowest, (Nuaillé, France). Fetal bovine serum (FBS) was provided by Gibco (MA, USA). Horse serum, human epidermal growth factor, human insulin, hydrocortisone and cholera toxin were obtained from Sigma-Aldrich (MO, USA). Betulinic acid (≥90% purity) and ursolic acid (≥98% purity) were purchased from Molekula GmbH (Munchen, Germany). Dimethylsulfoxide (DMSO, cell culture grade) was obtained from Applichem (Gatersleben, Germany). 3-(4,5-dimethylthiazol-2-yl)-2,5-diphenyltetrazolium bromide (MTT) and propidium iodide were purchased from Calbiochem (San Diego, CA, USA). Methanol was obtained from Merk (Darmstadt, Germany) and chloroform from Normapur (VWR, Radnor, PA, USA). RNase was obtained from Sigma Chemicals Co. (Madrid, Spain).

4.2.2. Cell culture

The human breast cancer cell line MDA-MB-231 and the immortalized normal breast epithelial cell line MCF-10A were purchased from American Type Cell Culture (ATCC, Manassas, VA, USA). MDA-MB-231 cells were cultured in DMEM supplemented with 10% (v/v) heat-inactivated FBS. MCF-10A cells were cultured in DMEM/F12 medium, supplemented with 5% (v/v) heat-inactivated horse serum, human epidermal growth factor (20 ng/ml), human insulin (10 µg/ml), hydrocortisone (100 ng/ml) and cholera toxin (0.1 nM). Both cell lines were cultured at 37ºC in a 5% CO_2 humidified atmosphere (C150, Binder GmbH, Tuttlingen, Germany). The cells were allowed to grow until they reached subconfluence. Then, cells were trypsinized with a trypsin (0.5 g/L) / EDTA (0.2 g/L) solution and suspended in fresh growth medium before platting.

4.2.3. Cell viability assay

Cells were cultured in 96-well plates at 2 x 10^5 cells/mL and treated the following day with either BA or UA (0.5-50 µM), for 24h, 48h and 72h. Vehicle solvent control cells received DMSO (0.25% (v/v)). Cell viability was estimated by the 3-(4,5-dimethylthiazol-2-yl)-2,5-diphenyltetrazolium bromide (MTT) assay as previously described [20]. After treatment, 20 µL of MTT stock solution was added to each well (final concentration 0.5 mg/mL), and plates were incubated at 37ºC, for 4h. Then, the medium was removed and the formed formazan crystals were dissolved using a DMSO/ethanol (1:1) solution. Finally, absorbance of the formed product was measured at 570 nm using a microplate reader (MultiSkan FC, ThermoScientific, Rochester, USA). The IC_{50}, defined as the concentration necessary to cause 50% inhibition of cell viability, was calculated using GraphPad Prism 5.0 (GraphPad Prism Software Inc., San Diego, USA), by plotting the percentage of cell viability as a function of sample concentration logarithm. Three independent experiments were performed for each treatment.

4.2.4. Cell cycle analysis by flow cytometry

MDA-MB-231 and MCF-10A cells were seeded in six-well plates at a density of 4 x 10^5 cells/mL and cultured for 24h at 37ºC. In this assay, and for the following assays, cells were treated for 48h with 15 µM of BA, or 20 µM of UA (selected based on the MTT results). Vehicle solvent control cells received DMSO (0.10% (v/v)) only. After being incubated, the cells were trypsinized, collected, washed with PBS and fixed with 85% cold ethanol. At the time of analysis, cells were centrifuged at 300*g* for 5 min at 4°C and resuspended in PBS, before being treated with RNase (50 µg/mL) and propidium iodide staining solution (50 µg/mL) and incubated, in the dark, for at least 20 min at room temperature. Propidium iodide–stained cells were analyzed on a Coulter EPICS XL (Beckman Coulter, Hialeah, FL, USA) flow cytometer. The results were acquired using the SYSTEM II software (version 3.0 Beckman-Coulter®). Four replicates were performed for each treatment, and for each sample at least 5000 nuclei were acquired. Analysis of cell cycle distribution was performed using the FlowJo software (Tree Star, Ashland, OR, USA).

4.2.5. Cell exposure for metabolomics assays

MDA-MB-231 and MCF-10A cells were cultured in 10 cm diameter Petri dishes, at a density of 6 x 10^5 cells/mL. In the following day, new medium containing 5 or 15 µM of BA and 10 or 20 µM of UA was added to the cells

(concentrations selected based on MTT results). Vehicle solvent control cells received DMSO (0.10% (v/v)) only. Both cell lines were then incubated with the TAs for 48h. Samples were collected after 48h incubation or, to assess cellular recovery, medium was replaced with fresh growth medium (without TAs), and cells were incubated for additional 24h before collection (48h+24h samples).

4.2.6. Sample collection and preparation for NMR analysis

After incubation, culture medium was collected and centrifuged (1000*g*, 5min) and the supernatant stored at -80ºC until analysis. Culture medium without cells, placed under the same conditions, was also collected. Extraction was performed as described by Carrola *et al*. [21]. Briefly, cells were washed 4 times with PBS and extracted with a mixture of methanol:chloroform:water (1:1:0.7). The resulting polar and organic phases were collected and then dried under vacuum or under a stream of nitrogen gas, respectively. All samples were stored at -80ºC and, at the time of analysis, dried polar extracts were reconstituted in 600 µL of deuterated phosphate buffer (100 mM, pH7.4) containing 0.1 mM TSP-d_4 and organic extracts in deuterated chloroform containing 0.03% TMS. For medium samples, 540 µL of thawed medium were mixed with 60 µL of D_2O containing 0.25% TSP-d_4. Prior to analysis, 550 µL of each sample were transferred to 5 mm NMR tubes.

4.2.7. NMR data acquisition and processing

^{1}H NMR spectra of all samples were acquired on a Bruker Avance III HD 500 NMR spectrometer (University of Aveiro, Portuguese NMR Network) operating at 500.13 MHz for ^{1}H observation equipped with a 5 mm TXI probe. Standard 1D spectra (Bruker pulse programs ‘noesypr1d’, with water suppression, for medium samples and aqueous extracts, and ‘zg’ for organic extracts) were recorded with a 7002.8 Hz spectral width, 32 k data points, a 2 s relaxation delay and 512 scans. Spectral processing comprised exponential multiplication with 0.3 Hz line broadening, zero filling to 64 k data points, manual phasing, baseline correction, and chemical shift calibration to the TSP or TMS signal at 0 ppm. 2D ^{1}H-^{1}H total correlation (TOCSY) spectra, ^{1}H-^{13}C heteronuclear single quantum correlation (HSQC) spectra and *J*-resolved spectra were also registered for selected samples to assist spectral assignment. The main acquisition and processing parameters for these experiments are provided in Supplementary Table S2.1. Metabolites were identified with the support of 2D spectra (Figure 2.2; Figure 2.5; Figure 2.8) and the

spectral reference databases BBIOREFCODE-2-0-0 (Bruker Biospin, Rheinstetten, Germany) and HMDB [22].

4.2.8. Multivariate analysis and spectral integration of NMR spectra

Spectra were normalized by total spectral area, to compensate for differences in cell numbers, and using SIMCA-P 11.5 software (Umetrics, Umeå, Sweden), scaled to Unit Variance (UV), giving equal variance to all variables. PCA was then applied in the SIMCA-P 11.5 software (Umetrics, Umeå, Sweden) and the results were visualized through scores scatter plots. Selected signals in the normalized 1D spectra were integrated using the AmixViewer software (version 3.9.14, Bruker BioSpin, Rheinstetten, Germany) and normalized by the total spectral area. The magnitude of each metabolite change was assessed through the percentage of variation (and its respective error) in exposed samples relatively to controls, and through the effect size (ES) adjusted for small sample numbers (and respective standard error) [23]. Metabolites variations with absolute ES greater than 0.8 were expressed in a heatmap**,** colored as a function of the percentage of variation, employing the R statistical software version 3.4.1. (R Core Team (2017). R: A language and environment for statistical computing. R Foundation for Statistical Computing, Vienna, Austria. http://www.R-project.org/). Moreover, the statistical significance of the difference between the means of two groups (control and exposed) was assessed using the two-sample t-test.

4.2.9. Statistical analysis

For sections 4.2.3. and 4.2.4, all parameters measured were analyzed using the PROC GLM option of SAS (SAS Institute Inc., Cary, NC, USA). Where differences existed, the source of the differences at $P < 0.05$ significance level was identified by all pairwise multiple comparison procedures via the Tukey's test.

4.3. Results

4.3.1. Inhibitory effects of betulinic and ursolic acids on MDA-MB-231 and MCF-10A cellular viability

MDA-MB-231 and MCF-10A cells were treated with various concentrations (0- 50 µM) of either BA or UA for 24h, 48h and 72h, and cell viability assessed through the MTT assay. Table 4.1 presents the IC_{50} values obtained.

Table 4.1. IC_{50} values regarding cell viability inhibition by betulinic acid (BA) and ursolic acid (UA) on the MDA-MB-231 and MCF-10A cell lines, as determined through the MTT assay.

	IC_{50} (μM)[1]			
	MDA-MB-231		**MCF-10A**	
	BA	**UA**	**BA**	**UA**
24h	31.28±5.94^{a,b}	24.54±4.61^{b,c}	22.42±6.49^{c}	37.87±8.93^{a}
48h	13.20±2.30^{d,e,f}	17.21±0.86^{c,d,e,f}	10.99±1.83^{e,f,g}	18.68±3.27^{c,d,e}
72h	8.39±0.98^{f,g}	17.70±2.81^{c,d,e}	2.38±1.36^{g}	21.49±4.55^{c,d}

[1] Each value is expressed as mean ± standard deviation. Three independent experiments were carried out. Means marked with different letters are statistically different (P <0.05).

The effect of BA on MDA-MB-231 cancer cells was highly dependent on incubation time, the IC_{50} value being significantly higher (P<0.05) for the shortest incubation period (24h). The IC_{50} value for 48h was 13.20±2.30 μM (Table 4.1), hence, a concentration of 15 μM, as well a concentration of 5 μM (lowest concentration for which a decrease in viability was already observed) were chosen for subsequent assays. The impact of UA on MDA-MB-231 cells was less dependent on incubation time. Based on the IC_{50} value for 48h (17.21±0.86 μM), concentrations of 20 and 10 μM (lowest concentration for which a decrease in viability was already observed) were selected for subsequent assays.

As for MCF-10A normal epithelial cells, they were more susceptible to BA than cancer cells, as seen by the lower IC_{50} values determined for all incubation periods (Table 4.1). This was not observed in the case UA, for which the 48h IC_{50} in MCF-10A cells (18.68±3.27 μM) was similar to that found in cancer cells. In general, both cell lines were more sensitive to BA than to UA.

4.3.2. Effect of betulinic and ursolic acids on MDA-MB-231 and MCF-10A cell cycle

The effects of BA and UA on cell cycle phases (G0/G1, S and G2) of MDA-MB-231 and MCF-10A cells, as assessed by flow cytometry, are shown in Figure 4.1.

Betulinic acid (15 μM) led to a significant (P<0.05) accumulation of MDA-MB-231 cells at the G2 phase, together with a decreased cell population at the S phase, in comparison with non-exposed control cells. MCF-10A breast epithelial cells treated with BA also displayed a statistically significance cell cycle arrest at G2 phase (P<0.05), and also an increase in S phase, with a concomitant decrease in G0/G1 phase.

Ursolic acid (20 µM) had less marked effects on the cell cycle phases of both MDA-MB-231 and MCF-10A cells. We only observed a significant decrease in the S phase for UA-treated MDA-MB-231 TNBC cells, and no effect in MCF-10A epithelial cells.

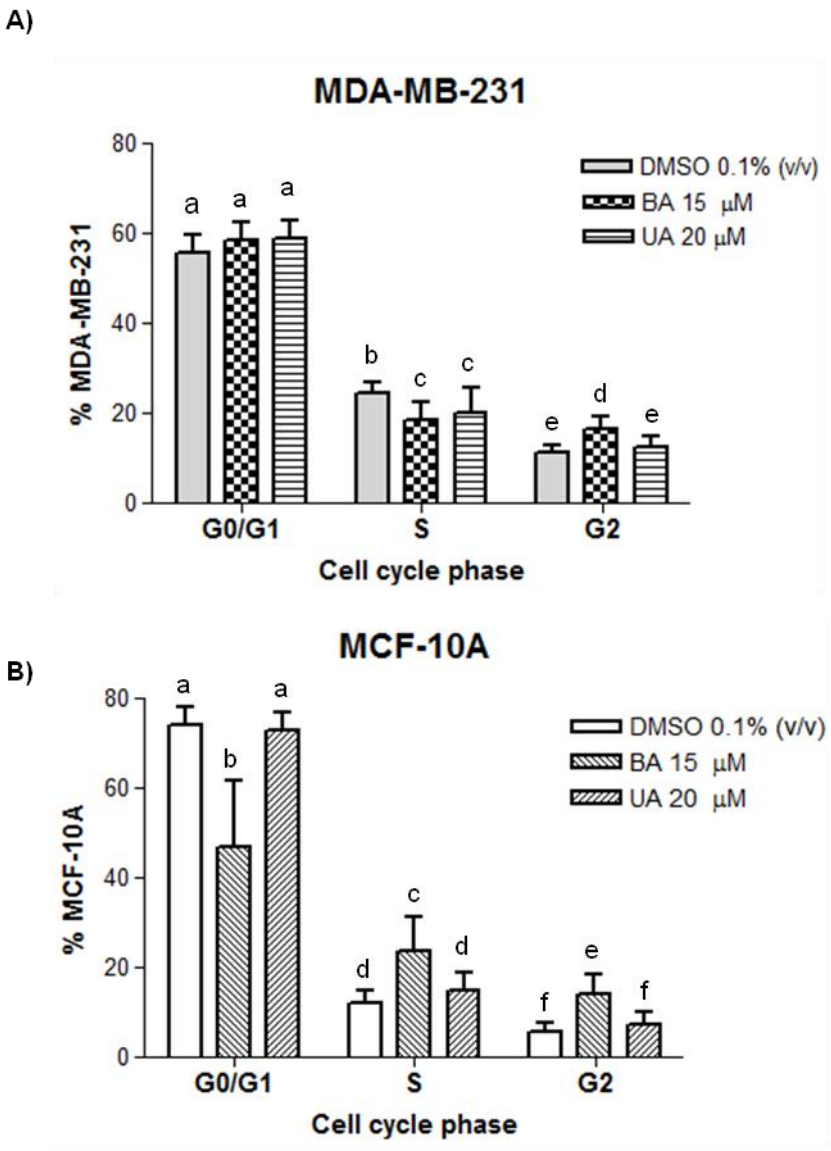

Figure 4.1. Cell cycle phase distribution of A) MDA-MB-231 and B) MCF-10A cells, treated with 20 µM UA and 15 µM BA, after 48h-incubation. DMSO was the solvent control. Each column and bar represent, respectively, the mean and the standard deviation. Four replicates were performed. Different letters are statistically different (*P*-value < 0.05, Tukey's test).

4.3.3. Variations induced by betulinic and ursolic acids on the metabolome of MDA-MB-231 and MCF-10 breast cells

Metabolic alterations induced by BA and UA on MDA-MB-231 breast cancer and MCF-10A breast epithelial cells were assessed immediately after 48h incubations, as well as after a 24h recovery period in fresh growth medium (without

TAs). NMR analysis of culture medium supernatants allowed the exometabolome profiling of cells, while intracellular metabolic variations were assessed through analysis of aqueous and organic cell extracts.

4.3.3.1. Extracellular metabolic changes induced by betulinic and ursolic acids

Alterations in metabolite consumption and excretion patterns upon incubation of breast cells with BA or UA were assessed by comparing metabolite levels in cell-conditioned media with those in acellular growth media. The results are shown in Figures 4.2 and 4.3 for MDA-MB-231 and Figures 4.4 and 4.5 for MCF-10A cells.

MDA-MB-231 cells incubated for 48h with 15 µM BA showed a significant ($P < 0.05$) increase in glucose consumption and lactate excretion, the latter being already noticed at the lower concentration tested (5 µM) BA (Figure 4.2A). On the other hand, the consumption of leucine decreased significantly with exposure to 5 µM. Upon medium replacement and a 24h incubation in fresh growth medium (without TAs), cells that had been treated with BA (48h+24h samples) still displayed differences in their exometabolome, as compared to control cells (Figure 4.2B). In particular, they consumed less leucine and pyruvate and excreted less 2-oxoisovalerate, citrate and alanine.

In regard to MDA-MB-231 cancer cells exposed to UA for 48h, there were no differences in the amounts of metabolites consumed or excreted in relation to untreated control cells (results not shown). However, when cells were allowed to recover in fresh culture medium for 24h, those that had been previously incubated with UA (48h+24h samples) presented significant differences in several extracellular metabolites, as compared to untreated control cells (Figure 4.3). In particular, they showed significantly decreased consumption of glucose, leucine and choline, accompanied by decreased excretion of lactate, 2-oxoisovalerate, citrate, alanine and glutamate.

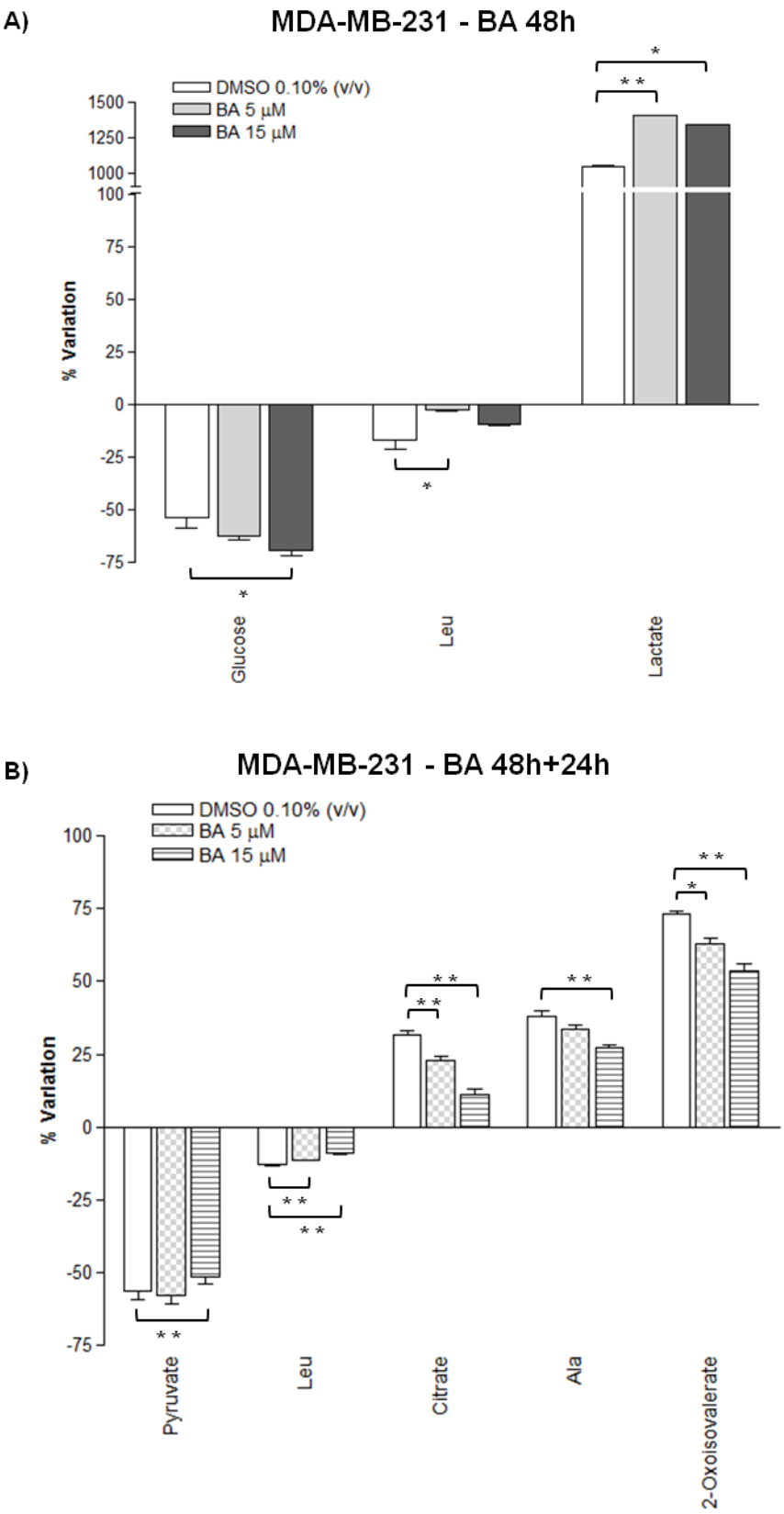

Figure 4.2. Variations in metabolites consumed (negative bars) and excreted (positive bars) by MDA-MB-231 breast cancer cells, under control conditions and upon treatment with BA (5 µM and 15 µM) for 48h (A) or 48h+24h (B), as assessed by comparison between acellular culture media and cells-conditioned media. DMSO was the solvent control. ***P*-value < 0.01; **P*-value < 0.05. Three-letter code used for amino acids.

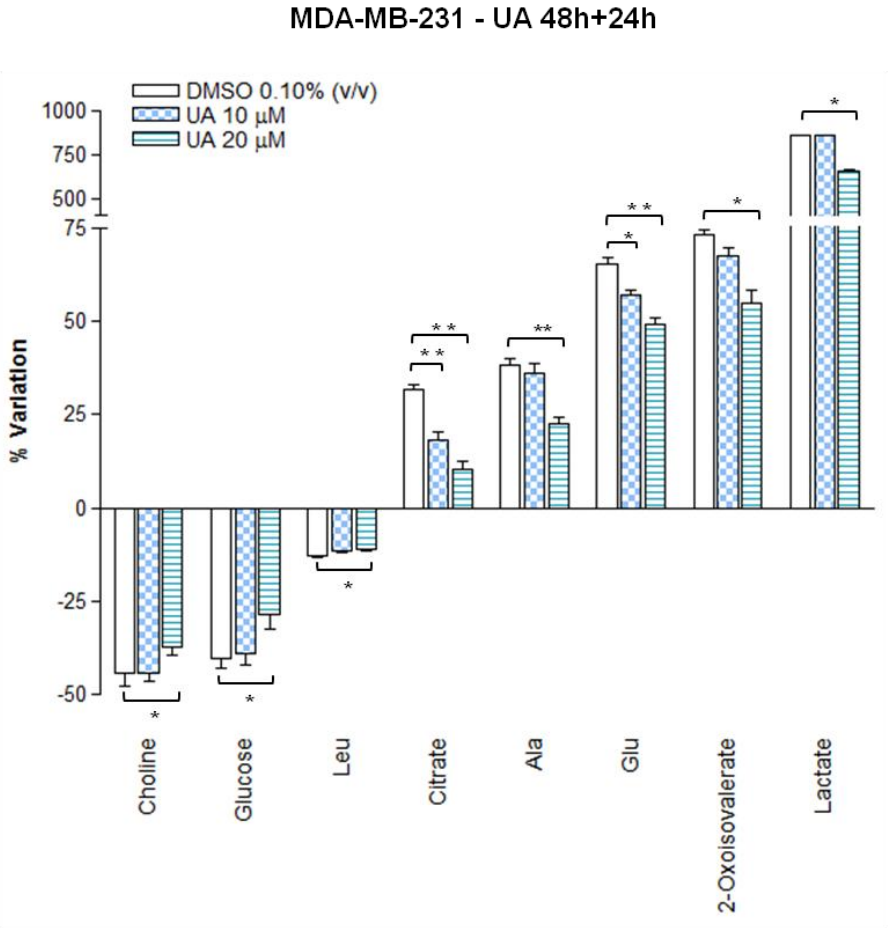

Figure 4.3. Variations in metabolites consumed (negative bars) and excreted (positive bars) by MDA-MB-231 breast cancer cells, under control conditions and upon treatment with UA (10 µM and 20 µM) for 48h+24h, as assessed by comparison between acellular culture media and cells-conditioned media. DMSO was the solvent control. ***P*-value < 0.01; **P*-value < 0.05. Three-letter code used for amino acids.

The exometabolome of MCF-10A epithelial cells was greatly affected by incubation with either BA or UA (Figures 4.4 and 4.5). Compared to untreated controls, BA-treated cells significantly reduced the consumption of several amino acids, namely branched chain amino acids, glutamine, phenylalanine and tyrosine (Figure 4.4A). This was accompanied by decreased excretion of alanine and fumarate. On the other hand, these cells increased the consumption of glucose and pyruvate, as well as the excretion of lactate and formate. Upon incubation for additional 24h in fresh culture medium, MCF-10A cells pre-treated with BA maintained decreased consumption of some amino acids (BCAA, serine) and decreased excretion of alanine and fumarate, in relation to controls (Figure 4.4B). However, the consumption of glucose, pyruvate and acetate was decreased, and so was the excretion of lactate and 2-oxoisovalerate. On the other hand, formate excretion increased in BA pre-treated cells (48h+24h samples).

In regard to MCF-10A cells treated with UA for 48h (Figure 4.5A), they decreased the consumption of several amino acids and the excretion of some of their metabolic products (e.g. 2-oxoisovalerate, 3-hydroxyisovalerate), while increasing the consumption of glucose and pyruvate and the excretion of lactate, similarly to BA-treated cells. Most of these changes were maintained in UA-treated cells allowed for a 24h recovery period (Figure 4.5B).

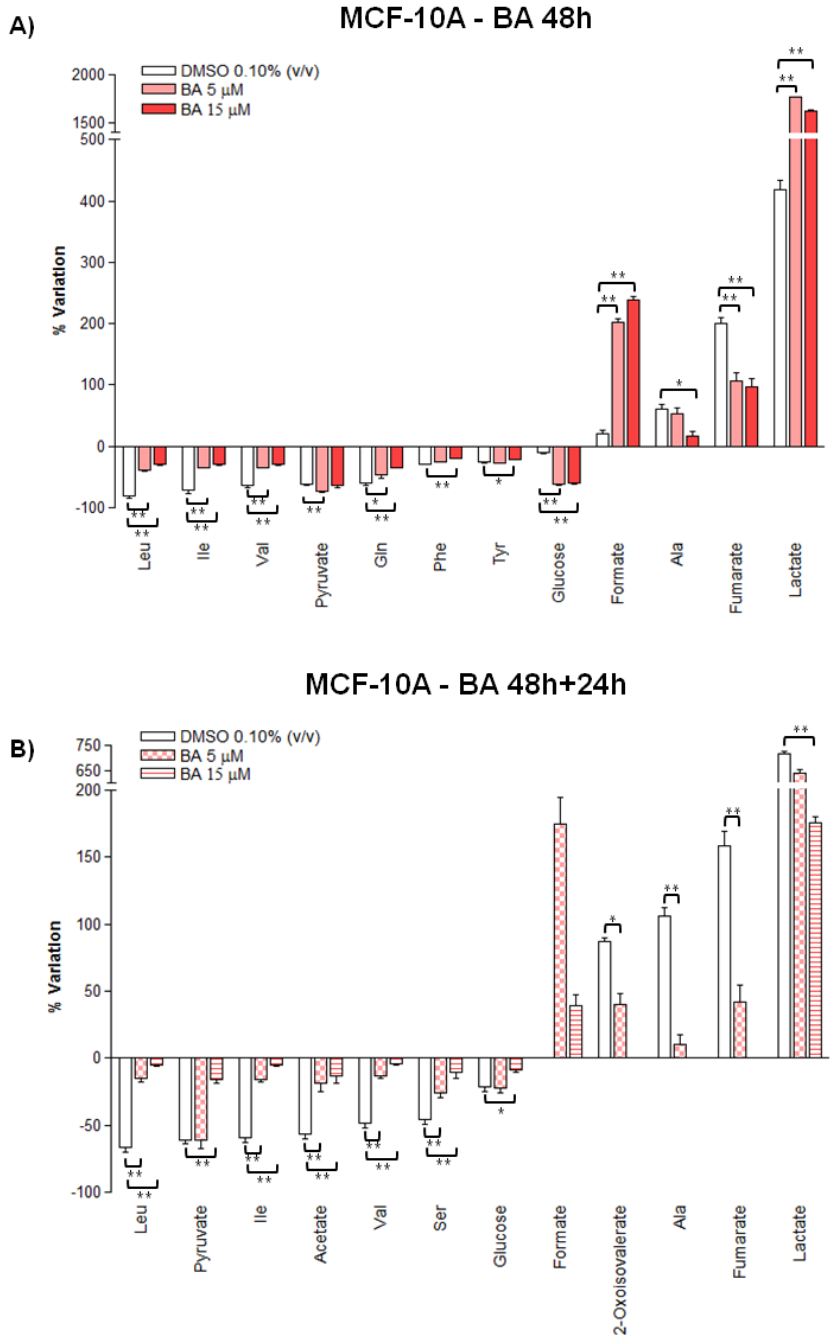

Figure 4.4. Variations in metabolites consumed (negative bars) and excreted (positive bars) by MCF-10A breast epithelial cells, under control conditions and upon treatment with BA (5 µM and 15 µM) for 48h (A) and 48h+24h (B), as assessed by comparison between acellular culture media and cells-conditioned media. DMSO was the solvent control. ***P*-value < 0.01; **P*-value < 0.05. Three-letter code used for amino acids.

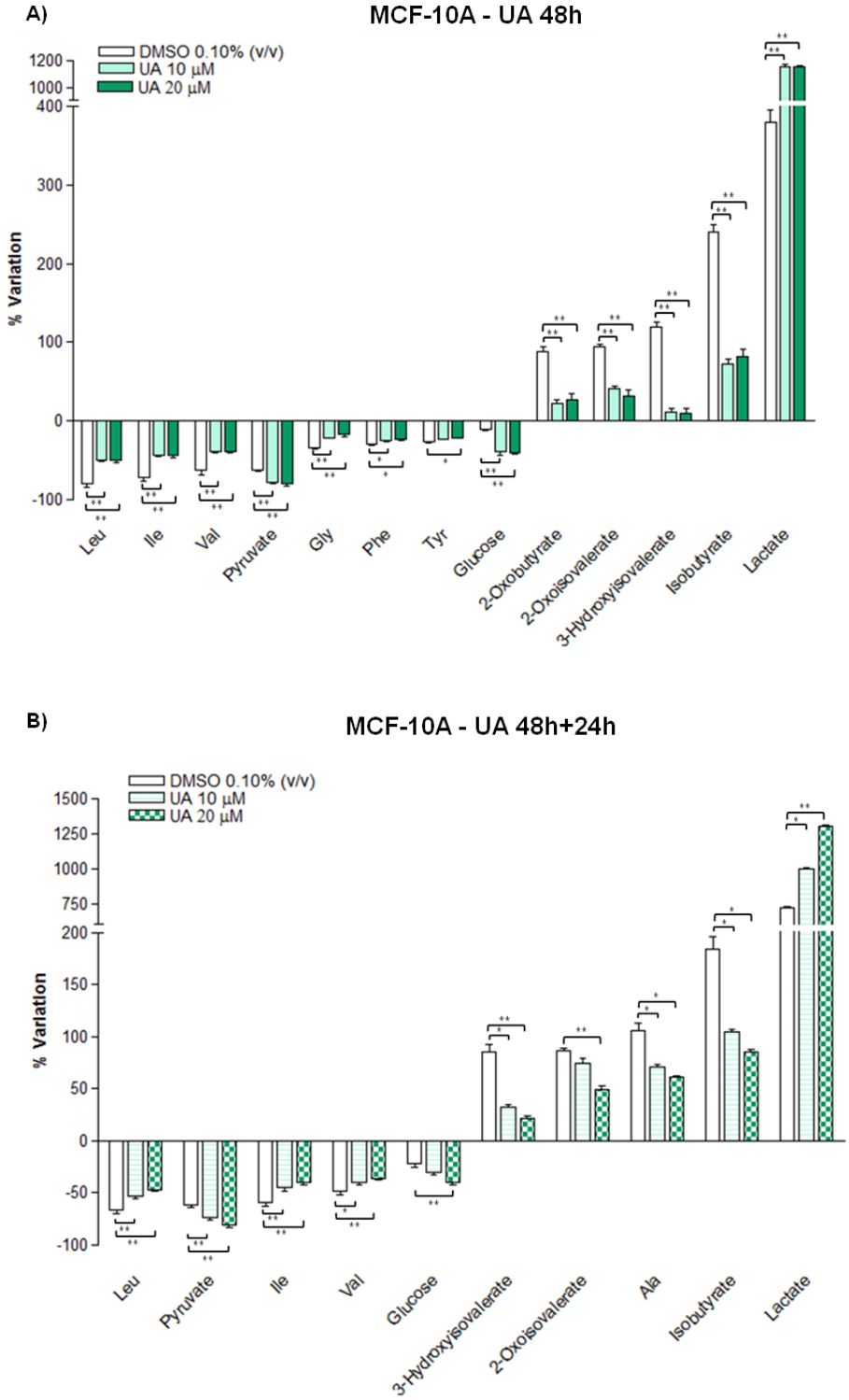

Figure 4.5. Variations in metabolites consumed (negative bars) and excreted (positive bars) by MCF-10A breast epithelial cells, under control conditions and upon treatment with UA (10 µM and 20 µM) for 48h (A) and 48h+24h (B), as assessed by comparison between acellular culture media and cells-conditioned media. DMSO was the solvent control. ***P*-value < 0.01; **P*-value < 0.05. Three-letter code used for amino acids.

4.3.3.2. Intracellular metabolic changes induced by betulinic and ursolic acids

Analysis of ^{1}H NMR spectra from cellular aqueous extracts enabled the identification of 60 intracellular metabolites based on matching 1D and 2D NMR sample data to spectral data recorded in-house for standard compounds and/or deposited in other available databases (Table S2.3).

As a first approach to assess intracellular metabolic alterations in BA- and UA-exposed cells, multivariate analysis was applied to the 1D ^{1}H NMR spectra of aqueous extracts. Principal Component Analysis (PCA) results obtained for MDA-MB-231 and MCF-10A cells are shown in Figure 4.6 and Figure 4.7, respectively. For MDA-MB-231 cells, the PCA scores scatter plot showeded a good separation between all sample groups, except for cells treated with the low UA concentration (10 µM), which overlapped with controls (Figure 4.6A). These results were confirmed by separate PCA analysis of spectral data collected for cells treated for 48h with each TA (Figure 4.6B and Figure 4.6C). When considering the recovery period after exposure to each TA, the resulting PCA scores plots showed that the samples incubated in fresh medium after treatment with low BA or UA concentrations tended to cluster near untreated controls. On the other hand, cells that had been treated with the high BA or UA concentrations before the recovery period separated from controls, while also clustering away from cells treated for 48h and not allowed to recover (Figure 4.6D and Figure 4.6E).

In the case of MCF-10A cells, the spectra of polar extracts obtained for cells treated with the high BA concentration (15 µM) were considerably noisier than all others, likely reflecting a lower number of cells collected for analysis. This could relate to the particularly strong impact of BA on the viability of MCF-10A cells, as shown in Table 4.1. Hence, in the case of BA-exposed MCF-10A cells, only the low concentration (5 µM) samples were included in further spectral treatment and interpretation.

The PCA scores plot obtained for all MCF-10A samples shows 3 clusters for control, BA-treated and UA-treated cells, without separation according to UA concentrations (Figure 4.7A), as also verified when the two TAs were considered separately (Figure 4.7B and Figure 4.7C). Figure 4.7D and Figure 4.7E display, for BA and UA, respectively, the PCA comparisons between cells treated for 48h and immediately collected or left to recover in fresh medium for additional 24h (48h+24h samples). In both cases, 48+24h samples cluster away from controls and also from cells collected immediately after treatment. Moreover, the 48h+24h samples pre-

treated with 10 and 20 µM UA form two separate clusters, the one corresponding to the lower concentration being closer to controls.

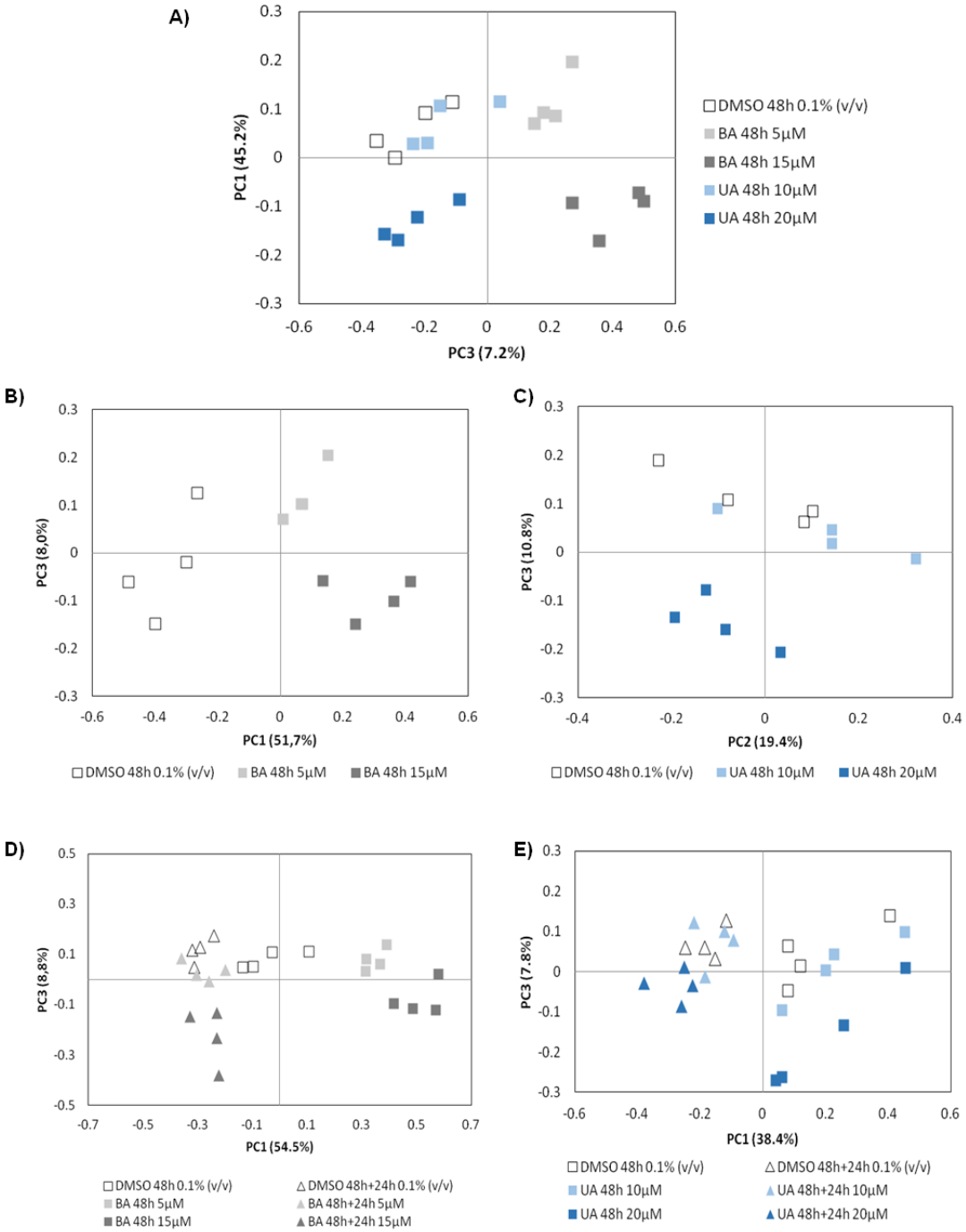

Figure 4.6. Multivariate analysis of ^{1}H NMR spectra from aqueous extracts of MDA-MB-231 control cells and cells exposed to TAs considering: A) All samples from 48h incubations (control, BA and UA); B) controls and samples from 48h BA incubations; C) controls and samples from 48h UA incubations; D) samples from 48h and 48+24h BA incubations, together with respective controls; E) samples from 48h and 48+24h UA incubations, together with respective controls.

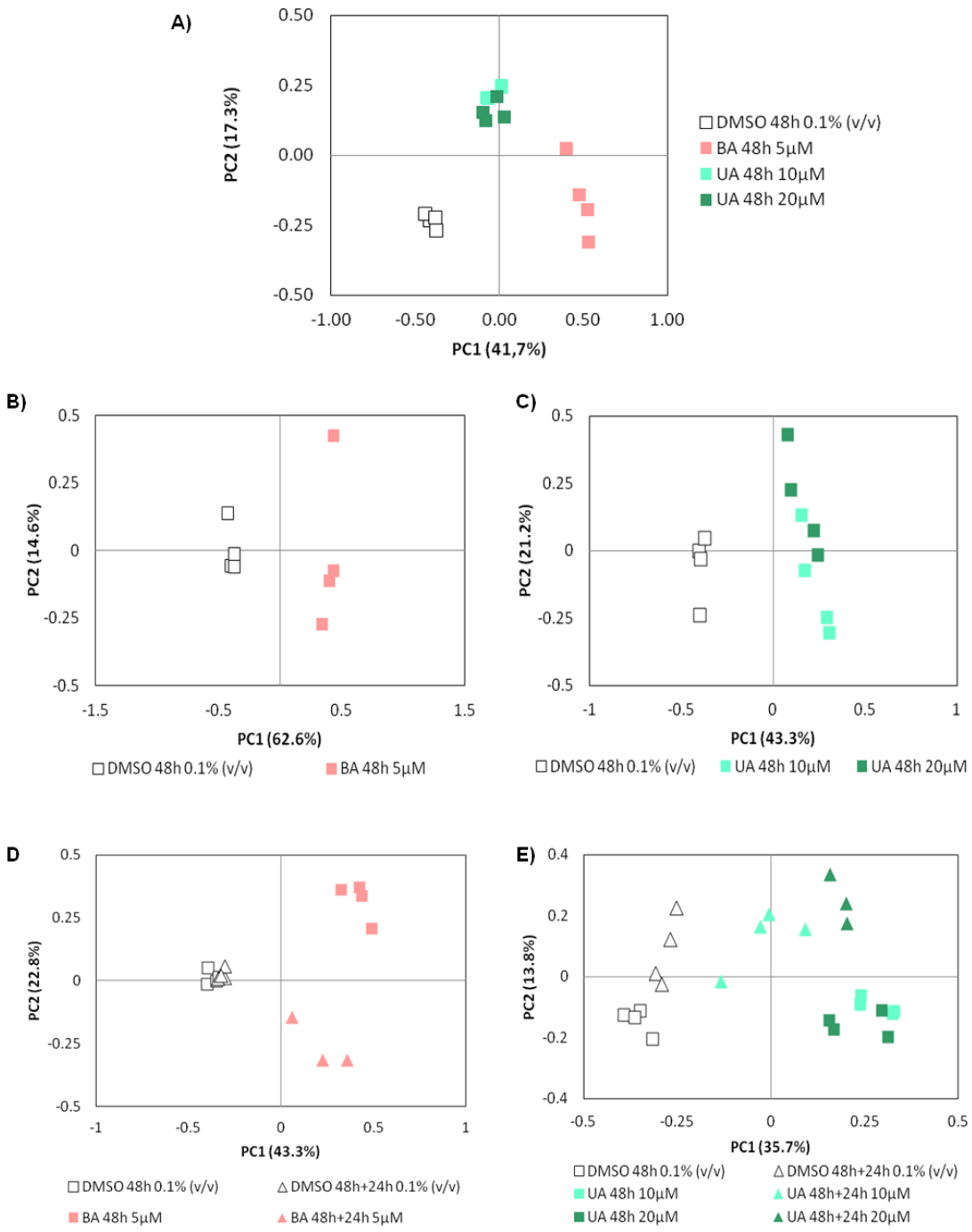

Figure 4.7. Multivariate analysis of ^{1}H NMR spectra from aqueous extracts of MCF-10A control cells and cells exposed to TAs considering: A) All samples from 48h incubations (control, BA and UA); B) controls and samples from 48h BA incubations; C) controls and samples from 48h UA incubations; D) samples from 48h and 48+24h BA incubations, together with respective controls; E) samples from 48h and 48+24h UA incubations, together with respective controls.

In order to perform a more detailed analysis of BA- and UA-induced metabolic variations in MDA-MB-231 and MCF-10A cells, spectral integration of individual metabolites was carried out. Full results are presented in Supplementary Table S4.1 and Table S4.2 and summarized in the form of colour-coded heatmaps for MDA-MB-231 (Figure 4.8) and MCF-10A cells (Figure 4.9).

Based on Figure 4.8, a few general observations can be made regarding the metabolic effects of BA and TA on MDA-MB-231 breast cancer cells. One is that BA had a much higher impact on the intracellular polar metabolome than UA, as seen by consistent alterations in 23 *vs.* 10 metabolites in cells treated with BA *vs.* UA for 48h, at concentrations of 15 µM and 20 µM, respectively. The other is that, in the case of BA, only a small number of changes remained (7 out of 23) or newly appeared (decrease in ATP) in cells that were allowed to recover in fresh growth medium after treatment. On the other hand, cells treated with the higher UA concentration kept their changed metabolic profile even after the 24h recovery period and even displayed additional differences relatively to controls.

Describing the results in more detail, the intracellular metabolic changes arising from 48h incubation of MDA-MB-231 cells with BA (5 or 15 µM) were: i) increases in acetate and lactate, a set of amino acids comprising proline, branched chain and aromatic amino acids, creatine, choline, glycerophosphocholine (GPC) and taurine, together with ii) decreases in citrate and fumarate, another set of amino acids (glutamine, glutamate, aspartate, alanine and glycine), phosphocholine (PC), glutathione (GSH) and myo-inositol. The increase in acetate was only noticed for cells treated with 15 µM BA and several other changes intensified with increasing BA concentration (e.g. upregulation of amino acids; changes in choline compounds and GSH). Moreover, as already mentioned, most changes were not detected after a 24h recovery period (in BA-free medium), with the exception of ATP, which did not vary in 48h samples (relatively to untreated controls) but showed decreased levels in 48h+24h samples.

As for the UA intracellular metabolic effects, they comprised: i) increases in acetate, aspartate, GPC and taurine, together with ii) decreases in citrate, fumarate, glycine, phosphocreatine, PC and GSH. Interestingly, the variations in PC and GPC were inverted when cells treated with the high BA concentration were incubated in fresh medium (48h+24h samples). Also, decreased ATP levels were only noticed in 48h+24h samples, as observed for BA.

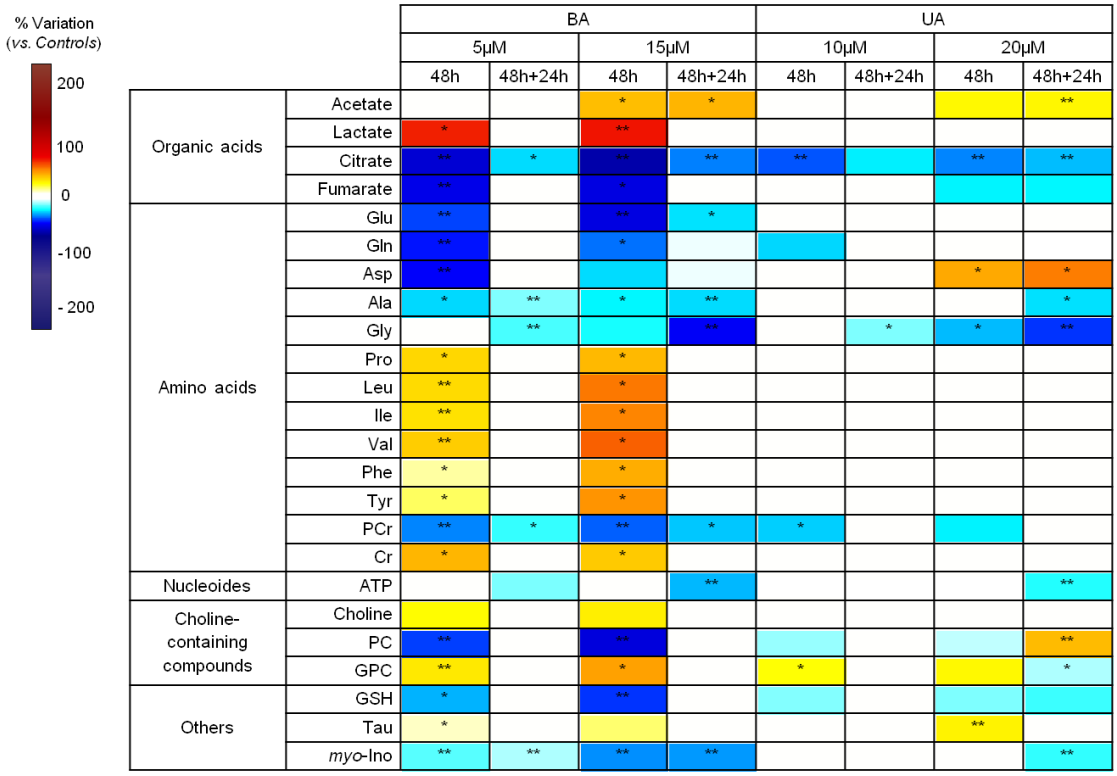

Figure 4.8. Heatmap of the main metabolite variations in polar extracts from MDA-MB-231 cells exposed to 5 µM and 15 µM of BA and 10 µM and 20 µM of UA, colored according to % variation in relation to controls. * *P*-value <0.05, ** *P*-value < 0.01. Three letter code used for amino acids; Cr, creatine; PCr, phosphocreatine; ADP/ATP, adenosine di/triphosphate; GSH, reduced glutathione; PC, phosphocholine; GPC, glycerophosphocholine.

The metabolic impact of BA and UA on MCF-10A breast epithelial cells was clearly greater than in cancer cells (at the same exposure concentrations), as seen by the more intense colouring of the respective heatmap (Figure 4.9). In total, a 48h incubation with BA (5 µM) altered the intracellular levels of 31 polar metabolites. Out of these, 18 metabolites kept altered levels in 48h+24h samples. As for 48h UA-treated epithelial cells, they showed alterations in 27/22 metabolites (at low/high UA concentration). Out of these, 17 compounds maintained their variation in cells allowed to recover in UA-free medium (48h+24h samples), while 4/6 new variations emerged in these cells (after low/high UA pre-treatment).

Looking closer at BA effects, they comprised: i) increases in uridine diphosphate N-acetyl glucosamine and galactosamine (UDP-GlcNAc and UDP-GalNAc), lactate, formate, acetate, some amino acids (glycine, proline and branched chain amino acids), creatine, NADH, 1-methylnicotinamide, choline and GPC, along with ii) decreases in glucose, glucose-1-phosphate and UDP-glucose, citrate and fumarate, 3-hydroxyisobutyrate, other amino acids (glutamate,

aspartate, histidine and tyrosine), phosphocholine, glutathione (GSH), myo-inositol and dimethylamine.

Most of the above-mentioned variations were also found in UA-treated epithelial cells. Exceptions were seen for i) lactate, formate and histidine (no change in UA-exposed cells), ii) glutamine, ATP and phosphocreatine (variations detected in UA but not in BA-treated cells), and iii) alanine, phenylalanine and tyrosine (opposite variations in BA and UA-exposed cells).

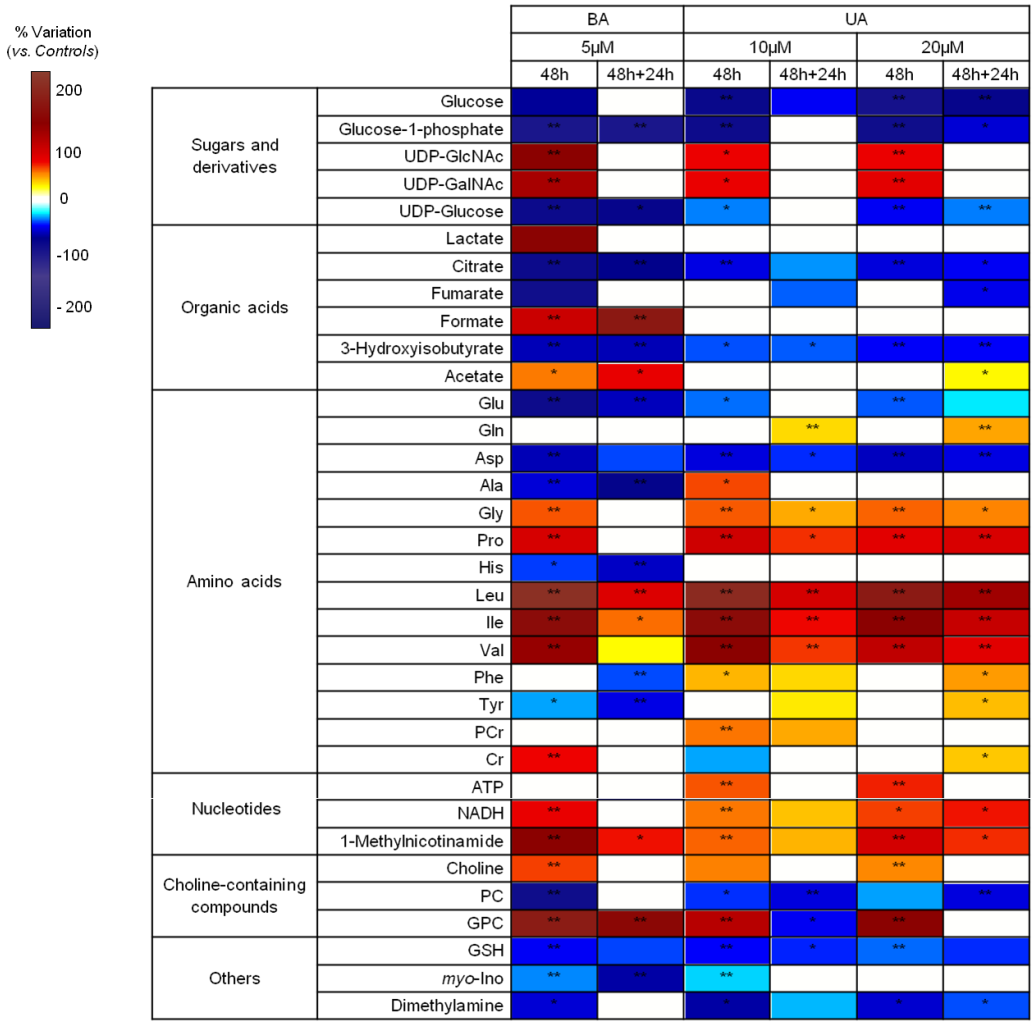

Figure 4.9 Heatmap of the main metabolite variations in polar extracts from MCF-10A cells exposed to 5 µM of BA and 10 µM and 20 µM of UA, colored according to % variation in relation to controls. * *P*-value <0.05, ** *P*-value < 0.01. Three letter code used for amino acids; Cr, creatine; PCr, phosphocreatine; ADP/ATP, adenosine di/triphosphate; NAD^+/NADH , nicotinamide adenine dinucleotide/reduced form; GSH, reduced glutathione; PC, phosphocholine; GPC, glycerophosphocholine; UDP, uridine diphosphate; UDP-GalNAc, UDP-N-acetyl-galactosamine; UDP-GlcNAc, UDP-N-acetyl-glucosamine.

Changes in cellular lipids were assessed through NMR analysis of cells organic extracts. A first important finding was that the signals of BA and UA were clearly detected in the 1D ^{1}H NMR spectra of exposed cells, confirming their direct interaction with both MDA-MB-231 cancer cells and MCF-10A epithelial cells

(internalization and/or membrane association). This is shown for MDA-MB-231 cells in Figure 4.10, where the spectra of control and BA/UA-treated cells are displayed together with the spectra of pure BA/UA. Additionally, spiking experiments definitely confirmed the identification of TAs in treated cell organic extracts (not shown).

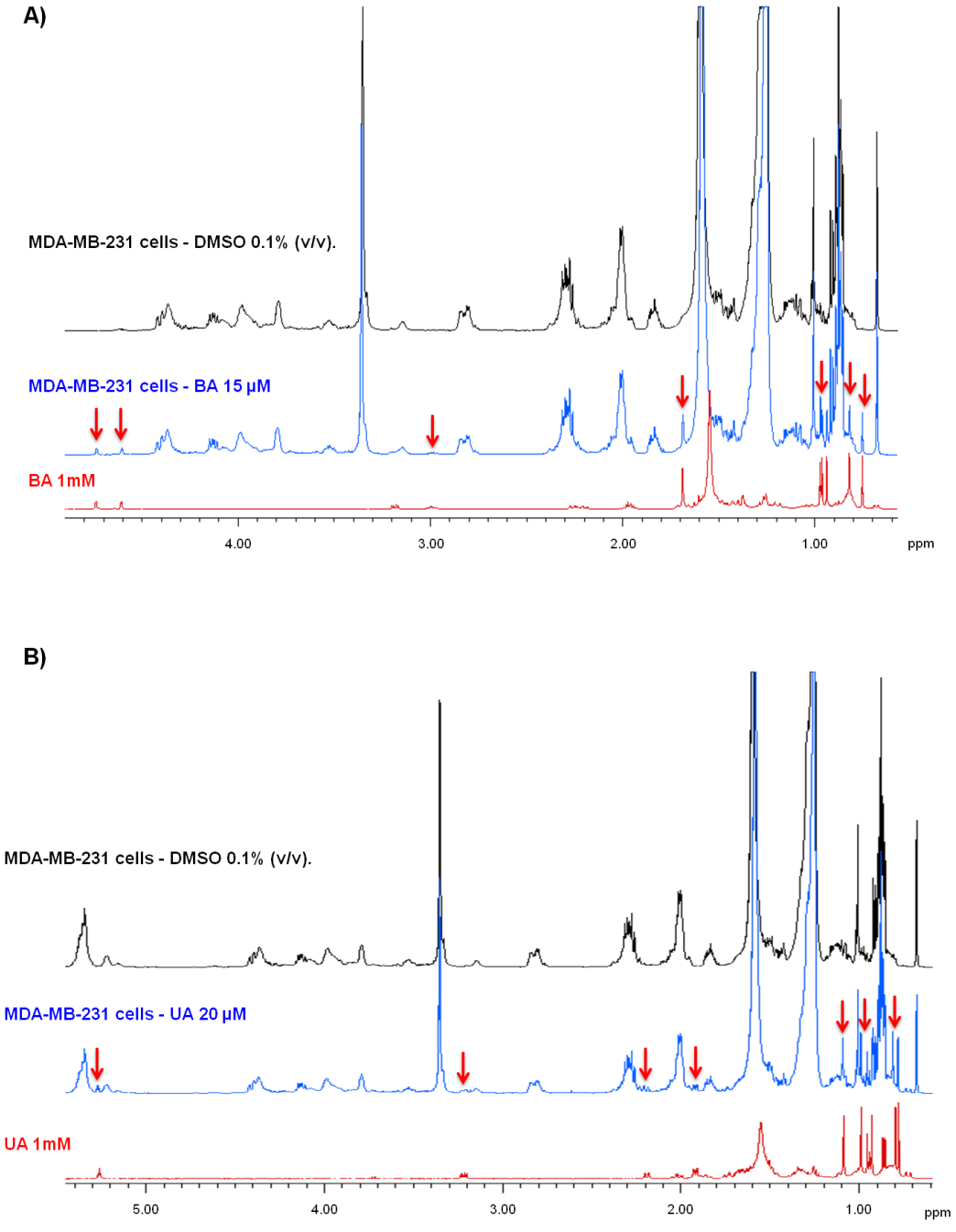

Figure 4.10. A) ^{1}H NMR spectra of organic extracts collected from MDA-MB-231 cells treated for 48h with BA (blue) and with DMSO (control cells- black). BA 1mM in $CDCl_3$ ^{1}H NMR spectra is represented in red. B) A) ^{1}H NMR spectra of organic extracts collected from MDA-MB-231 cells treated for 48h with UA (blue) and with DMSO (control cells- black). UA 1mM in $CDCl_3$ ^{1}H NMR spectra is represented in red. The signals arising from TAs in treated cells are indicated in the respective spectra with red arrows.

The changes in cellular lipid components were then assessed through spectral integration and normalization of signal areas to the total spectral area, excluding not only residual solvent signals but also the TA signals identified. The significant variations obtained for MDA-MB-231 and MCF-10A cells are presented in Figure 4.11 and Figure 4.12, respectively.

When MDA-MB-231 breast cancer cells were incubated with BA for 48h, the levels of neutral lipids (cholesteryl esters and triglycerides) decreased significantly relatively to control cells (Figure 4.11A). Plasmalogen lipids (glycerophospholipids with a vinyl-ether bond at the *sn*-1 position) also decreased, at the high exposure concentration only, while total glycerophospholipids and free cholesterol increased in BA-treated cells. However, except for triglyceride reduced levels, all other changes were reversed in BA-treated cells that were incubated for additional 24h in BA-free fresh medium.

The UA-induced variations in the lipid composition of MDA-MB-231 breast cancer cells are presented in Figure 4.11B. As it was found for BA, 48h cellular incubations with UA resulted in decreased levels of plasmalogen (high UA concentration) cholesteryl esters and triglycerides (both UA concentrations), along with an increase in free cholesterol (seen only at the low exposure concentration). However, contrarily to BA, most changes occurring in 48h UA-treated cells persisted after the 24h UA-free incubation period. In addition, cancer cells treated with 20 µM UA displayed a reduced relative proportion of unsaturated (namely, polyunsaturated) fatty acyl chains composing cellular lipids.

Compared to MDA-MB-231 cells, MCF-10A cells showed a very different profile of lipid variations upon incubation with BA or UA. As shown in Figure 4.12A, BA-treated epithelial cells displayed decreased levels of glycerophospholipids (including plasmalogen) and increased levels of triglycerides. The relative amount of free cholesterol was also increased, and so was the contribution of polyunsaturated fatty acids (such as linoleic acid) to the total fatty acyl content. All changes persisted after the 24h recovery period. As for UA-treated MCF-10A cells, significant variations in comparison to control cells were confined to increases in triglycerides and the linoleic/PUFA ratio (Figure 4.12B). The latter change was more pronounced in 48h+24h samples.

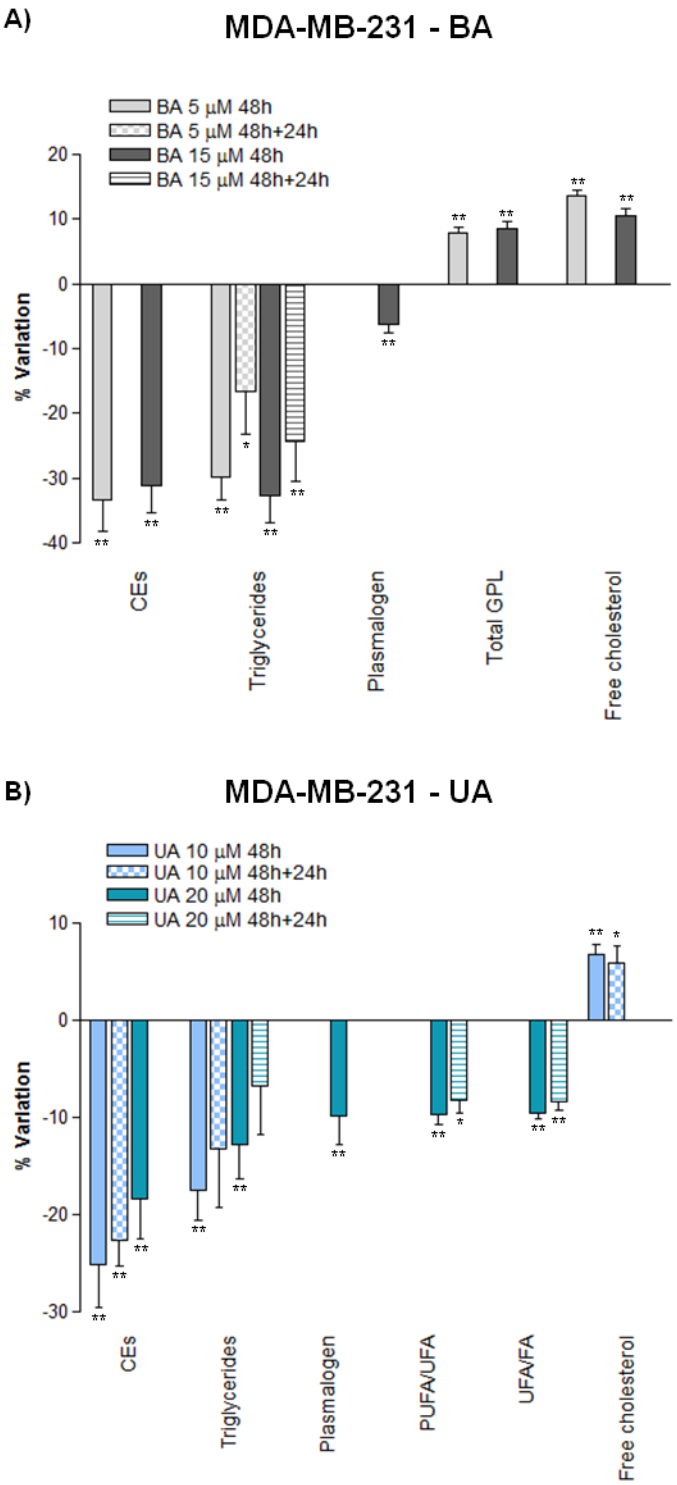

Figure 4.11. Lipid-related variations in organic extracts from MDA-MB-231 breast cancer cells treated for 48h or 48h+24h with A) BA 5 µM or 15 µM, B) UA 10 µM or 20 µM. DMSO was the solvent control. ***P*-value<0.01; **P*-value<0.05. CEs, cholesteryl esters; PUFA, polyunsaturated fatty acyl chains, UFA, unsaturated fatty acyl chains; GPL, Glycerophospholipids; FA, total fatty acids.

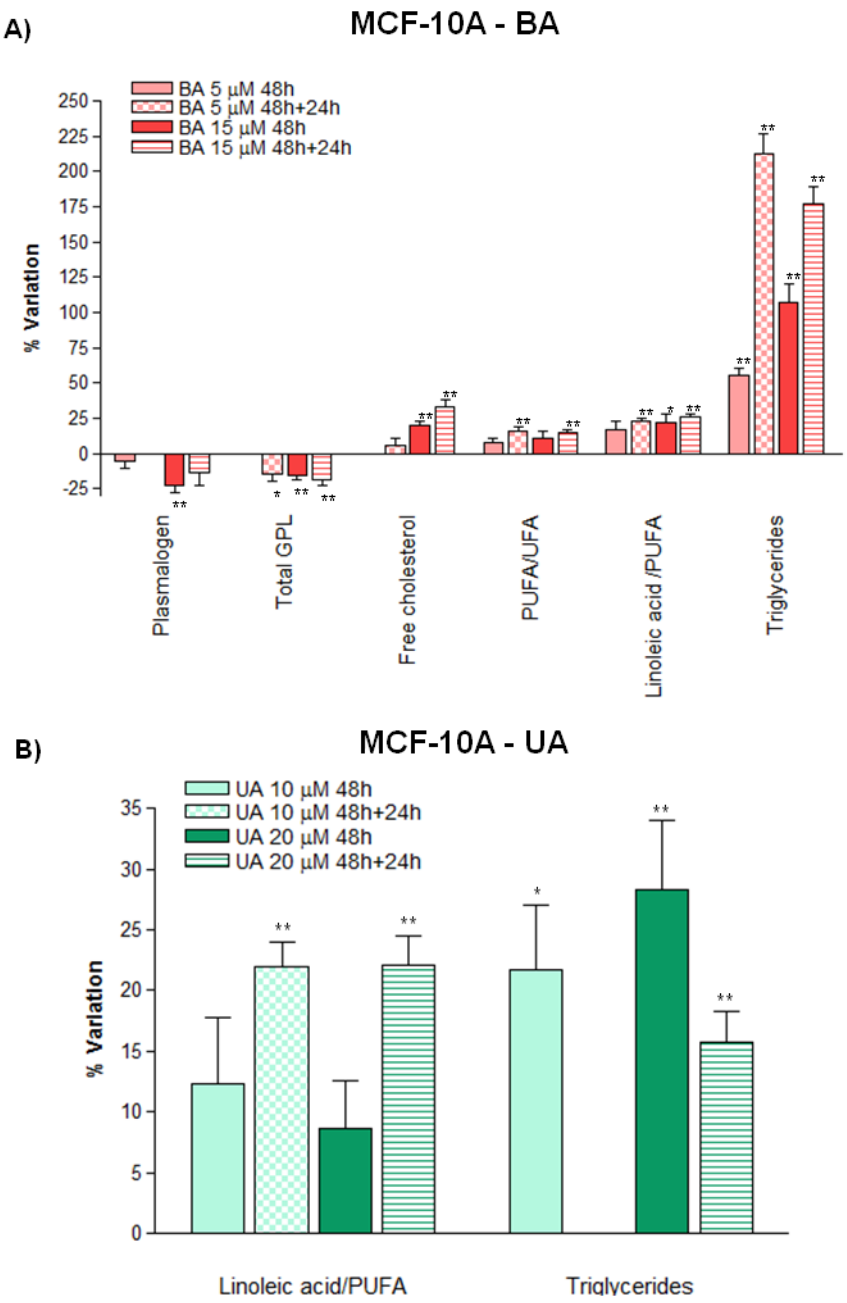

Figure 4.12. Lipid-related variations in organic extracts from MCF-10A breast epithelial cells treated for 48h or 48h+24h with A) BA 5 µM or 15 µM, B) UA 10 µM or 20 µM. DMSO was the solvent control. ***P*-value<0.01; **P*-value<0.05. PUFA, polyunsaturated fatty acyl chains, UFA, unsaturated fatty acyl chains; GPL, Glycerophospholipids; FA, total fatty acids.

4.4. Discussion

This work aimed at characterizing the metabolic effects of two pentacyclic triterpenes – betulinic acid (BA) and ursolic acid (UA) – in both TNBC cells (MDA-MB-231) and non-malignant breast epithelial cells (MCF-10A).

The results of the MTT assay, which reflect overall cellular metabolic activity and viability [24], indicated that both cell lines were susceptible to BA and UA, in a

dose- and time-dependent manner. The IC_{50} values determined for 24h incubations of MDA-MB-231 cells with BA (31.28 µM) and UA (24.54 µM) were very similar to those recently reported in the literature (30.6 and 22.9 µM, for BA and UA respectively) [25]. For this incubation period, UA appeared to be more cytotoxic than BA. However, for longer incubations (48 and 72h) of MDA-MB-231 cells with each of these TAs, BA had a higher impact on MTT-assessed metabolic activity, and the respective IC_{50} values were lower than those determined for UA. Regarding MCF-10A epithelial cells, they were more susceptible to BA treatment than cancer cells (lower IC_{50} values for all incubation periods). This is in contrast with previous studies where BA was reported to have no influence on MCF-10A cells viability [26, 27]. In the case of UA, we have found IC_{50} values in MCF-10A similar to those determined in MDA-MB-231 cells, while lower effects were also reported in the literature [28-31]. Differences in cell densities and incubation periods could possibly justify these discrepancies.

Untargeted NMR metabolomics was then employed to provide a more detailed picture of the cells metabolic reprogramming upon 48h incubations with either BA (5 and 15 µM) or UA (10 and 20 µM), the higher concentrations tested corresponding approximately to the IC_{50} values determined in MDA-MB-231 cells by the MTT assay. Moreover, the metabolic profiles of BA/UA-treated cells incubated for additional 24h in fresh growth media (without TAs) were also characterized to assess the persistence/reversibility of changes. The integrated analysis of variations in cells consumption and excretion patterns, polar intracellular metabolites and lipid composition, compared to adequate controls, allowed several hypotheses on BA/UA-induced metabolic modulation of each cell type to be proposed, as discussed below.

Exposure of MDA-MB-231 breast cancer cells to BA induced increased glucose consumption, lactate excretion and intracellular lactate levels, suggesting upregulation of glycolytic activity (Figure 4.13). MDA-MB-231 cells treated with common chemotherapy drugs (cisplatin and doxorubicin) have also been reported to increase lactate content [32]. However, in another study, a 24h treatment of MDA-MB-231 cells with BA (up to 20 µM) did not alter lactate levels nor the expression of glycolytic enzymes [25], while BA-treated SK-BR-3 and MCF-7 breast cancer cells displayed decreased protein levels of hexokinase (HK2) and/or pyruvate kinase PKM2 [25, 33]. These different results illustrate the dependence of metabolic modulation on the specific cell line considered, as well on other factors such as exposure time and concentration (the latter being also influenced by cell density).

BA-treated MDA-MB-231 cells further showed decreased intracellular levels of citrate and fumarate, as well as decreased levels of several amino acids (glutamate, glutamine, aspartate, alanine and glycine) that could be used as TCA cycle anaplerotic substrates, thus suggesting enhanced flux through this metabolic pathway [34]. On the other hand, the increases in other intracellular amino acids (proline, branched chain and aromatic amino acids) could be indicative of autophagic protein degradation. Indeed, MDA-MB-231 cells have been reported to present upregulated levels of several amino acids in response to nutrient deprivation leading to protein degradation [35]. A significant decrease in phosphocreatine accompanied by a concomitant increase in creatine further suggests the involvement of phosphocreatine-creatine kinase (CK) shuttle, likely to maintain ATP homeostasis. Indeed, the ability of this system to affect intracellular energy status has been recognized as an important factor in the regulation of cell cycle progression in cancer cells [36].

Redox imbalance has been previously reported to arise from exposure of breast cancer cells to triterpenic acids [25]. Our results showed a significant BA-induced decrease in the antioxidant tripeptide glutathione (GSH), stated by others to be crucial for neutralizing reactive oxygen species (ROS) in TNBC cells and to sustain their survival [37]. Hence, its decrease in BA-treated cancer cells suggests that its use to maintain cellular redox homeostasis surpassed its production, possibly also in relation with the limited availability of precursor amino acids [38, 39].

The levels of choline-containing metabolites, which are involved in phospholipid metabolism and associated with breast cancer progression [40], were also significantly affected in BA-treated MDA-MB-231 cells. The most marked variation was the decrease in phosphocholine. This could eventually be related to the increase in total glycerophospholipids (GPL) observed through NMR analysis of organic cell extracts. Indeed, BA-treated MDA-MB-231 cells displayed significant decreases in triglycerides and cholesteryl esters, typically found in cytosolic lipid droplets [41] and increased levels of GPL and free cholesterol (major membrane constituents). This suggests lipid metabolism reprogramming towards membrane formation (Figure 4.13), which is in accordance with the cell cycle results, namely with an increase of BA-treated cancer cells at G2 phase, during which cells enhance phospholipid synthesis to prepare for the mitotic phase [42]. This observation also agrees with the previously reported cell cycle arrest at G2/M phase in MDA-MB-231 cells treated with BA (2.5-10 μM) for 48h [43].

Although most of the metabolic variations described above were abrogated in MDA-MB-231 cells allowed to recover for 24h in BA-free fresh growth medium, 48+24h BA-treated cells still displayed a few differences in relation to controls. These included decreased consumption of pyruvate, decreased extracellular and intracellular levels of citrate and alanine, together with decreased intracellular phosphocreatine and ATP levels. It may thus be suggested that after the initial metabolic boost during BA incubation, BA-exposed cancer cells could not fully recover their ability to maintain metabolic and energetic homeostasis.

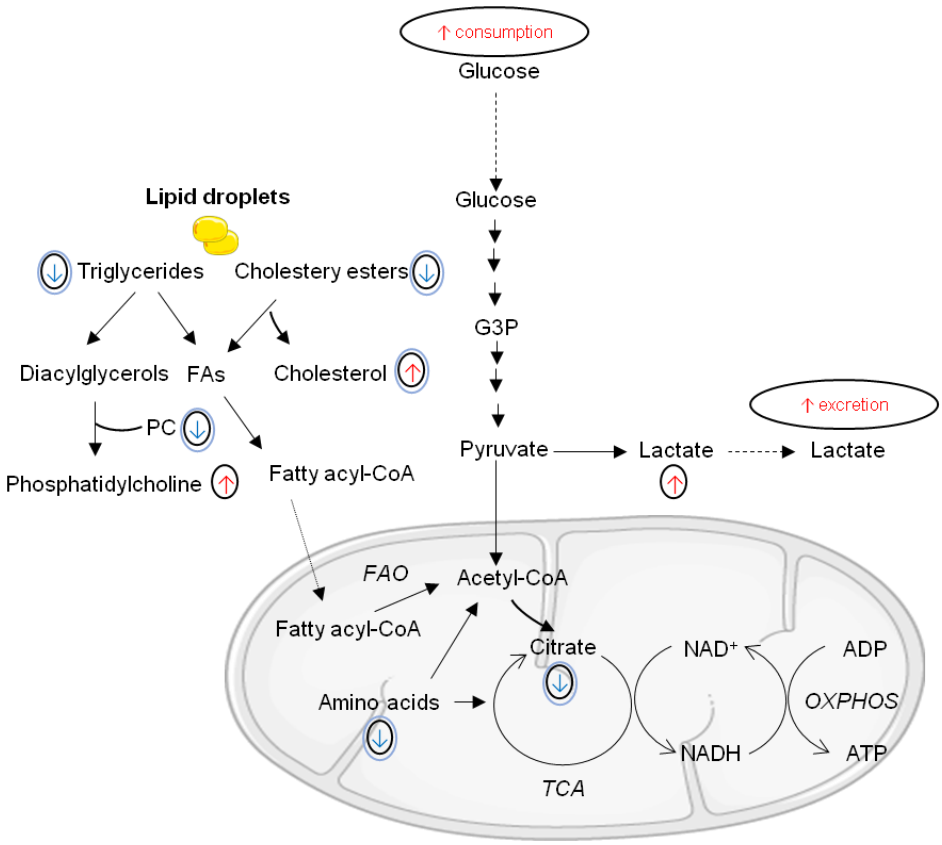

Figure 4.13. Proposed metabolic reprogramming of MDA-MB-231 breast cancer cells upon 48h incubation with BA or UA. Effects of BA and UA are represented by black and blue circles, respectively. NAD^+/NADH , nicotinamide adenine dinucleotide/reduced form; PC, phosphocholine; FAs, fatty acids; TCA, tricarboxylic acid cycle; OXPHOS; Oxidative phosphorylation.

Globally, UA had a lower impact on MDA-MB-231 cells metabolome than BA. It did not alter metabolite consumption nor excretion upon 48h incubation and induced considerably less changes in intracellular polar metabolites (Figure 4.8). However, after a 24h recovery period, UA-induced effects in cancer cells become more noticeable. For instance, cells consumed less glucose and excreted less lactate and alanine, suggesting downregulation of glycolysis (Figure 4.3). At the same time, intracellular ATP levels were decreased. This is in line with the results

of Lewinska and co-workers, where the expression of glycolytic enzymes (HK2 and PKM2) and ATP content decreased in MDA-MB-231 treated with UA (5-20 µM) [25]. Other noticeable variations after the recovery period comprised elevated aspartate levels (not seen in BA-treated cells) and an inversion of the PC to GPC ratio, i.e., in 48h+24h samples PC increased and GPC decreased, contrarily to what was observed in 48h-incubated cells. Analysis of lipid variations (Figure 4.11B) further showed that, although TG and CE contents decreased and free cholesterol increased, as seen for BA-treated cells, GPL did not increase, suggesting that membrane formation was not upregulated. On the other hand, the fate of fatty acids released from TG hydrolysis could possibly be beta-oxidation in the mitochondria. Additionally, UA-exposed cancer cells displayed a decrease in the relative proportion of (poly)unsaturated fatty acyl chains, suggesting reduced membrane fluidity.

The metabolic responses of MCF-10A breast epithelial cells to BA and UA differed greatly from those of cancer cells and were globally more pronounced. On the other hand, there were less marked differences between the metabolic signatures of the two TAs. After a 48h incubation with either BA or UA, MCF-10A cells showed profound reprogramming of glucose metabolism (Figure 4.14). In particular, integrated analysis of variations in extracellular and intracellular polar metabolites suggested enhancement of both glycolytic activity (supported not only by higher extracellular glucose consumption, but apparently also by glycogen degradation) and TCA cycle activity (supported by anaplerotic fueling of amino acids). Moreover, increased levels of UDP-N-acetyl glucosamine/galactosamine suggested upregulation of the hexosamine biosynthetic pathway (HBP). Intensification of glycolytic and TCA cycle activities are also consistent with increased NADH levels. Notably, in UA-treated MCF-10A cells, intracellular ATP even increased, possibly reflecting the overall boost in glucose metabolism. This could eventually lead to increased ROS production [44], which is consistent with the markedly decreased GSH levels. Analysis of variations in choline compounds and lipids further helped to build our working hypothesis, summarized in Figure 4.14. Both BA and UA caused marked decreases in phosphocholine and elevations in choline and glycerophosphocholine, which could reflect inhibition of choline to phosphocholine conversion (the first step in phosphatidylcholine biosynthesis) and membrane degradation. Indeed, BA-treated cells showed reduced levels of total glycerophospholipids. On the other hand, triglycerides increased in both BA and UA-treated cells, this accumulation being more extensive in the former, for which an

increase in cholesterol levels was also observed. The formation of cytosolic lipid droplets (LD) incorporating neutral lipids is a common adaptation to cellular stress triggered by factors such as redox imbalance, excessive free fatty acids or nutrient starvation [41, 45]. Indeed, LD are currently recognized to function not only as energy reserves, but also as storage sites for otherwise-harmful lipids or proteins and as regulators of lipid homeostasis in membranes. The observed increase in PUFA, especially linoleic acid, is also consistent with their sequestration from membranes into LDs, where they are thought to be less susceptible to peroxidation reactions [46]. Additionally, BA-treated MCF-10A cells showed increased cholesterol and formate levels which suggest upregulation of cholesterol synthesis.

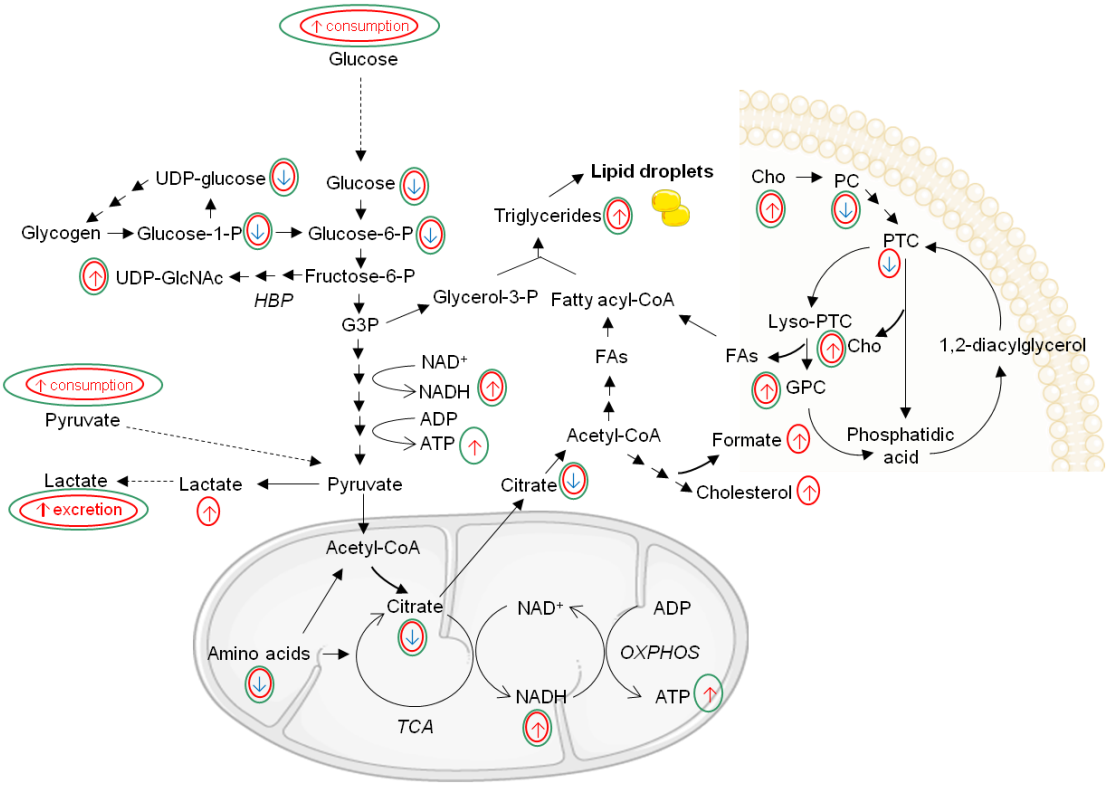

Figure 4.14. Proposed metabolic reprogramming of MCF-10A breast epithelial cells upon 48h incubation with BA or UA. Effects of BA and UA are represented by red and green circles, respectively. ADP/ATP, adenosine di/triphosphate; NAD^+/NADH , nicotinamide adenine dinucleotide/reduced form;Cho, choline; PC, phosphocholine; GPC, glycerophosphocholine; PTC, phosphatidylcholine; UDP, uridine diphosphate; UDP-GlcNAc, UDP-N-acetyl-glucosamine; FAs, fatty acids; HBP, hexosamine biosynthetic pathway; TCA, tricarboxylic acid cycle; G3P, glyceraldehyde 3-phosphate; OXPHOS; Oxidative phosphorylation.

The recovery behavior of MCF-10A cells upon incubation in fresh growth medium was partially different for the two TAs. Contrarily to 48h BA-treated cells, 48h+24h samples decreased the consumption of glucose, pyruvate and acetate, as

well as the excretion of lactate, and normalized intracellular glucose, lactate and ATP levels in relation to controls. On the other hand, UA-treated cells incubated for additional 24h in UA-free medium maintained enhance glycolysis and glutamine levels became more elevated.

4.5. Conclusions

This untargeted metabolomics study revealed a panoply of unanticipated metabolic alterations in TNBC and non-tumor breast epithelial cells, upon incubation with pure triterpenic acids, BA and UA. By integrating the changes observed in cell-conditioned culture medium, intracellular polar extracts and organic extracts, it was possible to propose several interconnections between multiple metabolic pathways (involving glucose, amino acids, nucleotides and lipid metabolisms) to be implicated in the TAs cellular effects. Notably, these effects were markedly different in TNBC and breast epithelial cells, which supports the idea that TAs may be promising candidates for the differential metabolic modulation of tumor cells, potentially targeting their metabolic vulnerabilities.

4.6. References

1. Pareja, F., Geyer, F.C., Marchio, C., Burke, K.A., Weigelt, B.and Reis-Filho, J.S., (2016). Triple-negative breast cancer: the importance of molecular and histologic subtyping, and recognition of low-grade variants. *Npj Breast Cancer*, 2, 16036.

2. Gusterson, B. and Eaves, C.J., (2018). Basal-like breast cancers: from pathology to biology and back again. *Stem Cell Reports*, 10(6), 1676-1686.

3. Schneeweiss, A., Denkert, C., Fasching, P.A., Fremd, C., Gluz, O., Kolberg-Liedtke, C., Loibl, S.and Luck, H.J., (2019). Diagnosis and therapy of Triple-Negative Breast Cancer (TNBC) - Recommendations for daily routine practice. *Geburtshilfe Und Frauenheilkunde*, 79(6), 605-617.

4. Vojtek, M., Marques, M.P.M., Ferreira, I.M.P.L.V.O., Mota-Filipe, H.and Diniz, C., (2019). Anticancer activity of palladium-based complexes against triple-negative breast cancer. *Drug Discovery Today*, 24(4), 1044-1058.

5. Harvey, A.L., Edrada-Ebel, R.and Quinn, R.J., (2015). The re-emergence of natural products for drug discovery in the genomics era. *Nature Reviews Drug Discovery*, 14(2), 111-129.

6. Guerra, A.R., Duarte, M.F.and Duarte, I.F., (2018). Targeting tumor metabolism with plant-derived natural products: Emerging trends in cancer therapy. *Journal of Agricultural and Food Chemistry*, 66(41), 10663-10685.

7. Xu, R., Fazio, G.C.and Matsuda, S.P.T., (2004). On the origins of triterpenoid skeletal diversity. *Phytochemistry*, 65(3), 261-291.

8. Laszczyk, M.N., (2009). Pentacyclic triterpenes of the lupane, oleanane and ursane group as tools in cancer therapy*. Planta Medica*, 75(15), 1549-1560.

9. Rufino-Palomares, E.E., Perez-Jimenez, A., Reyes-Zurita, F.J., Garcia-Salguero, L., Mokhtari, K., Herrera-Merchan, A., Medina, P.P., Peragon, J.and Lupianez, J.A., (2015). Anti-cancer and anti-angiogenic properties of various natural pentacyclic triterpenoids and some of their chemical derivatives*. Current Organic Chemistry*, 19(10), 919-947.

10. Salvador, J.A.R., Leal, A.S., Valdeira, A.S., Goncalves, B.M.F., Alho, D.P.S., Figueiredo, S.A.C., Silvestre, S.M.and Mendes, V.I.S., (2017). Oleanane-, ursane-, and quinone methide friedelane-type triterpenoid derivatives: Recent advances in cancer treatment*. European Journal of Medicinal Chemistry*, 142 95-130.

11. Domingues, R.M.A., Guerra, A.R., Duarte, M., Freire, C.S.R., Neto, C.P., Silva, C.M.S.and Silvestre, A.J.D., (2014). Bioactive triterpenic acids: from agroforestry biomass residues to promising therapeutic tools*. Mini-Reviews in Organic Chemistry*, 11(3), 382-399.

12. Ali-Seyed, M., Jantan, I., Vijayaraghavan, K.and Bukhari, S.N.A., (2016). Betulinic acid: Recent advances in chemical modifications, effective delivery, and molecular mechanisms of a promising anticancer therapy*. Chemical Biology & Drug Design*, 87(4), 517-536.

13. Luo, R.L., Fang, D.Y., Chu, P., Wu, H.J., Zhang, Z.and Tang, Z.Y., (2016). Multiple molecular targets in breast cancer therapy by betulinic acid*. Biomedicine & Pharmacotherapy*, 84 1321-1330.

14. Zhang, X., Hu, J.Y.and Chen, Y., (2016). Betulinic acid and the pharmacological effects of tumor suppression*. Molecular Medicine Reports*, 14(5), 4489-4495.

15. Yin, R., Li, T., Tian, J.X., Xi, P.and Liu, R.H., (2018). Ursolic acid, a potential anticancer compound for breast cancer therapy*. Critical Reviews in Food Science and Nutrition*, 58(4), 568-574.

16. Chan, E.W.C., Soon, C.Y., Tan, J.B.L., Wong, S.K.and Hui, Y.W., (2019). Ursolic acid: an overview on its cytotoxic activities against breast and colorectal cancer cells*. Journal of Integrative Medicine-Jim*, 17(3), 155-160.

17. Feng, X.M. and Su, X.L., (2019). Anticancer effect of ursolic acid via mitochondria-dependent pathways*. Oncology Letters*, 17(6), 4761-4767.

18. Domingues, R.M.A., Patinha, D.J.S., Sousa, G.D.A., Villaverde, J.J., Silva, C.M., Freire, C.S.R., Silvestre, A.J.D.and Neto, C.P., (2011). Eucalyptus biomass residues from agro-forest and pulping industries as sources of high-value triterpenic compounds*. Cellulose Chemistry and Technology*, 45(7-8), 475-481.

19. Guerra, A.R., Soares, B.I.G., Oliveira, H., Freire, C.S.R., Silvestre, A.J.D., Duarte, M.F.and Duarte, I.F., NMR metabolomics reveals different metabolic modulatory activity of a lipophilic Eucalyptus outer bark extract on human tumor and non-tumor breast epithelial cells*. (submitted)*.

20. Mosmann, T., (1983). Rapid colorimetric assay for cellular growth and survival - application to proliferation and cyto-toxicity assays*. Journal of Immunological Methods*, 65(1-2), 55-63.

21. Carrola, J., Bastos, V., de Oliveira, J.M.P.F., Oliveira, H., Santos, C., Gil, A.M.and Duarte, I.F., (2016). Insights into the impact of silver nanoparticles on human keratinocytes metabolism through NMR metabolomics*. Archives of Biochemistry and Biophysics*, 589 53-61.

22. Wishart, D.S., Feunang, Y.D., Marcu, A., Guo, A.C., Liang, K., Vazquez-Fresno, R., Sajed, T., Johnson, D., Li, C.R., Karu, N., Sayeeda, Z., *et al.*, (2018). HMDB 4.0: the human metabolome database for 2018*. Nucleic Acids Research*, 46(D1), D608-D617.

23. Berben, L., Sereika, S.M.and Engberg, S., (2012). Effect size estimation: Methods and examples*. International Journal of Nursing Studies*, 49(8), 1039-1047.

24. Stockert, J.C., Horobin, R.W., Colombo, L.L.and Blazquez-Castro, A., (2018). Tetrazolium salts and formazan products in cell biology: Viability assessment, fluorescence imaging, and labeling perspectives*. Acta Histochemica*, 120(3), 159-167.

25. Lewinska, A., Adamczyk-Grochala, J., Kwasniewicz, E., Deregowska, A.and Wnuk, M., (2017). Ursolic acid-mediated changes in glycolytic pathway promote cytotoxic autophagy and apoptosis in phenotypically different breast cancer cells*. Apoptosis*, 22(6), 800-815.

26. Cai, Y.L., Zheng, Y.F., Gu, J.Y., Wang, S.Q., Wang, N., Yang, B.W., Zhang, F.X., Wang, D.M., Fu, W.J.and Wang, Z.Y., (2018). Betulinic acid chemosensitizes breast cancer by triggering ER stress-ediated apoptosis by directly targeting GRP78*. Cell Death & Disease*, 9(6), 636.

27. Jiao, L., Wang, S.Q., Zheng, Y.F., Wang, N., Yang, B.W., Wang, D.M., Yang, D.P., Mei, W.J., Zhao, Z.M.and Wang, Z.Y., (2019). Betulinic acid suppresses breast cancer aerobic glycolysis via caveolin-1/NF-kappa B/c-Myc pathway*. Biochemical Pharmacology*, 161 149-162.

28. Gu, G.W., Barone, I., Gelsomino, L., Giordano, C., Bonofiglio, D., Statti, G., Menichini, F., Catalano, S.and Ando, S., (2012). Oldenlandia diffusa extracts exert antiproliferative and apoptotic effects on human breast cancer cells through ER alpha/Sp1-mediated p53 activation*. Journal of Cellular Physiology*, 227(10), 3363-3372.

29. Mishra, T., Arya, R.K., Meena, S., Joshi, P., Pal, M., Meena, B., Upreti, D.K., Rana, T.S.and Datta, D., (2016). Isolation, characterization and anticancer potential of cytotoxic triterpenes from Betula utilis bark*. Plos One*, 11(7), e0159430.

30. Wen, L.R., Guo, R.X., You, L.J., Abbasi, A.M., Li, T., Fu, X.and Liu, R.H., (2017). Major triterpenoids in Chinese hawthorn "Crataegus pinnatifida" and their effects on cell proliferation and apoptosis induction in MDA-MB-231 cancer cells*. Food and Chemical Toxicology*, 100 149-160.

31. Zheng, G.R., Shen, Z.C., Xu, A.X., Jiang, K., Wu, P.Y., Yang, X., Chen, X.and Shao, J.W., (2017). Synergistic chemopreventive and therapeutic effects of co-drug UA-Met: Implication in tumor metastasis*. Journal of Agricultural and Food Chemistry*, 65(50), 10973-10983.

32. Maria, R.M., Altei, W.F., Selistre-de-Araujo, H.S.and Colnago, L.A., (2017). Impact of chemotherapy on metabolic reprogramming: Characterization of the metabolic profile of breast cancer MDA-MB-231 cells using H-1 HR-MAS NMR spectroscopy*. Journal of Pharmaceutical and Biomedical Analysis*, 146 324-328.

33. Potze, L., Di Franco, S., Grandela, C., Pras-Raves, M.L., Picavet, D.I., van Veen, H.A., van Lenthe, H., Mullauer, F.B., van der Wel, N.N., Luyf, A., van Kampen, A.H.C., Kemp, S., Everts, V., Kessler, J.H., Vaz, F.M. and Medema, J.P., (2015). Betulinic acid induces a novel cell death pathway that depends on cardiolipin modification*. Oncogene*, 35(4), 427-437.

34. Haukaas, T.H., Euceda, L.R., Giskeodegard, G.F.and Bathen, T.F., (2017). Metabolic portraits of breast cancer by HR MAS MR spectroscopy of intact tissue samples*. Metabolites*, 7(2), E18.

35. Willmann, L., Schlimpert, M., Halbach, S., Erbes, T., Stickeler, E.and Kammerer, B., (2015). Metabolic profiling of breast cancer: Differences in central metabolism between subtypes of breast cancer cell lines*. Journal of Chromatography B-Analytical Technologies in the Biomedical and Life Sciences*, 1000 95-104.

36. Yan, Y.B., (2016). Creatine kinase in cell cycle regulation and cancer*. Amino Acids*, 48(8), 1775-1784.

37. Beatty, A., Fink, L.S., Singh, T., Strigun, A., Peter, E., Ferrer, C.M., Nicolas, E., Cai, K.Q., Moran, T.P., Reginato, M.J., Rennefahrt, U.and Peterson, J.R., (2018). Metabolite profiling reveals the glutathione biosynthetic pathway as a therapeutic target in triple-negative breast cancer*. Molecular Cancer Therapeutics*, 17(1), 264-275.

38. Timmerman, L.A., Holton, T., Yuneva, M., Louie, R.J., Padro, M., Daemen, A., Hu, M., Chan, D.A., Ethier, S.P., van 't Veer, L.J., Polyak, K., McCormick, F.and Gray, J.W., (2013). Glutamine sensitivity analysis identifies the xCT antiporter as a common triple-negative breast tumor therapeutic target*. Cancer Cell*, 24(4), 450-465.

39. Gross, M.I., Demo, S.D., Dennison, J.B., Chen, L., Chernov-Rogan, T., Goyal, B., Janes, J.R., Laidig, G.J., Lewis, E.R., Li, J., MacKinnon, A.L., Parlati, F., Rodriguez, M.L.M., Shwonek, P.J., Sjogren, E.B., Stanton, T.F., Wang, T.T., Yang, J.F., Zhao, F.and Bennett, M.K., (2014). Antitumor activity of the glutaminase inhibitor CB-839 in triple-negative breast cancer*. Molecular Cancer Therapeutics*, 13(4), 890-901.

40. Iorio, E., Caramujo, M.J., Cecchetti, S., Spadaro, F., Carpinelli, G., Canese, R.and Podo, F., (2016). Key players in choline metabolic reprograming in triple-negative breast cancer*. Frontiers in Oncology*, 6, 205.

41. Welte, M.A. and Gould, A.P., (2017). Lipid droplet functions beyond energy storage*. Biochimica Et Biophysica Acta-Molecular and Cell Biology of Lipids*, 1862(10), 1260-1272.

42. Icard, P., Fournel, L., Wu, Z.R., Alifano, M.and Lincet, H., (2019). Interconnection between metabolism and cell cycle in cancer*. Trends in Biochemical Sciences*, 44(6), 490-501.

43. Mertens-Talcott, S.U., Noratto, G.D., Li, X.R., Angel-Morales, G., Bertoldi, M.C.and Safe, S., (2013). Betulinic acid decreases ER-negative breast cancer cell growth in vitro and in vivo: Role of Sp transcription factors and microRNA-27a:ZBTB10*. Molecular Carcinogenesis*, 52(8), 591-602.

44. Liemburg-Apers, D.C., Willems, P.H.G.M., Koopman, W.J.H.and Grefte, S., (2015). Interactions between mitochondrial reactive oxygen species and cellular glucose metabolism*. Archives of Toxicology*, 89(8), 1209-1226.

45. Henne, W.M., Reese, M.L.and Goodman, J.M., (2018). The assembly of lipid droplets and their roles in challenged cells*. Embo Journal*, 37(12), e101816.

46. Pan, X.Y., Wilson, M., McConville, C., Arvanitis, T.N., Griffin, J.L., Kauppinen, R.A.and Peet, A.C., (2013). Increased unsaturation of lipids in cytoplasmic lipid droplets in DAOY cancer cells in response to cisplatin treatment*. Metabolomics*, 9(3), 722-729.

Supplementary information to Chapter 4

Table S4.1. Main metabolite variations in polar extracts of MDA-MB-231 cells exposed to 5 µM and 15 µM of BA and 10 µM and 20 µM of UA, in relation to controls, expressed as % variation (%var) and respective error (±), effect size (ES) and *P*-value (*P*). The variations with |ES| < 0.8 (or standard error > |ES|, or mean error > |% variation|) were considered null.

		BA				UA			
		5µM		15µM		10µM		20µM	
		48h	48h+24h	48h	48h+24h	48h	48h+24h	48h	48h+24h
Acetate	%var	0	0	21.07	22.70	0	0	10.69	11.02
	±			6.65	4.17			7.27	1.74
	ES	0	0	1.76	3.01	0	0	0.86	3.70
	P			0.0479	0.0145			0.2390	0.0033
Lactate	%var	53.08	0	55.73	0	0	0	0	0
	±	8.85		9.41					
	ES	2.91	0	2.85	0	0	0	0	0
	P	0.0115		0.0072					
Citrate	%var	-40.97	-12.45	-51.74	-19.78	-23.26	-10.99	-19.44	-15.02
	±	6.03	2.83	4.92	4.29	3.54	6.13	3.20	4.21
	ES	-5.25	-2.88	-8.72	-3.15	-4.58	-1.17	-4.14	-2.37
	P	0.0002	0.0169	1.0804E-05	0.0022	0.0014	0.1232	0.0052	0.0085
Fumarate	%var	-35.42	0	-37.50	0	0	0	-10.42	-10.34
	±	9.58		17.01				9.75	6.30
	ES	-2.76	0	-1.67	0	0	0	-0.69	-1.06
	P	0.0043		0.0497				0.3040	0.1817
Glu	%var	-24.61	0	-37.41	-11.90	0	0	0	0
	±	5.09		5.86	3.07				
	ES	-3.39	0	-4.83	-2.53	0	0	0	0
	P	0.0029		0.0003	0.0186				
Gln	%var	-28.49	0	-20.94	-5.26	-13.00	0	0	0
	±	5.90		6.99	4.20	7.36			
	ES	-3.46	0	-2.06	-0.79	-1.16	0	0	0
	P	0.0094		0.0172	0.2604	0.1079			
Asp	%var	-30.52	0	-12.45	0	0	0.00	24.90	32.91
	±	8.61		8.21				6.51	9.58
	ES	-2.57	0	-0.99	0	0	0.00	2.09	1.81
	P	0.0096		0.1632				0.0205	0.0390

Table S4.1. (cont.)

		BA				UA			
		5µM		15µM		10µM		20µM	
		48h	48h+24h	48h	48h+24h	48h	48h+24h	48h	48h+24h
Ala	%var	-12.64	-7.44	-10.34	-12.62	0	0.00	0	-12.11
	±	4.36	1.59	4.24	1.60				3.37
	ES	-1.90	-2.98	-1.58	-5.19	0	0.00	0	-2.35
	P	0.0219	0.0063	0.0429	0.0009				0.0162
Gly	%var	0	-8.57	-9.59	-31.75	0	-7.50	-15.08	-25.85
	±		1.94	6.90	1.84		2.44	5.06	1.37
	ES	0	-2.83	-0.90	-12.58	0	-1.96	-1.98	-13.32
	P		0.0052	0.1990	1.0429E-06		0.0297	0.0219	4.8081E-06
Pro	%var	16.73	0	21.93	0	0	0	0	0
	±	3.54		4.78					
	ES	2.68	0	2.54	0	0	0	0	0
	P	0.0112		0.0184					
Leu	%var	15.91	0	33.86	0	0	0	0	0
	±	2.07		6.04					
	ES	4.38	0	2.95	0	0	0	0	0
	P	0.0037		0.0112					
Ile	%var	14.68	0	30.97	0	0	0	0	0
	±	2.06		6.19					
	ES	4.08	0	2.66	0	0	0	0	0
	P	0.0044		0.0157					
Val	%var	18.46	0	38.79	0	0	0	0	0
	±	1.97		6.70					
	ES	5.28	0	2.98	0	0	0	0	0
	P	0.0008		0.0127					
Phe	%var	6.80	0	24.06	0	0	0	0	0
	±	2.51		6.82					
	ES	1.61	0	1.94	0	0	0	0	0
	P	0.0499		0.0403					

Table S4.1. (cont.)

		BA				UA			
		5µM		15µM		10µM		20µM	
		48h	48h+24h	48h	48h+24h	48h	48h+24h	48h	48h+24h
Tyr	%var	8.11	0	28.53	0	0	0	0	0
	±	2.49		6.45					
	ES	1.93	0	2.38	0	0	0	0	0
	P	0.0418		0.0202					
PCr	%var	-19.36	0	-22.44	-14.19	-13.59	0	-10.77	0
	±	4.46		5.44	4.07	4.18		5.40	
	ES	-2.95	0	-2.86	-2.31	-2.15	0	-1.30	0
	P	0.0077		0.0037	0.0134	0.0279		0.0797	
Cr	%var	22.45	0	18.99	0	0	0	0	0
	±	6.47		4.87					
	ES	1.92	0	2.19	0	0	0	0	0
	P	0.0274		0.0120					
ATP	%var	0	-7.54	0	-15.36	0	0	0	-9.33
	±		3.18		2.60				1.38
	ES	0	-1.52	0	-3.93	0	0	0	-4.37
	P		0.0814		0.0045				0.0007
Choline	%var	10.16	0	12.46	0	-6.23	0	0	0
	±	4.87		7.21		4.52			
	ES	1.22	0	1.00	0	-0.87	0	0	0
	P	0.0962		0.1752		0.2050			
PC	%var	-24.96	0	-38.62	0	-7.00	0	-6.17	21.66
	±	3.54		7.32		4.26		4.36	2.40
	ES	-4.96	0	-4.02	0	-1.05	0	-0.90	5.01
	P	0.0002		0.0029		0.1479		0.2042	0.0011
GPC	%var	13.50	0	26.27	0	9.94	0	10.72	-6.52
	±	2.21		5.30		3.24		5.81	2.25
	ES	3.52	0	2.69	0	1.80	0	1.08	-1.84
	P	0.0048		0.0125		0.0275		0.1575	0.0275

Table S4.1. (cont.)

		BA				UA			
		5µM		15µM		10µM		20µM	
		48h	48h+24h	48h	48h+24h	48h	48h+24h	48h	48h+24h
GSH	%var	-15.77	0	-25.87	0	-7.40	0	-7.50	-8.79
	±	4.65		6.40		5.98		5.29	3.95
	ES	-2.26	0	-2.86	0	-0.79	0	-0.91	-1.43
	P	0.0223		0.0035		0.2457		0.1939	0.0870
Tau	%var	6.09	0	7.79	0	0	0	11.82	0
	±	1.92		2.61				1.46	
	ES	1.90	0	1.76	0	0	0	4.70	0
	P	0.0407		0.0561				0.0013	
myo-Ino	%var	-8.23	-6.52	-18.58	-17.84	0	0	0	-9.02
	±	1.20	1.59	2.70	2.57				1.41
	ES	-4.41	-2.61	-4.67	-4.69	0	0	0	-4.13
	P	0.0011	0.0062	0.0014	0.0014				0.0005

Table S4.2. Main metabolite variations in polar extracts of MCF-10A cells exposed to 5 µM and 15 µM of BA and 10 µM and 20 µM of UA, in relation to controls, expressed as % variation (%var) and respective error (±), effect size (ES) and *P*-value (*P*). The variations with |ES| < 0.8 (or standard error > |ES|, or mean error > |% variation|) were considered null.

		BA			UA		
		5µM		10µM		20µM	
		48h	48h+24h	48h	48h+24h	48h	48h+24h
Glucose	*%var*	-56.45	0	-71.26	-31.96	-85.89	-67.35
	±	29.74		15.82	16.86	15.82	21.76
	ES	-1.63	0	-4.30	-1.39	-5.85	-2.87
	P	0.0567		0.0007	0.0810	0.0007	0.0067
Glucose-1-phosphate	*%var*	-93.58	-92.25	-75.94	0	-78.61	-40.85
	±	16.11	35.07	17.96		12.98	16.06
	ES	-6.71	-3.00	-4.19	0	-6.14	-1.97
	P	0.0001	0.0057	0.0005		0.0006	0.0187
UDP-GlcNAc	*%var*	151.53	0	60.69	0	61.45	0
	±	9.25		10.15		6.32	
	ES	5.73	0	2.82	0	4.57	0
	P	0.0015		0.0128		0.0009	
UDP-GalNAc	*%var*	123.58	0	62.26	0	68.87	0
	±	13.12		12.79		12.12	
	ES	3.58	0	2.28	0	2.60	0
	P	0.0026		0.0109		0.0060	
UDP-Glucose	*%var*	-75.09	-66.89	-19.78	0	-32.23	-20.07
	±	9.60	20.53	6.86		7.47	4.37
	ES	-7.70	-3.01	-1.97	0	-3.16	-3.14
	P	0.0000	0.0139	0.0187		0.0021	0.0024
Lactate	*%var*	161.49	0	0	0	0	0
	±	34.30					
	ES	1.60	0	0	0	0	0
	P	0.0786					
Citrate	*%var*	-74.68	-61.27	-36.91	-18.09	-38.52	-32.19
	±	3.76	5.96	3.57	8.81	3.85	8.84
	ES	-19.48	-9.11	-7.80	-1.39	-7.61	-2.67
	P	2.8047E-06	0.0001	0.00002	0.0943	0.00002	0.0144

Table S4.2. (cont.)

		BA			UA		
		5µM		10µM		20µM	
		48h	48h+24h	48h	48h+24h	48h	48h+24h
Fumarate	*%var*	-80.00	0	0	-22.45	0	-34.69
	±	54.43			17.15		14.18
	ES	-1.51	0	0	-0.91	0	-1.82
	P	0.0849			0.1908		0.0401
Formate	*%var*	91.07	287.80	0	0	0	0
	±	13.94	19.51				
	ES	2.76	3.72	0	0	0	0
	P	0.0092	0.0086				
3-Hydroxyisobutyrate	*%var*	-48.45	-48.51	-23.71	-22.77	-30.93	-30.69
	±	8.28	6.18	8.07	7.27	7.11	6.58
	ES	-4.75	-6.38	-2.05	-2.17	-3.16	-3.39
	P	0.0012	0.0006	0.0176	0.0124	0.0082	0.0018
Acetate	*%var*	33.50	63.78	0	0	0	10.61
	±	7.76	13.91				3.19
	ES	2.27	2.14	0	0	0	1.94
	P	0.0138	0.0389				0.0236
Glu	*%var*	-75.91	-47.27	-21.17	0	-23.01	-11.32
	±	8.73	8.30	6.62		6.62	7.41
	ES	-8.61	-4.59	-2.20	0	-2.41	-1.00
	P	0.00003	0.0005	0.0128		0.0088	0.1665
Gln	*%var*	0	0	0	16.14	0	25.50
	±				2.45		2.43
	ES	0	0	0	3.75	0	5.72
	P				0.0023		0.0004
Asp	*%var*	-48.70	-24.38	-38.30	-26.58	-46.10	-37.26
	±	4.01	14.06	4.21	9.00	4.90	10.00
	ES	-9.87	-1.21	-6.92	-2.09	-7.52	-2.82
	P	0.0003	0.1111	0.0001	0.0146	0.00003	0.0038

Table S4.2. (cont.)

		BA			UA		
		5µM		10µM		20µM	
		48h	48h+24h	48h	48h+24h	48h	48h+24h
Ala	*%var*	-39.74	-65.18	44.32	0	0	0
	±	10.37	7.36	11.33			
	ES	-2.94	-8.08	1.97	0	0	0
	P	0.0031	0.0001	0.0299			
Gly	*%var*	41.70	0	40.31	24.70	38.29	31.50
	±	5.34		4.91	6.74	4.53	5.56
	ES	3.97	0	4.20	2.01	4.36	3.01
	P	0.0010		0.0006	0.0435	0.0004	0.0137
Pro	*%var*	80.04	0	87.39	49.66	69.18	78.81
	±	5.11		3.36	7.94	5.64	6.79
	ES	6.88	0	11.13	3.08	5.60	5.12
	P	0.0003		4.9446E-06	0.0102	0.0009	0.0018
His	*%var*	-25.16	-44.80	0	0	0	0
	±	9.10	4.76				
	ES	-1.95	-7.45	0	0	0	0
	P	0.0281	0.0001				
Leu	*%var*	418.85	75.04	389.84	82.57	297.70	130.47
	±	9.04	8.46	10.01	9.08	15.33	6.93
	ES	9.21	3.97	8.12	3.96	4.80	7.01
	P	0.0002	0.0020	0.0001	0.0010	0.0002	0.0002
Ile	*%var*	218.16	36.26	211.80	58.71	156.93	94.71
	±	6.74	8.03	8.75	8.29	13.07	6.37
	ES	9.52	2.35	7.23	3.37	4.14	6.20
	P	0.0003	0.0149	0.00003	0.0018	0.0008	0.0003
Val	*%var*	138.35	10.36	151.36	47.98	101.22	70.45
	±	7.05	7.17	7.07	7.20	10.19	6.25
	ES	7.14	0.84	7.50	3.31	4.05	5.12
	P	0.0005	0.2444	0.0002	0.0021	0.0006	0.0003

Table S4.2. (cont.)

		BA			UA		
		5µM		10µM		20µM	
		48h	48h+24h	48h	48h+24h	48h	48h+24h
Phe	*%var*	0	-24.03	22.52	16.59	0	27.29
	±		3.87	4.02	5.94		5.68
	ES	0	-4.33	3.10	1.59	0	2.60
	P		0.0007	0.0129	0.0563		0.0112
Tyr	*%var*	-16.91	-36.13	0	13.28	0	21.23
	±	6.33	4.38		6.11		6.07
	ES	-1.79	-6.19	0	1.25	0	1.95
	P	0.0306	0.0002		0.1023		0.0290
PCr	*%var*	0	0	34.32	24.82	0	0
	±			5.07	8.78		
	ES	0	0	3.55	1.55	0	0
	P			0.0066	0.0625		
Cr	*%var*	59.47	0	-16.76	0	0	28.29
	±	7.16		7.24			5.90
	ES	3.94	0	-1.55	0	0	2.32
	P	0.0010		0.0504			0.0233
ATP	*%var*	0	0	41.52	0	53.13	0
	±			8.28		4.46	
	ES	0	0	2.55	0	5.79	0
	P			0.0099		0.0003	
NADH	*%var*	62.88	0	34.09	20.35	46.21	55.81
	±	9.38		7.12	12.26	10.93	12.96
	ES	3.14	0	2.52	0.93	2.11	2.07
	P	0.0030		0.0095	0.1871	0.0185	0.0155
1-MethylNicotinamide	*%var*	152.75	56.61	38.46	22.91	83.24	50.44
	±	6.98	12.39	4.12	11.32	5.37	11.40
	ES	7.62	2.19	4.81	1.12	6.73	2.17
	P	0.0006	0.0194	0.0003	0.1249	0.0003	0.0174

Table S4.2. (cont.)

		BA			UA		
		5µM		10µM		20µM	
		48h	48h+24h	48h	48h+24h	48h	48h+24h
Choline	*%var*	46.22	0	31.99	0	30.58	0
	±	5.48		10.12		5.34	
	ES	4.21	0	1.68	0	3.05	0
	P	0.0005		0.0515		0.0027	
PC	*%var*	-78.42	0	-26.30	-38.35	-17.27	-38.16
	±	9.97		10.76	11.54	8.07	8.48
	ES	-7.96	0	-1.73	-2.53	-1.44	-3.42
	P	0.00004		0.0360	0.0081	0.0578	0.0016
GPC	*%var*	307.70	188.81	108.51	-32.45	160.13	0
	±	7.34	17.03	7.69	11.53	8.43	
	ES	10.15	3.51	5.63	-2.07	6.49	0
	P	0.0003	0.0068	0.0015	0.0364	0.0012	
GSH	*%var*	-31.85	-24.73	-30.60	-27.29	-21.64	-26.66
	±	4.66	20.84	5.71	11.44	4.28	12.31
	ES	-4.99	-0.83	-3.89	-1.70	-3.48	-1.54
	P	0.0003	0.2549	0.0008	0.0382	0.0019	0.0559
myo-Lno	*%var*	-19.23	-52.77	-13.14	0	0	0
	±	5.02	9.47	3.34			
	ES	-2.60	-4.65	-2.59	0	0	0
	P	0.0090	0.0022	0.0057			
Dimethylamine	*%var*	-40.51	0	-53.26	-15.34	-41.93	-23.93
	±	17.23		17.87	8.94	17.00	8.69
	ES	-1.81	0	-2.50	-1.14	-1.92	-1.92
	P	0.0480		0.0266	0.1253	0.0458	0.0379

Chapter 5

FINAL REMARKS AND FUTURE PERSPECTIVES

The work performed in this thesis addressed the bioactive potential of Eucalyptus compounds in the field of anticancer therapy, focusing on their metabolic effects towards tumor and non-tumor breast cellular models. Eucalyptus harvesting and industrial processing, for the pulp and paper industry, produce considerable amounts of biomass residues, especially bark. Currently, these residues are mainly burned for energy production. However, they can also be further refined to value-added compounds, with relevance in chemical and pharmaceutical industries, contributing to more feasible economic valorization of these side-streams and prompting a transition for a circular-economy within the forestry-based sector. *Eucalyptus nitens* outer barks are particularly generous sources of pentacyclic triterpenoids, mostly triterpenic acids (TAs), a group of compounds with limited availability and very high priced in the market. Among multiple biological properties, TAs have been demonstrated to exert potent anticancer activity in diverse models, modulating numerous signaling pathways involved in carcinogenesis. This is particularly relevant for the discovery and development of more selective and efficient therapies for highly aggressive and refractory cancers. Triple negative breast cancer (TNBC) represents 10-20% of all BC cases and is amongst the most difficult to treat, remaining associated with poor overall survival and high risk of early relapse. Hence, motivated by the need to find novel therapeutics for this highly lethal disease, the driving goal of this work was to improve current knowledge on how Eucalyptus compounds affect cellular adaptation mechanisms and vulnerabilities, at the metabolic level, in order to trigger and/or potentiate anticancer responses.

There is cumulative evidence that tumor cells profoundly alter their metabolism to face exacerbated energetic and biosynthetic needs and to achieve survival advantages over normally proliferating cells. Moreover, some metabolites are known to have pro-oncogenic functions and to promote more aggressive and invasive phenotypes. Hence, reprogramming of cell metabolism is widely accepted as one of cancer hallmarks, with substantial associations with cancer-related signaling pathways. This knowledge has also boosted the interest in identifying and modulating metabolic targets in order to eliminate or sensitize tumor cells. While some pharmacological agents have been explored for this purpose since several years, the potential of plant-derived compounds as anticancer metabolic modulators has only recently begun to be appreciated. The work developed in this thesis is believed to give an important contribute for highlighting the metabolic modulatory activity of a Eucalyptus bark lipophilic bark extract and of two triterpenic acids (betulinic and ursolic acids) widely abundant in this kind of biomass.

NMR metabolomics was the main methodology employed in this thesis to investigate cells metabolic profiles and their responses to Eucalyptus compounds. In a first instance, we have characterized the basal metabolic activity and composition of the two cellular models used in this work, a TNBC cell line (MDA-MB-231) and a non-tumor breast epithelial cell line (MCF-10A) (Chapter 2). In this way, based on consumption and excretion patterns, together with analysis of polar endometabolome and lipid composition, we could infer on the more active metabolic pathways in each cell type. In line with the existing literature, breast cancer cells displayed very distinct metabolic features compared to breast epithelial cells. Some of the main differences were: upregulated glycolytic and TCA cycle activity, relatively lower mitochondrial respiration and energetic pool, active hexosamine biosynthetic pathway, high phosphocholine content (likely reflecting upregulation of choline kinase), redox imbalance with decreased levels of the endogenous antioxidant glutathione, and enrichment in neutral lipids (likely forming cytosolic droplets). This knowledge was important to interpret the differences in cellular responses to the exogeneous stimuli used thereafter.

The impact of a Eucalyptus (*E. nitens*) lipophilic bark extract on the metabolism of TNBC and epithelial breast cells was described in Chapter 3. Incubation for 48h of MDA-MB-231 breast cancer cells with the *E. nitens* extract at a concentration of 15 µg/mL, caused multiple metabolic effects, which suggested

modulation of several pathways. Some of these were proposed to relate more directly to the potential therapeutic effect of *E. nitens* lipophilic outer bark extract in TNBC and are here highlighted. One marked effect was the enhancement of the NAD^+/NADH ratio, likely reflecting a shift to mitochondrial respiration, which appeared to be fueled by oxidation of fatty acids resulting from hydrolysis of neutral lipids (triglycerides and cholesteryl esters), and/or by aminoacids which could arise from autophagic protein degradation. To further support these findings, possible interference of the *E. nitens* extract with complex I of MDA-MB-231 cells respiratory chain, increased FAO and autophagy induction should be investigated in the future. Another significant change regarded the downregulation of choline kinase (ChoK-α) expression and the significant reduction of the phosphocholine content, often regarded as a marker of breast cancer aggressiveness.

The *E. nitens* lipophilic outer bark extract presented a much higher cytotoxicity towards non-tumor breast epithelial cells (MCF-10A), hence it was not possible to use the same concentration for metabolomics assays as the one used for MDA-MB-231 cells. Instead, for the results to be comparable, a concentration which corresponded approximately to the MTT-determined IC_{50} was used (0.25 µg/mL). Interestingly, the overall metabolic impact of the *E. nitens* extract in MCFA-10A cells appeared to be less marked and clearly distinct from that produced in cancer cells. In MCF-10A epithelial cells, the *E. nitens* lipophilic outer bark extract appeared to intensify glycolysis and the TCA cycle (resulting in decreased $NAD^{+/}$NADH ratio) and had no effect on the cells lipid composition. Interestingly, the hexosamine biosynthetic pathway, through which nucleotide sugars involved in glycosylation reactions are produced, appeared to be upregulated by the *E. nitens* extract in both cell lines, but its biological relevance remains to be determined.

Given the abundance of triterpenic acids (TAs) in the *E. nitens* lipophilic outer bark extract, and their promising anticancer activities, we have also investigated the metabolic effects of betulinic and ursolic acids (BA and UA, respectively) on MDA-MB-231 and MCF-10A breast cells (Chapter 4). Here, 48h incubations at two concentrations of each acid (one closer to the IC_{50} and a lower one) were performed, together with a recovery assay, where BA/UA-treated cells were incubated for additional 24h in fresh growth medium. The metabolic responses of the two cell types to each TA were drastically different. In MDA-MB-231 cancer cells, the main effects of BA appeared to be the upregulation of glycolysis and TCA cycle activity, together with hydrolysis of neutral lipids and use of fatty acids,

possibly in membrane building. Not all these effects were reverted upon incubation in fresh medium, in fact, the ATP content decreased, suggesting impairment of energy homeostasis. Interestingly, the effects of UA were milder upon 48h incubation and became more noticeable after the recovery period, including downregulation of glycolysis and decreased ATP levels. In MCF-10A cells, both BA and UA had very pronounced effects, especially upon 48h incubation, which mainly suggested a significant reprogramming of glucose metabolism towards glycogen degradation, upregulation of HBP and intensification of glycolysis, membrane degradation and formation of lipid droplets, likely to scavenge otherwise-toxic species. These changes were only partially abrogated after 24h incubation in BA/UA-free medium. Overall, it may be concluded that neither BA nor UA alone recapitulated the metabolic effects of the *E. nitens* lipophilic outer bark extract. It could thus be interesting to investigate in the future the action of other extract components (e.g. oleanolic acid) either alone or in combination.

Another important observation was that TNBC and breast epithelial cells responded differently to the pure TAs, as well as to the *E. nitens* extract. This finding supports the idea that metabolic pathways specifically altered in tumors may constitute vulnerabilities that can potentially be targeted with minimum negative impact on healthy cells. Also of notice is that the *E. nitens* extract appeared to reprogram the metabolism of MDA-MB-231 cancer cells towards a less malignant metabolic phenotype. This is a good indication that it can possibly be useful in anticancer therapies through low dose, continued metabolic modulation, rather than through direct cytotoxic action.

As attested by the findings summarized above, NMR metabolomics enabled the simultaneous detection and relative quantification of unanticipated changes in a wide range of metabolites involved in several metabolic pathways. Unlike typical molecular and biochemical approaches that investigate a small number of pre-defined compounds, this untargeted approach newly revealed a comprehensive view of cellular metabolic adaptations and enabled some mechanistic hypotheses to be generated. On the other hand, there were also some important limitations, such as the high cell numbers required for analysis, which implied time-consuming cell culture procedures, and hindered the inclusion of additional time points and/or concentrations, or the incapability to detect metabolites present at low abundance (< µM concentrations). The use of 2D monocultures of cell lines, which poorly mimic

the *in vivo* tumor microenvironment is another limitation, which could be addressed in future studies by using 3D cellular/tissue models or even small animal models.

Finally, it should be stressed that the biochemical questions and hypotheses generated in this work represent a great amount of novel information that would greatly benefit from further testing and validation in the future. As this work demonstrated, the complexity and plasticity of cell metabolism pose great challenges to biological interpretation of metabolite changes. Therefore, complementary assays involving independent measurements of metabolic parameters (e.g. oxygen consumption, mitochondrial membrane potential, ROS production), together with the assessment of the expression/activity of specific proteins and enzymes should be performed.